Year : 2014

MECHANISTIC INSIGHTS INTO CYTOSOLIC MOLECULAR CHAPERONES IN PROTEIN UNFOLDING AND DISAGGREGATION

Mattoo Rayees

UNIL | Université de Lausanne
Faculté de biologie et de médecine

Département de biologie moléculaire végétale

MECHANISTIC INSIGHTS INTO CYTOSOLIC MOLECULAR CHAPERONES IN PROTEIN UNFOLDING AND DISAGGREGATION

Thèse de doctorat ès sciences de la vie (Ph.D.)
Présentée à la
Faculté de biologie et de médecine
de l'Université de Lausanne

par

RAYEES U. H. MATTOO

Biochemistry diplômé ou Master de l'Université Aligarh Inde.

Jury

Prof. Jan Roelof van der Meer, Président
Prof. Pierre Goloubinoff, Directeur de thèse
Prof. Anat Ben-Zvi, expert
Prof. Didier Picard, expert

Lausanne, 2014.

UNIL | Université de Lausanne
Faculté de biologie
et de médecine

Ecole Doctorale

Doctorat ès sciences de la vie

Imprimatur

Vu le rapport présenté par le jury d'examen, composé de

Président	Monsieur	Prof. Jan Roelof **Van der Meer**
Directeur de thèse	Monsieur	Prof. Pierre **Goloubinoff**
Experts	Monsieur	Prof. Didier **Picard**
	Madame	Dr Anat **Ben-Zvi**

le Conseil de Faculté autorise l'impression de la thèse de

Monsieur Rayees Ul Hassan Mattoo

Master en biochimie de Aligarh Muslim University, Aligarh, Inde

intitulée

MECHANISTIC INSIGHTS OF CYTOSOLIC MOLECULAR CHAPERONES IN PROTEIN UNFOLDING AND DISAGGREGATION

Lausanne, le 25 juillet 2014

pour La Doyenne
de la Faculté de Biologie et de Médecine

Prof. Jan Roelof Van der Meer

TABLE OF CONTENT

Thesis Graphical Abstract

MECHANISTIC INSIGHTS INTO CYTOSOLIC MOLECULAR CHAPERONES IN PROTEIN UNFOLDING AND DISAGGREGATION

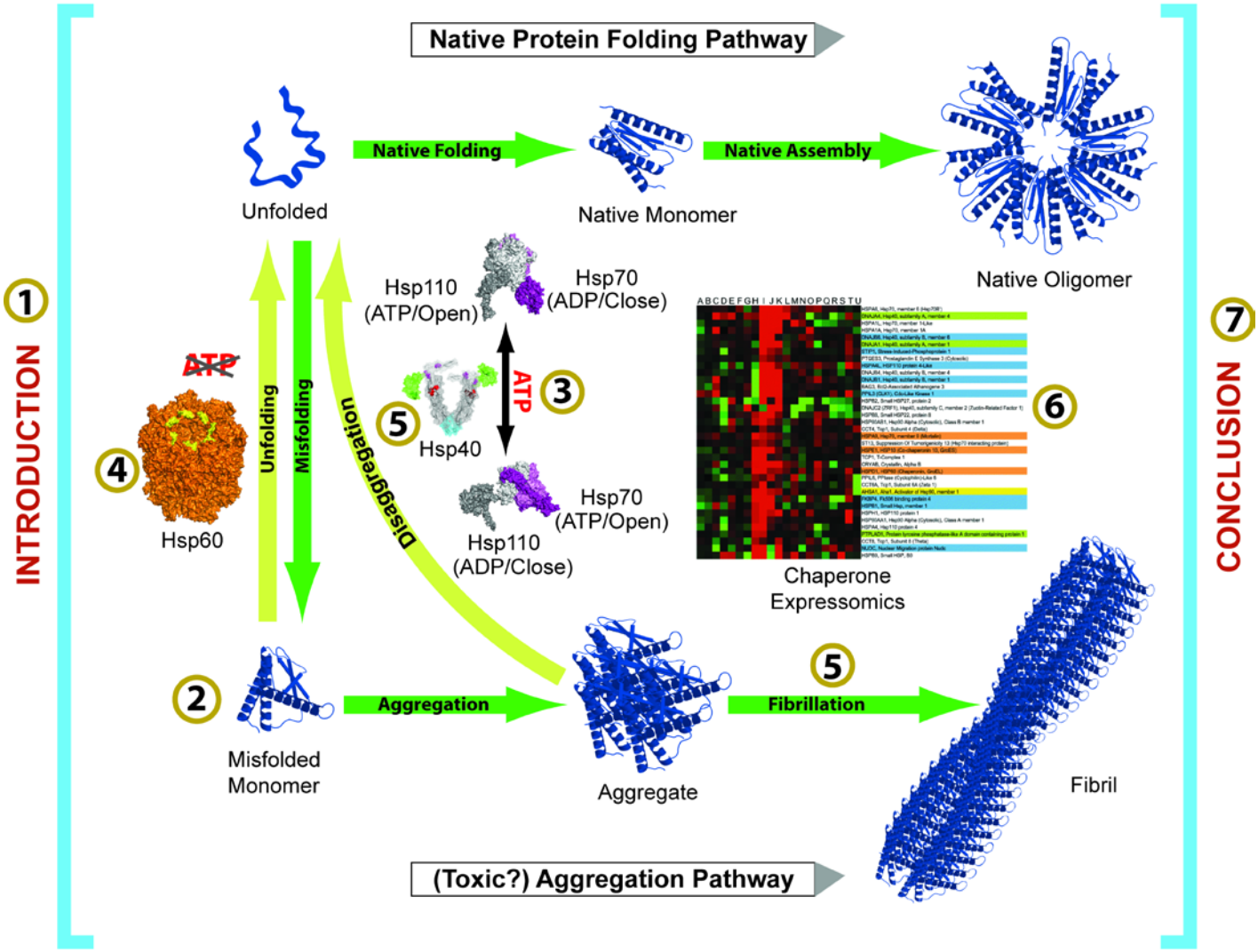

Cytosolic molecular chaperones reactivate misfolded or aggregated proteins by their polypeptide unfoldase activity. Protein synthesized *de novo* follow a native folding pathway under optimal conditions to acquire a terminal tertiary functional structure or may assemble to form a functional quaternary oligomer (upper pathway). Under stress or non-native conditions, protein may misfold (2) and enter an aggregation pathway (lower pathway), leading to the formation of aggregates and fibrils that can be cytotoxic. Chapter (2) presents an innovative method of preparation and biophysical characterization of stable misfolded monomers that were paradigmatic of the earliest species in the aggregation process and were unique chaperone amenable substrates that I used in most of the subsequent chapters of my thesis. In chapter (3), I addressed the disaggregation mechanism of stable protein aggregates by human Hsp70 and Hsp110 that acted as equal partners and synergistically combined their individual ATP-consuming polypeptide-unfoldase activity to reactivate stable protein aggregates. In chapter (4), my collaborators and I, showed that Hsp60 could act as a polypeptide unfoldase at reactivating stable misfolded proteins without ATP and without necessarily encaging them. In chapter (5) we investigated the role of Hsp40 (J-protein) at targeting Hsp70 onto the misfolded substrates and the inhibitory effect of potentially toxic protein aggregates on J-proteins that rendered Hsp70 unfolding activity less efficient, as in Parkinson's diseases. In chapter (6) we performed an innovative type of meta-analysis of chaperone expressomic data under various stress conditions that revealed possible co-expressions between core chaperone machineries and their co-chaperone regulators. *Encircled numbers in the figure represent chapters of the thesis.*

Abstract

Under optimal non-physiological conditions of low concentrations and low temperatures, proteins may spontaneously fold to the native state, as all the information for folding lies in the amino acid sequence of the polypeptide. However, under conditions of stress or high protein crowding as inside cells, a polypeptide may misfold and enter an aggregation pathway resulting in the formation of misfolded conformers and fibrils, which can be toxic and lead to neurodegenerative illnesses, such as Alzheimer's, Parkinson's or Huntington's diseases and aging in general. To avert and revert protein misfolding and aggregation, cells have evolved a set of proteins called molecular chaperones. Here, I focussed on the human cytosolic chaperones Hsp70 (DnaK) and Hsp110, and co-chaperone Hsp40 (DnaJ), and the chaperonin CCT (GroEL). The cytosolic molecular chaperones Hsp70s/Hsp110s and the chaperonins are highly upregulated in bacterial and human cells under different stresses and are involved both in the prevention and the reversion of protein misfolding and aggregation. Hsp70 works in collaboration with Hsp40 to reactivate misfolded or aggregated proteins in a strict ATP dependent manner. Chaperonins (CCT and GroEL) also unfold and reactivate stably misfolded proteins but we found that it needed to use the energy of ATP hydrolysis in order to evict over-sticky misfolded intermediates that inhibited the unfoldase catalytic sites.

In this study, we initially characterized a particular type of inactive misfolded monomeric luciferase and rhodanese species that were obtained by repeated cycles of freeze-thawing (FT). These stable misfolded monomeric conformers (FT-luciferase and FT-rhodanese) had exposed hydrophobic residues and were enriched with wrong β-sheet structures (Chapter 2). Using FT-luciferase as substrate, we found that the Hsp70 orthologs, called Hsp110 (Sse in yeast), acted similarly to Hsp70 as were *bona fide* ATP-fuelled polypeptide unfoldases and was much more than a mere nucleotide exchange factor, as generally thought. Moreover, we found that Hsp110 collaborated with Hsp70 in the disaggregation of stable protein aggregates in which Hsp70 and Hsp110 acted as equal partners that synergistically combined their individual ATP-consuming polypeptide unfoldase activities to reactivate the misfolded/aggregated proteins (Chapter 3). Using FT-rhodanese as substrate, we found that chaperonins (GroEL and CCT) could catalytically reactivate misfolded rhodanese monomers in the absence of ATP. Also, our results suggested that encaging of an unfolding polypeptide inside the GroEL cavity under a GroES cap was not an obligatory step as generally thought (Chapter 4). Further, we investigated the role of Hsp40, a J-protein co-chaperone of Hsp70, in targeting misfolded polypeptides substrates onto Hsp70 for unfolding. We found that even a large excess of monomeric unfolded α-synuclein did not inhibit DnaJ, whereas, in contrast, stable misfolded α-synuclein oligomers strongly inhibited the DnaK-mediated chaperone reaction by way of sequestering the DnaJ co-chaperone. This work revealed that DnaJ could specifically distinguish, and bind potentially toxic stably aggregated species, such as soluble α-synuclein oligomers involved in Parkinson's disease, and with the help of DnaK and ATP convert them into from harmless natively unfolded α-synuclein monomers (chapter 5). Finally, our meta-analysis of microarray data of plant and animal tissues treated with various chemicals and abiotic stresses, revealed possible co-expressions between core chaperone machineries and their co-chaperone regulators. It clearly showed that protein misfolding in the cytosol elicits a different response, consisting of upregulating the synthesis mainly of cytosolic chaperones, from protein misfolding in the *endoplasmic reticulum* (ER) that elicited a typical unfolded protein response (UPR), consisting of upregulating the synthesis mainly of ER chaperones. We proposed that drugs that best mimicked heat or UPR stress at increasing the chaperone load in the cytoplasm or ER respectively, may prove effective at combating protein misfolding diseases and aging (Chapter 6).

Résumé

Dans les conditions optimales de basse concentration et de basse température, les protéines vont spontanément adopter un repliement natif car toutes les informations nécessaires se trouvent dans la séquence des acides aminés du polypeptide. En revanche, dans des conditions de stress ou de forte concentration des protéines comme à l'intérieur d'une cellule, un polypeptide peu mal se replier et entrer dans un processus d'agrégation conduisant à la formation de conformères et de fibrilles qui peuvent être toxiques et causer des maladies neurodégénératives comme la maladie d'Alzheimer, la maladie de Parkinson ou la chorée de Huntington. Afin d'empêcher ou de rectifier le mauvais repliement des protéines, les cellules ont développé des protéines appelées chaperonnes. Dans ce travail, je me suis intéressé aux chaperonnes cytosoliques Hsp70 (DnaK) et Hsp110, la co-chaperones Hsp40 (DnaJ), le complexe CCT/TRiC et GroEL. Chez les bactéries et les humains, les chaperonnes cytosoliques Hsp70s/Hsp110s et les « chaperonines» sont fortement activées par différentes conditions de stress et sont toutes impliquées dans la prévention et la correction du mauvais repliement des protéines et de leur agrégation. Hsp70 collabore avec Hsp40 pour réactiver les protéines agrégées ou mal repliées et leur action nécessite de l'ATP. Les chaperonines (GroEL) déplient et réactivent aussi les protéines mal repliées de façon stable mais nous avons trouvé qu'elles utilisent l'ATP pour libérer les intermédiaires collant et mal repliés du site catalytique de dépliage.

Nous avons initialement caractérisé un type particulier de formes stables de luciférase et de rhodanese monomériques mal repliées obtenues après plusieurs cycles de congélation/décongélation répétés (FT). Ces monomères exposaient des résidus hydrophobiques et étaient plus riches en feuillets β anormaux. Ils pouvaient cependant être réactivés par les chaperonnes Hsp70+Hsp40 (DnaK+DnaJ) et de l'ATP, ou par Hsp60 (GroEL) sans ATP (Chapitre 2). En utilisant la FT-Luciferase comme substrat nous avons trouvé que Hsp110 (un orthologue de Hsp70) était une authentique dépliase, dépendante strictement de l'ATP. De plus, nous avons trouvé que Hsp110 collaborait avec Hsp70 dans la désagrégation d'agrégats stables de protéines en combinant leurs activités dépliase consommatrice d'ATP (Chapitre 3). En utilisant la FT-rhodanese, nous avons trouvé que les chaperonines (GroEL et CCT) pouvaient réactiver catalytiquement des monomères mal repliés en absence d'ATP. Nos résultats suggérèrent également que la capture d'un polypeptide en cours de dépliement dans la cavité de GroEL et sous un couvercle du complexe GroES ne serait pas une étape obligatoire du mécanisme, comme il est communément accepté dans la littérature (Chapitre 4). De plus, nous avons étudié le rôle de Hsp40, une co-chaperones de Hsp70, dans l'adressage de substrats polypeptidiques mal repliés vers Hsp70. Ce travail a révélé que DnaJ pouvait différencier et lier des polypeptide mal repliés (toxiques), comme des oligomères d'α-synucléine dans la maladie de Parkinson, et clairement les différencier des monomères inoffensifs d'α-synucléine (Chapitre 5). Finalement une méta-analyse de données de microarrays de tissus végétaux et animaux traités avec différents stress chimiques et abiotiques a révélé une possible co-expression de la machinerie des chaperonnes et des régulateurs de co-chaperonne. Cette meta-analyse montre aussi clairement que le mauvais repliement des protéines dans le cytosol entraîne la synthèse de chaperonnes principalement cytosoliques alors que le mauvais repliement de protéines dans le réticulum endoplasmique (ER) entraine une réponse typique de dépliement (UPR) qui consiste principalement en la synthèse de chaperonnes localisées dans l'ER. Nous émettons l'hypothèse que les drogues qui reproduisent le mieux les stress de chaleur ou les stress UPR pourraient se montrer efficaces dans la lutte contre le mauvais repliement des protéines et le vieillissement (Chapitre 6).

Acknowledgements

I would like to express my deepest appreciation to my thesis supervisor Prof. Pierre Goloubinoff. He provided me with a great opportunity to work in his laboratory and has been instrumental in realizing this thesis. His stimulating and critical scientific discussions have tremendously improved my scientific temperament. His effort to inculcate me with the scientific skills has remained one among the top priorities and I thank him for that.

I would like to mention that I thoroughly enjoyed working with my colleagues among them Dr. Sandeep sharma deserves special thanks for the advice and all the help he provided. Dr. Andrija Finka and Dr. Smriti Priya were also a great support throughout my stay. It would be unfair if I don't mention America Farina, Maude Muriset, Anika Braune, Flavia Canellas, Alberto Merli and John Perrin for their great company and for extending their help whenever I needed.

I am grateful to my collaborators, Prof. Hilal Lashuel, Prof. Silvia Maria Doglia and Prof. Juan Pelta for broadening my scientific skills by sharing their knowledge and expertise.

I would like to thank Guillaume Fabre for helping me in the French translation of the thesis abstract. I express my gratitude to all the members of Département de Biologie moléculaire végétale for maintaining a friendly and healthy scientific atmosphere.

I am also highly thankful to my friends, Dr. Tanveer for his critical scientific discussions, and Imene, Dr. Amir, Dr. Imran, Dr. Rouf and Zeeshan for their moral support.

Finally, I would like to thank Dr. Humaira and my parents for their love, encouragement and care that was truly a great motivation all through these years.

GENERAL OVERVIEW

Anfinsen demonstrated that under optimal conditions of low protein concentrations and low temperatures, the primary amino acid sequence of a polypeptide contains all the necessary instructions for its spontaneous acquisition of its functional three dimensional native conformation (Anfinsen, 1973). Yet, the refolding process is often inefficient because hydrophobic residues that become abnormally exposed to the aqueous phase in stress-unfolded or *de novo*-synthesized polypeptides, may spontaneously seek intra-molecular stability by forming wrong beta sheets and improper inter-molecular ensembles generally called aggregates. The aggregates-entrapped polypeptides are precluded from dissociating and reaching their native state within a biologically relevant time-scale (Dobson, 2003). Moreover, aggregates may be cytotoxic, especially to animal cells and cause degenerative disorders, such as Parkinson's, Huntington's and Alzheimer's diseases (Hinault et al., 2006). In order to prevent and retard the onset of protein conformational diseases, prokaryotes and eukaryotes have evolved a complex network of molecular chaperones. The most abundant chaperones are classified into five canonical families on the basis of sequence homology and have been named (1) the small-Hsps (IbpA/B), (2) the Hsp90s (HtpG), (3) the Hsp70s (DnaK), (4) the Hsp104s (ClpB), and (5) the chaperonins Hsp60 (GroEL) (*E. coli* orthologs shown in parentheses). Apart from sequence homology, molecular chaperones share high structural and functional homologies within their respective classes. Molecular chaperones are abundant and can be found in all the compartments of the cell. Thus, Hsp70 and Hsp90, which together may be 2 % of the protein mass of a human cell, are present in all the ATP-containing compartments of the eukaryotic cell (Finka and Goloubinoff, 2013; Hemmingsen et al., 1988; Mattoo and Goloubinoff, 2014). In addition to the canonical molecular chaperones, prokaryotic and eukaryotic cells harbour other protein molecules, such as foldases (peptidyl-prolyl-isomerases and protein disulphide isomerases) and proteases (ClpAP, FtsH, DegP, Lon and 26S protease) and chemical chaperones that maintain protein homeostasis. Chaperones likely form the first line of the cellular defence against stress-induced protein aggregation by unfolding misfolded, aggregated or alternatively-folded proteins, thereby favouring their refolding to the native state, foldases directly assist the native folding of polypeptides by alleviating blockages caused by wrongly oriented prolines or wrongly associate disulfide bounds, and proteases degradation unnecessary or damaged proteins (for further details on chemical chaperones, protein chaperones and foldases please see chapter 1).

Under physiological conditions, molecular chaperones and proteases control house-keeping processes of cellular proteostasis, such as assisting the proper *de novo* folding of polypeptides exiting the ribosome, or of cytoplasmic proteins exiting the import pores in the *endoplasmic reticulum* lumen or the mitochondrial matrix. Molecular chaperones also activate or inhibit various signalling pathways, such as the activation of the steroid hormone receptor or the inhibition of heat-shock transcription factor-1 (Picard, 2006; Voellmy and Boellmann, 2007; Weiss et al., 2007). Molecular chaperones like Hsc70 (an Hsp70 member) control vesicle formation by de-oligomerizing clathrin cages (Sousa and Lafer, 2006). Hsp70s also serve as molecular motors that pull, unfold and translocate across membranes proteins that are synthesized on cytoplasmic ribosomes, into the ER lumen or the mitochondrial matrix. Other chaperones may also target short-lived or stress-damaged proteins to proteasomal or lysosomal degradation and reorient mutant proteins prone to aggregation back on track of the native folding pathway (Hinault et al., 2006). Under stress conditions, such as heat-shock or oxidative stresses, molecular chaperones like Hsp70s and

Hsp60s can prevent actively avert protein misfolding and aggregation (Sharma et al., 2009).

The first *in vitro* chaperone assay showed that the GroEL chaperonin without ATP could effectively bind and prevent the aggregation of misfolding intermediates of urea- or acid-unfolded RubisCO enzymes, with a RubisCO:GroEL stoichiometry of about 1:14 (protomers) (Goloubinoff et al., 1989). Both ATP and the co-chaperone GroES were necessary to subsequently induce the release of the inactive GroEL-bound RubisCO species, into soluble, natively refolded RubisCO enzymes (Goloubinoff et al., 1989). Later, a similar situation was described with other types of chaperones and various model unfolded or misfolded substrates. For instance, GroEL/GroES and DnaK/DnaJ/GrpE chaperones with urea- or Guanidine-HCl-unfolded malate dehydrogenase (MDH) and rhodanese (Langer et al., 1992) and MDH that was pre-bound with GroEL during heat-denaturation without ATP and released from the chaperone after the heat-stress upon addition of ATP and GroES (Diamant et al., 1995). These experiments suggested that the primary role of chaperone binding is primarily to prevent the obligate aggregation of an unfolded polypeptide, a function also called *holdase*, and the role of ATP hydrolysis is generally thought to release the high-affinity chaperone-bound intermediates to allow them refold in solution. However, the precise state of the chaperone-bound polypeptides remained unclear.

A central question in the field, which is yet unresolved for lack of being asked by most chaperone specialists is, what is the nature of the polypeptide substrate when tightly bound to a chaperone such as GroEL or DnaK? Is it unfolded, alternatively folded, misfolded and/or partly aggregated?

It has long been assumed, albeit on the basis of scarce experimental evidence, that the bound polypeptides are nearly completely unfolded. This served the widely accepted model assuming that sequestration within the GroEL or CCT cavities is at the centre of the mechanism by which cage-like chaperonins mediate the native refolding of aggregation-prone polypeptides (Hayer-Hartl et al., 1996; Horovitz and Willison, 2005; Weber et al., 1998). Hence, the 2011 Lasker prize was awarded to A. Horwich and FU. Hartl “For discoveries concerning the cell's protein-folding machinery, exemplified by cage-like structures that convert newly made proteins into their biologically active forms.” (http://www.laskerfoundation.org/awards/2011basic.htm).

Although other chaperones like Hsp90, Hsp70, Hsp40 and the small-Hsps do not necessarily form anti-aggregation cages, it is still generally maintained that in their case too the high-affinity bound polypeptide substrate are unfolded. It was assumed that these chaperones act primarily as passive devices that prevent aggregation (Horwich et al., 2009), rather than as active unfolding motors that extend and unwind misfolded and aggregated species to convert them into natively-refoldable species (Mattoo et al., 2013; Sharma et al., 2010).

A first indication that some molecular chaperones may also interact with already stably misfolded polypeptides, and not exclusively with completely unfolded species, already came from the very first *in vitro* chaperone refolding assay 25 years ago (Goloubinoff et al., 1989). The assay showed that inactive acid-denatured RubisCO, which contained many misfolded β-sheets, as revealed by circular dichroism, was nearly as an amenable substrate for subsequent GroEL-GroES + ATP dependent refolding, as completely urea-pre-unfolded RubisCO. This suggested that the chaperonin can apply an unfolding force on stable pre-formed misfolded substrate species during initial binding (Stan et al., 2003). Subsequent ATP hydrolysis and GroES binding, would allow the thus unfolded substrate polypeptide to spontaneously refold to the native state upon release. A similar ability of chaperones to act upon stably misfolded polypeptide species,

formed beforehand in the absence of chaperones, was confirmed *in vitro* with the bacterial Hsp70 chaperone system (DnaK/DnaJ/GrpE) using preformed heat-denatured (Diamant et al., 2000). The mechanism involved first unfolding of the stable aggregates in a strict ATP-dependent manner, then their refolding to the native state upon release. Similarly, DnaK/DnaJ/GrpE, assisted by the bacterial co-chaperone ClpB, could solubilise stable pre-formed MDH aggregates (Goloubinoff et al., 1999) and yeast SSA and Hsp104 (ClpB like) could reactivate stable preformed luciferase aggregates in a strict ATP-dependent manner (Glover and Lindquist, 1998). Metazoans lack ClpB-like proteins but have Hsp110 chaperones, members of Hsp70 family described as mere nucleotide exchange factors that upon collaboration with Hsp70 functionally resemble ClpB-Hsp70 system. Hsp110 was found to collaborate with Hsp70 at disaggregating large stable protein aggregates, such as luciferase aggregates, α-synuclein fibrils and aggregated polyglutamine repeats (Duennwald et al., 2012; Mattoo et al., 2013; Rampelt et al., 2012; Shorter, 2011). All these findings used molecular chaperones in molar excess over the substrate, rendering the process of reversing the protein aggregation process energetically expensive. Moreover, the substrates that were used for chaperone-mediated refolding were generally prepared in presence of chaperones, which limited the estimation of the real effect of chaperones on already stable misfolded or aggregated proteins. This raised the need to develop and characterize obligate stable chaperone substrates that were pre-formed in the absence of chaperones and moreover that were neither obligatorily prone to aggregation nor tended to spontaneously refold to the native state in the absence of chaperones.

To this aim, the Goloubinoff laboratory has used in the last decade several new forms of chaperone substrates that were prepared in the absence of chaperones, such as heat-inactivated G6PDH and MDH, and, which were then refolded upon addition of chaperones (and ATP). The use of these substrates conducted to seminal discoveries. For instance, Hsp100 (ClpB) was found to cooperate with Hsp70 (DnaK) and use ATP to solubilise and reactivate stable inactive protein aggregates. Moreover, it was discovered that the size of the stable pre-aggregated chaperone substrates determined the efficiency and the degree of cooperation between chaperone systems. It was found that without ClpB, DnaK can efficiently solubilize and reactivate small aggregates and that the efficiency of the reaction decreased as the size of the aggregates increased. The refolding efficiency was restored by adding either an excess DnaK, or substoichiometric amounts of ClpB (Diamant et al., 2000; Goloubinoff et al., 1999). Recently, the Goloubinoff laboratory generated inactive misfolded luciferase monomers that neither tended to aggregate nor to spontaneously refold without the assistance of chaperones. The substrates were generated by repeated freeze thaw (FT) cycles and were optimally refolded by the bacterial Hsp70 system (DnaK/DnaJ/GrpE). These results provided a first proof that molecular chaperones, even in sub-stoichiometric amount compared to the misfolded substrate, can use the energy of ATP-hydrolysis to efficiently unfold and reactivate its misfolded inactive polypeptide substrate. In this study by Sharma et al., 2010, the misfolded (FT-luciferase) substrate was shown to bind bacterial Hsp40 and Hsp70 where, as a result of ATP hydrolysis it became completely unfolded. The unfolded substrate was then released from the Hsp70 in a nucleotide exchange factor (GrpE)-accelerated manner. The released unfolded substrate finally spontaneously refolded to the native state, much like in the original experiments of Anfinsen, i.e. free in solution apparently solely directed by the primary amino acid sequence (for details please see chapters 1 and 7). These results showed that theHsp70 chaperone acts as ATP-fuelled polypeptide *unfoldase* and not as a *foldase per se* (Sharma et al., 2010). This study suggested that unfolding of a misfolded monomeric luciferase substrate by a

single DnaK molecule can result from a forceful, ATP-fuelled, local "clamping" effect by DnaK on a bulky misfolded segment in a polypeptide substrate. However, in case the polypeptides were severely damaged, the clamping of a single DnaK molecule was apparently insufficient to cause productive unfolding (Diamant et al., 2000). In this case, several DnaKs needed to become concomitantly clamped onto the same misfolded polypeptide, in order to exert a fruitful cooperative unfolding force on the misfolded segments that were located in-between the chaperone-clamped binding sites. This mechanism involving several Hsp70s cooperating at pulling on an individual misfolded polypeptide entangled within an aggregate was called "entropic pulling". Entropic pulling also applied to the mechanism by which an organellar Hsp70 can cooperate with an import membrane pore, to pull upon and unfold an imported cytoplasmic polypeptide into the lumen of the *endoplasmic reticulum* or the matrix of mitochondria and chloroplasts (De Los Rios et al., 2006). Moreover, the study by Sharma et al., 2010 reported the most efficient *in vitro* chaperone mediated refolding assay to date. Only 5 ATPs were needed to be hydrolysed in order to recover one native luciferase from a stable misfolded state. Apart from mechanistic insights and energy costs of Hsp70 folding cycle, this study provided a method of generating new chaperone-amenable substrates that can act as novel tool to study the mechanisms of other chaperones.

At this juncture, I joined Goloubinoff laboratory in 2009 and took forward the ongoing challenges and obtained several results, which I am presenting here in the form of a thesis. The thesis is divided into seven chapters. A short description of all the interlinked chapters is given below:

The first chapter is an introduction on the different classes of molecular chaperones and their mechanisms of action with special emphasis on bacterial chaperones that are involved in the prevention and reversion of protein aggregation.

The second chapter presents the biochemical and biophysical characterization of two freeze thaw (FT)-generated misfolded monomeric species (luciferase and rhodanese) that were further used in most experiments presented in the subsequent chapters. These misfolded species neither tend to spontaneously refold to the native state nor to aggregate. We found that FT-luciferase and FT-rhodanese were differently processed by the Hsp70 chaperone machinery and their conformational properties were investigated by biophysical techniques: Fourier transform infrared spectroscopy (FTIR), Circular dichroism **(**CD) spectroscopy and Fluorescence spectroscopy. In spite of their monomeric nature, they displayed more non-native β-sheets, and tertiary structures with surface-accessible hydrophobic patches, but differed in their conformational stability and aggregation propensity. Interestingly, minor structural differences between the two misfolded species could account for their markedly different behaviour in chaperone-mediated unfolding/refolding assays. Indeed, only a single DnaK molecule was sufficient to unfold by direct ATP-fuelled "clamping" a misfolded luciferase monomer. In contrast, several DnaK molecules proved to be necessary to unfold the more resistant misfolded rhodanese monomer by a combination of direct clamping and cooperative entropic pulling.

The third chapter addressed the role of human cytoplasmic Hsp70 and Hsp110 in protein homeostasis. In this chapter, I showed that human cytosolic Hsp110, a member of Hsp70 family, acted as *bona fide* ATP-dependent polypeptide unfoldase like Hsp70 and not as a mere nucleotide exchange factor as generally thought. Moreover, Hsp70 and Hsp110 acted as equal partners in the disaggregation of soluble protein aggregates where they combine their individual polypeptide unfolding activity and synergistically reactivate inactive protein aggregates in an ATP dependent manner.

The fourth chapter addressed the mechanism by which cytosolic chaperonins, Hsp60s (GroEL and CCTs), can efficiently process to the native state, the stable FT-rhodanese misfolded substrate that we characterized in chapter 2, even without co-chaperones (GroES) and ATP. We showed that both GroEL and the eukaryotic chaperonin can unfold the stable misfolded polypeptide conformers and readily release them from the access ways to the cage. Reconciling earlier disparate experimental observations to ours, we presented a comprehensive model whereby following unfolding on the upper cavity, in-cage confinement was not needed and even counter-productive for the released intermediates to slowly reach their native state while being free in solution. As over-sticky intermediates occasionally stalled the catalytic unfoldase sites, GroES mobile loops and ATP were found to be necessary to dissociate the inhibitory species and regenerate the unfolding activity of GroEL. Thus, chaperonin rings were found to be non-obligate confining anti-aggregation cages. They were rather revealed to be polypeptide unfoldases that could iteratively convert stable off-pathway conformers into functional proteins but needed an ancillary ATP-fuelled removal mechanism to evict over-sticky intermediates acting at time as competitive inhibitors to the intrinsic catalytic polypeptide unfoldase reaction of GroEL and CCT.

The fifth chapter addressed the role of Hsp40 in the Hsp70 folding cycle and the consequences of potentially toxic protein aggregates (α-synuclein oligomers) on bacterial Hsp40 that cause the inhibition of Hsp70 folding cycle. We developed a protocol for preparing a homogeneous population of highly stable β-sheet enriched α-synuclein oligomers with a diameter typical of toxic pore-forming oligomers. These oligomers were partially resistant to *in vitro* unfolding by the bacterial Hsp70 chaperone system (DnaK, DnaJ, GrpE) and ATP. Moreover, both bacterial and human Hsp70/Hsp40 unfolding/refolding activities of model chaperone substrates were found to be strongly inhibited by the oligomers but, remarkably, not by the unstructured α-synuclein monomers, even in large 20 fold excess. The oligomers acted as a specific competitive inhibitor of the J-domain co-chaperones, indicating that J-domain co-chaperones may preferably bind to exposed bulky misfolded structures in misfolded proteins and, thus, complement Hsp70s that lock onto extended segments. Together, our findings suggested that Inhibition of the Hsp70/Hsp40 chaperone system by α-synuclein oligomers may contribute to the disruption of protein homeostasis in dopaminergic neurons, leading to apoptosis and tissue loss in Parkinson disease and related neurodegenerative diseases.

The sixth chapter presented a meta-analysis of up-regulated chaperone networks under different stress conditions in mammalian and plant cells and brought new avenues of research for chaperone inducing drugs. We performed a meta-analysis of published microarray data and compared expression profiles of HSP genes from mammalian and plant cells in response to heat or isothermal treatments with various drugs. The differences and overlaps between HSP and chaperone genes were analysed, and expression patterns were clustered and organized in a network. HSPs and chaperones only partly overlapped. Heat-shock induced a subset of chaperones, which organized into a network with a central core of Hsp90s, Hsp70s and sHsps, primarily targeted to the cytoplasm and organelles but not to the *endoplasmic reticulum*. Heat was best mimicked by isothermal treatments with Hsp90 inhibitors, whereas less toxic drugs, some of which non-steroidal anti-inflammatory drugs, weakly expressed different subsets of Hsp chaperones. This type of analysis may uncover new HSP-inducing drugs to improve protein homeostasis in misfolding and aging diseases.

The seventh chapter is a review that summarized and integrated the major themes of

my thesis about the mechanisms of molecular chaperones that act mainly as polypeptide unfolding enzymes.

All the chapters of the thesis have been published in peer-reviewed international journals and are available online. My contribution in the published chapters is explained in detail on a page appended before the start of each chapter.

REFERENCES

Anfinsen, C.B. (1973). Principles that govern the folding of protein chains. Science *181*, 223-230.

De Los Rios, P., Ben-Zvi, A., Slutsky, O., Azem, A., and Goloubinoff, P. (2006). Hsp70 chaperones accelerate protein translocation and the unfolding of stable protein aggregates by entropic pulling. Proc Natl Acad Sci U S A *103*, 6166-6171.

Diamant, S., Azem, A., Weiss, C., and Goloubinoff, P. (1995). Effect of free and ATP-bound magnesium and manganese ions on the ATPase activity of chaperonin GroEL14. Biochemistry *34*, 273-277.

Diamant, S., Ben-Zvi, A.P., Bukau, B., and Goloubinoff, P. (2000). Size-dependent disaggregation of stable protein aggregates by the DnaK chaperone machinery. Journal of Biological Chemistry *275*, 21107-21113.

Dobson, C.M. (2003). Protein folding and misfolding. Nature *426*, 884-890.

Duennwald, M.L., Echeverria, A., and Shorter, J. (2012). Small heat shock proteins potentiate amyloid dissolution by protein disaggregases from yeast and humans. PLoS Biol *10*, e1001346.

Finka, A., and Goloubinoff, P. (2013). Proteomic data from human cell cultures refine mechanisms of chaperone-mediated protein homeostasis. Cell Stress Chaperones *18*, 591-605.

Glover, J.R., and Lindquist, S. (1998). Hsp104, Hsp70, and Hsp40: a novel chaperone system that rescues previously aggregated proteins. Cell *94*, 73-82.

Goloubinoff, P., Christeller, J.T., Gatenby, A.A., and Lorimer, G.H. (1989). Reconstitution of active dimeric ribulose bisphosphate carboxylase from an unfoleded state depends on two chaperonin proteins and Mg-ATP. Nature *342*, 884-889.

Goloubinoff, P., Mogk, A., Zvi, A.P., Tomoyasu, T., and Bukau, B. (1999). Sequential mechanism of solubilization and refolding of stable protein aggregates by a bichaperone network. Proc Natl Acad Sci U S A *96*, 13732-13737.

Hayer-Hartl, M.K., Weber, F., and Hartl, F.U. (1996). Mechanism of chaperonin action: GroES binding and release can drive GroEL-mediated protein folding in the absence of ATP hydrolysis. EMBO J *15*, 6111-6121.

Hemmingsen, S.M., Woolford, C., van der Vies, S.M., Tilly, K., Dennis, D.T., Georgopoulos, C.P., Hendrix, R.W., and Ellis, R.J. (1988). Homologous plant and bacterial proteins chaperone oligomeric protein assembly. Nature *333*, 330-334.

Hinault, M.P., Ben-Zvi, A., and Goloubinoff, P. (2006). Chaperones and proteases: cellular fold-controlling factors of proteins in neurodegenerative diseases and aging. J Mol Neurosci *30*, 249-265.

Horovitz, A., and Willison, K.R. (2005). Allosteric regulation of chaperonins. Curr Opin Struct Biol *15*, 646-651.

Horwich, A.L., Apetri, A.C., and Fenton, W.A. (2009). The GroEL/GroES cis cavity as a passive anti-aggregation device. FEBS Lett *583*, 2654-2662.

Langer, T., Lu, C., Echols, H., Flanagan, J., Hayer, M.K., and Hartl, F.U. (1992). Successive action of DnaK, DnaJ and GroEL along the pathway of chaperone-mediated protein folding. Nature *356*, 683-689.

Mattoo, R.U., and Goloubinoff, P. (2014). Molecular chaperones are nano-machines that catalytically unfold misfolded and alternatively folded proteins. Cellular and Molecular Life Sciences, In Press.

Mattoo, R.U., Sharma, S.K., Priya, S., Finka, A., and Goloubinoff, P. (2013). Hsp110 is a bona fide chaperone using ATP to unfold stable misfolded polypeptides and reciprocally collaborate with Hsp70 to solubilize protein aggregates. Journal of Biological Chemistry.

Picard, D. (2006). Chaperoning steroid hormone action. Trends Endocrinol Metab *17*, 229-235.

Rampelt, H., Kirstein-Miles, J., Nillegoda, N.B., Chi, K., Scholz, S.R., Morimoto, R.I., and Bukau, B. (2012). Metazoan Hsp70 machines use Hsp110 to power protein disaggregation. EMBO J *31*, 4221-4235.

Sharma, S.K., Christen, P., and Goloubinoff, P. (2009). Disaggregating chaperones: an unfolding story. Curr Protein Pept Sci *10*, 432-446.

Sharma, S.K., De Los Rios, P., Christen, P., Lustig, A., and Goloubinoff, P. (2010). The kinetic parameters and energy cost of the Hsp70 chaperone as a polypeptide unfoldase. Nat Chem Biol *6*, 914-920.

Shorter, J. (2011). The mammalian disaggregase machinery: Hsp110 synergizes with Hsp70 and Hsp40 to catalyze protein disaggregation and reactivation in a cell-free system. PLoS One *6*, e26319.

Sousa, R., and Lafer, E.M. (2006). Keep the traffic moving: mechanism of the Hsp70 motor. Traffic *7*, 1596-1603.

Stan, G., Thirumalai, D., Lorimer, G.H., and Brooks, B.R. (2003). Annealing function of GroEL: structural and bioinformatic analysis. Biophys Chem *100*, 453-467.

Voellmy, R., and Boellmann, F. (2007). Chaperone regulation of the heat shock protein response. Adv Exp Med Biol *594*, 89-99.

Weber, F., Keppel, F., Georgopoulos, C., Hayer-Hartl, M.K., and Hartl, F.U. (1998). The oligomeric structure of GroEL/GroES is required for biologically significant chaperonin function in protein folding. Nat Struct Biol *5*, 977-985.

Weiss, Y.G., Bromberg, Z., Raj, N., Raphael, J., Goloubinoff, P., Ben-Neriah, Y., and Deutschman, C.S. (2007). Enhanced heat shock protein 70 expression alters proteasomal degradation of IkappaB kinase in experimental acute respiratory distress syndrome. Crit Care Med *35*, 2128-2138.

CHAPTER 1

An introduction to thesis

Recruiting unfolding chaperones to solubilize misfolded recombinant proteins

Recruiting unfolding chaperones to solubilize misfolded recombinant proteins.

Mattoo, R.U. and Goloubinoff, P.

I contributed to this work conceptually and in the manuscript writing.
I provided the data for the Fig 2.1.

2

RECRUITING UNFOLDING CHAPERONES TO SOLUBILIZE MISFOLDED RECOMBINANT PROTEINS

Rayees U.H. Mattoo and Pierre Goloubinoff

2.1 INTRODUCTION

Anfinsen demonstrated that under optimal conditions, artificially unfolded proteins can spontaneously refold into their native conformation without requiring external assistance from other molecules. This seminal finding implied that the amino acid sequence of a polypeptide suffices to determine its native biologically active conformation (Anfinsen, 1973). Yet Anfinsen also observed that following artificial unfolding by urea, the yield of recovered native proteins decreased significantly as the temperature and protein concentration increased, suggesting that alternative nonproductive misfolding and aggregation pathways can compete with the physiological native refolding pathway of proteins. Destabilizing mutations, high temperatures, and prolonged stresses in general can cause more frequent transient unfolding events in proteins, which can be followed by misfolding and aggregation events. Moreover, early misfolded and aggregated species can be toxic to animal cells, neurons in particular. Thus, compact fibrils and amyloids are a hallmark of degenerative pathologies such as Parkinson's and Alzheimer's diseases (Hinault et al., 2006; Uversky, 2008).

Protein Aggregation in Bacteria: Functional and Structural Properties of Inclusion Bodies in Bacterial Cells, First Edition. Edited by Silvia Maria Doglia and Marina Lotti.

As observed while cooking an egg, the higher and longer the exposure to denaturing temperatures, the higher will be the oligomeric state, stability, compactness, SDS resistance, β-sheet content, and hydrophobic exposure of the resulting protein aggregates (Bagriantsev et al., 2006; Khare and Dokholyan, 2007; Uversky, 2008; Vendruscolo et al., 2011). With the advent of recombinant DNA technology, gene overexpression in bacteria became a central tool in biomedical and fundamental research as well as for industry (Ventura and Villaverde, 2006). Yet overexpression of recombinant polypeptides in bacteria produce inactive polypeptide species tightly compacted within insoluble inclusion bodies (IBs). Whereas IB formation can be a simple way to isolate large amounts of relatively pure recombinant polypeptides, subsequent steps to convert them into soluble functional proteins are often limiting. Thus, the effectiveness of iterative rounds of IB solubilization and unfolding by urea, guanidinium-HCl, and/or mild detergents, followed by refolding to the native state, typically by slow dialysis in the presence of osmolytes at low temperatures, determines whether initial IB formation is a favorable or a counterproductive prerequisite for the effective massive production of a given recombinant protein (Hagel et al., 1971; Vallejo and Rinas, 2004).

To obtain higher cellular amounts of recombinant proteins in their soluble, natively folded functional state, several parameters can be modified, which, however, generally correlate with a reduction in polypeptide production rates by bacteria. Thus, to reduce IB formation, the promoter strength can be decreased, the culture media impoverished, and the codon usage rarefied. The growth temperature can also be decreased and salts and osmolytes can be added to the medium to increase viscosity of the folding environment (Diamant et al., 2001; de Marco et al., 2007; Bandyopadhyay et al., 2012). Additionally, increasing the number of members of the chaperone network can improve the native folding of aggregation-prone recombinant proteins, either by plasmid-encoded chaperone genes, or by increasing the fluidity of the plasma membrane by chemical fluidizers, or naturally by heat shock, increasing the bacterial production of endogenous chaperones. Yet chaperone overexpression can reduce yields of the recombinant protein of interest, artificial fluidizers can be poisonous and impair protein synthesis, and heat shock can increase the propensity of a labile protein to misfold and aggregate rather than reach its native state (Worrall and Goss, 1989; Strandberg and Enfors, 1991; de Marco et al., 2005).

In the next section we discuss the various mechanisms by which chemical chaperones, foldases, and unfolding molecular chaperones can prevent IB formation in bacteria and convert *in vivo*, stable misfolded recombinant polypeptides into soluble active proteins.

2.2 CHEMICAL CHAPERONES

Osmolytes are naturally occurring small organic molecules, such as trehalose, glycerol, free proline, glycine betaine, trimethylamineN-oxide (TMAO) and trimethylglycine, which can be specifically absorbed by cells from the surroundings against a gradient of concentrations, or synthetized by cells in response to salt dehydration and/or osmotic stress (Diamant et al., 2001, 2003; Bandyopadhyay et al., 2012; De Los Rios and Goloubinoff, 2012). Osmolytes have been shown to inhibit *in vitro* protein aggregation during refolding of unfolded/misfolded proteins and can be considered as chemical chaperones standing first in line of the cellular defenses against stress-induced protein aggregation. Thus, the accumulation of osmolytes, such as free amino acids (proline in particular) and sugars in the cytoplasm, or their presence in molar amounts in the *in vitro* refolding buffer during dialysis, generally results in higher refolding yields of various recombinant proteins from urea-unfolded IBs (Yancey et al., 1982; de Marco et al., 2005). Arginine, glutamic acid, and proline are among the most commonly used folding aids to recover soluble proteins from IBs (Tsumoto et al., 2010; Wu et al., 2011). The present understanding of the mechanism of action of many osmolytes can be attributed to their presumed ability to destabilize unstructured segments in polypeptides, thereby shifting the free-energy balance in favor of protein conformers with a higher content of secondary structures (Cho et al., 2011). Moreover, depending on the amino acid composition of polypeptides, various osmolytes may be preferentially attracted to, or repulsed from, different unstructured segments of the polypeptide. Thus, TMAO may interact more strongly with α-helices than with β-structures (Cho et al., 2011). As misfolded proteins generally accumulate more misfolded β-structures at the expense of native α-helices, the presence of TMAO could favor the refolding of unfolded polypeptides into stable native structures and disfavor misfolded structures (De Los Rios and Goloubinoff, 2012). Osmolytes alone can act as buffers of protein evolution by stabilizing mutants with new functions that have not yet reached an optimal folding pathway to the native state (Bandyopadhyay et al., 2012). Osmolytes such as glycine betaine, glycerol, proline, alone or at best in combination with molecular chaperones (e.g., GroEL, DnaK, and ClpB), can assist the de novo folding of polypeptides and stabilization of the native end products of the folding reaction (Diamant et al., 2001; Tokuriki and Tawfik, 2009). Thus, whereas under nonstressed conditions, polypeptides emerging from the ribosome, especially short single-domain polypeptides, may not need particular assistance and readily follow the folding path dictated by their primary amino acid sequence and reach the native state. Yet when mutated or subject to external stress, they may, instead, misfold and aggregate (Figure 2.1, cycle I).

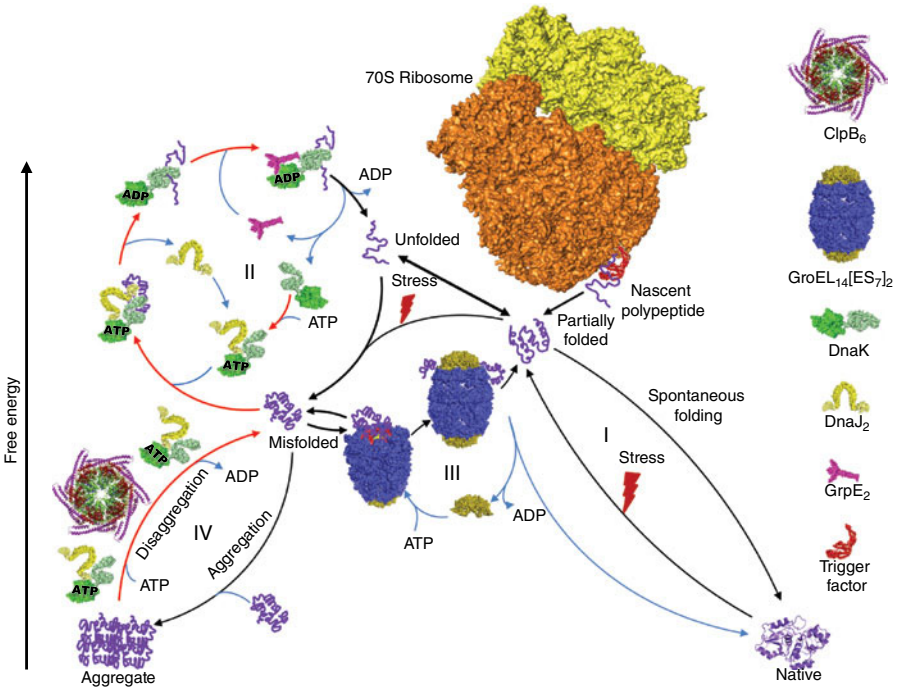

FIGURE 2.1 Schematic representation of the *E. coli* unfolding chaperone network promoting the native folding of aggregation-prone recombinant proteins. As nascent polypeptides (purple) emerge from the ribosome, the trigger factor, which is a PDI associated with the ribosome, assists in the sequential shaping of small native-like domains. Once released from the rhibosome and trigger factor, the partially folded proteins may reach the native state spontaneously, possibly assisted by chemical chaperones (cycle I). Yet, under stress or when mutated, they may instead misfold and become unfolded by the DnaK (KJE) system (cycle II), or by the GroEL/GroES chaperonin system (cycle III). In case the misfolded monomers escape unfolding by KJE or GroELS, they may form stable aggregates and IBs, but the KJE system can collaborate with ClpB to use the energy of ATP hydrolysis to unfold and solubilize individual polypeptides from the stable aggregates (cycle IV), thereby allowing them to reach their native state spontaneously. (*See insert for color representation of the figure*.)

2.3 PPIs AND PDIs ARE FOLDING ENZYMES

The native folding of some polypeptides may be limited by unfavorable distribution between *cis*- and *trans*-prolines and by the formation of the wrong disulfide bonds, requiring assistance of folding enzymes of peptidyl prolyl isomerases (PPIs) and protein disulfide isomerases (PDIs), respectively.

Native proteins have a strong bias in favor of *cis*-prolines, which may be lost in the unfolded state. Reacquisition of biased *cis*-prolines can be rate limiting for native folding and lead to aggregation (Brandts et al., 1977). Several classes of PPIases, such as cyclophilins, FK-506 binding proteins (FKBPs), and parvulins, can accelerate the *cis-trans* isomerization of prolines in refolding proteins and thus overcome rate-limiting steps in the folding pathway. Hence, the *Escherichia coli* trigger factor (TF), which is the first protein to interact with nascent chains exiting the ribosome (Deuerling and Bukau, 2004) (Figure 2.1), can catalyze prolyl-*cis-trans* isomerization of the nascent polypeptide while assisting in the sequential shaping of small protein domains (Stoller et al., 1995).

In the oxidative environment of the *endoplasmic reticulum* lumen, the cysteines of secreted proteins can wrongly associate with one another and lead to protein misfolding and aggregation. Thus, in his experiment with ribonuclease A, Anfinsen found that removing β-mercaptoethanol before removing the urea led to a dramatic decrease in the recovery of activity. This was attributed to the formation of random disulfide bridges between the eight cysteines present in the protein. Protein disulfide isomerases (PDIs) are folding enzymes, which, by virtue of their ability to disallow nonnative disulfide bonds can accelerate the formation of properly aligned disulfide bonds in native structures. However, because the bacterial cytoplasm is reduced and correspondingly less favorable to disulfide bonds than the *endoplasmic reticulum* lumen, the role of PDIs in the production of soluble recombinant proteins in the cytoplasm of bacteria is less relevant than for eukaryotes, where secreted proteins such as immunoglobins and pro-insulin need to be stabilized by properly aligned disulfide bonds.

2.4 MOLECULAR CHAPERONES

Behind the chemical chaperones and alongside the PPIs and PDIs foldases, the molecular chaperones form another line of active cellular defenses against stress- and mutation-induced protein misfolding and aggregation. Noticeably, although generally referred to misleadingly as being heat-shock proteins (Hsps), many molecular chaperones but not all are stress-inducible proteins. For example, of about 120 identified molecular chaperones, co-chaperones, and foldases that form the human genome, only a third are heat-induced (Finka et al., 2011). All molecular chaperones control cellular proteostasis by sharing the ability to screen the surfaces of potential misfolded or alternatively folded protein substrates, for nonnative structural elements, such as abnormal β-sheets associated with hydrophobic patches exposed to the aqueous phase (Hinault et al., 2006). They may act as passive

"holding" chaperones upon mere binding to misfolding polypeptide intermediates, thus preventing further aggregations, and/or as active polypeptide unfoldases, which upon hydrolyzing ATP can pull apart stable aggregates and open stable misfolded structures in misfolded polypeptides, thereby promoting spontaneous folding to the native state (Nollen et al., 1999; Sharma et al., 2009). In addition to their role under stress, heat shock in particular, molecular chaperones may also carry housekeeping cellular functions, such as controlling the assembly and activity of native protein complexes (Morgan et al., 2001; Weiss et al., 2007); targeting and importing proteins into organelles; and blocking or activating various receptors, signaling proteins, and transcription factors. Importantly, chaperones are also involved in the selection of proteins to be targeted for degradation (Muchowski and Wacker, 2005).

Most molecular chaperones can be classified within five canonical families on the basis of sequence homologies and have been named according to their approximate molecular mass on SDS gels (in kilodaltons): (1) the small Hsps (IbpA/B), (2) the HSP90s (HtpG), (3) the HSP70s (DnaK), (4) the HSP104s (ClpB), and (5) the chaperonins HSP60 (GroEL) (*E. coli* orthologs shown in parentheses).

2.5 THE SMALL Hsps

The small Hsps (sHsps) are a family of ubiquitous chaperones found in bacteria and most cellular compartments of plants, fungi, and animal cells. They share a conserved 80- to 100-amino acid α-crystallin domain. The small Hsps do not hydrolyze ATP. They include mammalian Hsp27 and α-crystallins; organellar Hsp23, Hsp17, and Hsp16; and bacterial IbpA/B (*E. coli*) and Hsp17 (*Synechocystis*). IbpA and IbpB were originally isolated from inclusion bodies formed during the overproduction of recombinant proteins in *E. coli* cells and accordingly named *inclusion body binding protein A/B*. IbpA/B can also coaggregate with endogenous *E. coli* proteins and stress-misfolded proteins (Laskowska et al., 1996, 2003). Deletion of the *ibpA/B* operon resulted in a twofold increase in aggregated proteins and a 10-fold decrease in cell viability under stress conditions (Kuczynska-Wisnik et al., 2002). Indicating a possible overlap with other chaperone functions, overexpression of IbpB can alleviate thermo-sensitive point mutations of GroEL (Veinger et al., 1998). The oligomeric state and chaperone-like activity of IbpB is temperature responsive: Heat shock decreases IbpB's oligomeric size while increasing its chaperone-like activity (Jiao et al., 2005). By virtue of their association with misfolded proteins in IBs, the two *E. coli* sHsps (IbpA/B) are pivotal to the possible solubilization of IBs, as they

can optimally present bound misfolded polypeptides to other unfolding chaperone systems, such as DnaK/DnaJ/GrpE and GroEL/GroES (Veinger et al., 1998) or to the disaggregating machinery ClpB-DnaK/DnaJ/GrpE (Mogk et al., 2003; Lethanh et al., 2005). In addition to preventing aggregation by passive binding, sHsps may also mediate the refolding of unfolded species to the native state (Lee and Vierling, 2000; Basha et al., 2004).

2.6 Hsp90

Hsp90s, named HtpG in bacteria and tumor necrosis factor receptor-associated protein (TRAP) in animal mitochondria, are among the most abundant proteins in human cells. They form dimers that can interact with a broad spectrum of misfolded, translocating, and native "client" proteins, particularly with polypeptides involved in signal transduction (Pearl and Prodromou, 2006). Structurally and mechanistically, it is not clear precisely where and how the various clients bind the Hsp90 dimers. The ATPase cycle is intimately coupled to the opening and closing of the dimer, which could act as a molecular clamp (Chadli et al., 2000; Prodromou et al., 2000), suggesting that Hsp90 may unfold its various misfolded or alternatively folded "clients," similar to other ATPase chaperones, (Walerych et al., 2010). Whereas eukaryotes require a functional cytoplasmic Hsp90 for viability (Borkovich et al., 1989; Versteeg et al., 1999), the *E. coli* HtpG knockout has no apparent phenotype. Thus, although HtpG is a highly conserved heat-inducible molecular chaperone, it is not a primary *E. coli* chaperone to improve the transitions between aggregated and native state in recombinant proteins.

2.7 Hsp70/Hsp40

The Hsp70 system, which in eubacteria is composed principally of DnaK and of its two co-chaperones DnaJ and GrpE, forms the central hub of the *E. coli* chaperone network (Hesterkamp and Bukau, 1998). Without ATP, DnaK and its co-chaperone DnaJ can prevent protein aggregation by mere passive "holding" of the labile proteins. Yet in the presence of DnaJ and ATP, prevention of aggregation by DnaK can be improved dramatically, suggesting an active process (Sharma et al., 2011). Moreover, the bacterial DnaK–DnaJ–GrpE (KJE) system can act as powerful polypeptide unfolding machinery that can catalytically unfold misfolded polypeptide monomers (Figure 2.1, cycle II) and disaggregate small soluble complexes of heat-denatured proteins (Diamant et al., 2000; Sharma et al., 2010). The mechanism by which the bacterial Hsp70 (KJE) system may facilitate substrate native

folding comprises five main steps: (1) DnaJ and low-affinity ATP-DnaK bind a high-affinity misfolded polypeptide substrate. This triggers ATP hydrolysis in DnaK and the dissociation of the J-domain of DnaJ; (2) the ADP-DnaK "locks" onto the misfolded substrate and, by doing so, unfolds the substrate; (3) Unfolding of the polypeptide causes DnaJ dissociation from it (Hinault, 2010); (4) GrpE drives the release of ADP from DnaK and the release of the unfolded intermediate from DnaK; (5) the released intermediate spontaneously refolds in solution into a low-affinity native product, or misfolds again and re-enters the chaperone cycle as a high affinity substrate (Sharma et al., 2010) (Figure 2.1, cycle II). When, despite the unfolding activity of KJE, misfolded polypeptide became entangled and packed within IBs, the bacterial KJE system can recruit the disaggregating co-chaperone ClpB (Diamant et al., 2000) (Figure 2.1, cycle IV), which is a member of the AAA+superfamily (ATPases associated with a variety of cellular activities). The KJE system can activate and recruit the ClpB hexameric rings to the polypeptide aggregates (Oguchi et al., 2012). Individual polypeptides become disentangled upon being partially threaded in an ATP-dependent manner through the central channel of the ClpB hexameric ring (Haslberger et al., 2008) This may lead to dissociation of individual misfolded polypeptides from the aggregates, whose final refolding to the native state may, further, need partial unfolding by the KJE system (Goloubinoff et al., 1999) (Figure 2.1, cycle IV).

By virtue of its strong ATP-fueled unfolding and disaggregating activities, the KJE system is the most important chaperone machinery to maintain overexpressed recombinant proteins in a soluble form in *E. coli* cells and *in vitro*. It may also act in concert with other chaperones, such as GroEL, either upstream, by conditioning misfolded monomers to be fed to the GroEL cavity (Langer et al., 1992; Veinger et al., 1998), or downstream, by processing GroEL-released inactive species into natively refoldable species (Buchberger et al., 1996) (Figure 2.1, cycle III).

2.8 GroEL CHAPERONINS

GroEL is a complex of 14 identical 57-kDa subunits arranged as two back-to-back heptameric rings with two noncommunicating open cavities. The distal surfaces of the GroEL cavities exposed hydrophobic residues that nonnative polypeptide substrates can access from the external solution (Braig et al., 1994). GroES is a seven-membered ring of 10-kDa subunits that can cap one or both open ends of the GroEL cavities. The cage-like structure of GroEL is thought to mediate its chaperone activity (Horwich, 2011). Upon transiently sequestering stress-denatured or newly synthesized polypeptides in the cavity under GroES caps, GroEL is thought to prevent deleterious misfolding and

aggregation events during the folding process (Figure 2.1, cycle III). Increased expression of both GroEL and GroES on a high-copy-number plasmid has been shown to increase the solubility and activity of recombinant cyanobacterial RubisCO (Goloubinoff et al., 1989). Moreover, co-expression on the same plasmid of up to four different complementing chaperone systems—IbpA/B, DnaK/DnaJ/GrpE, ClpB, and GroEL/GroES—can produce very high yields of soluble, natively folded recombinant proteins (de Marco et al., 2007).

2.9 CONCLUSIONS

A detailed understanding of the mechanisms by which chemical chaperones, folding enzymes, and various molecular chaperones can collaborate to prevent and actively revert misfolding and aggregation events in the cell is necessary for the successful massive production of soluble native recombinant proteins in bacteria. This can be achieved by reducing the synthesis rate, and thus the burden on the protein quality-control network, as well as by increasing the concentrations of chemical and protein chaperones in the cytoplasm. In addition to the advantages for biotechnology, finding new ways to increase the cellular levels of various molecular chaperones, particularly in animal cells, holds biomedical promises to find cures to protein-conformational diseases.

REFERENCES

Anfinsen, CB (1973) Principles that govern the folding of protein chains. Science 181:223–230.

Bagriantsev SN, Kushnirov VV, Liebman SW (2006) Analysis of amyloid aggregates using agarose gel electrophoresis. Methods Enzymol 412:33–48.

Bandyopadhyay A, Saxena K, Kasturia N, Dalal V, Bhatt N, Rajkumar A, Maity S, Sengupta S, Chakraborty, K (2012) Chemical chaperones assist intracellular folding to buffer mutational variations. Nat Chem Biol 8:238–245.

Basha E, Lee GJ, Demeler B, Vierling E (2004) Chaperone activity of cytosolic small heat shock proteins from wheat. Eur J Biochem 271:1426–1436.

Borkovich KA, Farrelly FW, Finkelstein DB, Taulien J, Lindquist S (1989) hsp82 is an essential protein that is required in higher concentrations for growth of cells at higher temperatures. Mol Cell Biol 9:3919–3930.

Braig K, Otwinowski Z, Hegde R, Boisvert DC, Joachimiak A, Horwich AL, Sigler PB (1994) The crystal structure of the bacterial chaperonin GroEL at 2.8 Å. Nature 371:578–586.

Brandts JF, Brennan M, Lung-Nan L (1977) Unfolding and refolding occur much faster for a proline-free proteins than for most proline-containing proteins. Proc Natl Acad Sci U S A 74:4178–4181.

Buchberger A, Schroder H, Hesterkamp T, Schonfeld HJ, Bukau B (1996) Substrate shuttling between the DnaK and GroEL systems indicates a chaperone network promoting protein folding. J Mol Biol 261:328–333.

Chadli A, Bouhouche I, Sullivan W, Stensgard B, McMahon N, Catelli MG, Toft DO (2000) Dimerization and N-terminal domain proximity underlie the function of the molecular chaperone heat shock protein 90. Proc Natl Acad Sci U S A 97:12524–12529.

Cho SS, Reddy G, Straub JE, Thirumalai D (2011) Entropic stabilization of proteins by TMAO. J Phys Chem B 115:13401–13407.

De Los Rios P, Goloubinoff P (2012). Protein folding: chaperoning protein evolution. Nat Chem Biol 8:226–228.

de Marco A, Vigh L, Diamant S, Goloubinoff P (2005) Native folding of aggregation-prone recombinant proteins in *Escherichia coli* by osmolytes, plasmid- or benzyl alcohol-overexpressed molecular chaperones. Cell Stress Chaperones 10:329–339.

de Marco A, Deuerling E, Mogk A, Tomoyasu T, Bukau B (2007) Chaperone-based procedure to increase yields of soluble recombinant proteins produced in *E. coli*. BMC Biotechnol 7:32.

Deuerling E, Bukau B (2004) Chaperone-assisted folding of newly synthesized proteins in the cytosol. Crit Rev Biochem Mol Biol 39:261–277.

Diamant S, Ben-Zvi AP, Bukau B, Goloubinoff P (2000) Size-dependent disaggregation of stable protein aggregates by the DnaK chaperone machinery. J Biol Chem 275:21107–21113.

Diamant S, Eliahu N, Rosenthal D, Goloubinoff P. (2001) Chemical chaperones regulate molecular chaperones in vitro and in cells under combined salt and heat stresses. J Biol Chem 276:39586–39591.

Diamant S, Rosenthal D, Azem A, Eliahu N, Ben-Zvi AP, Goloubinoff P (2003) Dicarboxylic amino acids and glycine-betaine regulate chaperone-mediated protein-disaggregation under stress. Mol Microbiol 49:401–410.

Finka A, Mattoo RU, Goloubinoff P (2011) Meta-analysis of heat- and chemically upregulated chaperone genes in plant and human cells. Cell Stress Chaperones 16:15–31.

Goloubinoff P, Gatenby AA, Lorimer GH (1989) GroE heat-shock proteins promote assembly of foreign prokaryotic ribulose bisphosphate carboxylase oligomers in *Escherichia coli*. Nature 337:44–47.

Goloubinoff P, Mogk A, Zvi AP, Tomoyasu T, Bukau B (1999) Sequential mechanism of solubilization and refolding of stable protein aggregates by a bichaperone network. Proc Natl Acad Sci U S A 96:13732–13737.

Hagel P, Gerding JJ, Fieggen W, Bloemendal H (1971) Cyanate formation in solutions of urea: I. Calculation of cyanate concentrations at different temperature and pH. Biochim Biophys Acta 243:366–373.

Haslberger T, Zdanowicz A, Brand I, Kirstein J, Turgay K, Mogk A, Bukau B (2008) Protein disaggregation by the AAA+chaperone ClpB involves partial threading of looped polypeptide segments. Nat Struct Mol Biol 15:641–650.

Hesterkamp T, Bukau B (1998) Role of the DnaK and HscA homologs of Hsp70 chaperones in protein folding in *E. coli*. EMBO J 17:4818–4828.

Hinault MP, Ben-Zvi A, Goloubinoff P (2006) Chaperones and proteases: cellular fold-controlling factors of proteins in neurodegenerative diseases and aging. J Mol Neurosci 30:249–265.

Hinault MP, Cuendet AF, Mattoo RU, Mensi M, Dietler G, Lashuel HA, Goloubinoff P (2010) Stable alpha-synuclein oligomers strongly inhibit chaperone activity of the Hsp70 system by weak interactions with J-domain co-chaperones. J Biol Chem 285: 38173–38182.

Horwich AL (2011). Protein folding in the cell: an inside story. Nat Med 17:1211–1216.

Jiao W, Qian M, Li P, Zhao L, Chang Z (2005) The essential role of the flexible termini in the temperature-responsiveness of the oligomeric state and chaperone-like activity for the polydisperse small heat shock protein IbpB from *Escherichia coli*. J Mol Biol 347:871–884.

Khare SD, Dokholyan NV (2007) Molecular mechanisms of polypeptide aggregation in human diseases. Curr Protein Pept Sci 8:573–579.

Kuczynska-Wisnik D, Kedzierska S, Matuszewska E, Lund P, Taylor A, Lipinska B, Laskowska E (2002) The *Escherichia coli* small heat-shock proteins IbpA and IbpB prevent the aggregation of endogenous proteins denatured in vivo during extreme heat shock. Microbiology 148:1757–1765.

Langer T, Lu C, Echols H, Flanagan J, Hayer MK, Hartl FU (1992) Successive action of DnaK, DnaJ and GroEL along the pathway of chaperone-mediated protein folding. Nature 356:683–689.

Laskowska E, Wawrzynow A, Taylor A (1996) IbpA and IbpB, the new heat-shock proteins, bind to endogenous *Escherichia coli* proteins aggregated intracellularly by heat shock. Biochimie 78:117–122.

Laskowska E, Kuczynska-Wisnik D, Bak M, Lipinska B (2003) Trimethoprim induces heat shock proteins and protein aggregation in *E. coli* cells. Curr Microbiol 47:286–289.

Lee GJ, Vierling E (2000) A small heat shock protein cooperates with heat shock protein 70 systems to reactivate a heat-denatured protein. Plant Physiol 122:189–198.

Lethanh H, Neubauer P, Hoffmann F (2005) The small heat-shock proteins IbpA and IbpB reduce the stress load of recombinant *Escherichia coli* and delay degradation of inclusion bodies. Microb Cell Fact 4:6.

Mogk A, Deuerling E, Vorderwulbecke S, Vierling E, Bukau B (2003) Small heat shock proteins, ClpB and the DnaK system form a functional triade in reversing protein aggregation. Mol Microbiol 50:585–595.

Morgan JR, Prasad K, Jin S, Augustine GJ, Lafer EM (2001) Uncoating of clathrin-coated vesicles in presynaptic terminals: roles for Hsc70 and auxilin. Neuron 32:289–300.

Muchowski PJ, Wacker JL (2005) Modulation of neurodegeneration by molecular chaperones. Nat Rev Neurosci 6:11–22.

Nollen EA, Brunsting JF, Roelofsen H, Weber LA, Kampinga HH (1999) In vivo chaperone activity of heat shock protein 70 and thermotolerance. Mol Cell Biol 19:2069–2079.

Oguchi Y, Kummer E, Seyffer F, Berynskyy M, Anstett B, Zahn R, Wade RC, Mogk A, Bukau B (2012) A tightly regulated molecular toggle controls AAA+disaggregase. Nat Struct Mol Biol.

Pearl LH, Prodromou C (2006) Structure and mechanism of the Hsp90 molecular chaperone machinery. Annu Rev Biochem 75:271–294.

Prodromou C, Panaretou B, Chohan S, Siligardi G, O'Brien R, Ladbury JE, Roe SM, Piper PW, Pearl LH (2000) The ATPase cycle of Hsp90 drives a molecular 'clamp' via transient dimerization of the N-terminal domains. EMBO J 19:4383–4392.

Sharma SK, Christen P, Goloubinoff P (2009) Disaggregating chaperones: an unfolding story. Curr Protein Pept Sci 10:432–446.

Sharma SK, De Los Rios P, Christen P, Lustig A, Goloubinoff P (2010) The kinetic parameters and energy cost of the Hsp70 chaperone as a polypeptide unfoldase. Nat Chem Biol 6:914–920.

Sharma SK, De Los Rios P, Goloubinoff P (2011) Probing the different chaperone activities of the bacterial HSP70–HSP40 system using a thermolabile luciferase substrate. Proteins 79:1991–1998.

Stoller G, Rucknagel KP, Nierhaus KH, Schmid FX, Fischer G, Rahfeld JU (1995) A ribosome-associated peptidyl-prolyl *cis*/*trans* isomerase identified as the trigger factor. EMBO J 14:4939–4948.

Strandberg L, Enfors SO (1991) Factors influencing inclusion body formation in the production of a fused protein in *Escherichia coli*. Appl Environ Microbiol 57:1669–1674.

Tokuriki N, Tawfik DS (2009) Chaperonin overexpression promotes genetic variation and enzyme evolution. Nature 459:668–673.

Tsumoto K, Abe R, Ejima D, Arakawa T (2010) Non-denaturing solubilization of inclusion bodies. Curr Pharm Biotechnol 11:309–312.

Uversky VN (2008) Amyloidogenesis of natively unfolded proteins. Curr Alzheimer Res 5:260–287.

Vallejo LF, Rinas U (2004) Strategies for the recovery of active proteins through refolding of bacterial inclusion body proteins. Microb Cell Fact 3:11.

Veinger L, Diamant S, Buchner J, Goloubinoff P (1998) The small heat-shock protein IbpB from *Escherichia coli* stabilizes stress-denatured proteins for subsequent refolding by a multichaperone network. J Biol Chem 273:11032–11037.

Vendruscolo M, Knowles TP, Dobson CM (2011) Protein solubility and protein homeostasis: a generic view of protein misfolding disorders. Cold Spring Harbor Perspect Biol 3.

Ventura S, Villaverde A (2006) Protein quality in bacterial inclusion bodies. Trends Biotechnol 24:179–185.

Versteeg S, Mogk A, Schumann W (1999) The *Bacillus subtilis* htpG gene is not involved in thermal stress management. Mol Gen Genet 261:582–588.

Walerych D, Gutkowska M, Klejman MP, Wawrzynow B, Tracz Z, Wiech M, Zylicz M, Zylicz A (2010) ATP binding to Hsp90 is sufficient for effective chaperoning of p53 protein. J Biol Chem 285:32020–32028.

Weiss YG, Bromberg Z, Raj N, Raphael J, Goloubinoff P, Ben-Neriah Y, Deutschman CS (2007) Enhanced heat shock protein 70 expression alters proteasomal degradation of IkappaB kinase in experimental acute respiratory distress syndrome. Crit Care Med 35:2128–2138.

Worrall DM, Goss NH (1989) The formation of biologically active beta-galactosidase inclusion bodies in *Escherichia coli*. Aust J Biotechnol 3:28–32.

Wu B, Nemeth JF, Janecki DJ, Jones B, Obmolova G, Malia TJ, Baker A, Bethea D, Elloso MM, Naso M, et al. (2011) Expression, refolding and purification of a human interleukin-17A variant. Cytokine 53:107–114.

Yancey PH, Clark ME, Hand SC, Bowlus RD, Somero GN (1982) Living with water stress: evolution of osmolyte systems. Science 217:1214–1222.

CHAPTER 2

Biophysical characterization of two different stable misfolded monomeric polypeptides that are chaperone-amenable substrates

Biophysical characterization of two different stable misfolded monomeric polypeptides that are chaperone-amenable substrates.

Natalello, A.*, Mattoo, R.U.*, Priya, S., Sharma, S.K., Goloubinoff, P. and Doglia, S.M.

**Authors contributed equally to this work*

I contributed to this work conceptually and in the manuscript writing.
I contributed with Dr. Natalello in the data acquisition for the Fig 4 (a-f), Fig. 6 (a-d) and provided the data for Fig 5(a-d), supplementary Fig S1 and Table 1.
Dr. Priya and Dr. Sharma contributed by providing the data for Fig. 1(a-c), Fig. 2(a-d) and Fig. 3 (a and b).

jmb Article

Biophysical Characterization of Two Different Stable Misfolded Monomeric Polypeptides That Are Chaperone-Amenable Substrates

Antonino Natalello[1,2]†, Rayees U. H. Mattoo[3]†, Smriti Priya[3], Sandeep K. Sharma[3], Pierre Goloubinoff[3] and Silvia M. Doglia[1,2,4]

*1 - **Department of Biotechnology and Biosciences,** University of Milano-Bicocca, Piazza della Scienza 2, 20126 Milan, Italy*
*2 - **Consorzio Nazionale Interuniversitario per le Scienze Fisiche della Materia (CNISM),** UdR Milano-Bicocca, Milan, Italy*
*3 - **Department of Plant Molecular Biology,** Faculty of Biology and Medicine, University of Lausanne, 1015 Lausanne, Switzerland*
*4 - **Department of Physics,** University of Milano-Bicocca, Piazza della Scienza 3, 20126 Milan, Italy*

Correspondence to Pierre Goloubinoff and Silvia M. Doglia: *Pierre.Goloubinoff@unil.ch; silviamaria.doglia@unimib.it*
http://dx.doi.org/10.1016/j.jmb.2012.12.025
Edited by J. Buchner

Abstract

Misfolded polypeptide monomers may be regarded as the initial species of many protein aggregation pathways, which could accordingly serve as primary targets for molecular chaperones. It is therefore of paramount importance to study the cellular mechanisms that can prevent misfolded monomers from entering the toxic aggregation pathway and moreover rehabilitate them into active proteins. Here, we produced two stable misfolded monomers of luciferase and rhodanese, which we found to be differently processed by the Hsp70 chaperone machinery and whose conformational properties were investigated by biophysical approaches. In spite of their monomeric nature, they displayed enhanced thioflavin T fluorescence, non-native β-sheets, and tertiary structures with surface-accessible hydrophobic patches, but differed in their conformational stability and aggregation propensity. Interestingly, minor structural differences between the two misfolded species could account for their markedly different behavior in chaperone-mediated unfolding/refolding assays. Indeed, only a single DnaK molecule was sufficient to unfold by direct clamping a misfolded luciferase monomer, while, by contrast, several DnaK molecules were necessary to unfold the more resistant misfolded rhodanese monomer by a combination of direct clamping and cooperative entropic pulling.

Introduction

Anfinsen demonstrated that the sole primary sequence of a polypeptide can dictate the three-dimensional structure of its native state.[1] However, under non-physiological and stressful conditions, mutant and labile proteins can misfold and assemble into oligomers and higher-molecular-weight aggregates, with various degrees of toxicity to cells, leading to degenerative tissue loss. Protein misfolding is the central cause for a number of pathological conditions, generally referred to as protein conformational diseases, associated with the formation of highly organized protein aggregates, as in the case of diabetes type 2, amyotrophic lateral sclerosis, cystic fibrosis, and a rising number of neurodegenerative diseases, such as Alzheimer, prion, and Parkinson diseases.[2–5] There is increasing evidence that cytotoxicity correlates with the more soluble misfolded protein conformers with a high surface-to-volume ratio. Presenting abnormally exposed hydrophobic surfaces, the misfolded conformers likely cause toxicity by partaking in aberrant interactions with the hydrophobic components of the cell, primarily cellular membranes and other hydrophobically exposed misfolded proteins that can co-aggregate and seed other amyloidogenic species into fibrils, tangles, amyloids, and even infectious prions.[6–10] In contrast, the later species in the misfolding pathway, such as large amyloid fibrils, tangles, and other insoluble aggregates, although still associated to a certain degree of toxicity,[11] are generally considered less harmful than the more soluble species. The active compaction in cells of

the soluble misfolded protein species by the aggresome thus appears to be a costly, yet effective mechanism to detoxify protein aggregates.[12–14]

Whereas oligomers and end products of the aggregation pathway have been widely characterized by various biochemical and biophysical means,[2,7,10,15] little is known about the structural properties of full-length misfolded monomeric polypeptides[16] at the state where they waver between reverting to the native state or further proceeding into the aggregation pathway. This knowledge is of great importance to the understanding of how proteotoxic species develop in protein conformational diseases and more efforts are required to identify the initial events that lead to the formation of early species, misfolded monomers in particular.

Molecular chaperones are key components of the cell that can counteract and actively revert potentially toxic misfolded polypeptides into non-toxic active species and reorient them from the aggregation pathway onto the native refolding pathway.[4,17] Recently, a stable misfolded full-length 63 kDa monomeric luciferase species [freezing-thawing luciferase (FT-Luc)] has been isolated, which tends to neither spontaneously refold to the native state nor aggregate within the experimental time frame.[18] Thus, although monomeric, FT-Luc is a stringent chaperone substrate,[19] whose unique ability to stay un-aggregated was used to demonstrate that chaperones do not need to act as mere anti-aggregation devices but also use ATP to catalytically unfold stable misfolded polypeptide substrates into natively refoldable products. Hence, in the presence of substoichiometric amounts of DnaK, and of its co-chaperones DnaJ and GrpE (KJE), the misfolded FT-Luc can become transiently unfolded in a strict ATP-dependent manner. Subsequent to GrpE-accelerated ADP and luciferase release, the unfolded luciferase polypeptide spontaneously refolds into the native state with a very high efficiency.[18] Therefore, DnaK acts as a catalytic ATP-dependent polypeptide unfoldase enzyme, capable, together with DnaJ, to recognize and iteratively bind misfolded luciferase monomers, unfold, and subsequently release them in a sufficiently unfolded state, allowing them to thereafter spontaneously refold to the native state. When polypeptides are more severely damaged, as in the case of the small soluble aggregates of heat-denatured glucose-6-phosphate dehydrogenase (G6PDH),[20] the clamping of a single DnaK molecule is not sufficient to cause productive unfolding. In this case, several DnaKs need to become concomitantly clamped onto the same misfolded polypeptide, to exert a fruitful cooperative unfolding force on in-between misfolded segments, in a mechanism called entropic pulling.[21]

The unfoldase activity of the Hsp70 chaperones thus provides cells with a unique mechanism to actively counteract protein aggregation by neutralizing early species such as misfolded monomers and small oligomers on the misfolding pathway, before they can reach critical concentrations to aggregate into more toxic species. The energy cost to unfold early misfolded monomers was estimated to be a thousand fold less than for heavily aggregated species to be first degraded by ATP-consuming proteases and then resynthesized into new functional polypeptides.[18]

Because it is essential to understand the mechanisms by which the cellular machinery can prevent misfolded monomeric species from entering the aggregation pathway, we investigated here the conformational properties of two stable full-length misfolded monomeric polypeptides generated by iterative cycle of freeze–thawing, a misfolded 63-kDa luciferase monomer (FT-Luc)[18] and a stable misfolded 33-kDa rhodanese monomer [freezing-thawing rhodanese (FT-Rho)]. We characterize here FT-Rho for the first time and show it to be a stringent amenable substrate to the Hsp70 chaperone machinery. In particular, we examined through various complementary biophysical approaches the structural differences between the two misfolded monomeric species. Compared with their native conformers, the FT-Rho and FT-Luc displayed a similar gel-filtration profile typical of globular monomers with, however, appreciably increased exposure of hydrophobic patches. Although both misfolded monomeric species contained a similar amount of non-native intramolecular β-sheets and tertiary structures, they markedly differed in terms of their intrinsic stability in urea and aggregation propensity under heat stress. Interestingly, in correlation with the markedly higher stability in urea of FT-Rho, compared to FT-Luc, we found that FT-Rho was also more resistant to chaperone-mediated unfolding than FT-Luc. Unlike FT-Luc, FT-Rho could be refolded only by a large molar excess of DnaK necessary to unfold very resistant misfolded species by cooperative entropic pulling, highlighting that minor structural differences can be relevant to the chaperone specificity and unfolding/refolding efficacy.

Results

Production of the misfolded monomers

We have reported earlier that consecutive cycles of rapid freezing-thawing can generate, in phosphate buffer, a high proportion of stable misfolded monomers of diluted solutions (less than 3 μM) of *Photinus pyralis* luciferase (Luc) variant.[18] This misfolded monomer (FT-Luc) was found to bind 1.8 times more thioflavin T (ThT) than the native luciferase (Nat-Luc). As it did not significantly refold

to the native state without chaperones and ATP, FT-Luc was a stringent substrate of the bacterial chaperone unfoldase system KJE.[18] We developed here a similar protocol to generate and purify a seemingly uniform population of metastable misfolded monomeric rhodanese (FT-Rho) species that, similarly to FT-Luc, was inclined to neither spontaneously aggregate nor significantly convert into the native state within the experimental time frame of our *in vitro* chaperone assays and biophysical measurements. Figure 1a shows that following 10 successive cycles of freezing at −160 °C and slow (45 min) thawing to 4 °C, the native rhodanese (Nat-Rho) became stably inactive up to 93%. After centrifugation (12,000*g*, 10 min) that removed about 40–45% of the protein in the form of insoluble aggregates, gel filtration showed that most of the remaining soluble FT-Rho eluted as inactive monomers (Fig. 1b). Although non-globular misshaped elongated proteins may elute sooner on gel filtration and be mistaken for larger proteins, it is not known that oligomeric proteins abnormally elute later, precisely where monomers do. Similar to native, but unlike heat-denatured rhodanese (HD-Rho), FT-Rho did not scatter light (Fig. 1c). Limited cross-linking confirmed its monomeric nature (Fig. S1). Indeed, whereas treatment with 0.012% glutaraldehyde (GA) fully cross-linked HD-Rho aggregates, as evidenced by their inability to enter and migrate in the SDS gel, GA-treated Nat-Rho and FT-Rho entered the gel and resolved as SDS-soluble monomers (Fig. S1). Thus, as previously demonstrated by analytical ultracentrifugation in the case of FT-Luc,[18] both FT-Rho and FT-Luc are inactive metastable species that are mostly monomeric.

Fluorescence spectroscopy showed that FT-Rho bound 3.5 times more ThT than the native protein (Fig. 1c), as already found in the case of FT-Luc that displayed a 1.8-fold increase in ThT fluorescence, compared to Nat-Luc.[18] Lengthy incubations of FT-Rho in buffer (i.e., without chaperones) at 22 °C showed a very low rate of spontaneous refolding of about 3% in the first hour (Fig. 2b), reaching ~12% after 18 h (data not shown). Therefore, we generated here a second example of a metastable inactive misfolded monomeric species, whose chaperone

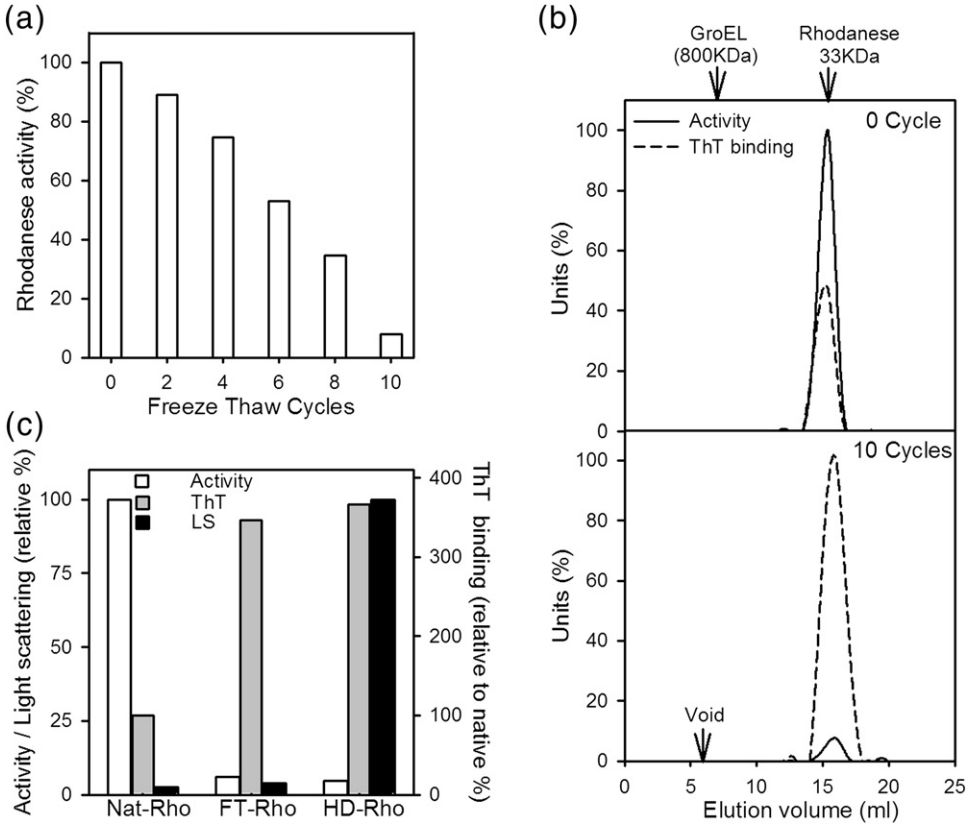

Fig. 1. Nat-Rho can be inactivated by freeze–thawing and isolated as stable misfolded monomers. (a) Rhodanese activity before and after successive rounds of rapid freezing-thawing for 45 min at 4 °C. (b) Gel-filtration elution profile of enzymatic activity and ThT binding of Nat-Rho (upper) and FT-Rho (lower panel). Arrows show the elution volume of the void volume, of the 800-kDa GroEL14 oligomers, and of the 33-kDa Nat-Rho monomers. (c) Relative enzymatic activity (empty bars) and levels of ThT binding (gray bars) and of light scattering (black bars) of Nat-Rho, FT-Rho, and HD-Rho.

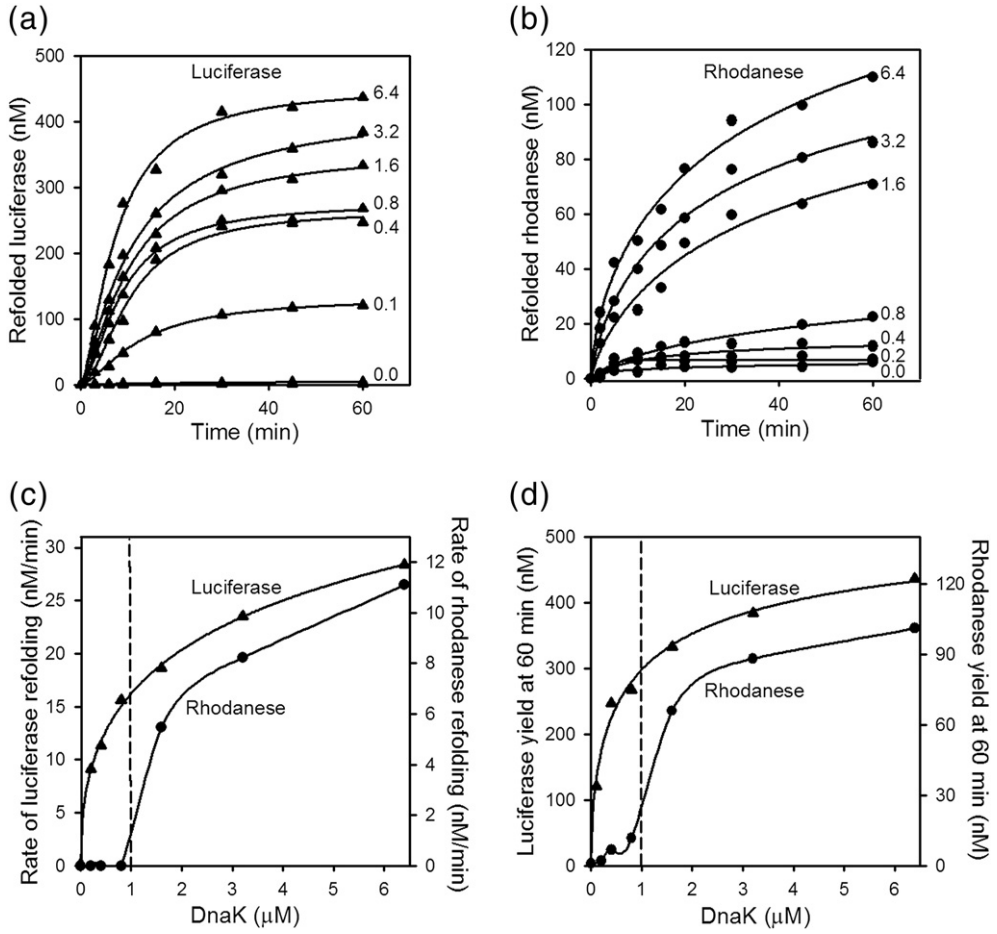

Fig. 2. Stable misfolded FT-Luc and FT-Rho monomers are refolded to the native state by the bacterial DnaKJE chaperone system in a strict ATP-dependent manner. (a and b) Time-dependent refolding to the native state of 1 μM FT-Luc (a) and 1 μM FT-Rho (b) in the presence of increasing DnaK concentrations (from 0 up to 6.4 μM, as indicated) and of a constant concentration of 0.5 μM DnaJ, 0.7 μM GrpE, and 5 mM ATP. Refolding at 22 °C was evaluated from the recovered enzymatic activity. (c and d) Initial rates (c) and yields of refolding after 60 min (d), evaluated from the data reported in (a) and (b), are shown as a function of the DnaK concentration. Broken lines indicate the equimolar concentration of DnaK and substrate.

amenabilities and biophysical properties could be further analyzed.

Both stable misfolded luciferase and rhodanese monomers are chaperone substrates

FT-Luc has been previously shown to be a stable misfolded monomeric species that behaved as a stringent substrate of the KJE chaperone unfoldase system, where ATP hydrolysis fueled substrate unfolding, whereas subsequent native refolding occurred spontaneously.[18] We therefore next tested the ability of FT-Rho to be converted into Nat-Rho by the ATP-fueled KJE chaperone system, as compared to FT-Luc (Fig. 2a and b). FT-Rho was found to behave as a specific, stringent ATP-dependent KJE substrate (Fig. 2b), albeit it refolded to the native state at lower rates than FT-Luc. Thus, in the presence of 1.6 μM DnaK, FT-Rho was refolded three times more slowly than FT-Luc and the yields were 3.5 lower, a difference that dramatically increased when DnaK was equimolar or substoichiometric to the substrate (Fig. 2c and d). As expected, the ATP cost of the unfolding/refolding reaction was also different. The addition of 1 μM FT-Rho doubled the rates of ATP hydrolysis by 6.4 μM DnaK (0.5 μM DnaJ, 0.7 μM GrpE), while Nat-Rho had no significant effect (Table S1), confirming that FT-Rho is a substrate that strongly interacts with DnaK and that Nat-Rho is a low-affinity product of the chaperone reaction. Yet, as expected from the slow rate of FT-Rho refolding, the apparent ATP cost of the unfolding/refolding reaction by DnaK was high. Indeed, a 6.4-fold molar excess of DnaK over the FT-Rho substrate reactivated a single Rho polypeptide, at the approximate net cost of 850 ATPs (Table S1). Similarly high ATP costs have been observed with urea heat-denatured G6PDH,[20] in contrast with

the low net cost of 5 ATPs for substoichiometric amounts of DnaK to refold FT-Luc molecule.[18] Although slow and energy consuming, 6.4 μM DnaK specifically accelerated the rate of spontaneous FT-Rho refolding by 100-fold, qualifying FT-Rho as a stringent chaperone substrate. Moreover, the chaperone reaction was not inhibited by the presence of up to a 16-fold molar excess of native malate dehydrogenase, or native G6PDH (Fig. S2), both of which are typical native products of KJE-mediated refolding reactions.[20,22] Thus, FT-Rho is a *bona fide* chaperone substrate because it does not significantly refold to the native state without chaperones and because DnaK can identify it as a high-affinity substrate, in contrast to low-affinity native products of the chaperone reaction.

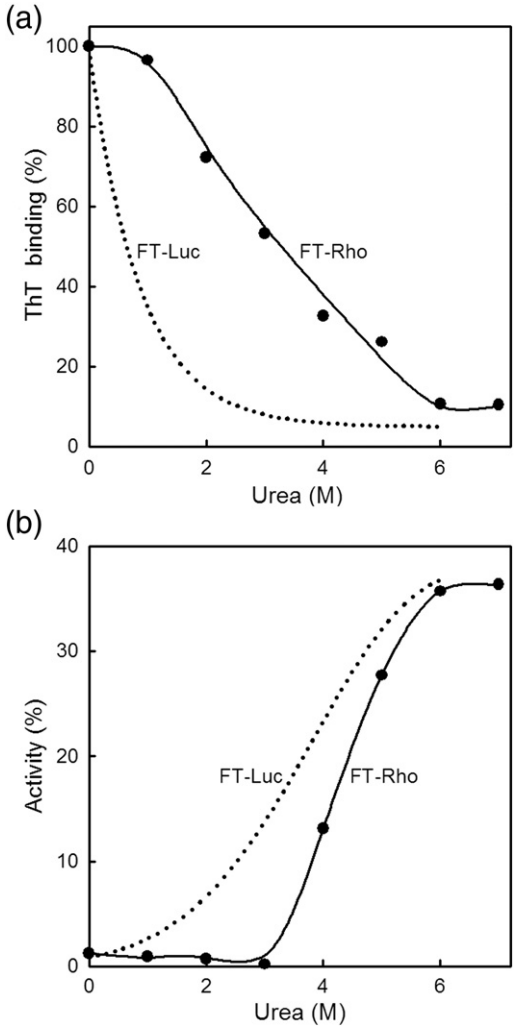

Fig. 3. FT-Rho is more stable than FT-Luc. Stable inactive FT-Rho (continuous line) and FT-Luc (dotted line) were incubated for 1 h at 25 °C in the presence of increasing concentrations of urea and of 60 μM ThT. (a) ThT fluorescence was measured and normalized to the signal without urea, with (100% intensity) and without (0% intensity) proteins. (b) The samples from (a) were then diluted in refolding buffer, and after 3 h at 25 °C, the recovered rhodanese or luciferase activities were measured. The reported FT-Rho results are representative of three independent experiments. The FT-Luc data were taken from a previous work[18] and shown here for comparison.

FT-Rho is more stable than FT-Luc

To address the reasons for the difference of chaperone amenability between the two species, we next measured their steady-state ThT fluorescence in the presence of increasing urea concentrations. Remarkably, FT-Luc lost half of its misfolded ThT-binding structures in the presence of as little as 0.7 M urea, as compared to 3.3 M urea in the case of FT-Rho (Fig. 3a). Similarly, following dilution of the urea-treated samples, half-maximal yields of spontaneously refolded species were obtained with FT-Luc pretreated with 3.6 M urea, as compared to 4.3 M in the case of FT-Rho (Fig. 3b). Together, this shows that FT-Rho is a much more stable misfolded species than FT-Luc. Indeed, FT-Rho needed higher concentrations of urea, or of unfolding chaperones, to become sufficiently unfolded to thereafter regain its ability to spontaneously refold to the native state.

We next used various complementary biophysical techniques to characterize the two stable misfolded monomers, in an attempt to find the structural differences accounting for their different degrees of chaperone amenabilities.

Misfolded monomers contain non-native β-sheet structures

The secondary structures of native and FT luciferase and rhodanese were first analyzed by Fourier transform infrared (FTIR) spectroscopy and CD. In Fig. 4a and b, the infrared (IR) absorption spectra of native proteins were reported in the amide I region, where the stretching vibrations of the CO peptide bonds occur. This band is particularly sensitive to the protein secondary structures and to the presence of intermolecular β-sheets, diagnostic of protein aggregation. To extract this structural information from the IR absorption spectrum, its second derivative can be performed, since the minima in this derivative spectrum corresponds to the maxima of the band absorption, becoming in this way more resolved.[23–25]

The second-derivative spectrum of Nat-Luc (Fig. 4c) displayed well-resolved components, which could be assigned to the protein secondary structures. The ~1639 cm^{-1} component and the shoulder at ~1688 cm^{-1} could be assigned to intramolecular β-sheets; the ~1657 cm^{-1}, to α-helices and random coil; and the ~1681 cm^{-1}, to β-turns. Also, the second-derivative spectrum of Nat-

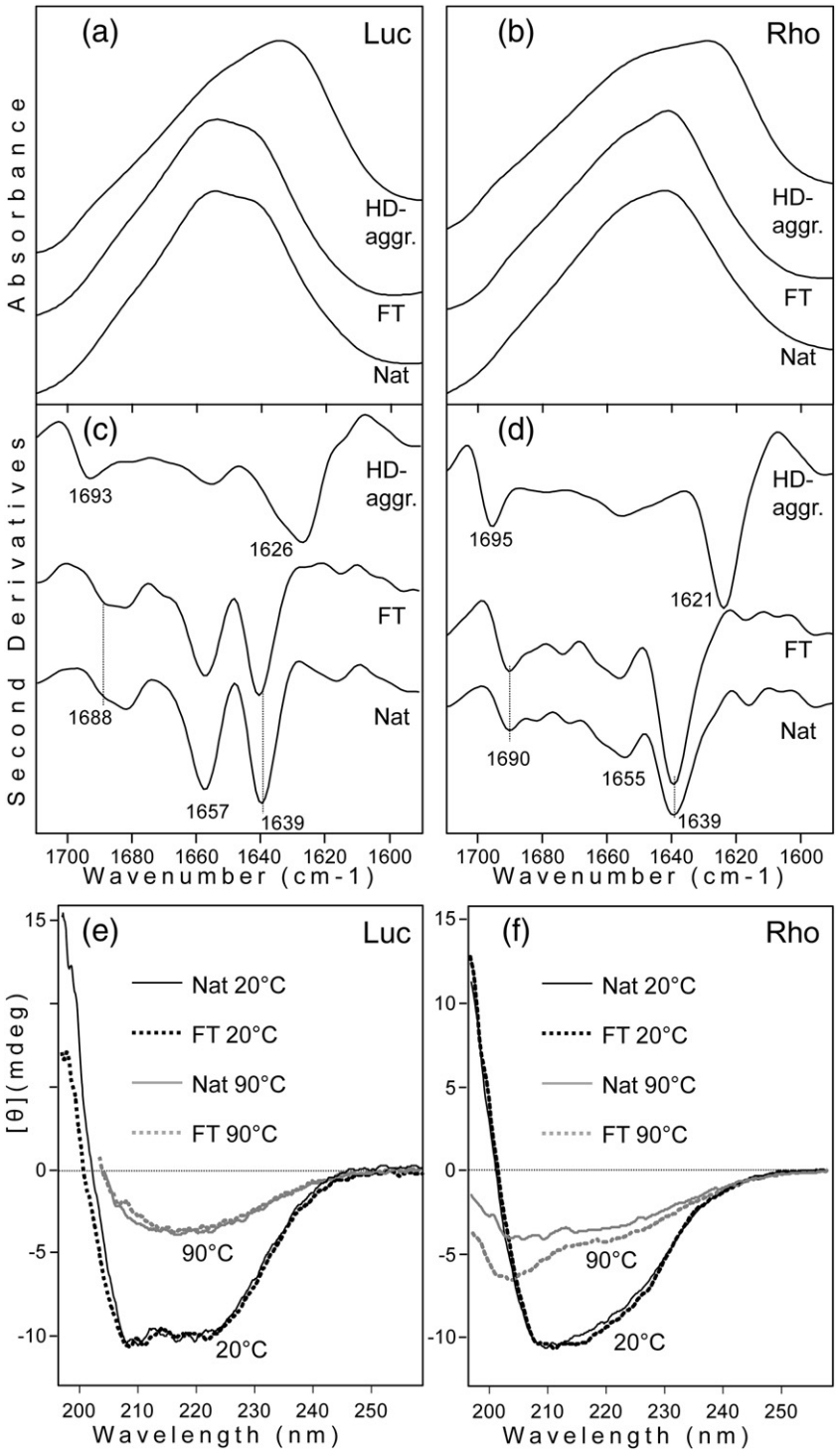

Fig. 4. Luciferase and rhodanese secondary structures. (a–d) The FTIR absorption (a and b) and second-derivative (c and d) spectra of luciferase and rhodanese, in the native (Nat) and misfolded (FT) forms, are reported in the amide I region, where peak positions of the main components are indicated. The spectra of heat-denatured aggregates (HD) are also presented. (e and f) Far-UV CD spectra of luciferase (e) and rhodanese (f) in the native and FT forms, both collected at 20 °C and 90 °C. The reported data are representative of more than four independent experiments.

Rho (Fig. 4d) was characterized by components at ~1639 and ~1690 cm^{-1} due to intramolecular β-sheets, and ~1655 cm^{-1}, which could be assigned to α-helices and random-coil secondary structures.[23]

The second-derivative spectra of the misfolded monomers (Fig. 4c and d) displayed only small differences, compared to that of the native proteins. In the case of luciferase, the intramolecular β-sheet component was upshifted from 1639.1 ± 0.2 cm^{-1} in the Nat-Luc to 1640.0 ± 0.2 cm^{-1} in the FT-Luc, suggesting the presence of slightly loosely packed and/or distorted β-sheet structures in the misfolded monomer, as compared to the native state.[23,24,26,27] A similar shift of the β-sheet component was reported for monomeric β-galactosidase after freeze–thaw in 100 mM sodium phosphate buffer.[28]

In the case of rhodanese second-derivative spectra, the IR response of intramolecular β-sheets of FT-Rho occurred at the same wavenumber as in the native protein but displayed a higher intensity and a narrower bandwidth. It should be noted that the absorption spectra of the two forms (Fig. 4b) were almost superimposable, indicating that the differences in the second-derivative spectra mainly reflected a structural rearrangement of the native β-sheets. As also suggested by the CD data reported below, these FTIR results indicate that the misfolded monomers retained their intramolecular β-sheet structures to a similar extent compared to the native proteins, but in a different conformation, which could also account for their increased ThT binding, 1.8 times higher in the case of FT-Luc[18] and 3.5 times higher in the case of FT-Rho (Fig. 1c).

One should note that the IR marker bands of protein aggregation (i.e., the intermolecular β-sheet bands)[23–25,27,29] were absent in the spectra of the two native species and also were remarkably absent in the spectra of the two FT variants, confirming their monomeric, non-aggregated state, in agreement with the gel-filtration and light-scattering data for both FT-Luc[18] and FT-Rho, and with the results of GA cross-linking (Fig. 1; Fig. S1). In contrast, the IR spectra of the thermally denatured proteins (Fig. 4a–d) displayed a clear reduction of the native secondary-structure components and the appearance of two new bands, due to the formation of intermolecular β-sheet structures in protein aggregates,[24,25,27,29] respectively, at ~1626 cm^{-1} and at ~1693 cm^{-1} for heat-denatured luciferase and at ~1621 cm^{-1} and at ~1695 cm^{-1} for HD-Rho, which we show here for the first time not to occur in the misfolded species.

The secondary structures of the two FT species were also investigated by CD. Nat-Luc and FT-Luc displayed almost superimposable CD spectra at 20 °C (Fig. 4e), characteristic of an α/β protein.[30] However, a minor unfolding of the protein secondary structures seemed to have occurred after FT treatment, as indicated by the decreased CD signal around 200 nm in the FT-Luc spectrum (Fig. 4e). In the case of rhodanese, again, the CD spectra of native and FT conformers at 20 °C were almost superimposable (Fig. 4f), displaying a spectral shape in agreement with an α/β protein.[30]

Misfolded monomers display an increased exposure of hydrophobic patches

To highlight possible tertiary-structure changes induced by FT treatment, we next investigated the intrinsic fluorescence of the protein aromatic amino acids. Upon excitation at 280 nm, both FT-Luc and FT-Rho displayed a strongly reduced fluorescence emission, compared to that of their native conformers (Fig. 5a and b). These results suggest that FT treatment caused in both proteins a higher solvent accessibility of the aromatic residues. In

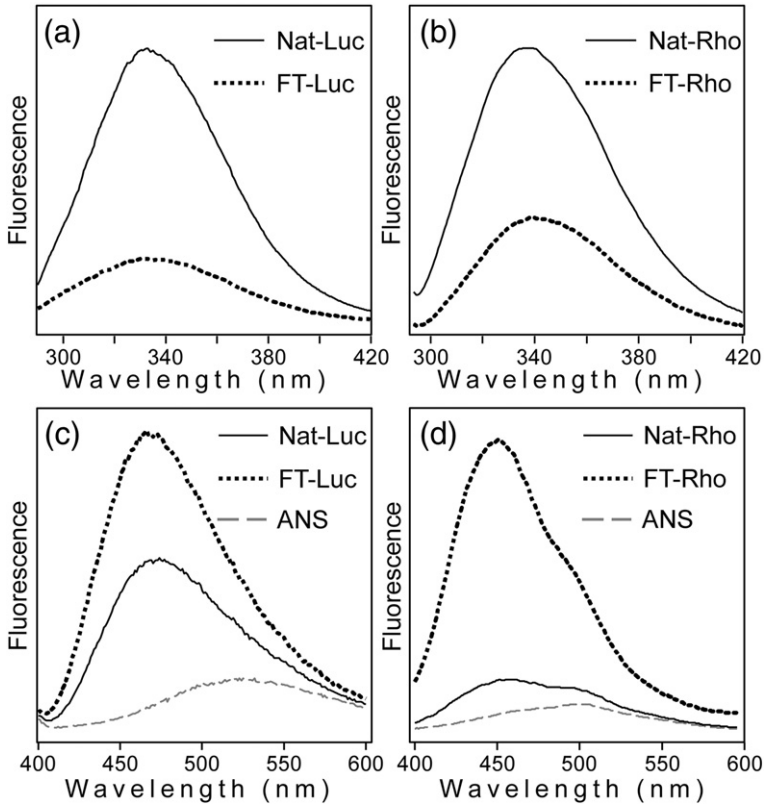

Fig. 5. Tertiary structures of native and FT luciferase and rhodanese. (a and b) Intrinsic fluorescence emission spectra are reported for luciferase (a) and rhodanese (b) in the native and FT forms, with excitation at 280 nm. (c) Fluorescence emission spectra of ANS at 30 μM concentration are presented in the absence (broken line) and in the presence of 1 μM Nat-Luc (continuous line) or of 1 μM FT-Luc (dotted line). (d) Fluorescence emission spectra of ANS at 30 μM concentration are presented in the absence (broken line) and in the presence of 4 μM Nat-Rho (continuous line) or of 4 μM FT-Rho (dotted line). ANS fluorescence was excited at 350 nm. The reported data are representative of more than three independent experiments.

addition, the structural properties of luciferase and rhodanese were further investigated using the fluorescent dye 8-naphthalene-1-anilino-sulfonate (ANS). When ANS binds to the protein's exposed hydrophobic patches, its fluorescence quantum yield is strongly enhanced and its emission maximum is shifted to lower wavelengths. Interestingly, both in the case of Nat-Luc and FT-Luc, the ANS fluorescence emission was increased and shifted. Similar results of ANS interactions were recently reported for the native luciferase.[31] However, a much higher fluorescence was observed for FT-Luc, indicating more exposure of hydrophobic patches on its surface, compared to the native protein (Fig. 5c). This structural difference, that is, the increased exposure of hydrophobic patches after FT treatment, was more pronounced in the case of FT-Rho (Fig. 5d).

FT-Rho and FT-Luc have different degrees of thermal stability and aggregation propensity

We next investigated the thermal stability of FT-Rho and FT-Luc by CD, monitoring the ellipticity changes at 222 nm, while gradually heating the samples from 20 °C to 90 °C (Fig. 6a and b). The Nat-Luc was found to be stable up to ~40 °C. Above 40 °C, the protein rapidly lost its CD signal with a midpoint at ~43 °C (Fig. 6a). Noticeably, FT-Luc displayed a reduction of about 4 °C of thermal stability. During the thermal treatment, luciferase aggregation occurred, as indicated by the high tension voltage (HT[V]) changes (Fig. 6c), which allow to monitor the variation of the solution's turbidity, induced by the formation of protein aggregates.[32,33] In particular, the HT[V] signal at 222 nm firstly increased, as the ellipticity at the same wavelength, and then decreased, as a consequence of protein precipitation. Again, the HT[V] plots indicated a reduced stability of the FT-Luc. After heating up to 90 °C, the direct inspection of the CD spectra (Fig. 4e) for both native and FT-Luc indicated that the aggregated protein still in solution displayed the spectral response of β-sheet structures, as expected from the FTIR results.

When Nat-Rho was heated, the ellipticity at 222 nm changed (Fig. 6b) with a similar trend as for native luciferase, but with a midpoint temperature at ~50 °C, indicating higher stability of Nat-Rho, as compared to both Nat-Luc and FT-Luc. Also in the case of Nat-Rho, the increase of HT[V] indicated that the thermal treatment induced protein aggregation, leading to a higher turbidity of the solution. Above ~55 °C, the HT[V] decreased due to protein precipitation (Fig. 6d).

A markedly different behavior was observed with FT-Rho, where a gradual ellipticity variation at 222 nm was observed, with no evident transition (Fig. 6b). Moreover, for FT-Rho, the 50% change of ellipticity occurred at a higher temperature, as compared to Nat-Rho. The HT[V] signal (Fig. 6d) of FT-Rho decreased very slowly in the ~30–57 °C temperature range, while it dropped abruptly at higher temperature. This behavior suggests the formation of small soluble aggregates that did not

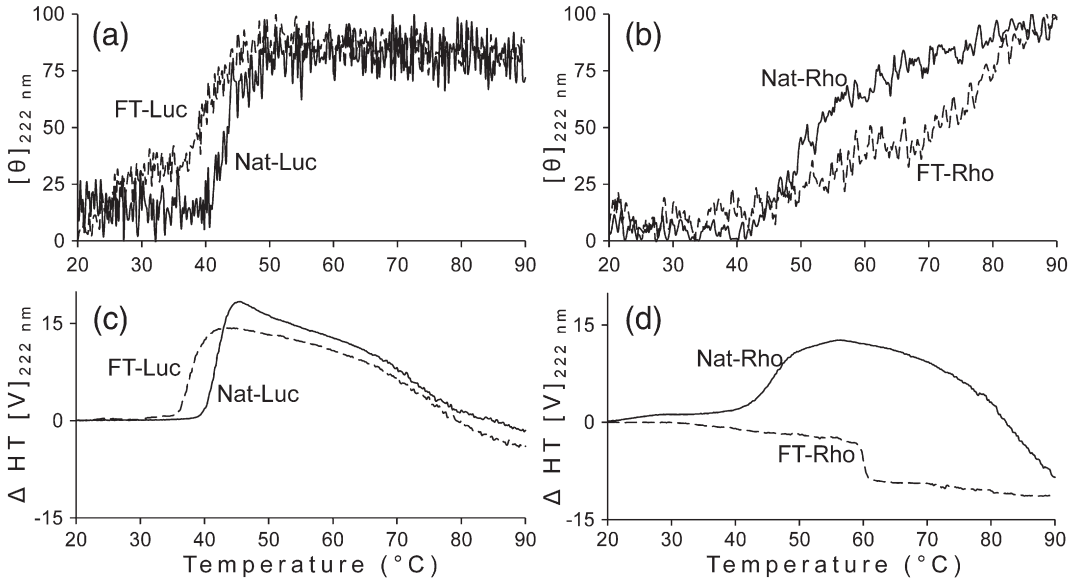

Fig. 6. Luciferase and rhodanese thermal stability and aggregation. (a and b) The ellipticity changes monitored at 222 nm for luciferase (a) and rhodanese (b) conformers during thermal treatment, from 20 °C to 90 °C, are reported as percentage of variation. (c and d) The HT[V] changes monitored at 222 nm for luciferase (c) and rhodanese (d) conformers during thermal treatment, from 20 °C to 90 °C, are reported as absolute voltage variations. The displayed data are representative of more than four independent experiments.

contribute to the solution turbidity, but interacted as "sticky" protein intermediates, leading to insoluble aggregates that simultaneously precipitated at a critical temperature. The different thermal behavior of FT-Rho and Nat-Rho was also evident by the direct inspection of their CD spectra collected at 90 °C (Fig. 4f). In the case of FT-Rho, the fraction of protein still in solution at this temperature in the CD spectrum displayed a more evident minimum around 203 nm, indicative of less ordered secondary structures.

Discussion

In this work, we focused on the structural characterization of two stable misfolded monomers of luciferase and rhodanese, obtained by iterative cycles of freezing–thawing. They were both stringent DnaK chaperone-amenable substrates, yet, interestingly, they displayed very different behaviors in *in vitro* chaperone refolding assays. Whereas FT-Rho was slowly refolded only by a molar excess of the chaperone, FT-Luc was rapidly and efficiently refolded already by substoichiometric amounts of DnaK. To better understand the mechanism of chaperone-mediated unfolding/refolding, it was thus important to investigate the biophysical properties of these two unique stable monomeric species and gain insights on the structural characteristics favoring specific chaperone interactions with misfolded substrates and disfavoring interactions with the unfolded and natively refolded products of the chaperone reaction.

Alongside chaperone amenability, there is an increasing interest in studying protein species at the very early stage of their aggregation in view of understanding their role in the early onset of protein conformational diseases. It is a major concern for medicine, pharmacology, and biotechnology to reach a better understanding of the natural mechanisms by which young cells may succeed to rescue themselves from pathological protein misfolding conditions, while the natural defense mechanisms in aging cells and diseased tissues apparently fail at protecting themselves from proteotoxic damages. The two newly characterized, stable misfolded monomeric species might serve as new tools to study the ways cells counteract toxic protein misfolding events at very early stages of the aggregation pathway, before they become irreversibly damaged. Indeed, the partial unfolding of globular proteins, or partial folding of intrinsically disordered proteins, is often considered to be the first event in protein fibrillogenesis.[2,16,34,35] Whereas oligomers and mature aggregates are extensively studied to highlight their structure and toxic properties,[2,7,10,15] little is known about the initial misfolded monomers that enter the aggregation pathway. Due to their unstable structure under native-like conditions, a thorough description of their conformational properties and possibly of their toxic properties has been only rarely reported. Nevertheless, they might represent a very important therapeutic target of protein conformational diseases.[36] The full relevance of the misfolded monomeric species is apparent when considering that during their lifetime, cells are continuously challenged by external stresses, such as cold stress and heat shock, and they need molecular defenses to counteract and rescue potentially toxic misfolded species that may sporadically form, even under physiological conditions.

Here, we performed a detailed biophysical characterization of the two stable inactive misfolded monomers of luciferase and rhodanese, investigating their secondary and tertiary structures, conformational stability in urea and under heat stress, and their aggregation propensity. In particular, we found that the secondary structures of the native proteins and of their misfolded monomers displayed minor but significant differences, mainly involving the quality of their β-sheet structures that displayed, after the FT treatment, a different structural rearrangement, as indicated by FTIR and CD spectroscopy.

Interestingly, the aromatic amino acids in the misfolded monomers were also found to be more accessible to the solvent, as observed by intrinsic fluorescence measurements. Furthermore, the misfolded monomers were found to expose more hydrophobic patches than the native proteins, as detected by ANS fluorescence studies. These properties could account for the expected higher affinity of chaperone for the misfolded FT-Luc and FT-Rho substrates, compared to their native conformers.[37,38]

Moreover, ThT fluorescence gave new insights on the conformational changes that were induced by the iterative FT treatments of native luciferase and rhodanese. Although ThT fluorescence is the most used method for staining amyloid material, both *in vivo* and *in vitro*, the ThT interactions with fibrils and misfolded species at the molecular level still need to be better understood (see, for reviews, Refs. 39 and 40). Among different proposals, the "channel" model suggests that ThT binds to grooves formed by the amino acid side chains of the fibril β-sheets, with ThT aligned to the fibril axis, perpendicularly to the β-strands. The side chains are required to produce a surface channel-like structure on flat β-sheets, involving at least four to five β-strands. Moreover, they should contain aromatic and hydrophobic amino acids, avoiding charged side chains in order to reduce repulsive electrostatic interactions. The central role of hydrophobic cavities of proper size in the ThT–fibril interaction has been underlined in the literature.[39,40] These studies highlight that structural constraints are required for ThT binding, justifying why most native proteins, even rich in β-sheets, interact relatively poorly with the dye. Indeed, native β-sheets are typically highly twisted, that is, not flat

enough and do not always expose side chains to support efficient ThT binding. Both luciferase and especially rhodanese misfolded monomers displayed a markedly higher ThT fluorescence compared to their native conformer, a result that might help to understand ThT interactions with non-aggregated protein species. This can be explained by the structural changes detected in this work, namely, (i) the structural rearrangement of the intramolecular β-sheets, (ii) the increased surface exposure of hydrophobic patches, and (iii) the increased accessibility of aromatic amino acids to the solvent.

Therefore, the FT-Luc and FT-Rho could be taken as novel model species for a detailed study on ThT interactions with non-aggregated misfolded species. Interestingly, we found that up to 60 μM, ThT did not inhibit or activate the enzymatic activities of native chaperone products Nat-Luc, Nat-Rho (data not shown), and G6PDH.[41] Moreover, 60 μM ThT did not affect the ATPase activities of KJE, the rates and yields of spontaneous refolding, the aggregation propensity of misfolded species, or the stability of already aggregated species (data not shown). Thus, ThT can be used as a specific molecular probe to monitor online structural changes into non-native β-sheet structures of misfolded and aggregated conformers during chemical and physical treatments, as well as during ATP-fueled chaperone-mediated unfolding and refolding assays, as reported here and earlier.[18,42]

Steady-state ThT fluorescence in the presence of increasing concentrations of urea clearly demonstrated that FT-Luc is much less stable than FT-Rho (Fig. 3a), in agreement with their different levels of intrinsic ThT binding (1.8 and 3.5, respectively) and their various degrees of chaperone amenability. Concerning the thermal stability, the two misfolded monomers displayed a very different behavior. In the case of luciferase, while at the temperature used in the chaperone assay, the native and misfolded monomers were both stable; above ~35 °C, the FT-Luc displayed a reduced thermal stability (Fig. 6a) and underwent a fast aggregation process (Fig. 6c). This behavior was in agreement with the increased presence of hydrophobic patches in FT-treated species (Fig. 5c). It confirmed that hydrophobic exposure is the main intrinsic physicochemical property determining the propensity of a misfolded species to aggregate or bind a molecular chaperone. In particular, it has been found that the protein regions involved in the first stage of aggregation are those with higher hydrophobicity and propensity to form β-sheets.[43]

In the case of rhodanese, it has been previously reported that above ~40 °C, the protein first forms small active oligomers in a concentration-dependent manner, which thereafter aggregate in large assemblies at higher temperature.[44] It has been suggested that the small oligomers protect the protein from thermal inactivation[45] and are the starting material for larger aggregates.[44] In light of these studies, a possible explanation of the peculiar thermal profiles reported here for FT-Rho is that the increased exposure of hydrophobic patches during FT treatment (Fig. 5d) might increase the propensity to form small oligomers at high temperature, leading to a temperature-dependent ellipticity change smoother for FT-Rho than for Nat-Rho (Fig. 6b). However, above a critical temperature, these oligomers might undergo aggregation into large insoluble assemblies, resulting in a drop of the solution turbidity observed in the HT[V] plot (Fig. 6d).

As conclusive remarks, our biophysical characterization disclosed minor structural differences between the native and the two misfolded FT monomers (i.e., increased hydrophobic patches and misfolded β-sheets) that could account for the expected difference of chaperone affinity. Moreover, our results provide an explanation for the different behavior of the two stable misfolded monomers as chaperone substrates: whereas a substoichiometric amount of DnaK (Fig. 2c, left of the broken line) can efficiently unfold/refold FT-Luc by the unfolding action of a single DnaK molecule per luciferase substrate at a time—likely by a direct clamping mechanism[18,46]—only a stoichiometric excess of DnaK could efficiently unfold FT-Rho (Fig. 2c, right of the broken line). This suggests that in the case of the more stable and therefore more chaperone-resistant FT-Rho species, the unfolding action likely involves the concomitant binding of several DnaK molecules at different positions of the same misfolded rhodanese polypeptide. This concomitant binding enables them to apply an unfolding force resulting from the combined effect of chaperone clamping and cooperative entropic pulling. Such a cooperative mode of DnaK action has been previously reported in the case of stable soluble heat-denatured G6PDH aggregates.[21,41]

Accordingly, the FT-Rho structure was found to be significantly more stable than that of FT-Luc (Figs. 3 and 6a and b), accounting for the need of an additional unfolding mechanism, both clamping and cooperative entropic pulling, in the case of FT-Rho. In contrast, FT-Luc required only the unfolding by a direct chaperone clamping. Moreover, the propensity of rhodanese to form non-productive and aggregation-prone intermediates during its refolding process[47] could further contribute to the reduced refolding yields of chaperone, as compared to FT-Luc (Fig. 2d).

Materials and Methods

Materials

DnaK of *Escherichia coli* was expressed and purified as described previously.[48] DnaJ and GrpE of *E. coli*[49] were a gift from H. J. Schönfeld, F. Hoffmann-La Roche, Basel,

Switzerland. The plasmid pT7lucC-His, carrying the luciferase gene of *P. pyralis* with the additional His6-coding sequence[50] was a gift from A. S. Spirin, Institute of Protein Research, Russian Academy of Sciences, Pushchino, Moscow Region, Russia. His-tagged luciferase was purified as described previously[18] and stored only once in 15% glycerol at −80 °C. Bovine rhodanese was purchased from Sigma.

Activity assay

Luciferase activity was measured using a Victor Light 1420 Luminescence Counter from Perkin–Elmer as described previously.[18] Rhodanese activity was measured by a colorimetric method (monitored at 460 nm) based on the formation of the complex between ferric ions and one of the reaction products, thiocyanate.[51,52] Rates of ATP hydrolysis during the first 4 min of the chaperone reactions, reported in Fig. 2b, were measured as previously described.[18]

Purification of stable misfolded monomeric rhodanese and luciferase

The misfolded monomeric rhodanese was prepared by repeated cycles of freezing-thawing (rapid freezing at −160 °C and slow thawing at 4 °C) of Nat-Rho (not more than 5 μM) in the presence of 20 mM sodium phosphate, pH 7.5, 20 mM DTT, and 50 mM $Na_2S_2O_3$. Once stably inactivated to 95%, the protein was centrifuged at 12,000***g*** for 10 min and the supernatant was injected on a gel-filtration column (Superose 6HR10/30). The fractions corresponding to inactive and monomeric rhodanese were collected and further concentrated, on Amicon ultra-10 concentrator with a 10-kDa cutoff, to about 5 μM and stored in 10% glycerol at −80 °C. The purification of stable misfolded monomeric luciferase species was as previously described.[18]

Preparation of HD-Rho

Rhodanese was incubated for 10 min at 62 °C in 50 mM Tris–HCl, pH 7.5, 150 mM potassium chloride, and 20 mM magnesium chloride. The residual activity after heat exposure was <2% of the initial value.

Thioflavin T fluorescence and light-scattering measurements

Rhodanese (1 μM) was incubated in the presence of 60 μM ThT (from Sigma), which we found to have no detectable effects on the activity of the chaperones and Nat-Rho enzyme, as previously reported to be the case for G6PDH[41] and luciferase[18] as well. ThT fluorescence was measured with a Perkin–Elmer LS55 luminescence spectrometer at 25 °C. Fluorescence was recorded online for 30 min (excitation 450 nm, bandwidth 15 nm; emission 485 nm, bandwidth 2.5 nm). Light scattering was measured online at 550 nm (excitation wavelength 550 nm) at 25 °C with a Perkin–Elmer LS55 luminescence spectrometer.

Chaperone activity assay

Refolding assays were performed in refolding buffer (50 mM Tris–acetate, pH 7.8, 50 mM KCl, and 10 mM $MgCl_2$) in the presence of 5 mM ATP. The concentrations of chaperones, except DnaK, were kept constant for DnaJ (0.5 μM) and GrpE (0.7 μM). Rates of luciferase and rhodanese refolding were derived from the initial linear phase of the time curves of recovered enzymatic activity.

Urea unfolding experiments

The urea unfolding of FT-Rho was performed as previously reported for FT-Luc.[18] Briefly, 1 μM FT-Rho or FT-Luc was incubated for 1 h at 25 °C in the presence of 60 μM ThT and different concentrations of urea, as indicated in Fig. 3. The ThT fluorescence was then measured as described in the previous paragraph and expressed as the percentage of the maximal ThT fluorescence measured after pretreatment with 0 M urea.

FTIR spectroscopy

FTIR spectroscopy measurements in attenuated total reflection were performed on protein hydrated film following an already standardized approach,[29,53,54] which allows to obtain spectra with high signal-to-noise ratio also for proteins at low concentrations. In particular, luciferase has been analyzed at 5 μM in 20 mM phosphate buffer and 100 mM NaCl, pH 7.5, whereas rhodanese has been measured at 5–12 μM concentration in 20 mM phosphate buffer, pH 7.5. Sample aliquots of 3 μl were deposed on the diamond plate of the nine-reflection attenuated total reflection device (DuraSamplIRII, Smith Detection) and dried at room temperature in order to obtain a protein hydrated film. Spectra were collected by the Varian 670-IR spectrometer (Varian Australia Pty Ltd., Mulgrave, VIC, Australia) equipped with a nitrogen-cooled mercury cadmium telluride detector under accurate dry air purging. The following conditions were employed: 2 cm^{-1} spectral resolution, 25 kHz scan speed, 1000 scan co-addition, and triangular apodization. The buffer spectrum, collected under identical conditions, has been then subtracted to that of the protein. All the measured spectra were reported after normalization to the amide I band area, to compensate for possible differences in protein content. The second derivatives were obtained by the Savitsky–Golay method (third-grade polynomial, 5 smoothing points) after a binomial smoothing (11 points) of the absorption spectra using the GRAMS/32 software (Galactic Industries Corporation, Salem, NH, USA).

Circular dichroism

CD spectra were recorded on the same samples employed for FTIR measurements using the Jasco J-815 (Jasco Corp., Tokyo, Japan) spectropolarimeter. For both luciferase (at 2.5 μM) and rhodanese (at 8 μM), far-UV spectra were collected in a 0.1-cm path-length quartz cell, in the 260–190 nm spectral range, and averaged over four scans. The bandwidth and time-response parameters were respectively set to 1 nm and 1 s for

luciferase and 2 nm and 2 s for rhodanese. CD spectra are presented after buffer subtraction and binomial smoothing. For thermal stability experiments, the sample temperature was varied from 20 to 90 °C at 1 °C/min and the ellipticity and the HT[V] signals were monitored at 222 nm every 0.2 °C.

Intrinsic fluorescence and ANS binding measurements

Fluorescence measurements were performed using Cary Eclipse (Varian, Palo Alto, CA, USA) and the LS55 Perkin–Elmer luminescence spectrometers (Waltham, MA, USA). Intrinsic fluorescence of the aromatic protein amino acid was recorded, exciting the sample at 280 nm. Luciferase conformers have been measured at 2.5 μM (in 20 mM phosphate buffer and 100 mM NaCl, pH 7.5) and rhodanese conformers have been measured at 1 μM (in 20 mM phosphate buffer, pH 7.5). For ANS binding studies, the fluorescence emission of the dye excited at 350 nm was recorded for luciferase at 1 μM protein and at 30 μM ANS concentrations (20 mM phosphate buffer and 100 mM NaCl, pH 7.5). For rhodanese, ANS fluorescence was collected at 4 μM protein and at 30 μM ANS concentrations (in 20 mM phosphate buffer, pH 7.5). Quartz cuvette of 1 cm path length was employed.

Acknowledgements

S.M.D. acknowledges the financial support of the Fondo di Ateneo per la Ricerca of the University of Milano-Bicocca, Italy. P.G. acknowledges the financial support from the Faculty of Biology and Medicine of Lausanne University and Grant 31003A-140512/1 from the Swiss National Fund.

Conflict of Interest Statement. The authors declare no conflict of interest.

Supplementary Data

Supplementary data to this article can be found online at http://dx.doi.org/10.1016/j.jmb.2012.12.025

Received 30 August 2012;
Received in revised form 21 December 2012;
Accepted 31 December 2012
Available online 7 January 2013

Keywords:
chaperone substrate;
luciferase;
misfolded monomer;
protein aggregation;

† A.N. and R.U.H.M. contributed equally to this work.

Abbreviations used:
ANS, 8-naphthalene-1-anilino-sulfonate; KJE, the DnaK, DnaJ, GrpE chaperone system; FT-Luc, freezing-thawing luciferase; FT-Rho, freezing-thawing rhodanese; FTIR, Fourier transform infrared; G6PDH, glucose-6-phosphate dehydrogenase, GA, glutaraldehyde; HD-Rho, heat-denatured rhodanese; HT[V], high tension voltage; IR, infrared; Nat-Luc, native luciferase; Nat-Rho, native rhodanese; ThT, thioflavin T.

References

1. Anfinsen, C. B. (1973). Principles that govern folding of protein chains. *Science*, **181**, 223–230.
2. Chiti, F. & Dobson, C. M. (2006). Protein misfolding, functional amyloid, and human disease. *Annu. Rev. Biochem.* **75**, 333–366.
3. Pinney, J. H. & Hawkins, P. N. (2012). Amyloidosis. *Ann. Clin. Biochem.* **49**, 229–241.
4. Hinault, M. P., Farina-Henriquez-Cuendet, A. & Goloubinoff, P. (2011). Molecular chaperones and associated cellular clearance mechanisms against toxic protein conformers in Parkinson's disease. *Neurodegener. Dis.* **8**, 397–412.
5. Uversky, V. N. (2008). Amyloidogenesis of natively unfolded proteins. *Curr. Alzheimer Res.* **5**, 260–287.
6. Bucciantini, M., Giannoni, E., Chiti, F., Baroni, F., Formigli, L., Zurdo, J. *et al.* (2002). Inherent toxicity of aggregates implies a common mechanism for protein misfolding diseases. *Nature*, **416**, 507–511.
7. Campioni, S., Mannini, B., Zampagni, M., Pensalfini, A., Parrini, C., Evangelisti, E. *et al.* (2010). A causative link between the structure of aberrant protein oligomers and their toxicity. *Nat. Chem. Biol.* **6**, 140–147.
8. Bolognesi, B., Kumita, J. R., Barros, T. P., Esbjorner, E. K., Luheshi, L. M., Crowther, D. C. *et al.* (2010). ANS binding reveals common features of cytotoxic amyloid species. *ACS Chem. Biol.* **5**, 735–740.
9. Olzscha, H., Schermann, S. M., Woerner, A. C., Pinkert, S., Hecht, M. H., Tartaglia, G. G. *et al.* (2011). Amyloid-like aggregates sequester numerous metastable proteins with essential cellular functions. *Cell*, **144**, 67–78.
10. Fandrich, M. (2012). Oligomeric intermediates in amyloid formation: structure determination and mechanisms of toxicity. *J. Mol. Biol.* **421**, 427–440.
11. Bucciantini, M., Nosi, D., Forzan, M., Russo, E., Calamai, M., Pieri, L. *et al.* (2012). Toxic effects of amyloid fibrils on cell membranes: the importance of ganglioside GM1. *FASEB J.* **26**, 818–831.
12. Kaganovich, D., Kopito, R. & Frydman, J. (2008). Misfolded proteins partition between two distinct quality control compartments. *Nature*, **454**; 1088-U36.
13. Tyedmers, J., Mogk, A. & Bukau, B. (2010). Cellular strategies for controlling protein aggregation. *Nat. Rev. Mol. Cell Biol.* **11**, 777–788.
14. Hinault, M. P., Ben-Zvi, A. & Goloubinoff, P. (2006). Chaperones and proteases—cellular fold-controlling factors of proteins in neurodegenerative diseases and aging. *J. Mol. Neurosci.* **30**, 249–265.

15. Uversky, V. N. (2010). Mysterious oligomerization of the amyloidogenic proteins. *FEBS J.* **277**, 2940–2953.
16. Neudecker, P., Robustelli, P., Cavalli, A., Walsh, P., Lundstrom, P., Zarrine-Afsar, A. *et al.* (2012). Structure of an intermediate state in protein folding and aggregation. *Science*, **336**, 362–366.
17. Sharma, S. K., Christen, P. & Goloubinoff, P. (2009). Disaggregating chaperones: an unfolding story. *Curr. Protein Pept. Sci.* **10**, 432–446.
18. Sharma, S. K., De Los Rios, P., Christen, P., Lustig, A. & Goloubinoff, P. (2010). The kinetic parameters and energy cost of the Hsp70 chaperone as a polypeptide unfoldase. *Nat. Chem. Biol.* **6**, 914–920.
19. Apetri, A. C. & Horwich, A. L. (2008). Chaperonin chamber accelerates protein folding through passive action of preventing aggregation. *Proc. Natl Acad. Sci. USA*, **105**, 17351–17355.
20. Diamant, S., Ben-Zvi, A. P., Bukau, B. & Goloubinoff, P. (2000). Size-dependent disaggregation of stable protein aggregates by the DnaK chaperone machinery. *J. Biol. Chem.* **275**, 21107–21113.
21. De los Rios, P., Ben-Zvi, A., Slutsky, O., Azem, A. & Goloubinoff, P. (2006). Hsp70 chaperones accelerate protein translocation and the unfolding of stable protein aggregates by entropic pulling. *Proc. Natl Acad. Sci. USA*, **103**, 6166–6171.
22. Diamant, S. & Goloubinoff, P. (1998). Temperature-controlled activity of DnaK–DnaJ–GrpE chaperones: protein-folding arrest and recovery during and after heat shock depends on the substrate protein and the GrpE concentration. *Biochemistry*, **37**, 9688–9694.
23. Barth, A. & Zscherp, C. (2002). What vibrations tell us about proteins. *Q. Rev. Biophys.* **35**, 369–430.
24. Zandomeneghi, G., Krebs, M. R. H., McCammon, M. G. & Fandrich, M. (2004). FTIR reveals structural differences between native beta-sheet proteins and amyloid fibrils. *Protein Sci.* **13**, 3314–3321.
25. Natalello, A., Prokorov, V. V., Tagliavini, F., Morbin, M., Forloni, G., Beeg, M. *et al.* (2008). Conformational plasticity of the Gerstmann–Straussler–Scheinker disease peptide as indicated by its multiple aggregation pathways. *J. Mol. Biol.* **381**, 1349–1361.
26. Kauffmann, E., Darnton, N. C., Austin, R. H., Batt, C. & Gerwert, K. (2001). Lifetimes of intermediates in the beta-sheet to alpha-helix transition of beta-lactoglobulin by using a diffusional IR mixer. *Proc. Natl Acad. Sci. USA*, **98**, 6646–6649.
27. Ami, D., Ricagno, S., Bolognesi, M., Bellotti, V., Doglia, Silvia M. & Natalello, A. (2012). Structure, stability, and aggregation of β-2 microglobulin mutants: insights from a Fourier transform infrared study in solution and in the crystalline state. *Biophys. J.* **102**, 1676–1684.
28. Pikal-Cleland, K. A., Rodriguez-Hornedo, N., Amidon, G. L. & Carpenter, J. F. (2000). Protein denaturation during freezing and thawing in phosphate buffer systems: monomeric and tetrameric beta-galactosidase. *Arch. Biochem. Biophys.* **384**, 398–406.
29. Natalello, A., Frana, A. M., Relini, A., Apicella, A., Invernizzi, G., Casari, C. *et al.* (2011). A major role for side-chain polyglutamine hydrogen bonding in irreversible ataxin-3 aggregation. *PLoS One*, **6**, e18789.
30. Kelly, S. M., Jess, T. J. & Price, N. C. (2005). How to study proteins by circular dichroism. *Biochim. Biophys. Acta*, **1751**, 119–139.
31. Amini-Bayat, Z., Hosseinkhani, S., Jafari, R. & Khajeh, K. (2012). Relationship between stability and flexibility in the most flexible region of *Photinus pyralis* luciferase. *Biochim. Biophys. Acta*, **1824**, 350–358.
32. Benjwal, S., Verma, S., Rohm, K. H. & Gursky, O. (2006). Monitoring protein aggregation during thermal unfolding in circular dichroism experiments. *Protein Sci.* **15**, 635–639.
33. Natalello, A., Ami, D., Collini, M., D'Alfonso, L., Chirico, G., Tonon, G. *et al.* (2012). Biophysical characterization of Met-G-CSF: effects of different site-specific mono-pegylations on protein stability and aggregation. *PLoS One*, **7**, e42511.
34. Uversky, V. N. & Fink, A. L. (2004). Conformational constraints for amyloid fibrillation: the importance of being unfolded. *Biochim. Biophys. Acta*, **1698**, 131–153.
35. Hervas, R., Oroz, J., Galera-Prat, A., Goni, O., Valbuena, A., Vera, A. M. *et al.* (2012). Common features at the start of the neurodegeneration cascade. *PLoS Biol.* **10**, e1001335.
36. Nagai, Y., Inui, T., Popiel, H. A., Fujikake, N., Hasegawa, K., Urade, Y. *et al.* (2007). A toxic monomeric conformer of the polyglutamine protein. *Nat. Struct. Mol. Biol.* **14**, 332–340.
37. Fenton, W. A., Kashi, Y., Furtak, K. & Horwich, A. L. (1994). Residues in chaperonin GroEL required for polypeptide binding and release. *Nature*, **371**, 614–619.
38. Rudiger, S., Schneider-Mergener, J. & Bukau, B. (2001). Its substrate specificity characterizes the DnaJ co-chaperone as a scanning factor for the DnaK chaperone. *EMBO J.* **20**, 1042–1050.
39. Biancalana, M. & Koide, S. (2010). Molecular mechanism of thioflavin-T binding to amyloid fibrils. *Biochim. Biophys. Acta*, **1804**, 1405–1412.
40. Groenning, M. (2010). Binding mode of thioflavin T and other molecular probes in the context of amyloid fibrils—current status. *J. Chem. Biol.* **3**, 1–18.
41. Ben-Zvi, A., De los Rios,, P., Dietler, G. & Goloubinoff, P. (2004). Active solubilization and refolding of stable protein aggregates by cooperative unfolding action of individual Hsp70 chaperones. *J. Biol. Chem.* **279**, 37298–37303.
42. Sharma, S. K., De Los Rios, P. & Goloubinoff, P. (2011). Probing the different chaperone activities of the bacterial HSP70–HSP40 system using a thermolabile luciferase substrate. *Proteins*, **79**, 1991–1998.
43. Chiti, F., Taddei, N., Baroni, F., Capanni, C., Stefani, M., Ramponi, G. & Dobson, C. M. (2002). Kinetic partitioning of protein folding and aggregation. *Nat. Struct. Biol.* **9**, 137–143.
44. Bhattacharyya, A. M. & Horowitz, P. M. (2002). Isolation and characterization of rhodanese intermediates during thermal inactivation and their implications for the mechanism of protein aggregation. *Biochemistry*, **41**, 422–429.
45. Dungan, J. M. & Horowitz, P. M. (1993). Thermally perturbed rhodanese can be protected from inactivation by self-association. *J. Protein Chem.* **12**, 311–321.

46. Baneyx, F. & Nannenga, B. L. (2010). Chaperones: a story of thrift unfolds. *Nat. Chem. Biol.* **6**, 880–881.
47. Panda, M., Gorovits, B. M. & Horowitz, P. M. (2000). Productive and nonproductive intermediates in the folding of denatured rhodanese. *J. Biol. Chem.* **275**, 63–70.
48. Feifel, B., Sandmeier, E., Schonfeld, H. J. & Christen, P. (1996). Potassium ions and the molecular-chaperone activity of DnaK. *Eur. J. Biochem.* **237**, 318–321.
49. Schonfeld, H. J., Schmidt, D., Schroder, H. & Bukau, B. (1995). The DnaK chaperone system of *Escherichia coli*—quaternary structures and interactions of the DnaK and GrpE components. *J. Biol. Chem.* **270**, 2183–2189.
50. Svetlov, M. S., Kolb, V. A. & Spirin, A. S. (2007). Folding of the firefly luciferase polypeptide chain with the immobilized C terminus. *Mol. Biol. (Moscow)*, **41**, 86–92.
51. Lahti, M., Vilpo, J. & Hovinen, J. (1999). Spectrophotometric determination of thiocyanate in human saliva. *J. Chem. Educ.* **76**, 1281–1282.
52. Sörbo, B. H. (1955). Rhodanese: $CN^- + S_2O_3^{--} \rightarrow CNS^- + SO_3^{--}$. In *Methods in Enzymology*, vol. 2, pp. 334–337, Academic Press, New York, NY.
53. Apicella, A., Natalello, A., Frana, A. M., Baserga, A., Casari, C. S., Bottani, C. E. *et al.* (2012). Temperature profoundly affects ataxin-3 fibrillogenesis. *Biochimie*, **94**, 1026–1031.
54. Cerf, E., Sarroukh, R., Tamamizu-Kato, S., Breydo, L., Derclaye, S., Dufrêne, Y. F. *et al.* (2009). Antiparallel β-sheet: a signature structure of the oligomeric amyloid β-peptide. *Biochem. J.* **421**, 415–423.

SUPPLEMENTARY MATERIALS

FIGURE S1: Cross-linking shows that FT-Rho is not aggregated and similar to monomeric Nat-Rho.

2µM of native or heat-denatured (HD) Rhodanese, both from the stock solution, and of gel-filtered purified freeze thaw (FT) Rhodanese, were incubated in phosphate buffer for 1 hour at 25 °C with increasing concentrations of glutaraldehyde (GA), as indicated. The reaction was stopped with SDS sample buffer and, following boiling for 30 seconds, samples were resolved by SDS-PAGE and coomassie blue stained.

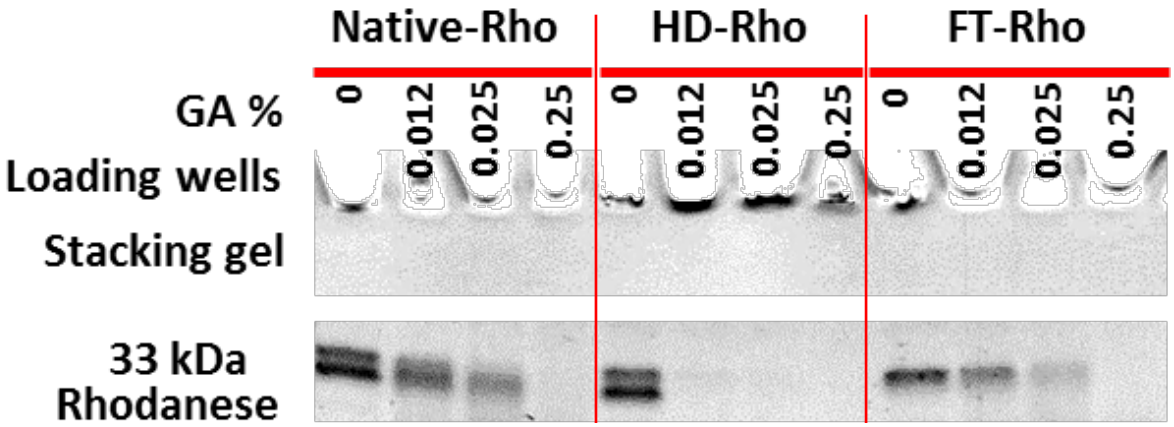

FIGURE S2: The FT-Rho refolding is not affected by the presence of native chaperone products.

FT-Rho (0.5µM) was incubated with DnaK (2.5µM), DnaJ (1.25µM), and GrpE (1.75µM) with and without 5 mM ATP (-ATP), and with different concentrations of native MDH and G6PDH, as indicated. After 60 minutes at 22°C, Rhodanese activity was measured. Basal FT-Rho activity without chaperones is shown (labeled as "Nothing"). Error bars represent s.e.m. of three independent measurements.

Up to a 16 fold molar excess of typical natively folded chaperone products (MDH or G6PDH), as compared to the FT-Rho substrate, does not inhibit the KJE- and ATP-dependent refolding reaction. These results indicate that the FT-Rho substrate have a much higher affinity to the chaperone system than the natively refolded products.

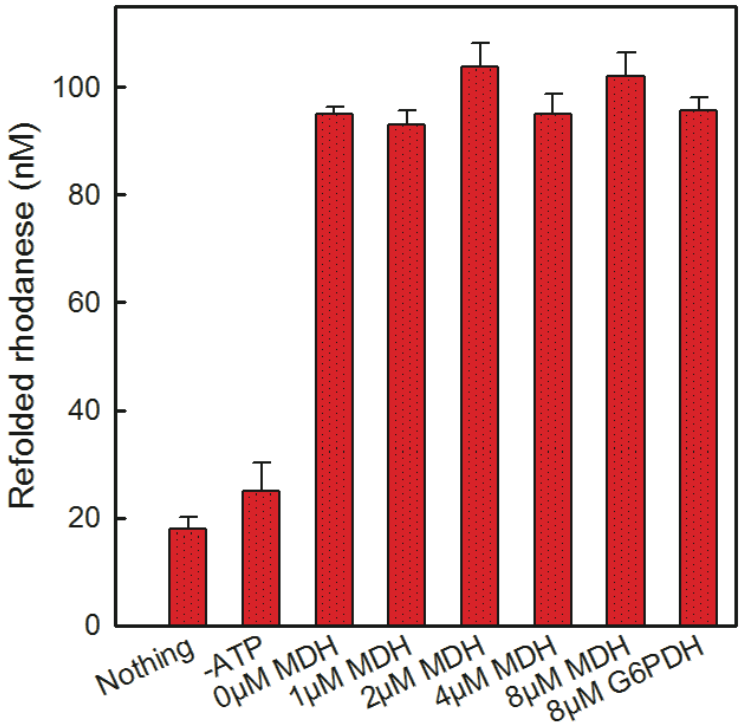

SUPPLEMENTARY TABLE 1

Rates of ATP hydrolysis during chaperone-mediated refolding of FT-Rho at 22°C, as in Fig. 2B. ATP was incubated during 4 minutes without or with 6.4 µM DnaK, 0.5 µM DnaJ, 0.7 µM GrpE (KJE), without or with 1 µM FT-Rho, or 1 µM Nat-Rho, as indicated.

Sample	nM ATP/min	ATP $DnaK^{-1}$ min^{-1}	Net ATP/refolded Rho
FT-Rho	200	-	-
Nat-Rho	260	-	-
KJE	9700	1.52	-
KJE + FT-Rho	19500	3.02	857
KJE + Nat-Rho	10700	1.63	-

CHAPTER 3

Hsp110 is a *bona fide* chaperone using ATP to unfold stable misfolded polypeptides and reciprocally collaborate with Hsp70 to solubilize protein aggregates

Hsp110 is a *bona fide* chaperone using ATP to unfold stable misfolded polypeptides and reciprocally collaborate with Hsp70 to solubilize protein aggregates.

Mattoo, R.U., Sharma, S.K., Priya, S., Finka, A. and Goloubinoff, P.

I contributed to this work conceptually and in the manuscript writing.
I provided the data for Fig. 1 (A-H), Fig. 3 (B-C), Fig. 5 (A-D) and Fig. 7 (A and B). I contributed with Dr. Sharma and Dr. Priya in the data acquisition for the Fig. 2 (A-D), Fig. 4, Fig. 6 (A and B) and Table 1. I also contributed with Dr. Finka in the data acquisition for Fig. 3 (A).

THE JOURNAL OF BIOLOGICAL CHEMISTRY VOL. 288, NO. 29, pp. 21399–21411, July 19, 2013

Hsp110 Is a *Bona Fide* Chaperone Using ATP to Unfold Stable Misfolded Polypeptides and Reciprocally Collaborate with Hsp70 to Solubilize Protein Aggregates*

Received for publication, April 22, 2013, and in revised form, May 24, 2013 Published, JBC Papers in Press, June 4, 2013, DOI 10.1074/jbc.M113.479253

Rayees U. H. Mattoo[‡], **Sandeep K. Sharma**[‡§], **Smriti Priya**[‡], **Andrija Finka**[‡], **and Pierre Goloubinoff**[‡1]

From the [‡]*Department of Plant Molecular Biology, Faculty of Biology and Medicine, University of Lausanne, 1015 Lausanne, Switzerland and the* [§]*Department of Biochemistry, University of Zurich, 8057 Zurich, Switzerland*

Background: Hsp110s are considered as mere nucleotide exchange factors of the Hsp70s.
Results: Human cytosolic Hsp110s can use ATP to unfold misfolded polypeptides and act as equal partner with Hsp70 to solubilize stable protein aggregates.
Conclusion: Hsp110s are Hsp70-like polypeptide unfolding chaperones.
Significance: Hsp110s are powerful disaggregating chaperones that can collaborate with Hsp70s to detoxify misfolding proteins in degenerative diseases.

Structurally and sequence-wise, the Hsp110s belong to a subfamily of the Hsp70 chaperones. Like the classical Hsp70s, members of the Hsp110 subfamily can bind misfolding polypeptides and hydrolyze ATP. However, they apparently act as a mere subordinate nucleotide exchange factors, regulating the ability of Hsp70 to hydrolyze ATP and convert stable protein aggregates into native proteins. Using stably misfolded and aggregated polypeptides as substrates in optimized *in vitro* chaperone assays, we show that the human cytosolic Hsp110s (HSPH1 and HSPH2) are *bona fide* chaperones on their own that collaborate with Hsp40 (DNAJA1 and DNAJB1) to hydrolyze ATP and unfold and thus convert stable misfolded polypeptides into natively refolded proteins. Moreover, equimolar Hsp70 (HSPA1A) and Hsp110 (HSPH1) formed a powerful molecular machinery that optimally reactivated stable luciferase aggregates in an ATP- and DNAJA1-dependent manner, in a disaggregation mechanism whereby the two paralogous chaperones alternatively activate the release of bound unfolded polypeptide substrates from one another, leading to native protein refolding.

Under optimal *in vitro* conditions, such as low protein concentrations and low temperature, the primary amino acid sequences may contain all the necessary information for small unfolded polypeptide chains to spontaneously reach their native three-dimensional structure (1). However, the cytoplasm of human cells may contain as much as 200 mg/ml proteins (2, 3), a highly crowded environment that may interfere with the productive native folding pathway of *de novo* synthesized or translocated multidomain polypeptides and with the proper refolding of stress-unfolded polypeptides (4–6). When a new polypeptide chain exits the ribosome or an organellar import pore or when a labile native protein becomes transiently heat- or cold-denatured, it may transiently unfold and expose hydrophobic segments to the aqueous environment (7, 8). It may then seek higher stability either by refolding to the native state or by generating non-native intramolecular misfolded structures, predominantly short β-strands with exposed hydrophobic residues (8). Depending on the intensity and duration of a stress and the degree of hydrophobic exposure, the misfolded monomers may then further proceed into the misfolding pathway by seeking intermolecular hydrophobic associations, leading to the formation of various insoluble disordered complexes, generally termed aggregates, that may further condense *in vitro* into compact protofilaments and insoluble fibrils, or *in vivo*, into tangles, protofibrils, and extracellular amyloids (7, 9–11). Stable misfolded monomers, such as freeze-thaw-inactivated luciferase (FTluc)[2] (12) or freeze-thaw-inactivated rhodanese (8, 13), may thus serve as the start points of an alternative protein misfolding and aggregation pathway, which, at variance with the native folding pathway, may be toxic to animal cells, neurons in particular (10, 14, 15). Because of their high surface-to-volume ratio, intermediate misfolded proteins, such as stable soluble aggregates (16) and protofibrils, may be among the most toxic species (17), causing mammalian cell leakage, inflammation-induced oxidative stress, apoptosis, and tissue loss in neurodegenerative diseases such as Alzheimer, Huntington, and Parkinson diseases, amyotrophic lateral sclerosis, and aging in general (10, 17, 18).

Opportunely, both prokaryotes and eukaryotes have evolved a complex network of chemical and protein chaperones (19, 20), which can prevent the conversion of stress-labile native proteins into toxic aggregates. Moreover, proteotoxic species that already formed can be actively converted by disaggregating and unfolding chaperones into harmless natively refoldable proteins or be degraded by chaperone-gated proteases into reusable amino acids (14). Therefore, stress-induced or crowd-

* This work was supported in part by the Faculty of Biology and Medicine of Lausanne University of Lausanne and by Grant 31003A-140512/1 from the Swiss National Fund.
[1] To whom correspondence should be addressed. E-mail: Pierre.Goloubinoff@unil.ch.

[2] The abbreviations used are: FTluc, freeze-thaw inactivated luciferase; PDB, Protein Data Bank; SBD, substrate-binding domain; ThT, thioflavin T; Luc, luciferase; NEF, nucleotide exchange factor; NBD, nucleotide-binding domain.

ing-induced protein misfolding and aggregation can be efficiently counteracted by a network of so-called "holding" chaperones that upon binding to exposed hydrophobic residues on the surface of the misfolded polypeptides can prevent the formation of large aggregates (21–24). However, with the exception of the small Hsps, the other canonical families of molecular chaperones are ATPases with demonstrated abilities to act as polypeptide unfolding enzymes. Thus, even without ATP, apoGroEL and apoCCT chaperonins can act as effective enzymes, unfolding metastable misfolded monomeric species and thus averting further proceeding into the misfolding pathway and instead promoting native refolding (10, 12, 13, 24). Other molecular chaperones, such as Hsp104 and Hsp70, are strict ATP-dependent polypeptide unfoldases that can disentangle stable protein aggregates and unfold stable misfolded monomeric polypeptides species. Thus, Hsp70 (DnaK; the names of the *Escherichia coli* proteins are shown in parentheses), co-chaperoned by Hsp40 (DnaJ), regulated by nucleotide exchange factors (GrpE), and the disaggregating co-chaperone Hsp104 (ClpB) can use the energy of ATP hydrolysis to scavenge stable insoluble aggregates and unfold stably misfolded polypeptides by binding, clamping, and pulling apart entangled misfolded structures and whole polypeptides (12, 25–27).

Whereas in bacteria, chloroplasts, mitochondria, and the cytosol of plants and yeast, Hsp104/ClpB type chaperones can use their hexameric ring structure to pull apart stably entangled polypeptides in aggregates and collaborate with Hsp70 to recover native proteins, animal cells lack obvious Hsp104 orthologs. However, animal cells are not devoid of disaggregating chaperones, because recent *in vivo* and *in vitro* data showed that the mammalian Hsp110 (HSPH2, Apg-2) can act in synergy with Hsp70 (HSPA8, Hsc70) and Hsp40 (Ydj1, DNAJB1) to catalyze the ATP-dependent disentanglement, solubilization, and native refolding of various stable protein aggregates (28, 29).

The human cytosol contains three distinct Hsp110s: HSPH2 (Apg-2), HSPH1 (Hsp105), and HSPH3, present in 800, 510, and 130 copies per cubic micron of HeLa cell, respectively (28). Amounts and stoichiometries indicate that ~15% of the cytosolic Hsp70 pool may be involved in the formation of Hsp70-Hsp110-dependent disaggregating machineries (3). Here, we tested with stringent *in vitro* refolding assays the chaperone activity of purified recombinant human HSPH1 in various combinations with HSPA1A and DNAJA, which are abundant cytosolic members of the Hsp70/110/40 chaperone family in human cells (3). This allowed us to assess the precise mechanistic contribution of Hsp110, individually as an independent molecular chaperone and as a possible chaperone that reciprocally collaborate with Hsp70 in the *in vitro* unfolding and reactivation of stable misfolded species and the disaggregation of extensively damaged protein substrates preformed in the absence of chaperones (12, 28, 29). We found that Hsp110 is by itself a *bona fide* ATP-dependent unfolding chaperone that can catalyze the unfolding of stable misfolded polypeptides and thus favor the conversion of stable, high affinity misfolded substrates in to stable low affinity native products of the chaperone reaction. Interestingly, even without ATP, Hsp110 could activate the release of a prebound luciferase substrate from Hsp70, and reciprocally Hsp70 could activate the release of a prebound luciferase substrate from Hsp110. Titration of the ATP- and HSP40-dependent luciferase refolding activity in the presence of various relative amounts of Hsp110 and Hsp70 showed optimal disaggregation activity at a 1:1 ratio. Confirming earlier *in vivo* and *in vitro* evidence with human HSPH2, yeast YDJ1, or the other major cytosolic human DNAJB1 (28, 29), our *in vitro* results mainly with HSPH1 (Hsp105) and DNAJA1 show that the cytosol and likewise the endoplasmic reticulum of mammalian cells contain powerful Hsp110/Hsp70 bichaperone machineries that can unfold and solubilize stably misfolded and aggregated protein species to combat the onset of protein conformational diseases.

EXPERIMENTAL PROCEDURES

Cloning—HSPA1A (HSP70, HsCD00002890) and DNAJA1 (HSP40, HsCD00002610) were amplified from cDNA, using following set of primers: HSPA1A forward, 5′-ATGATGGGCTCTTCTCATCATCATCATCATTCTTCTGGCCTGGTTCCGCGTGGCTCTCATATGGCCAAAGCCGCGGCGATCGGCATCG-3′; HSPA1A reverse, 5′-CGTGGCCACTAGTCTAATCCACCTCCTCAATGG-3′; DNAJA1 forward, 5′-ATGATGGGCTCTTCTCATCATCATCATCATTCTTCTGGCCTGGTTCCGCGTGGCTCTCATATGGTGAAAGAAACAACTTACTACG-3′; and DNAJA1 reverse, 5′-CGTGGCCACTAGTTTAAGAGGTCTGACACTGAACACCACCTC-3′. The PCR product with the N-terminal His_6 tag and the thrombin cleavage site was cloned in between restriction sites NcoI and SpeI of the pSE420 expression vector (Invitrogen) using BspHI and SpeI at the 5′ and 3′ ends of the amplified PCR product.

Purification of His-tagged HSPA1A, DNAJA1, Luciferase, and HSPH1—E. coli DH5α cells transformed with pSE420 vector carrying HSPA1A and DNAJA1 were grown in LB medium with 100 μg/ml ampicillin at 37 °C. 0.6 mM isopropyl β-D-thiogalactopyranoside (Sigma-Aldrich) was added at OD 0.6, and 12 h later, the cells were harvested by centrifugation at 6000 rpm. Cell pellet was resuspended and sonicated in Buffer A (20 mM sodium phosphate buffer, pH 7.5, and 500 mM NaCl, supplemented with phenylmethanesulfonyl fluoride (Sigma-Aldrich). The lysate was centrifuged at 16,000 rpm (JA 25.50 rotor, Beckman J2-21 centrifuge) for 30 min, and supernatant was filtered though a 0.2-μm membrane and loaded onto a nickel affinity column (HisPrep FF 16/10; GE Healthcare) with buffer A. After loading, column was extensively washed (30–40 column volumes). The bound protein was eluted with linear gradient of 10–500 mM imidazol in buffer A. The purity of the fractions was confirmed on SDS-PAGE. Proteins were concentrated and stored in 20 mM Tris-HCl, pH 7.5, 10% glycerol, and 200 mM NaCl at −80 °C.

Cells harboring pET28a-HSP110 (Hsp105) plasmid (a gift from Dr. E. Lafer Department of Biochemistry, The University of Texas Health Science Center) were preincubated overnight at 37 °C on LB kanamycin (50 μg/ml) and chloramphenicol (34 μg/ml) plates. Cells from the plate were transferred to autoinduction media (for 1 liter: 10 g of tryptone, 5 g of yeast extract, 5 g of glycerol, 0.5 g of glucose, 2 g of lactose, 26.8 ml of 0.1 g/ml NH_4Cl, 2 ml of 1 M $MgSO_4$), then 100 ml of sterilized 10× salt

solution (stock: 35.49 g of Na_2HPO_4, 34.02 g of KH_2PO_4, 7.1 g of Na_2SO4) and kanamycin (50 μg/ml) were added, and cells were grown at 30 °C for 24 h. Afterward, the cells were harvested and sonicated in 20 mM sodium phosphate buffer, pH 8, and 300 mM NaCl, 0.2% Triton X-100, PMSF, and centrifuged at 16,000 rpm; supernatant was filtered and loaded onto previously equilibrated nickel affinity column. After loading, the column was extensively washed (30–40 column volumes) with wash buffer (20 mM sodium phosphate buffer at pH 8.0, 20 mM imidazole, and 500 mM NaCl), and the pure protein was eluted using elution buffer (20 mM sodium phosphate buffer at pH 8, 100 mM imidazole, and 500 mM NaCl). After confirming on SDS-PAGE, pure fractions were pooled, buffer was exchanged into storage buffer (20 mM Tris-HCl at pH 8, 100 mM NaCl, 5% glycerol, and 3 mM DTT), concentrated, and stored at −80 °C. DnaK and Luciferase was purified as in Ref. 12. DnaJ and GrpE of *E. coli* were a gift from Dr. H. J. Schönfeld (Pharmaceutical Research, F. Hoffman-La Roche Ltd., Basel, Switzerland).

Luciferase Assays—Luciferase activity was measured as described previously (12) using a Victor Light 1420 Luminescence Counter from PerkinElmer Life Sciences.

Immunoblotting—FTluc samples were incubated with chaperones in the presence of ATP; aliquots were taken at different time intervals and treated with trypsin for 2 min and immediately mixed with loading dye; and samples were incubated at 95 °C for 2 min, run on SDS-PAGE, and electrotransferred onto a 0.2-μm nitrocellulose membrane (Bio-Rad). Following seven 5-min rinses in TTBS, the membrane was incubated in primary goat luciferase antibody in TTBS (1:20,000; Sigma-Aldrich) for overnight, followed by secondary donkey HRP-goat antibody. The membrane was washed and then developed using the chemiluminescent Immunstar™ kit (Bio-Rad) according to the manufacturer's instructions.

Measurement of ATP Consumption—The ATP content ([2,5′,8-^{3}H]ATP from Amersham Biosciences) of the refolding solution supplemented with 0.5 μM Hsp70, 0.5 μM Hsp110, 0.25 μM Hsp40, 100 μM ATP, and 0.5 μM luciferase (FTLuc) was determined as a function of time at 25 °C. At 50–60-s intervals over a time period of 7 min, 5-μl aliquots were taken and processed as explained elsewhere (12).

Thioflavin T Binding—Thioflavin T (ThT) binding of luciferase was measured in the presence of 60 μM ThT as in Ref. 12 (excitation, 435 nm; and emission, 465 nm) using a PerkinElmer Life Sciences LS55 fluorescence spectrometer.

Protein Structural Analysis—Protein structures of Hsc70-Sse1 (Protein Data Bank (PDB) code 3C7N) complex and DnaK/Hsp70 (PDB code 4B9Q, 2KHO) were taken from PDB and by using PyMOL molecular graphics system, Hsc70 NBD was structurally aligned with the structure of ADP-bound DnaK (PDB code 2KHO) or ATP-bound DnaK/Hsp70 (PDB code 4B9Q). Based on the analogy of DnaK structure, the substrate-binding domain (SBD) of Sse1 was superimposed to match the SBD structure of ADP-bound DnaK/Hsp70.

RESULTS

Human Hsp110 Cooperates with Hsp40 to Prevent Protein Aggregation in an ATP-dependent Manner—We tested the ability of purified recombinant Hsp110 (HSPH1) to prevent the aggregation of native firefly luciferase, which is mildly thermolabile. When native luciferase was incubated at 34 °C without chaperones and ATP or with equimolar Hsp40 or Hsp110, it lost activity at similar rates of 2.4 ± 0.2% per minute. The presence of both Hsp40 and Hsp110 slightly slowed down luciferase denaturation, as expected from a mild nonspecific protective effect caused by the presence of native proteins (Fig. 1, *A* and *B*). Whereas ATP alone did not stabilize the heat-denaturing native luciferase, in the presence of ATP and Hsp40 (DNAJA1), Hsp110 drove the transient net reactivation of up to 120% of the initial luciferase activity during the first 10 min, indicating that the original native luciferase stock contained at least 20% of misfolded inactive chaperone-amenable luciferase species (13). Thereafter, the luciferase activity flattened and steadily decreased at the same rate, yet at a constant higher level by 35%, compared with without chaperones and ATP (Fig. 1*D*). Online light scattering measurements showed that without ATP, the presence of Hsp110, or of Hsp40 was mildly yet significantly effective at passively preventing the aggregation of the denaturing luciferase species. Together, their effect was additive (Fig. 1*A*), confirming that like Hsp70, the protein-binding domain of Hsp110 can also bind aggregating polypeptides. In the presence of ATP, Hsp110 or Hsp40 individually remained mildly effective at preventing the luciferase aggregation as without ATP. Remarkably, in the presence of ATP, Hsp110 together with Hsp40 became strongly synergic at preventing luciferase aggregation (Fig. 1*C*). A similar synergic ATP-dependent prevention of aggregation has been previously shown in the case of bacterial DnaK and DnaJ (24) and was also confirmed here with human Hsp70 (HSPA1A) and Hsp40 (Fig. 1*G*). Thus, Hsp110 is functionally indistinguishable from its structurally related Hsp70 and DnaK paralogs. This is also strong evidence that the Hsp40 co-chaperone undergoes an ATP-driven specific interaction with Hsp110, as it does with Hsp70.

The transient luciferase reactivation that we observed during the first 10 min of the reaction with the particular Hsp110 + Hsp40 + ATP combination (Fig. 1*D*) suggested that Hsp110 is a *bona fide* Hsp40- and ATP-dependent chaperone that can drive the transient renaturation of a misfolding protein against the general tendency of the substrate at 34 °C to remain inactive and become increasingly aggregated. Hsp70, Hsp40, and ATP presented the same ability to transiently protect and reactivate the heat-denaturing luciferase (Fig. 1*F*), implying that under the conditions of the *in vitro* assay, the Hsp110 was an Hsp40-dependent, ATP-fueled antiaggregation reactivating chaperone, functionally indistinguishable from its structurally related Hsp70 paralog.

Human Hsp110 Is a Bona Fide Polypeptide Unfolding/Refolding Chaperone—We next addressed the ability of Hsp110 (HSPH1) to act upon stable inactive misfolded luciferase monomers (FTluc), which were prepared beforehand without chaperones by iterative cycles of freeze-thawing (12) and convert them at 22 °C into native luciferase. Whereas ATP and/or Hsp40 (DNAJA1) alone did not cause a significant net native refolding of FTluc (Fig. 2*A*), the presence of equimolar Hsp110 with ATP regenerated a net 12% (120 nM) of native luciferase in 60 min. Remarkably, in the presence of Hsp40 (0.5 μM) and ATP, Hsp110 (1 μM) produced a net 44% (440 nM) of native

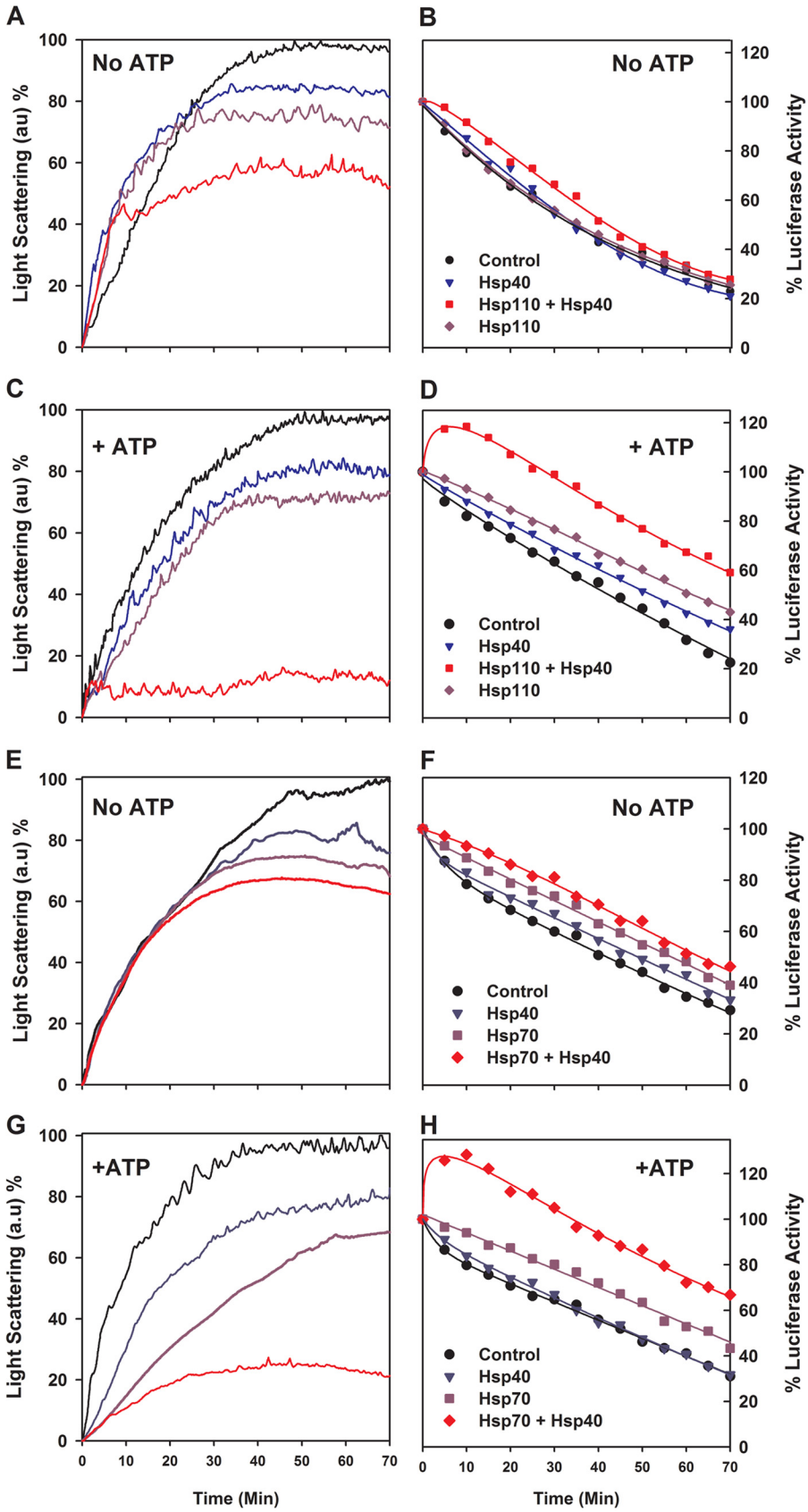

FIGURE 1. **Hsp110 (HSPH1) and Hsp40 (DNAJA1) are synergic at preventing aggregation and transiently reactivating thermo-labile luciferase.** *A–D*, native luciferase (1 μM) was incubated at 34 °C without or with Hsp110 (1 μM) and/or Hsp40 (0. 5 μM), without (*A* and *B*) or with (*C* and *D*) 5 mM ATP. Light scattering at 550 nm (*A* and *C*) and luciferase activity (*B* and *D*) were measured online during exposure to 34 °C. *E–H*, similarly, Hsp70 and Hsp40 are synergic at preventing aggregation and transiently reactivating thermolabile luciferase at 34 °C.

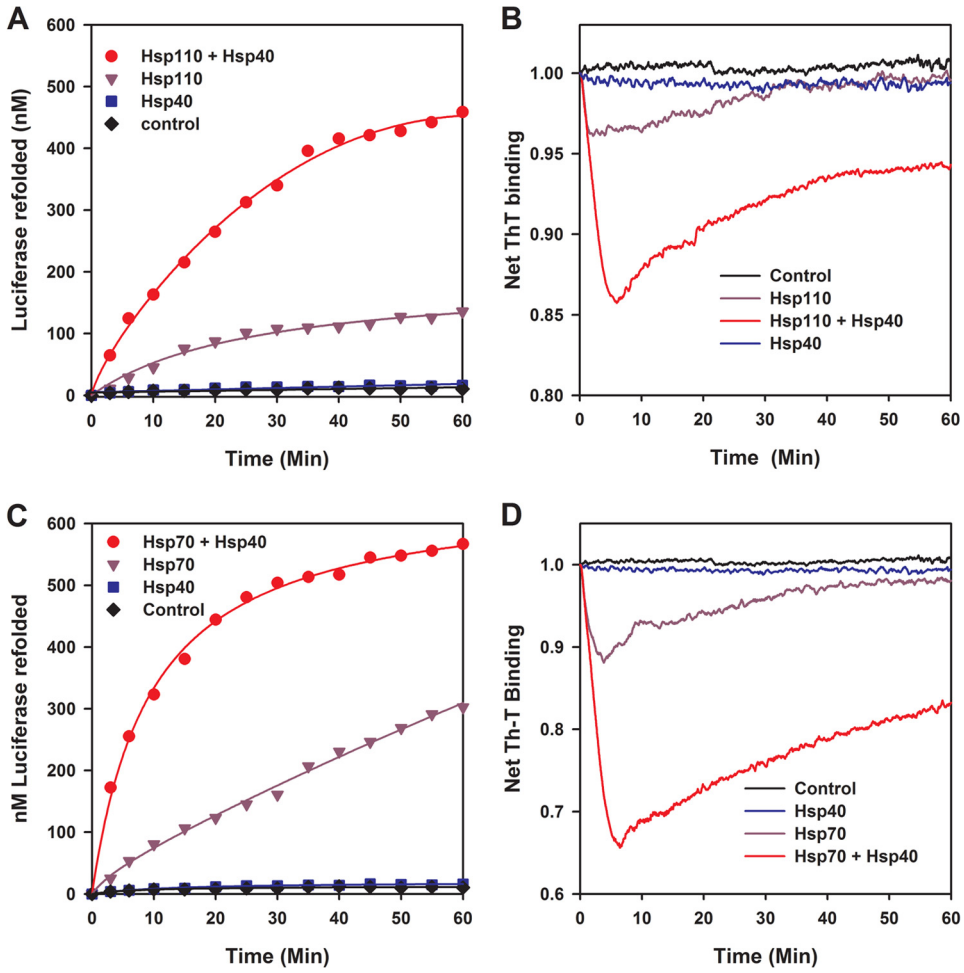

FIGURE 2. **Hsp110 (HSPH1) is an Hsp40- and ATP-dependent polypeptide unfolding/refolding chaperone similar to Hsp70.** *A* and *B*, the activity (*A*) and the net ThT fluorescence (*B*) of stable misfolded FT luciferase (1 μM) were measured online at 22 °C in the presence of ThT (60 μM) at various time points as indicated, in the absence (*black*) or presence of ATP (5 mM) with Hsp110 alone (1 μM, *purple*), Hsp40 (DNAJA1) alone (0.5 μM, *blue*), or both Hsp110 + Hsp40 (*red*). *C* and *D*, the activity (*C*) and the net ThT fluorescence (*D*) of stable misfolded FT luciferase (1 μM) measured online without (*black*) or with ATP as in *A* and *B*, in the presence of Hsp70 alone (1 μM, *purple*), Hsp40 alone (0.5 μM, blue), or both Hsp70 and Hsp40 (*red*).

luciferase, demonstrating that alone but preferably when assisted by Hsp40, Hsp110 can use the energy of ATP hydrolysis to convert stable preformed misfolded polypeptide species into their stable native state. Similar specific assisted refolding results were obtained when we used urea predenatured malate dehydrogenase or stable pre-heat-denatured G6PDH aggregates (Fig. 3, *A* and *B*). Thus, the chaperone activity of Hsp110 (Hsp105, HSPH1) is not limited to the special case of stable inactive FTluc monomers. Noticeably, using FTluc as substrate, Apg-2 (HSPH2) and DNAJB1, which are respectively the other most abundant human cytosolic Hsp110 and Hsp40, were found to be as effective refolding chaperones as HSPH1 and DNAJA1 (Fig. 3*C*). This was not unexpected, given that the human Apg-2 (HSPH2), together with DNAJB1 or yeast YDJ1 have recently been shown *in vivo* and *in vitro* to act in synergy with Hsc70 (HSPA8) at disaggregating preformed protein aggregates (28, 29). Thus, we show here that Apg-2 is as a *bona fide* ATP-fueled chaperone on its own, as HSPH1. Without Hsc70, Apg-2 may also use ATP to drive the conversion of stable misfolded polypeptide substrates into natively refolded products.

ThT is a fluorescent dye that specifically binds cross-β structures, both in native proteins, but more strongly and specifically in misfolded polypeptides entangled within dense protein aggregates, fibrils, and amyloids (30, 31). Because ThT does not interfere with chaperone activity (12, 24), this allows online measurements of the net time-dependent changes in the misfolded β-structures of the substrates during the chaperone reaction. When the Hsp110-mediated Hsp40-dependent refolding reaction as in Fig. 2*A* was carried in the presence of excess ThT, online fluorescence showed that addition of ATP at $T = 0$ min caused a sharp decrease in the net amount of ThT-binding sites in the misfolded FTluc, indicating that the chaperone caused a massive ATP-dependent loss of misfolded structures and the unfolding, at least in part of the FTluc (Fig. 2*B*). After 5 min, during which 130 nM luciferase became natively refolded, the decrease of ThT fluorescence leveled, and a net regain of ThT-binding structures was observed, alongside a parallel regain of up to 440 nM of native luciferase. The reactivation profiles confirmed that Hsp110 alone with ATP (but not Hsp40 alone with ATP) had a significant unfolding activity, whose maximal yield at 5 min was ~4.5 times lower than when

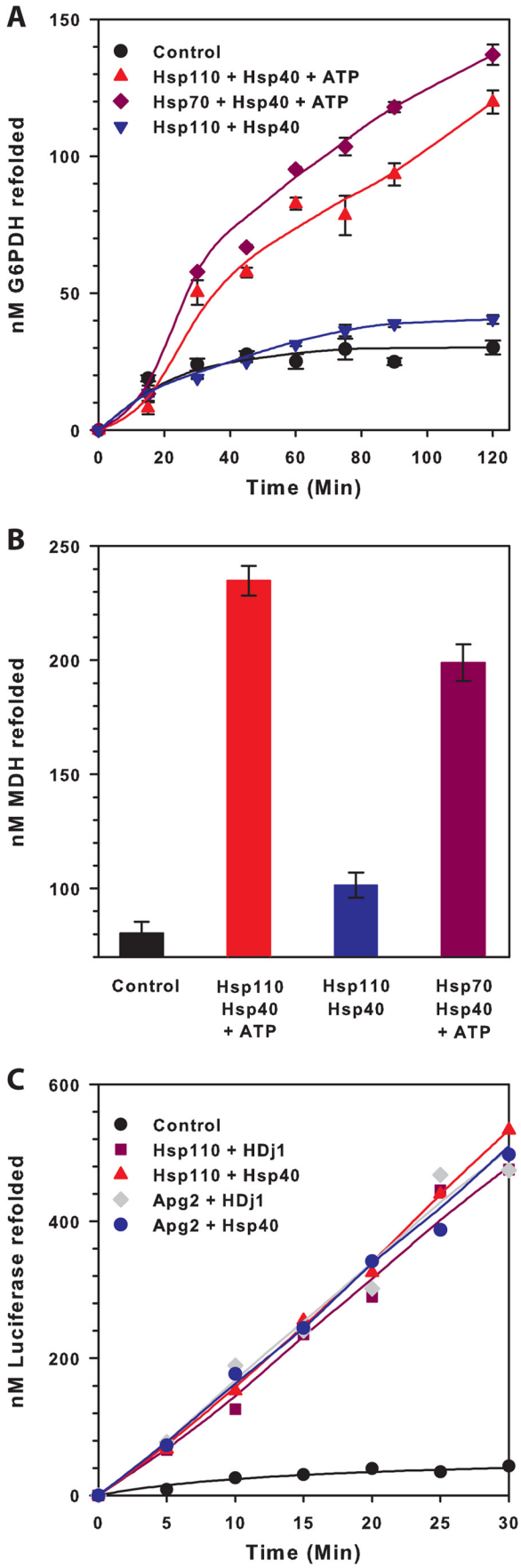

FIGURE 3. **Various Hsp110s and Hsp40s can collaborate to reactivate various misfolded protein substrates.** *A*, time-dependent refolding of thermally predenatured G6PDH following 30 min of incubation at 30 °C without or with ATP, 6 μM Hsp70 or Hsp110 (HSPH1), without or with 3 μM DNAJA1, as indicated. *B*, refolding yields of urea-preunfolded MDH (600 nM final concentration) at 34 °C. 60 μM MDH was incubated 30 min at 34 °C in 8 M urea and diluted 100-fold in refolding buffer also containing 5% glycerol, without or with 4 μM Hsp70, or Hsp110 (Hsp105) and 2 μM DNAJA1, as indicated. *C*, time-dependent refolding of 1 μM FTluc without or with ATP, 1 μM Apg-2 or Hsp105, and 0.5 μM DNAJA1 or DNAJB1. The protein combinations are indicated.

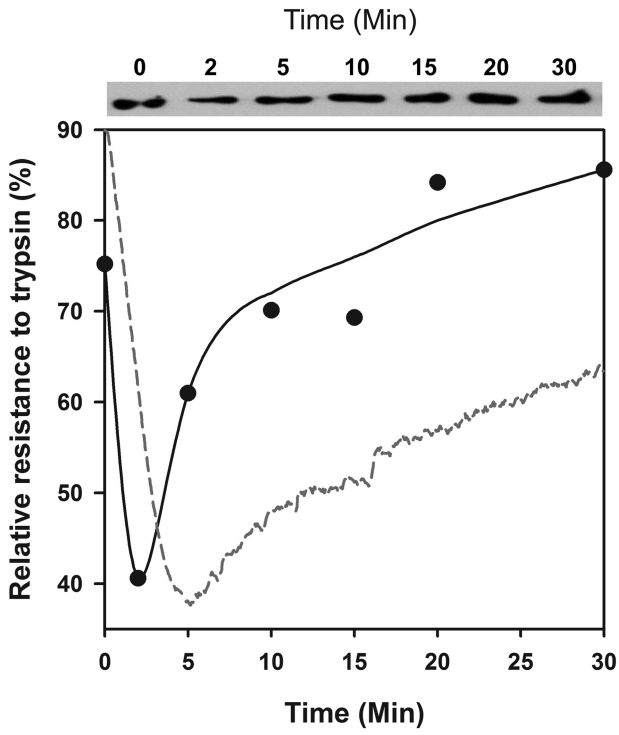

FIGURE 4. **Trypsin treatment of misfolded monomeric luciferase revealed unfolding by Hsp110/Hsp40.** *Upper panel*, Western blots of trypsin-treated luciferase. At the indicated time points of the Hsp110 + Hsp40 + ATP-dependent refolding reaction as in Fig. 2*A*, the samples were treated for 3 min with 0.04 mg/ml trypsin, separated on SDS gel, and detected on Western blots with luciferase antibodies. *Lower panel*, the relative semiquantitative luciferase signal at 60 kDa from the Western blot (*plain circles*). The relative net ThT fluorescence signal of FTluc under the same conditions from Fig. 2*B* is shown for comparison (*red dotted line*).

Hsp40 was also present. When in the same chaperone assay Hsp110 was replaced by Hsp70, slightly faster reactivation rates but overall similar refolding yields (Fig. 2*C*) and time-dependent ThT changes in the luciferase substrate were observed (Fig. 2*D*). Thus, as already shown with bacterial DnaK (12), both human cytoplasmic Hsp70 and Hsp110 can independently act as efficient polypeptide unfolding enzymes that use ATP hydrolysis to convert stable misfolded polypeptide substrates into stable natively refolded protein products.

Partial trypsin digestions for 2 min at various time points of the reaction and Western blots of SDS gels (Fig. 4) confirmed that Hsp110 is an ATP-dependent polypeptide-unfolding chaperone. Whereas at $T = 0$ min, FTluc was 75.2% trypsin-resistant, following addition of Hsp110 + Hsp40 + ATP, trypsin resistance dropped at $T = 5$ min to 40.6% and thereafter recovered to 85.6% within 30 min. Thus, confirming the chaperone-mediated transient loss of ThT binding misfolded β-sheets in the FTLuc substrate, partial trypsin digestions showed a transient loss of the FTLuc compactness under the

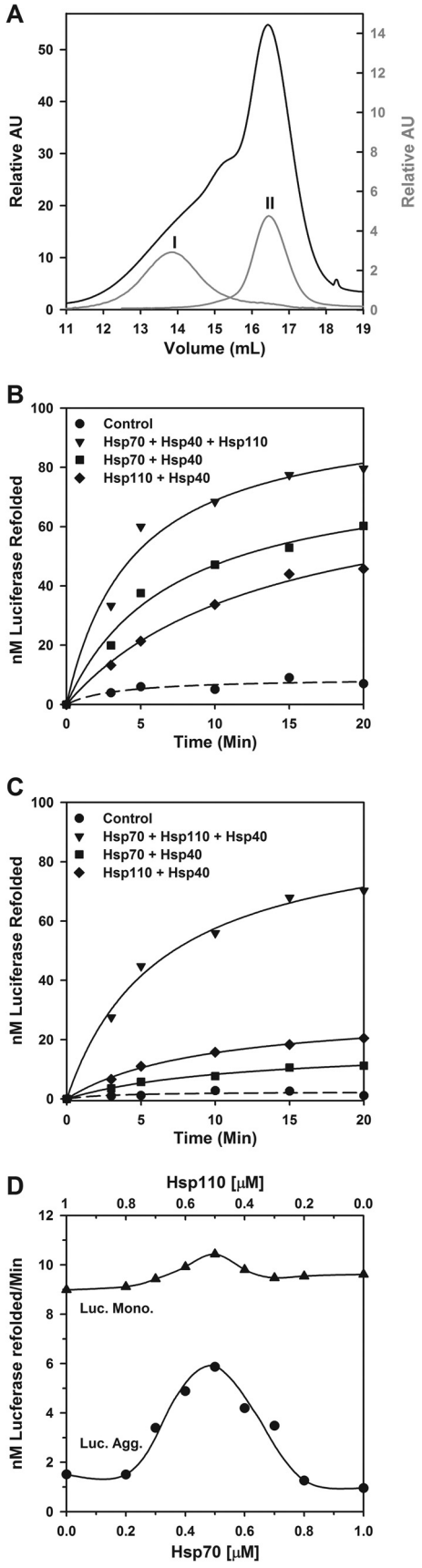

FIGURE 5. **Hsp110 (HSPH1) collaborates with Hsp70 (HSPA1A) to convert stable luciferase aggregates into native species.** *A*, purification and confirmation of freeze-thawed luciferase aggregates (fraction I) and monomers (fraction II). *B* and *C*, soluble monomeric misfolded FTluc (0.5 μM) from fraction II (*B*) or soluble oligomeric aggregates of FTluc monomers from fraction II (*C*) was incubated at 22 °C as in the presence of 5 mM ATP, 125 nM Hsp40, and either 250 nM Hsp70 alone (■) or 250 nM Hsp110 alone (♦) or 125 nM Hsp70 together with 125 nM Hsp110 (▼), as indicated. *D*, the rates of reactivation of monomeric FTluc (▲) or oligomeric FTluc (●) in the presence of 5 mM ATP, 0.5 μM Hsp40, and increasing concentrations of Hsp70 (0–1 μM) supplemented by corresponding decreasing concentrations of Hsp110 maintaining the sum of Hsp70 and Hsp110 molecules at 1 μM. *Luc.*, luciferase; *Mono.*, monomer; *Agg.*, aggregate.

combined ATP-fueled action of Hsp110, Hsp40, despite the additional chaperones that were also competing for the limiting amounts of trypsin. The subsequent regain of luciferase trypsin resistance, which paralleled that of ThT rebinding and regained luciferase activity (Fig. 2*B*), confirmed that the natively refolded chaperone product was, as expected, more compact than the chaperone-unfolded intermediate.

Equimolar Hsp110 and Hsp70 Form an Optimal Bi-chaperone Disaggregating Machine—A slow significant disaggregating activity has been demonstrated for mammalian Hsp110 (Apg-2, HSPH2) and Hsc70 (HSPA8), which dissolved large disordered aggregates but failed to act on α-synuclein fibrils (29). We thus next addressed the ATP-dependent chaperone activity of both human cytoplasmic Hsp110 (HSPH1) and Hsp70 (HSPA1A) in the presence of Hsp40 (DNAJA1), using two different substrates: stable oligomeric FTluc aggregates, which eluted on gel filtration with an apparent molecular weight of soluble 4–12-mers (fraction I; Fig. 5*A*), or misfolded FTluc monomers that eluted last (fraction II; Fig. 5*A*). At equal protomer concentrations, light scattering and ThT fluorescence of the various gel filtration fractions (data not shown) showed that, as initially demonstrated by analytical ultracentrifugation, the monomeric FTluc fraction was composed mostly of stable misfolded luciferase monomers that bound 1.8 times more ThT than native luciferase (12) but, similar to the native monomeric luciferase, did not scatter light. In contrast, the oligomeric fraction, although containing as many ThT binding misfolded structures, scattered light five times more than the monomeric species (data not shown). When 2 h after their first elution the 10-fold diluted oligomers were reinjected on the same column, at least 95% eluted at the same positions as the original oligomers, and the remaining 5% eluted at the same position as monomer (Fig. 5*A*, *peak I*), confirming that although soluble, the luciferase aggregates were stable and mostly dilution-resistant.

When the monomeric misfolded luciferase species (fraction II) were incubated with Hsp70 (HSPA1A), Hsp40 (DNAJA1), and ATP, a net minor amount of 50 nM native Luc was produced within 20 min, and similarly, Hsp110 (HSPH1) with ATP and Hsp40 produced 40 nM native Luc (Fig. 5*B*). In contrast, an equimolar mixture of half as concentrated Hsp70 and Hsp110 with Hsp40 and ATP produced 75 nM luciferase, *i.e.*, nearly twice more than the average yield of 45 nM expected if the two chaperones were acting independently from one another. Hsp70, Hsp40, and ATP produced only 5 nM of net native luciferase from stable aggregated species, as expected from less amenable aggregated substrates. Hsp110, Hsp40, and ATP produced twice more native protein than Hsp70, suggesting that Hsp110, by itself, may be slightly more competent a chaperone

to process large oligomeric misfolded polypeptides than Hsp70 (Fig. 5*C*). Remarkably, an equimolar mixture of half as concentrated Hsp70 and Hsp110 molecules produced 70 nM native luciferase, which was nine times higher than the expected average yield of 7.5 nM if the two chaperones were acting independently from one another. This strongly suggests that Hsp110 forms a functional complex with Hsp70, combining their individual chaperone unfolding abilities into a unique synergic polypeptide disentangling and unfolding mechanism to convert stable protein aggregates in native proteins.

Further addressing the optimal stoichiometry in the 1:1 Hsp110:Hsp70 disaggregating machinery, we measured the initial rates of luciferase reactivation, either with stable misfolded FTluc monomers as substrates or with stable misfolded FTluc oligomers, in the presence of increasing concentrations of Hsp70 (0–1 μM), supplemented with the corresponding decreasing concentrations of Hsp110 (1–0 μM) to keep a constant chaperone concentration of 1 μM. As initially observed in Fig. 5*A*, the reactivation rates of misfolded FTluc monomers by individual Hsp70, or individual Hsp110 were nearly equally high: ~9 nM min^{-1} with a minor optimal rate of 10.3 nM min^{-1} observed at equimolar Hsp70:Hsp110 (Fig. 5*D*, *upper line*). Whereas the reactivation rates of misfolded Luc oligomers by individual Hsp70 or Hsp110 was expectedly low in both cases (~1–1.5 nM min^{-1}), as the stoichiometry between Hsp70 and Hsp110 approached 1:1, the reactivation rates increased 5-fold, to reach up to 55% of the optimal rates obtained with misfolded FTluc monomers (Fig. 5*D*, *lower line*). Thus, corroborating the crystal 1:1 heterocomplexes between bovine Hsc70 and yeast Hsp110 (SSE, 32), the human Hsp110 (Hsp105) can form in solution with Hsp70 a functional 1:1 bichaperone complex to disaggregate proteins.

Hsp70 and Hsp110 Mutually Catalyze Substrate Release from One Another—We next assessed the ability of Hsp110 (HSPH1) to act as a presumed nucleotide exchange factor (NEF) of Hsp70 (33, 34). Because a NEF, by definition, should catalyze the ATP-dependent release of ADP and of polypeptide substrates from stable preformed (ADP-Hsp70-substrate) complexes, we use a simplified protocol from Ref. 12 in which FTluc was first incubated for 2 min with Hsp40, ATP, and Hsp70 (Fig. 6*A*). Because of the high ATPase activity of Hsp70 with Hsp40 even in the absence of a NEF, Luc expectedly started to refold at ~15 nM min^{-1}. Addition at $T = 2$ min of apyrase sharply reduced by 10-fold the rate of luciferase refolding to 0.2 nM min^{-1}. Thus, the instantaneous destruction of the ATP molecules reduced as expected the release and refolding of the unfolded luciferase substrate from the so-called "locking" state of the ADP-bound Hsp70 chaperone (12). Whereas the subsequent addition at $T = 30$ min of an equimolar amount of free Hsp70 did not change the slow ATP-independent rate of luciferase release and refolding from the preformed ADP-Hsp70-Luc complex, addition of equimolar Hsp110 caused a dramatic release and spontaneous refolding of the Hsp70-bound FTluc, at a rate that was three times faster than the initial rate with ATP, although release and refolding at $T = 30$ min took place in the total absence of ATP (Fig. 6*A*). Thus, justifying in part why it was initially described as a NEF of Hsp70, we found that Hsp110 is not a true NEF, because ATP binding was

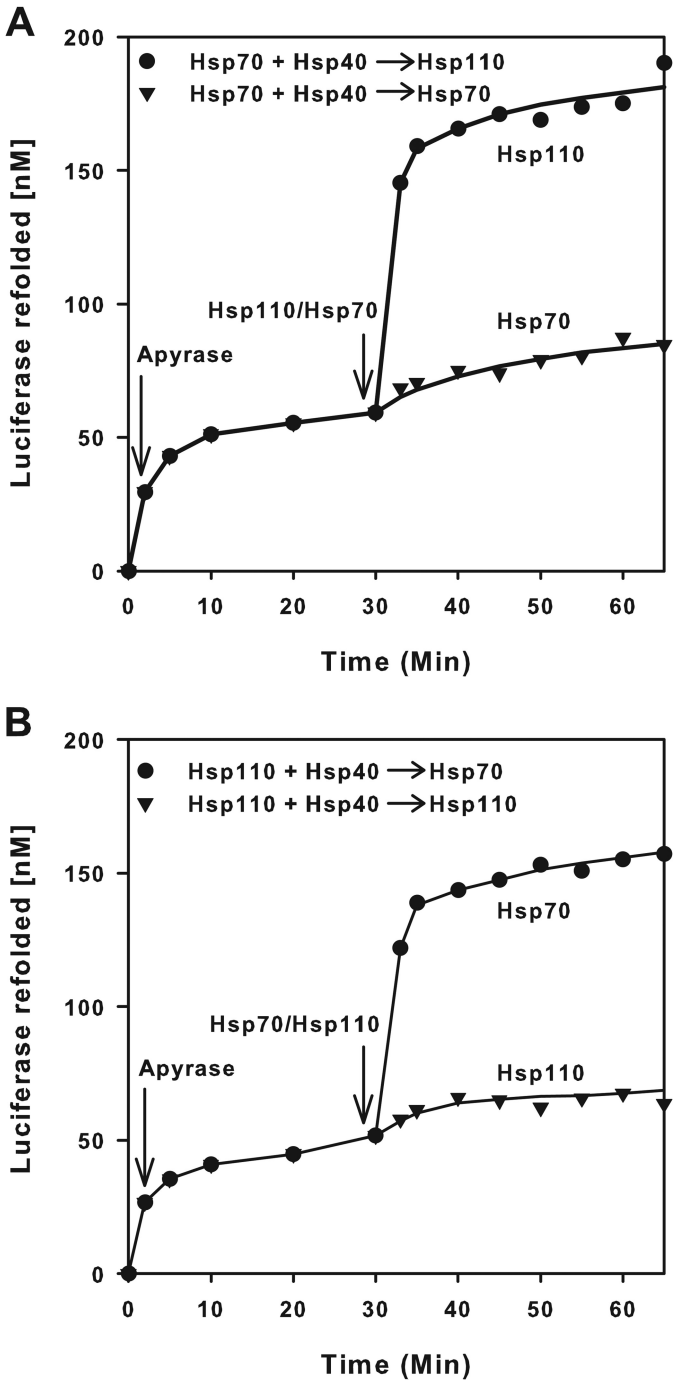

FIGURE 6. **Hsp70 (HSPA1A) and Hsp110 (HSPH1) mutually activate substrate release.** Misfolded luciferase monomers (1 μM) were supplemented with 0.1 mM ATP and Hsp70 (1 μM), Hsp40 (0.5 μM) (*A*), or Hsp110 (1 μM) and Hsp40 (0.5 μM) (*B*), and luciferase activity was followed in time. At $T = 2$ min, apyrase (2 μM) was added, which readily destroyed the ATP. At $T = 30$ min, 1 μM of Hsp110 in *A* and of Hsp70 in *B* was added, and luciferase activity was further measured up to $T = 65$ min.

apparently not necessary for its action upon Hsp70 as a substrate release factor. Surprisingly, swapping the roles between Hsp70 and Hsp110 in this experiment produced the same results. The addition at $T = 30$ min of equimolar amounts of free Hsp70 to apyrase-treated preformed Hsp110-Luc complexes caused a strong release and native refolding of the unfolded luciferase, whereas addition of substrate-free Hsp110

TABLE 1
Rate of ATP hydrolysis and ATP cost by various combinations of Hsp110, Hsp70, and Hsp40, without or with equimolar aggregated (Agg.) or misfolded monomeric (Mono.) luciferase (Luc.) substrates

Sample	ATP consumed by 500 nM chaperones only	ATP consumed by chaperones in the presence of substrates	ATP	Net ATP cost to refold a luciferase
	min^{-1}	*min*$^{-1}$	*chaperone*$^{-1}$ *min*$^{-1}$	
Hsp70	312		0.62	
Hsp110	252		0.50	
Hsp70 + Hsp40	624		1.25	
Hsp110 + Hsp40	516		1.03	
Hsp70 + Hsp110 + Hsp40	924		1.85	
Hsp70 + Hsp40 + Luc. Mono.		1392	2.78	77.45
Hsp110 + Hsp40 + Luc. Mono.		1644	3.29	168.6
Hsp70 + Hsp110 + Hsp40 + Luc. Mono		2772	5.54	148.9
Hsp70 + Hsp40 + Luc. Agg.		1536	3.07	650.7
Hsp110 + Hsp40 + Luc. Agg.		1890	3.8	485.4
Hsp70 + Hsp110 + Hsp40 + Luc. Agg.		2388	4.8	228.9

did not significantly affect the slow rate of luciferase release from Hsp110 (Fig. 6*B*). Thus, Hsp110 is symmetrically as much a substrate release factor for the Hsp70 unfolding chaperone as Hsp70 is a substrate release factor for the Hsp110 unfolding chaperone.

ATP Hydrolysis Assays Show Functional Interactions between Hsp110, Hsp70, Hsp40, and the Substrate—In the absence of substrate polypeptides, the highly conserved J-domain of Hsp40 spontaneously associates with the nucleotide-binding domain (NBD) of nucleotide-less or ATP-bound Hsp70 molecules, near the hinge region that connects the NBD to the SBD (35). Thus, even without a substrate polypeptide, DnaJ can activate futile ATP hydrolysis by bacterial Hsp70 (12, 36). Measures of steady state rates of ATP hydrolysis (Table 1) showed that the presence of Hsp40 expectedly nearly doubled the rate of ATP hydrolysis, both by Hsp70 alone and by Hsp110 alone. Thus, as previously shown in the case of SSE1 and Ydj1 (37), with regard to J-domain-induced ATPase activity, human Hsp110 is functionally indistinguishable from other *bona fide* Hsp70 chaperones.

Whereas, theoretically, half amounts of Hsp70 and Hsp110 (in the presence of constant Hsp40) should hydrolyze 1.1 ATP min^{-1}, they effectively hydrolyzed 1.8 ATP min^{-1} (Table 1). This 1.6-fold activation was in agreement with the refolding rates, suggesting that Hsp110 and Hsp70 form a functional 1:1 complex, and with the crystal structure of SSE1 with Hsc70 that showed that the two chaperones interact though their distal lobes in their respective NBDs, far away from where the J-domain of Hsp40 can bind Hsp110 or Hsp70.

Hsp110 ATPase Is Activated by FT Misfolded and Aggregated Luciferase Substrates—The ATPase activity of DnaK, with and without DnaJ and GrpE, has been shown to become activated severalfold upon binding of various short, mostly hydrophobic peptides (22, 38) and of artificially unfolded polypeptide substrates (39, 40), as well as of native polypeptide substrates, such as the σ32 (41). Here, we found that the ATPase rate of Hsp70 in the presence of Hsp40 was activated 2.2- or 2.5-fold by stable misfolded luciferase monomers or oligomers, respectively (Table 1). Similarly, the ATPase rate of Hsp110 (HSPH1) in the presence of Hsp40 (DNAJA1) was activated 3.2- and 3.7-fold by stable misfolded luciferase monomers or oligomers, respectively. Thus, with regard to substrate-induced ATPase activation, Hsp110 was functionally indistinguishable from a *bona fide* Hsp70 chaperone.

Although the luciferase aggregates were less efficiently refolded, they triggered the ATPase activity to a higher extent than the misfolded luciferase monomers, suggesting that there is more futile hydrolysis and that despite strong interactions with the chaperone, the misfolded oligomers are more resistant to ATP-fueled Hsp70- or Hsp110-mediated unfolding than the misfolded monomers. Theoretically, if equimolar Hsp70 and Hsp110 molecules were not collaborating with one another, 568 ATPs should be hydrolyzed while reactivating a single luciferase polypeptide entangled within a stable luciferase aggregate. We found that only 229 ATPs were hydrolyzed, indicating that the two chaperones collaborate in a way that increases the efficiency of ATP hydrolysis to unfold/refold stable protein aggregates (Table 1). In contrast, compared with the theoretical average of 123 ATPs, the equimolar mixture of Hsp110 and Hsp70 consumed 21% more ATP (149 ATPs) while reactivating a misfolded monomer, suggesting that the ATP-fueled unfolding/refolding of misfolded monomers does not require that the two chaperones collaborate.

DISCUSSION

The chaperone mechanism of Hsp70 has been extensively studied (42). Bacterial DnaK was shown to use ATP to apply an unfolding force on stable misfolded polypeptides and small aggregates by two complementary mechanisms likely involving both direct "clamping" by individual DnaK molecules that may unfold non-native β-structures in stable misfolded polypeptides (12, 43) and indirect "entropic pulling" by several concomitantly clamped DnaK molecules on the same misfolded polypeptide, cooperating to unfold by thermal movements local misfolded regions in between chaperone-bound segments (44). NEFs can accelerate both effects by promoting the dissociation of ADP and the consequent release of the unfolded polypeptides from the stable ADP-Hsp70-substrate clamped complexes, allowing the unfolded products to spontaneously refold to their native state (12). In eukaryotes, at least four classes of Hsp70 NEFs have been identified, all acting on the same distal NBD lobes (IB and IIB) of Hsp70s. Three conserved classes of the GrpE-like, HspBP1-like, and BAG1–5-like NEFs cannot bind misfolded polypeptides. Although they are also unable to bind ATP, they are considered to be ATP-dependent ADP release catalysts (20, 45–48). The Hsp110s have been categorized as a fourth class of NEFs (32, 48–51), despite the fact that sequence-wise and structure-wise, they are close orthologs of

their acknowledged Hsp70 co-chaperone partners in disaggregation. The Hsp110s have a very similar NBD and C-terminal SBD, in which the peptide binding β-sandwich subdomain (SBDβ) and the α-helical lid subdomain (SBDα) can be clearly recognized (52). *In vitro*, purified human Hsp110 (HSPH1) can drive the ATP-, Hsc70-, and DNAJC6-dependent disaggregation of clathrin baskets (32). Like Hsp70s, Hsp110 can hydrolyze ATP (33) and is activated by J-domain co-chaperones (34). Hsp110 can also bind nascent polypeptide chains (33, 34, 53) and small peptides with different specificities (54). By doing so, Hsp110 may act as a "holding" chaperone that passively prevents the aggregation of stress- or mutation-induced misfolding and aggregating proteins (55). Moreover, yeast Hsp110 (Sse1) has been co-crystallized in 1:1 complex with the NBD of bovine Hsp70 (Hsc70), showing a pseudosymmetrical dimer with many tight interactions between the two NBDs, mostly in the distal lobes (IB and IIB), precisely at the same locations where the other NEFs also interact with Hsp70 and DnaK (32). However, at variance with the DnaK structure, the crystal structure of Sse1 showed the SBDα lid in an extensively wide open conformation. Although this initially questioned the ability of Hsp110 to close on its base and consequently to act as unfolding chaperones on its own (28), the same extensively wide open conformation was observed with functional DnaK mutants that crystallized as dimers associated through their NBDs as in the case of the SSE1 and Hsp70 crystals (56).

Hsp70s are polypeptide-unfolding enzymes on their own with a significant disaggregase and reactivation activities, which need to be in a large stoichiometric excess to cooperatively solubilize misfolded polypeptides from small soluble aggregates (12, 16). Generalizing the initial finding that Hsp105, together with Hsc70, can efficiently disaggregate purified clathrin cages (32), less specific *in vitro* disaggregating assays recently showed that mammalian cytosol prepared from different sources possess a potent, ATP-dependent activity requiring the apparent NEF activity of mammalian Hsp110 (Apg-2), the chaperone activity of Hsc70, and the co-chaperoning of Hdj1, to slowly dissolve large disordered aggregates and recover natively refolded proteins. A similar significant disaggregase activity was also observed in the case of yeast Sse1 acting upon Ssa1 together with the Sis1 or Ydj1 J-domain proteins (29). Likewise, Hsp110 (Apg-2) promotes the ATP- and Hdj1-dependent disaggregation activity of Hsc70 on stable heat-denatured aggregates *in vitro* and *in vivo* (28). Thus, contrary to other co-chaperones, Hsp110 is a unique NEF by being able to turn Hsc70 into an effective disaggregating machinery that can solubilize and reactivate large stable proteins aggregates (33), thereby possibly reducing the need for a large molar excess of Hsp70 to obtain some disaggregation by cooperative entropic pulling (16, 25, 44).

Noticeably, prior *in vitro* chaperone assays have reported that Hsp110 (Apg-2) lacks a chaperone unfolding/refolding activity of its own (28). In contrast, using various sensitive misfolded substrates, we found here *in vitro* that HSPH1 (Hsp105) or HSPH2 (Apg-2), assisted by DNAJA1 or DNAJB1, can act as *bona fide* ATP-dependent unfolding/refolding chaperones, even when Hsp70 is not present. This difference may be attributed to the use of slightly different substrates: predominantly stable freeze-thawed misfolded luciferase monomers rather than urea preaggregated luciferase.

Our finding that human Hsp110 alone can act as a chaperone using ATP hydrolysis to drive the catalytic unfolding of stable misfolded polypeptide substrates and to efficiently convert them into natively refolded products suggests that in solution, the substrate-binding domain of Hsp110 can effectively "clamp" upon its misfolded substrate and apply a pressure leading to unfolding, as in the case of DnaK (43). We therefore suggest a model accounting for the polypeptide unfoldase activity of Hsp110, in which the α-helical lid may depart from its stable position alongside the nucleotide-binding domain observed in the crystal structures and adopt during ATP hydrolysis an extensively opened position capable of binding to large bulky hydrophobic misfolded domains of a substrate polypeptide and, upon ATP hydrolysis, operate a large clamping movement toward the β-sheet base subdomain, as in the case of DnaK (57), that may in turn cause the unfolding of the clamped misfolded polypeptide segment (43).

An allosteric communication between the NBD and the substrate-binding domain of Hsp110 has been recently reported (54). Our dose responses further showed that, as suggested from the crystal structure of yeast Hsp110 with bovine Hcp70 NBD, equimolar Hsp70 and Hsp110 can optimally refold stable aggregated luciferase, likely by binding to orthologous topological sites in their respective NBDs and by effective reciprocal allosteric signals of similar quality and intensities between the two orthologous SBDs (42). The presence of such symmetrical allosteric signals was confirmed by the reciprocal release of the unfolded luciferase that we observed in the presence of apyrase, upon addition of Hsp110 to stable preformed ADP-Hsp70-Luc complexes or symmetrically of Hsp70 to stable preformed ADP-Hsp110-Luc complexes.

Despite their optimal 1:1 functional association, Hsp110 and Hsp70 apparently form loose heterodimers, because gel filtration, dynamic light scattering, chemical cross-linking, and electrophoresis on native gels thus far failed to reveal the unambiguous presence of stable Hsp110-Hsp70 heterodimers. Noticeably, proteomic analysis showed that in the cytoplasm and the endoplasmic reticulum of human cells, the Hsp70s are respectively 7- and 14-fold more abundant than the Hsp110s (3). Thus, despite their low affinity, most of the Hsp110 molecules are expected to form loose but potent disaggregating heterocomplexes with Hsp70, leaving the remaining excess Hsp70 molecules free to carry Hsp70-specific functions, such as the catalytic unfolding of amenable misfolded monomers (12) and the pulling apart of native clathrin cages (32) or of active IκB complexes (58), the activation of steroid hormone receptors, the inhibition of the heat shock transcription factor (59), or mediating proteasomal and lysosomal degradation (60).

Analysis of the x-ray structures from various Hsp70s associated with NEFs (DnaK-GrpE, Hsp70-Bag1, and Hsp70-Bag2) shows a common region of interaction (data not shown) in the IB lobe of the Hsp70 NBD, which is structurally similar as in the reciprocal binding of the SSE1 to bovine Hsc70 NBD. This may justify initial description of Hsp110 acting as an apparent NEF of Hsp70 (33, 61). However, our results with apyrase suggested that Hsp110 does not need ATP to catalyze the release of a

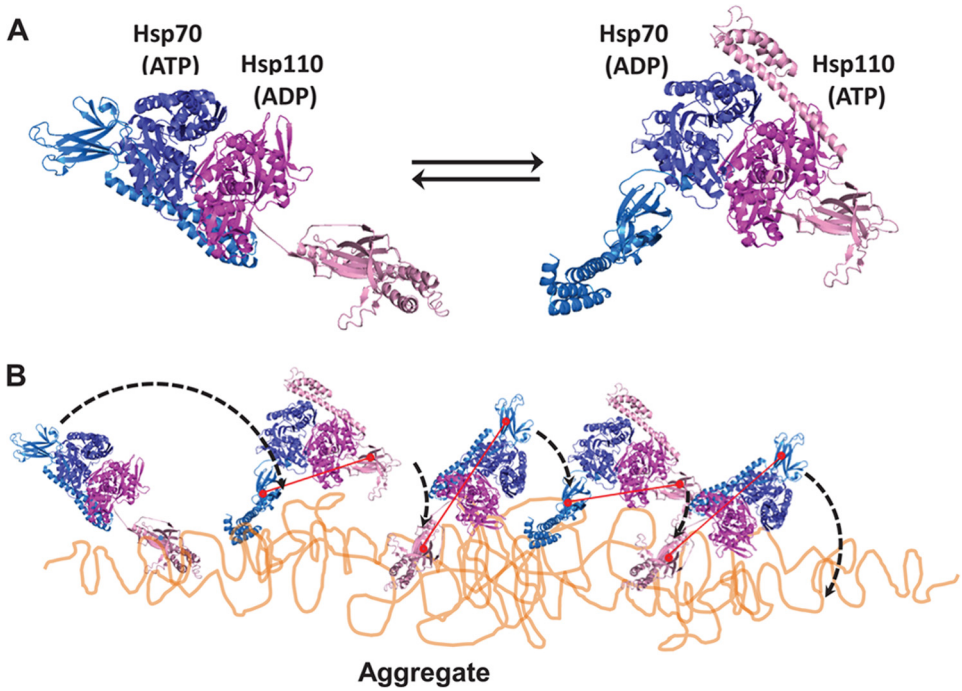

FIGURE 7. **Model for Hsp110-Hsp70-mediated disaggregation.** *A*, model of the two alternating functional HSPA8-SSE1 heterodimers, respectively, in the ATP-ADP state (*left panel*) and the ADP-ATP state (*right panel*), reconstructed by structural alignments of the SBDs from HSPA8 (*blue tones*) and SSE1 (*magenta tones*), either with the closed ADP-bound form of DnaK (PDB code 2KHO) or with the opened ATP-bound form of DnaK (PDB code 4B9Q). The association of the HSPA8 NBD with the SSE1 NBD was from PDB code 3C7N. The substrate binding sites of HSPA8 and SSE1 SBDs are shown as *red circles*. The connecting *red line* shows the distances between binding sites in the heterodimer. *B*, model for the disaggregation mechanism. The crystal structure of the HSPA8-SSE1 heterodimer (32) suggests that when one chaperone is ADP-bound, its SBD can be locked on an unfolded substrate, whereas the other chaperone is in the ATP-bound state with a widely opened SBD. During disaggregation, SSE1 and Hsp70 may thus alternate between a closed locked state, anchoring the whole chaperone heterodimer to the aggregate surface at a single misfolded loop (*left panel*), becoming unfolded by entropic pulling (44), and an opened state that can scan far from the anchor for new misfolded structures to bind to. Then, upon ATP hydrolysis, the second chaperone may bind and apply an unfolding pressure on the newly targeted misfolded loops (*right panel*). When successful, locking may unfold the misfolded structure, while concomitantly, an allosteric signal is sent from the NBD of the second locking chaperone to the NBD of the first chaperone to release ADP and thus unlock the SBD from a now newly enlarged unfolded anchoring loop, which may then refold to the native state.

locked polypeptide clamped into an ADP-bound Hsp70. Moreover, Hsp110 was found to be as much an ATP-independent substrate release factor for Hsp70, as Hsp70 was a substrate release factor for Hsp110.

A Possible Disaggregation Mechanism—The molecular mechanism by which Hsp110-Hsp70 heterodimers may utilize ATP to disentangle stable protein aggregates and fibrils is unclear. The core mechanism should include basic unfolding by individual Hsp70 and, as we found, also of Hsp110 molecules, amplified by the heterodimeric complex into a cooperative disaggregating machine. Inspired from the partial crystal structure of the heterodimer showing SSE1 and bovine Hsc70 in different nucleotide binding states (32), one could propose a "clamping and walking on the aggregate" mechanism, in which both SBDs of the Hsp110-Hsp70 heterodimer would side by side face the aggregate. The cycles of ATP hydrolysis would alternate between the ADP-Hsp110 (clamped):ATP-Hsp70 (open) state and the ATP-Hsp110 (open):ADP-Hsp70 (clamped) state (Fig. 7). Although one SBD would be firmly anchored onto the aggregate surface by way of an ADP-bound subunit clamping and unfolding a misfolded polypeptide segment, the flexible hinge between the SBD and the NBD would allow for the other ATP-binding chaperone molecule with its wide open SBD to scan the surrounding surfaces for new exposed hydrophobic surfaces to clamp upon (Fig. 7). Triggered by this "substrate-probing" chaperone subunit, ADP release from the NBD of the first subunit would "unclamp" its SBD and thus allow the heterodimer to "walk" on the aggregate surface, thus leaving behind a trail of unfolded polypeptide loops that would thereafter spontaneously seek more native-like conformations and thus gradually dissociate and refold into soluble native polypeptides.

In Vivo Relevance of Hsp110—The cytoplasm and endoplasmic reticulum of animal cells lack ClpB/Hsp104-like co-chaperones and may use only Hsp110-Hsp70 to disaggregate potential proteotoxic conformers. Thus, Hsp110 was co-localized to GFP-luciferase aggregates in human U2OS cells, and Hsp110 RNAi dramatically increased the number of heat-induced aggregates of Luciferase-YFP in whole *Caenorhabditis elegans* animals. Moreover, knockdown of Hsp110 decreased the nematode lifespan, particularly upon heat shock (28). Thus, functional Hsp70-Hsp110 complexes in the cytoplasm and the *endoplasmic reticulum* of human cells likely form a powerful unfolding/disaggregating machinery to counteract age- and mutation-induced toxic protein misfolding and aggregations, causing the onset of degenerative protein conformational diseases.

Acknowledgments—We thank Bernd Bukau for a gift of Apg-2 and DNAJB1, Rui Sousa and Eileen M. Lafer for expression plasmids encoding for human HSPH1, and Anika Braune and América Farina Henriquez Cuendet for technical assistance.

REFERENCES

1. Anfinsen, C. B. (1973) Principles that govern the folding of protein chains. *Science* **181,** 223–230
2. Geiger, T., Wehner, A., Schaab, C., Cox, J., and Mann, M. (2012) Comparative proteomic analysis of eleven common cell lines reveals ubiquitous but varying expression of most proteins. *Mol. Cell. Proteomics* **11,** M111.014050
3. Finka, A., and Goloubinoff, P. (2013) Proteomic data from human cell cultures refine mechanisms of chaperone-mediated protein homeostasis. *Cell Stress Chaperones* DOI 10.1007/s12192-013-0413-3
4. Cabrita, L. D., Dobson, C. M., and Christodoulou, J. (2010) Protein folding on the ribosome. *Curr. Opin. Struct. Biol.* **20,** 33–45
5. Ellis, R. J. (2001) Macromolecular crowding. Obvious but underappreciated. *Trends Biochem. Sci.* **26,** 597–604
6. Martin, J., and Hartl, F. U. (1997) The effect of macromolecular crowding on chaperonin-mediated protein folding. *Proc. Natl. Acad. Sci. U.S.A.* **94,** 1107–1112
7. Dobson, C. M. (2003) Protein folding and misfolding. *Nature* **426,** 884–890
8. Natalello, A., Mattoo, R. U., Priya, S., Sharma, S. K., Goloubinoff, P., and Doglia, S. M. (2013) Biophysical characterization of two different stable misfolded monomeric polypeptides that are chaperone-amenable substrates. *J. Mol. Biol.* **425,** 1158–1171
9. Gidalevitz, T., Ben-Zvi, A., Ho, K. H., Brignull, H. R., and Morimoto, R. I. (2006) Progressive disruption of cellular protein folding in models of polyglutamine diseases. *Science* **311,** 1471–1474
10. Hinault, M. P., Ben-Zvi, A., and Goloubinoff, P. (2006) Chaperones and proteases. Cellular fold-controlling factors of proteins in neurodegenerative diseases and aging. *J. Mol. Neurosci.* **30,** 249–265
11. Lashuel, H. A., Hartley, D., Petre, B. M., Walz, T., and Lansbury, P. T., Jr. (2002) Neurodegenerative disease. Amyloid pores from pathogenic mutations. *Nature* **418,** 291
12. Sharma, S. K., De los Rios, P., Christen, P., Lustig, A., and Goloubinoff, P. (2010) The kinetic parameters and energy cost of the Hsp70 chaperone as a polypeptide unfoldase. *Nat. Chem. Biol.* **6,** 914–920
13. Priya, S., Sharma, S. K., Sood, V., Mattoo, R. U., Finka, A., Azem, A., De Los Rios, P., and Goloubinoff, P. (2013) GroEL and CCT are catalytic unfoldases mediating out-of-cage polypeptide refolding without ATP. *Proc. Natl. Acad. Sci. U.S.A.* **110,** 7199–7204
14. Hinault, M. P., Farina-Henriquez-Cuendet, A., and Goloubinoff, P. (2011) Molecular chaperones and associated cellular clearance mechanisms against toxic protein conformers in Parkinson's disease. *Neurodegener. Dis.* **8,** 397–412
15. Priya, S., Sharma, S. K., and Goloubinoff, P. (2013) Molecular chaperones as enzymes that catalytically unfold misfolded polypeptides. *FEBS Lett.* **587,** 1981–1987
16. Diamant, S., Ben-Zvi, A. P., Bukau, B., and Goloubinoff, P. (2000) Size-dependent disaggregation of stable protein aggregates by the DnaK chaperone machinery. *J. Biol. Chem.* **275,** 21107–21113
17. Bucciantini, M., Giannoni, E., Chiti, F., Baroni, F., Formigli, L., Zurdo, J., Taddei, N., Ramponi, G., Dobson, C. M., and Stefani, M. (2002) Inherent toxicity of aggregates implies a common mechanism for protein misfolding diseases. *Nature* **416,** 507–511
18. Selkoe, D. J. (2004) Cell biology of protein misfolding. The examples of Alzheimer's and Parkinson's diseases. *Nat. Cell Biol.* **6,** 1054–1061
19. De Los Rios, P., and Goloubinoff, P. (2012) Protein folding. Chaperoning protein evolution. *Nat. Chem. Biol.* **8,** 226–228
20. Finka, A., Mattoo, R. U., and Goloubinoff, P. (2011) Meta-analysis of heat- and chemically upregulated chaperone genes in plant and human cells. *Cell Stress Chaperones* **16,** 15–31
21. Fenton, W. A., Kashi, Y., Furtak, K., and Horwich, A. L. (1994) Residues in chaperonin GroEL required for polypeptide binding and release. *Nature* **371,** 614–619
22. Rüdiger, S., Buchberger, A., and Bukau, B. (1997) Interaction of Hsp70 chaperones with substrates. *Nat. Struct. Biol.* **4,** 342–349
23. Rüdiger, S., Schneider-Mergener, J., and Bukau, B. (2001) Its substrate specificity characterizes the DnaJ co-chaperone as a scanning factor for the DnaK chaperone. *EMBO J.* **20,** 1042–1050
24. Sharma, S. K., De Los Rios, P., and Goloubinoff, P. (2011) Probing the different chaperone activities of the bacterial HSP70-HSP40 system using a thermolabile luciferase substrate. *Proteins* **79,** 1991–1998
25. Ben-Zvi, A., De Los Rios, P., Dietler, G., and Goloubinoff, P. (2004) Active solubilization and refolding of stable protein aggregates by cooperative unfolding action of individual hsp70 chaperones. *J. Biol. Chem.* **279,** 37298–37303
26. Glover, J. R., and Lindquist, S. (1998) Hsp104, Hsp70, and Hsp40. A novel chaperone system that rescues previously aggregated proteins. *Cell* **94,** 73–82
27. Goloubinoff, P., Mogk, A., Zvi, A. P., Tomoyasu, T., and Bukau, B. (1999) Sequential mechanism of solubilization and refolding of stable protein aggregates by a bichaperone network. *Proc. Natl. Acad. Sci. U.S.A.* **96,** 13732–13737
28. Rampelt, H., Kirstein-Miles, J., Nillegoda, N. B., Chi, K., Scholz, S. R., Morimoto, R. I., and Bukau, B. (2012) Metazoan Hsp70 machines use Hsp110 to power protein disaggregation. *EMBO J.* **31,** 4221–4235
29. Shorter, J. (2011) The mammalian disaggregase machinery. Hsp110 synergizes with Hsp70 and Hsp40 to catalyze protein disaggregation and reactivation in a cell-free system. *PLoS One* **6,** e26319
30. Hinault, M. P., Cuendet, A. F., Mattoo, R. U., Mensi, M., Dietler, G., Lashuel, H. A., and Goloubinoff, P. (2010) Stable α-synuclein oligomers strongly inhibit chaperone activity of the Hsp70 system by weak interactions with J-domain co-chaperones. *J. Biol. Chem.* **285,** 38173–38182
31. Biancalana, M., Makabe, K., Koide, A., and Koide, S. (2009) Molecular mechanism of thioflavin-T binding to the surface of β-rich peptide self-assemblies. *J. Mol. Biol.* **385,** 1052–1063
32. Schuermann, J. P., Jiang, J., Cuellar, J., Llorca, O., Wang, L., Gimenez, L. E., Jin, S., Taylor, A. B., Demeler, B., Morano, K. A., Hart, P. J., Valpuesta, J. M., Lafer, E. M., and Sousa, R. (2008) Structure of the Hsp110:Hsc70 nucleotide exchange machine. *Mol. Cell* **31,** 232–243
33. Andréasson, C., Fiaux, J., Rampelt, H., Mayer, M. P., and Bukau, B. (2008) Hsp110 is a nucleotide-activated exchange factor for Hsp70. *J. Biol. Chem.* **283,** 8877–8884
34. Raviol, H., Sadlish, H., Rodriguez, F., Mayer, M. P., and Bukau, B. (2006) Chaperone network in the yeast cytosol. Hsp110 is revealed as an Hsp70 nucleotide exchange factor. *EMBO J.* **25,** 2510–2518
35. Wisén, S., Bertelsen, E. B., Thompson, A. D., Patury, S., Ung, P., Chang, L., Evans, C. G., Walter, G. M., Wipf, P., Carlson, H. A., Brodsky, J. L., Zuiderweg, E. R., and Gestwicki, J. E. (2010) Binding of a small molecule at a protein-protein interface regulates the chaperone activity of hsp70-hsp40. *ACS Chem. Biol.* **5,** 611–622
36. Liberek, K., Marszalek, J., Ang, D., Georgopoulos, C., and Zylicz, M. (1991) *Escherichia coli* DnaJ and GrpE heat shock proteins jointly stimulate ATPase activity of DnaK. *Proc. Natl. Acad. Sci. U.S.A.* **88,** 2874–2878
37. Raviol, H., Bukau, B., and Mayer, M. P. (2006) Human and yeast Hsp110 chaperones exhibit functional differences. *FEBS Lett.* **580,** 168–174
38. Siegenthaler, R. K., and Christen, P. (2006) Tuning of DnaK chaperone action by nonnative protein sensor DnaJ and thermosensor GrpE. *J. Biol. Chem.* **281,** 34448–34456
39. Rüngeling, E., Laufen, T., and Bahl, H. (1999) Functional characterisation of the chaperones DnaK, DnaJ, and GrpE from *Clostridium acetobutylicum*. *FEMS Microbiol. Lett.* **170,** 119–123
40. Zolkiewski, M. (1999) ClpB cooperates with DnaK, DnaJ, and GrpE in suppressing protein aggregation. A novel multi-chaperone system from *Escherichia coli*. *J. Biol. Chem.* **274,** 28083–28086
41. Rodriguez, F., Arsène-Ploetze, F., Rist, W., Rüdiger, S., Schneider-Mergener, J., Mayer, M. P., and Bukau, B. (2008) Molecular basis for regulation of the heat shock transcription factor sigma32 by the DnaK and DnaJ chaperones. *Mol Cell* **32,** 347–358
42. Zhuravleva, A., and Gierasch, L. M. (2011) Allosteric signal transmission in the nucleotide-binding domain of 70-kDa heat shock protein (Hsp70) molecular chaperones. *Proc. Natl. Acad. Sci. U.S.A.* **108,** 6987–6992
43. Baneyx, F., and Nannenga, B. L. (2010) Chaperones. A story of thrift unfolds. *Nat Chem Biol* **6,** 880–881
44. De Los Rios, P., Ben-Zvi, A., Slutsky, O., Azem, A., and Goloubinoff, P. (2006) Hsp70 chaperones accelerate protein translocation and the unfold-

ing of stable protein aggregates by entropic pulling. *Proc. Natl. Acad. Sci. U.S.A.* **103,** 6166–6171
45. Brehmer, D., Gässler, C., Rist, W., Mayer, M. P., and Bukau, B. (2004) Influence of GrpE on DnaK-substrate interactions. *J. Biol. Chem.* **279,** 27957–27964
46. Kabani, M., Beckerich, J. M., and Brodsky, J. L. (2002) Nucleotide exchange factor for the yeast Hsp70 molecular chaperone Ssa1p. *Mol. Cell. Biol.* **22,** 4677–4689
47. Mayer, M. P., and Bukau, B. (2005) Hsp70 chaperones. Cellular functions and molecular mechanism. *Cell. Mol. Life Sci.* **62,** 670–684
48. Sondermann, H., Scheufler, C., Schneider, C., Hohfeld, J., Hartl, F. U., and Moarefi, I. (2001) Structure of a Bag/Hsc70 complex. Convergent functional evolution of Hsp70 nucleotide exchange factors. *Science* **291,** 1553–1557
49. Packschies, L., Theyssen, H., Buchberger, A., Bukau, B., Goody, R. S., and Reinstein, J. (1997) GrpE accelerates nucleotide exchange of the molecular chaperone DnaK with an associative displacement mechanism. *Biochemistry* **36,** 3417–3422
50. Shomura, Y., Dragovic, Z., Chang, H. C., Tzvetkov, N., Young, J. C., Brodsky, J. L., Guerriero, V., Hartl, F. U., and Bracher, A. (2005) Regulation of Hsp70 function by HspBP1. Structural analysis reveals an alternate mechanism for Hsp70 nucleotide exchange. *Mol Cell* **17,** 367–379
51. Steel, G. J., Fullerton, D. M., Tyson, J. R., and Stirling, C. J. (2004) Coordinated activation of Hsp70 chaperones. *Science* **303,** 98–101
52. Knappe, D., Zahn, M., Sauer, U., Schiffer, G., Sträter, N., and Hoffmann, R. (2011) Rational design of oncocin derivatives with superior protease stabilities and antibacterial activities based on the high-resolution structure of the oncocin-DnaK complex. *Chembiochem* **12,** 874–876
53. Polier, S., Hartl, F. U., and Bracher, A. (2010) Interaction of the Hsp110 molecular chaperones from *S. cerevisiae* with substrate protein. *J. Mol. Biol.* **401,** 696–707
54. Xu, X., Sarbeng, E. B., Vorvis, C., Kumar, D. P., Zhou, L., and Liu, Q. (2012) Unique peptide substrate binding properties of 110-kDa heat-shock protein (Hsp110) determine its distinct chaperone activity. *J. Biol. Chem.* **287,** 5661–5672
55. Oh, H. J., Chen, X., and Subjeck, J. R. (1997) Hsp110 protects heat-denatured proteins and confers cellular thermoresistance. *J. Biol. Chem.* **272,** 31636–31640
56. Kityk, R., Kopp, J., Sinning, I., and Mayer, M. P. (2012) Structure and dynamics of the ATP-bound open conformation of Hsp70 chaperones. *Mol. Cell* **48,** 863–874
57. Bertelsen, E. B., Chang, L., Gestwicki, J. E., and Zuiderweg, E. R. (2009) Solution conformation of wild-type *E. coli* Hsp70 (DnaK) chaperone complexed with ADP and substrate. *Proc. Natl. Acad. Sci. U.S.A.* **106,** 8471–8476
58. Weiss, Y. G., Bromberg, Z., Raj, N., Raphael, J., Goloubinoff, P., Ben-Neriah, Y., and Deutschman, C. S. (2007) Enhanced heat shock protein 70 expression alters proteasomal degradation of IκB kinase in experimental acute respiratory distress syndrome. *Crit. Care Med.* **35,** 2128–2138
59. Voellmy, R. (2004) On mechanisms that control heat shock transcription factor activity in metazoan cells. *Cell Stress Chaperones* **9,** 122–133
60. Muchowski, P. J., and Wacker, J. L. (2005) Modulation of neurodegeneration by molecular chaperones. *Nat. Rev. Neurosci.* **6,** 11–22
61. Dragovic, Z., Broadley, S. A., Shomura, Y., Bracher, A., and Hartl, F. U. (2006) Molecular chaperones of the Hsp110 family act as nucleotide exchange factors of Hsp70s. *EMBO J.* **25,** 2519–2528

CHAPTER 4

GroEL and CCT are catalytic unfoldases mediating Out-of-cage polypeptide refolding without ATP

GroEL and CCT are catalytic unfoldases mediating out-of-cage polypeptide refolding without ATP.

Priya, S., Sharma, S.K., Sood, V., Mattoo, R.U., Finka, A., Azem, A., De Los Rios, P. and Goloubinoff, P.

I contributed to the writing of the manuscript.

I contributed with Dr. Priya in the data acquisition for the Fig. 1(B and C), Fig. 2B, Fig. 5 and Fig. S7B.

GroEL and CCT are catalytic unfoldases mediating out-of-cage polypeptide refolding without ATP

Smriti Priya[a], Sandeep Kumar Sharma[a,b], Vishal Sood[c], Rayees U. H. Mattoo[a], Andrija Finka[a], Abdussalam Azem[d], Paolo De Los Rios[c], and Pierre Goloubinoff[a,1]

[a]Department of Plant Molecular Biology, Faculty of Biology and Medicine, University of Lausanne, CH-1015 Lausanne, Switzerland; [b]Biochemisches Institut, Universität Zürich, CH-8057 Zurich, Switzerland; [c]Laboratory of Statistical Biophysics, School of Basic Sciences, Ecole Polytechnique Fédérale de Lausanne, CH-1015 Lausanne, Switzerland; and [d]Department of Biochemistry and Molecular Biology, George S. Wise Faculty of Life Sciences, Tel Aviv University, Tel Aviv 69978, Israel

Edited by Alan R. Fersht, Medical Research Council Laboratory of Molecular Biology, Cambridge, United Kingdom, and approved March 20, 2013 (received for review November 16, 2012)

Chaperonins are cage-like complexes in which nonnative polypeptides prone to aggregation are thought to reach their native state optimally. However, they also may use ATP to unfold stably bound misfolded polypeptides and mediate the out-of-cage native refolding of large proteins. Here, we show that even without ATP and GroES, both GroEL and the eukaryotic chaperonin containing t-complex polypeptide 1 (CCT/TRiC) can unfold stable misfolded polypeptide conformers and readily release them from the access ways to the cage. Reconciling earlier disparate experimental observations to ours, we present a comprehensive model whereby following unfolding on the upper cavity, in-cage confinement is not needed for the released intermediates to slowly reach their native state in solution. As over-sticky intermediates occasionally stall the catalytic unfoldase sites, GroES mobile loops and ATP are necessary to dissociate the inhibitory species and regenerate the unfolding activity. Thus, chaperonin rings are not obligate confining antiaggregation cages. They are polypeptide unfoldases that can iteratively convert stable off-pathway conformers into functional proteins.

molecular chaperones | protein aggregation | protein misfolding | protein unfolding

Newly synthesized polypeptides, or stress-labile proteins destabilized by mutations, may fail to properly reach their native state and instead form misfolded species that may coalesce further into stable toxic aggregates (1–3). Molecular chaperones, such as the cage-like eukaryotic chaperonin containing t-complex polypeptide 1 (CCT/TRiC) and GroEL/GroES chaperonins and the heat shock protein (Hsp)70/Hsp40s (4, 5), form a first line of cellular defenses against early misfolded species on the cytotoxic protein aggregation pathway, leading to degenerative conformational diseases and aging (6). In vitro, chaperonins may prevent the aggregation of artificially unfolded proteins and use ATP hydrolysis to promote their native refolding but fail to act upon misfolded species already entangled into large aggregates (7, 8).

Eukaryotic cytosolic CCTs, bacterial GroEL, and mitochondrial Hsp60 are double-ring complexes with two central cavities. Their key role in cellular proteostasis is generally thought to be the ATP-driven transient confinement of aggregation-prone polypeptides within the central cavities, allowing "in-cage" protein refolding to the native state. The mechanistic steps first involve spontaneous binding of an unfolded or misfolded polypeptide to exposed hydrophobic residues on the apical domains facing the upper passageway of the chaperonin cavity (9). Next, the ATP-regulated movements of the apical domains cause the dissociation of the tightly bound polypeptide, either within the confined space of the cavity or directly into the external solution, especially in cases of large polypeptides (10). The transient capping of the cavity by a helical lid domain in CCT, or a $GroES_7$ cover in the case of $GroEL_{14}$ (5, 11), is generally thought to be an obligatory step to confine the released polypeptide within the cage, where it presumably needs to reach its native state while being secluded from other aggregating polypeptides. An allosteric signal from the empty *trans*-ring then prompts the uncapping of the substrate-containing *cis*-cavity (12, 13), causing the release of the natively refolded protein. Thus, ATP is thought to drive the reaction cycle of GroEL and CCT by timely alternating between an in-cage sequestration phase, to promote by confinement the spontaneous refolding of an unfolded polypeptide, and a dissociation phase, to release the natively refolded protein from the cage into the solution. However, exceptions also have been reported of large proteins being released directly from the GroEL cage without encapsulation, upon GroES binding to the opposite ring, possibly leading to out-of-cage refolding (14, 15).

Here, we revisit the obligate link between the mechanism by which chaperonins can convert a stable misfolded polypeptide into a native protein and the mechanism of encaging to avoid aggregation of the substrate during the various steps to native refolding. To this aim, we used as a unique type of stringent chaperone substrates in the form of stable misfolded inactive polypeptides that without chaperonins tended neither to aggregate nor to refold spontaneously to the native state. We found that both apoGroEL and apoCCT acted as efficient polypeptide unfolding molecular machines that could rapidly convert an excess of misfolded polypeptide substrates into unfolded intermediates that were released from the chaperonin to slowly reach the native state in solution. However, following several full turnovers of binding, unfolding, release, and out-of-cage refolding, both GroEL and CCT activities gradually became stalled by over-sticky intermediates, whose dissociation required the action of an ancillary regeneration mechanism that depended on ATP hydrolysis and, in the case of GroEL, also on GroES mobile loops (16).

Results

Freeze–Thaw Denatured Rhodanese Is a Stringent Substrate That Is Not Aggregation Prone. Unstable guanidinium HCl- or urea-unfolded rhodanese has been used in classic in vitro chaperonin assays by virtue of its high propensity to aggregate readily upon removal of the denaturant and form resistant species, unless readily assisted by a large molar excess of GroEL, GroES, and ATP (17). In contrast, here we used freeze–thaw (FT) denatured rhodanese (FTrho) as a unique type of substrate generated beforehand in the absence of GroEL, by iterative FT cycles. Similar to FT-denatured luciferase (FTluc) (18), inactive FTrho was found to be composed of stable, soluble, and mostly monomeric species (Fig. S1*A*) (19). Indicative of the presence of stable misfolded β-structures, FTrho bound 3.5 times more thioflavin T (Th-T) than native rhodanese (Nrho) (Fig. S1*B*). Without chaperones, less than 3% spontaneously converted into Nrho in 60 min at 25 °C. Remarkably, no FTrho converted into light-scattering aggregates in 18 h (Fig. S1*C*). The FTrho species were more resistant than Nrho to urea unfolding (Fig. S2), and

Author contributions: S.P., S.K.S., A.A., P.D.L.R., and P.G. designed research; S.P., R.U.H.M., and P.G. performed research; S.P., S.K.S., V.S., A.F., P.D.L.R., and P.G. analyzed data; and S.P., A.A., P.D.L.R., and P.G. wrote the paper.

The authors declare no conflict of interest.

This article is a PNAS Direct Submission.

[1]To whom correspondence should be addressed. E-mail: Pierre.Goloubinoff@unil.ch.

This article contains supporting information online at www.pnas.org/lookup/suppl/doi:10.1073/pnas.1219867110/-/DCSupplemental.

FTIR spectroscopy showed the presence of intramolecular misfolded β-sheets different from Nrho (19). Therefore, FTrho was a stringent candidate substrate with a potential to differentiate between the chaperonin's ability to mediate protein refolding per se and its ability to prevent aggregation.

ApoGroEL Can Catalytically Unfold FTrho Without ATP. Whereas during 18 h, up to 13% of the FTrho was converted spontaneously to Nrho, addition of equimolar apoGroEL (1 μM protomers, i.e., 71.4 nM of $GroEL_{14}$) produced the same amount of Nrho in 3 min, corresponding to a 360-fold acceleration of the native refolding reaction. Whereas without ATP other molecular chaperones and proteins in equimolar amounts [DnaK, DnaJ, Caseinolytic peptidase B protein (ClpB), HtpG, GroES, BSA] remained ineffective, up to a third of the substrate (330 nM) was refolded rapidly by apoGroEL in 15 min (T_{50} = 4 min 30 s; Fig. 1*A*) and similar high refolding yields were observed with equimolar single-ring $GroEL_7$-mutant SR1 mutants (20). On average, each $GroEL_7$ ring converted half the FTrho substrate per minute, generating 2.3 native products in 30 min. FTrho thus allowed chaperonins to work through multiple turnovers, overcoming the single-turnover limitation observed in previous in vitro refolding assays with aggregation-prone substrates (7, 17). Enzyme activity, kinetics of deuterium exchange, NMR, and FRET spectroscopy previously showed that mere binding to apoGroEL may cause the unfolding of metastable native or misfolding proteins, such as pre–β-lactamase (21), heat-denatured cyclophilin (22), barnase (23), or urea-denatured Ribulose 1,5-bisphosphate carboxylase/oxygenase (RubisCO) (24). However, here we show that a single apoGroEL ring may carry several complete, consecutive turnovers including substrate binding, unfolding, release, and native refolding.

Fluorescence spectroscopy showed that apoGroEL caused a rapid net loss of the high FTrho Th-T signal (T_{50} = 1 min), indicating that upon GroEL binding, FTrho lost a significant fraction of its intramolecular misfolded β-structures (18, 19), a result compatible with some degree of unfolding. Within 2 min, the apparent unfolding signal leveled and was followed by a slower net regain of Th-T signal, corresponding to the formation of some native β-structures (Fig. 1*B*), as suggested by a parallel regain of rhodanese activity (Fig. 1*A*). Time-lapse transient trypsin digestions at various time points of the reaction confirmed that binding of apoGroEL caused an initial decompaction and partial unfolding of the bound FTrho substrate. FTrho thus was incubated before and after GroEL addition with 0.02 mg/mL trypsin and, 3 min later, with an excess of the trypsin inhibitor *N*-α-tosyl-L-lysine chloromethyl ketone hydrochloride (TLCK). A prior short trypsin treatment of GroEL alone had no effect on its subsequent unfolding/refolding activity, and a prior short trypsin treatment of FTrho or Nrho alone followed by GroEL addition produced 82% and 91% Nrho, respectively, in 60 min (compared with the apoGroEL-mediated yield without trypsin pretreatment set to 100%; Fig. 1*C*). The similar elevated levels of trypsin resistance of FTrho and Nrho imply that they were comparably compact. Remarkably, when transient trypsin digestion of FTrho was applied 2 min after GroEL addition, only 18% of the refolding yield (mediated by apoGroEL in 60 min) was observed. A marked transient increase of sensitivity of FTrho to trypsin, despite a possible partial recruitment of trypsin by the added GroEL and a possible partial sequestration of the substrate in the cavity, is strong evidence that upon binding, GroEL caused a decompaction and, therefore, the partial unfolding of the compact misfolded FTrho species. When the trypsin digestions were applied later in the GroEL reaction, they progressively became less effective, and the GroEL-mediated refolding yields recovered up to a maximal 87%, with a T_{50} = 17 min (Fig. 1*C*). Thus, following an initial rapid drop of the compactness of the substrate, its subsequent slow regain of trypsin resistance is evidence of its slow conversion into new compact native species, as attested by its regained enzymatic activity.

In this reaction, each GroEL heptameric ring thus acted as an ATP-independent enzyme, which first rapidly unfolded the misfolded polypeptide substrate upon binding, then rapidly released it as a species highly sensitive to the trypsin molecules of the external solution, where it slowly refolded to the more compact protease-resistant native state. Other misfolded substrates in excess, by virtue of their low propensity to aggregate, could patiently wait their turn to be unfolded and released by the chaperonin in several successive turnovers. The same results were found with the single-ring SR1 mutants, indicating that the release step did not depend on an allosteric signal from the *trans*-ring.

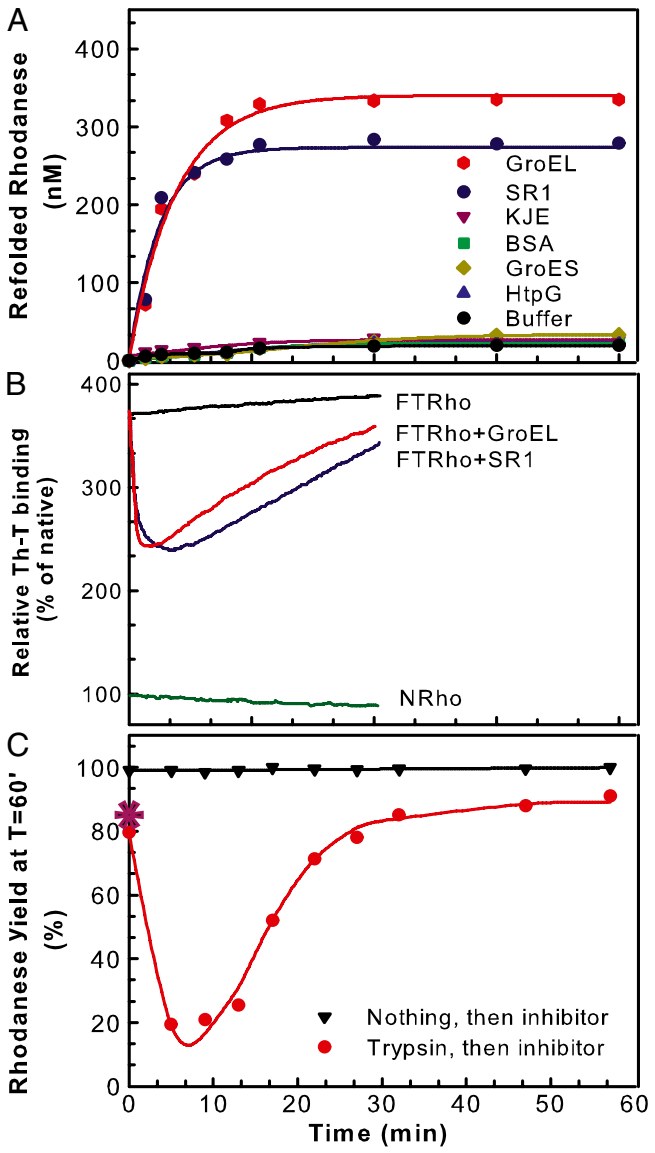

Fig. 1. GroEL is an ATP-independent catalytic polypeptide-unfolding enzyme. (*A*) Time course of stringent chaperonin-mediated refolding (reactivation) of FTrho (1 μM) at 22 °C without or with equimolar (expressed in protomers) $GroEL_{14}$, single $GroEL_7$ ring SR1, $GroES_7$, DnaK + DnaJ + GrpE (KJE), $HtpG_2$, or BSA. (*B*) Time-dependent net relative changes in FTrho Th-T fluorescence in the presence of equimolar $GroEL_{14}$, $SR1_7$, KJE, or only buffer as in *A*. Nrho is 100%. (*C*) Time-lapse trypsin sensitivity of FTrho. FTrho (1 μM) was incubated with equimolar GroEL (1 μM protomers) as in *A*. Three minutes before the indicated time points, 0.02 mg/mL trypsin was added, and at the indicated time points, trypsin activity was stopped by adding 100 μM trypsin inhibitor (TLCK). Refolding was allowed to continue until 60 min after GroEL addition, and the refolding relative yields (from *A*, 330 nM = 100%) were plotted against the time at which the (3-min) trypsin treatments were ended by TLCK addition. TLCK was added without (black ▼) or following (red ●) a prior 3-min trypsin treatment. Trypsin and inhibitor pretreatment of GroEL before FTrho addition at T = 0 min did not affect refolding yields (*). Lines in *A* and *C* are simple guides for the eyes.

Although exceptionally effective, the catalytic unfolding action of apoGroEL gradually halted after processing two to three misfolded polypeptides per ring. To address the reasons for arrest, we titrated the unfolding/refolding activity of increasing substoichiometric amounts of apoGroEL sequentially added to the reaction every 30 min, to a constant excess FTrho (2 μM). As little as 250 nM GroEL (i.e., 36 nM of $GroEL_7$ active sites) was found to refold up to 280 nM rhodanese in 25 min, corresponding to seven to eight turnovers per $GroEL_7$ ring; then, it stopped (Fig. 2*A*). The subsequent addition of fresh GroEL (36 nM $GroEL_7$ sites) produced nearly the same amount of Nrho, indicating that the first refolding reaction was not arrested because all the substrate had been consumed or turned into GroEL-resistant species, but rather that the initial GroEL molecules became inhibited. Further additions of substoichiometric amounts of fresh GroEL expectedly processed less and less FTrho, until equimolar GroEL (286 nM of $GroEL_7$ catalytic sites) was found saturating, yielding up to 46% of stable Nrho (Fig. 2*A*). Gel filtration chromatography, activity, and Western blots of FTrho preincubated with apoGroEL for 0 min or 60 min (Fig. 2*B*) confirmed that the catalytic unfoldase action of apoGroEL became stalled by inactive over-sticky rhodanese species acting as inhibitors of the unfoldase catalysis.

These observations were tested and confirmed by a mathematical model based on simple thermodynamic and kinetic considerations (*SI Text*, section S1 and Fig. S3) capturing the basic experimental observations (*SI Text*, section S1 and Fig. S4), which provided quantitative estimates of the parameters governing the different steps of the catalytic unfoldase cycle mediated by an apoGroEL heptameric ring: binding, unfolding, release, and refolding (Table S1). The model provided insight into the evolution of the various intermediate species produced in the reaction (*SI Text*, section S1 and Fig. S5). It showed best fits with the data when assuming rapid unfolding on the upper rim of the cavity (T_{50} < 1 min), followed by a slow out-of-cage refolding (T_{50} = 6 min 18 s) of the released unfolded FTrho species in solution (Fig. S4). The model could account for the slower refolding rates we observed in the presence of excess (7 μM) compared with limiting (0.5–1 μM) apoGroEL (Figs. S4 and S5), implying that the species released from the cage were in a nonnative, on-pathway state that, at variance with the lowest-affinity Nrho state, could be recaptured transiently by the excess of apoGroEL. Modifying the model to compel the protein to undergo obligate in-cage refolding, with the released product being native and averse to GroEL rebinding, produced much worse fits than when assuming out-of-cage refolding. Moreover, it predicted that an excess of chaperonin would accelerate the reaction, whereas the experiments showed a slowing down. The optimal out-of-cage refolding model thus predicted that binding, unfolding, and release of a first substrate should have been rapid enough (T_{50} < 1 min) to allow the binding of the next substrate, whereas the first released product continues its slow (T_{50} = 6 min 18 s) native refolding in solution. This might best account for the ability of each apoGroEL ring to undergo up to eight consecutive turnovers in several minutes (as in Fig. 2*A*, step one) while accommodating in their cavity, at most, a single 30-kDa substrate at a time.

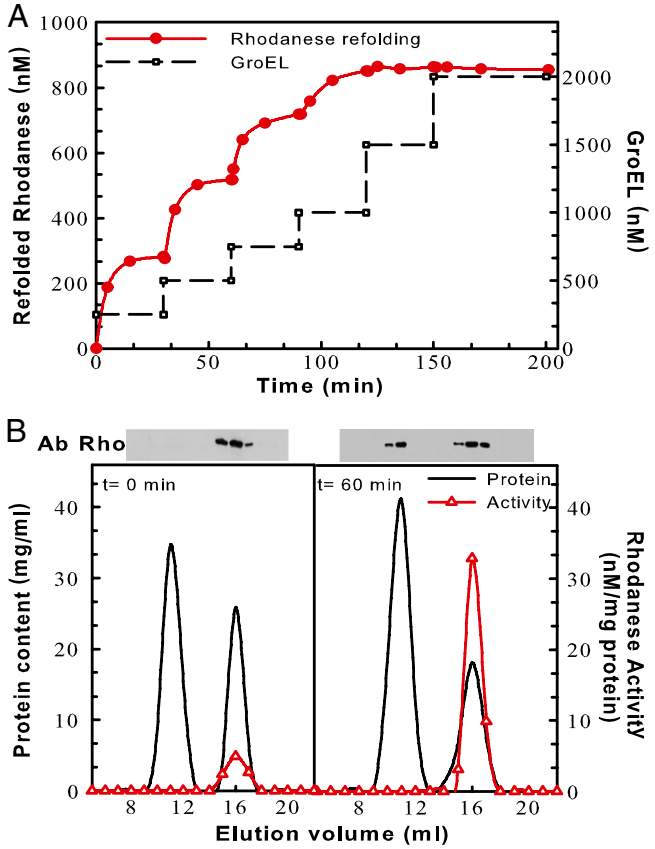

Fig. 2. The chaperonin unfoldase activity becomes stalled by over-sticky FTrho species. (*A*) An excess of FTrho substrate (2 μM) was supplemented stepwise every 30 min, first with substoichiometric amounts, then up to equimolar GroEL protomers (black lines), and rhodanese activity was measured as in Fig. 1*A* at the indicated time points. (*B*) GroEL complexes become stalled by over-sticky inactive rhodanese species. FTrho incubated for 0 (*Left*) or 60 min (*Right*) with equimolar GroEL as in Fig. 1*A* was separated by gel filtration chromatography. The eluted fractions were assayed for total protein concentration (black line) and rhodanese activity (red △) and further separated by SDS-gel electrophoresis to detect the presence of rhodanese by Western blots. Lines are simple guides for the eyes.

Role of ATP and GroES. Because cells contain several millimolars of ATP and mitochondria contain equimolar GroEL and GroES protomers (Table S2), chaperonins will unlikely stay long without binding ATP and GroES. Therefore, next we addressed the effect of ATP and GroES on stalled chaperonins. First, we incubated apoGroEL, apoSR1, or apoCCT with FTrho for 30 min until complete unfolding/refolding arrest was achieved; then, we added ATP, GroES, or both (Figs. 3*B* and 4).

Remarkably, apoCCT, but not the other chaperones tested, showed the same ability to drive the catalytic refolding of FTrho, with a similar number of turnovers and yields as apoGroEL (Fig. 4*A*), suggesting that catalytic unfolding/refolding is a particular functional feature of both classes of chaperonins. The presence of ATP from the start (Fig. 4*A*) or the subsequent addition of ATP to FTrho-stalled–apoCCT complexes caused the release and refolding of about 102 nM Nrho (Fig. S6*A*). This confirmed that ATP suffices to decrease the affinity for over-sticky polypeptides that may stall the catalytic unfoldase sites of CCT chaperonins. Addition of ATP alone to FTrho-stalled–apoGroEL complexes was less effective at releasing refoldable inhibitory species from GroEL or SR1, suggesting that the ATP-fueled upward and sidewise twisting of the GroEL apical domains (11) remained predominantly frustrated by the bound over-sticky species. GroES addition to FTrho-stalled apoGroEL released a more important fraction of stalling species. This showed that GroES can bind GroEL even without ATP and stabilize the low-affinity state for over-sticky substrates, as previously shown to be the case in GroEL prebound with heat-denatured malate dehydrogenase (MDH) (25). As expected, addition of both ATP and GroES caused an effective net release and native refolding of about 210 nM Nrho (Fig. 3*B*), demonstrating synergism between the two at dissociating high-affinity species (25). In the case of SR1 single rings, addition of ATP and GroES resulted only in a minor FTrho release and refolding (40 nM Nrho) (Fig. S6*B*). These species were previously shown to be in-cage refolded under the sealed GroES cap of SR1 (20). Remarkably, GroES and ATP-mediated refolding of apoGroEL-stalled species was six times more effective because of the ability of GroEL *trans*-ring to mediate the timely dissociation of GroES. Thus, although possible, obligate in-cage refolding appears to be considerably less effective than out-of-cage refolding, as independently suggested from model-based simulations of the data (Figs. S3–S5).

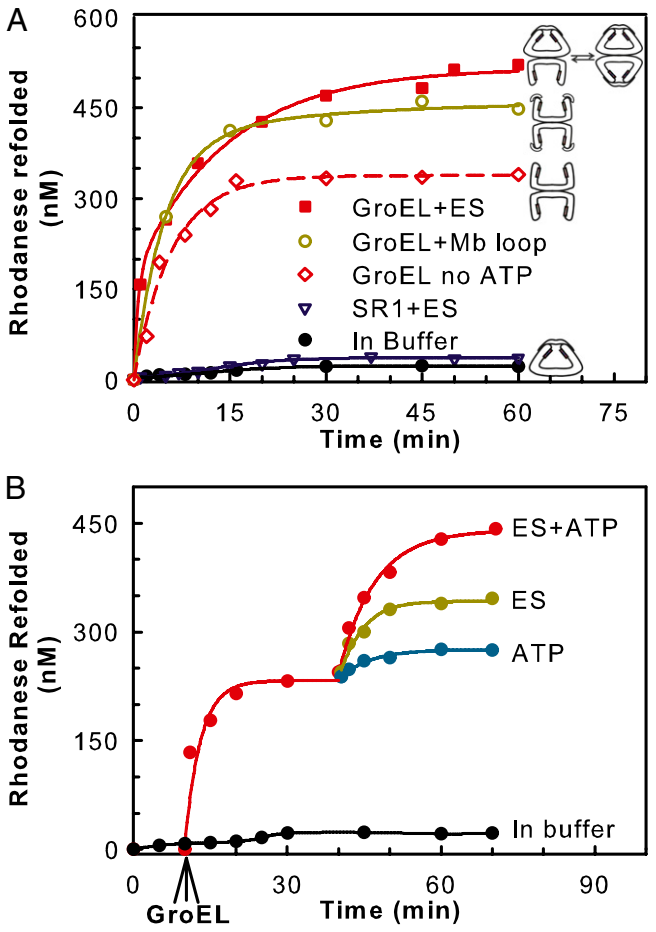

Fig. 3. The sequential additive effects of ATP + GroES on GroEL-mediated unfoldase/refoldase activity. (*A*) The effects of ATP and GroES or mobile loop preincubation on the GroEL unfoldase/refoldase activity. One-micromolar protomers of GroEL (red ■) or SR1 (blue ▽) first were preincubated with 5 mM ATP and 1 μM $GroES_7$ or 5 μM mobile loops (ML) (ETKSAGGIVLTGS; green ○) and subsequently supplemented at T = 0 min with 1 μM FTrho, and the time-dependent refolding rhodanese was measured. For comparison, the refolding of FTrho alone (black ●) or with GroEL (without ATP from Fig 1*A*; red ◇, dashed line) also is shown with illustrative schemes of the possible $GroEL_{14}$-$GroES_7$, $GroEL_{14}(GroES_7)_2$ (34–36), $SR1_7GroES_7$, or $GroEL_{14}(ML_7)_2$ complexes that may form under the various conditions. (*B*) Net chaperonin-assisted rhodanese refolding. FTrho (1 μM) first was incubated for 10 min in buffer at 22 °C then supplemented with equimolar GroEL protomers as in Fig 2*A*; then at T = 40 min it was supplemented with only ATP (5 mM), with only equimolar GroES, or with both as indicated. Lines are simple guides for the eyes.

Whereas apoSR1 was as effective as apoGroEL in refolding FTrho, preincubation of SR1 with GroES and ATP before FTrho addition completely inhibited refolding (Fig. 3*A*). Thus, the known irreversible binding of GroES to SR1, not only prevents the timely early exit of refolding species to complete optimal out-of-cage refolding, but also prevented new misfolded substrates from accessing the binding sites. This suggests that helices H and I, which are involved in substrate binding on the GroEL apical domains (11), also serve as the catalytic sites for unfolding.

To address the role of GroES binding in GroEL regeneration further, we used a minimal fragment of the GroES mobile loop, NH_2-ETKSAGGIVLTGS-COOH, that binds GroEL with high specificity but with a lower affinity than whole $GroES_7$ complexes (26). Remarkably, a fivefold molar excess of mobile loop peptides recovered GroEL-stalled FTrho nearly as effectively as equimolar GroES (in protomers; Fig. 3 and Fig. S6*D*), especially with ATP. Thus, mere binding of mobile loops to apoGroEL sufficed to drive the productive dissociation of sticky inhibitory species from the catalytic unfoldase sites of $GroEL_{14}$, leading to native refolding, an effect that was however poorly efficient with the SR1 mutants (Fig. S3*C*). Because individual mobile loops bind far from the cavity's entry (11, 26), encapsulation and in-cage refolding under sealed $GroES_7$ caps are not obligate steps of the basic catalytic unfolding mechanism by which apoGroEL may convert stable misfolded polypeptides into natively refoldable proteins.

In the case of CCT, ATP alone sufficed to dissociate and refold 106 nM of over-sticky intermediates in 60 min (T_{50} = 8 min) (Fig. S6*A*). This difference from GroEL was not unexpected, given that CCTs encode for small apical loops with putative GroES functions (27). Thus, GroEL and CCT strongly resemble each other in terms of ATP-independent catalytic unfoldase/refoldase activity. They both converted unbound misfolded substrates into free out-of-cage native proteins, and when they became stalled by sticky intermediates, they activated an ancillary regeneration mechanism with ATP (and mobile loops) to evict chaperonin-bound intermediates and convert them into free, natively refolded proteins.

FTrho Is Not an Unique Substrate. Because our results were obtained with a new type of substrate, FTrho, we next questioned whether other chaperonin substrates might be generated with similar characteristics. Early observations suggested the presence of FTrho-like chaperonin-amenable species in native protein stocks, as addition of GroEL + GroES + ATP to presumably

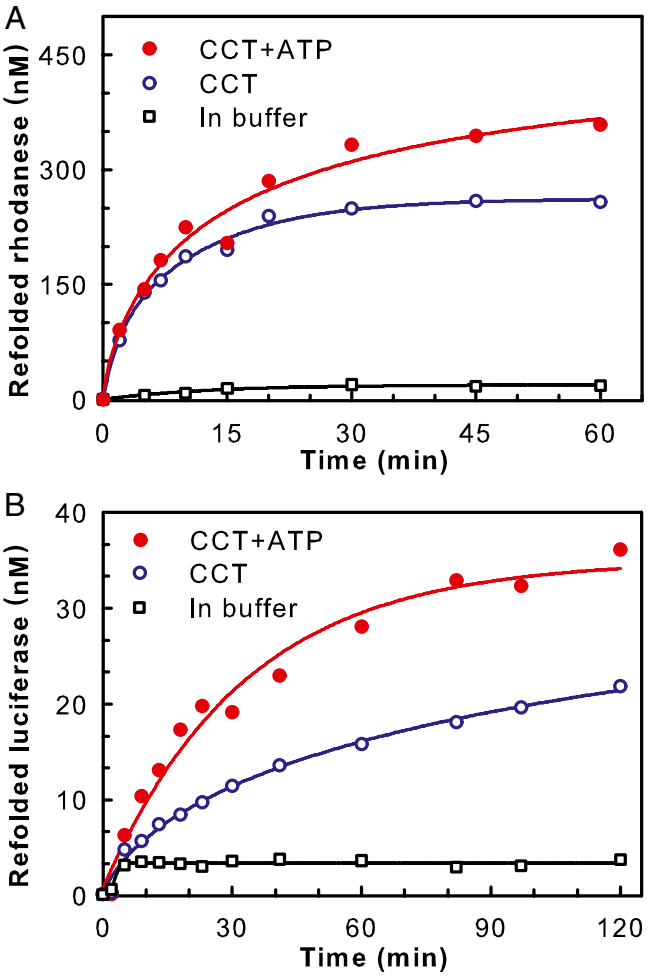

Fig. 4. CCT can mediate the ATP-independent refolding of both FTrho and FTluc. Time course of stringent chaperonin-mediated refolding of FTrho (1 μM) (*A*) or FTluc (*B*) at 22 °C in the presence of buffer (□) or 1 μM bovine CCT hetero-oligomers (protomers) without (blue ○) or with 5 mM ATP (red ●). Lines are simple guides for the eyes.

"all-native" stocks of rhodanese and pre–β-lactamase recovered 165% and 200% of active enzymes, respectively (21, 28). Here, we further tested whether such inactive species in native stocks might be processed by apoGroEL alone. Addition of apoGroEL + GroES to native stocks of Nrho or MDH produced 5% and 7% more native species, respectively (Fig. S7 *A* and *B*). Thus, native protein stocks in general may contain significant amounts of stable inactive misfolded species that can be refolded by apoGroEL. Following dilution of urea-unfolded rhodanese and completion of spontaneous refolding, which reached 30% Nrho (Fig. S7*C*), addition of apoGroEL also produced a net 4.5% increase of Nrho, and adding apoGroEL + GroES without ATP produced some additional Nrho (Fig. S7*C*), suggesting that a subpopulation of sticky urea-denatured species binds apoGroEL with an affinity similar to that of the GroEL-stalling FTrho species. Similarly, mild heat denaturation also generated some stable misfolded rhodanese species amenable to apoGroEL (Fig. S7*D*). Importantly, whereas apoGroEL remained ineffective at refolding FTluc (18), apoCCT was found to efficiently form up to 15%, and in the presence of ATP up to 22%, native luciferase (Fig. 4*B*). Thus, stable FTrho monomers are not exceptional substrates. Other in vitro denaturing conditions and different proteins may accumulate as apoGroEL-amenable stable inactive species. It is tempting to speculate that in stressed cells too, early misfolded species similar to FTrho, FTluc, and MDH may form and become as readily unfolded by GroEL or CCT and thus rehabilitated into nontoxic functional proteins at a very low ATP cost (6).

Discussion

We found that both classes of double-ring cage-like chaperonins act as polypeptide-unfolding enzymes, converting stable high-affinity misfolded polypeptide substrates into unstable high-affinity unfolded intermediates that subsequently refold into low-affinity native products. The unfoldase mechanism did not necessitate ATP or the in-cage confinement of the substrate. This was evidenced by the kinetic model that best fit the data and by comparing the volume of Nrho to that of the cavity in apoGroEL (Fig. 5). FTrho was a compact, structurally damaged inactive species that needed the ATP-dependent action of a large molar excess of DnaK chaperones to become unfolded enough to thereafter undergo spontaneous refolding to the native state (19); yet, we found here that it could become as sufficiently unfolded by equimolar apoGroEL or apoCCT (protomers) without ATP. Our data with FTrho also showed that without nucleotides, $GroES_7$ could cause the release and native refolding of GroEL-bound inactive species, confirming initial observations with GroEL–MDH complexes (25). Although this observation is important for the understanding of the chaperonin mechanism, it is likely irrelevant in cells that contain millimolars of ATP.

When FTrho was compelled to confinement in SR1 under a sealed $GroES_7$ cap, this was counterproductive compared with wild-type $GroEL_{14}$, indicating that for particular substrates, unrestricted out-of-the-cage refolding may be more effective than restricted in-cage refolding. The unfoldase activity was also found to be prone to gradual inhibition by over-sticky intermediates, and the regeneration of the catalytic activity necessitated ATP and the binding of GroES mobile loops. This further indicates that following binding and unfolding, tight confinement under apical loops in CCT, or a whole $GroES_7$ cap in GroEL, is not mandatory for the release of the intermediate. Moreover, our data suggest that when free in solution, folding intermediates may be more at liberty to sample various partially extended conformations to reach the native state than when detrimentally confined deep inside chaperonin cages. Thus, in general, chaperonins do not need to use their cage-like structures to carry their main activity as catalytic polypeptide unfoldases and to avert the formation of early off-pathway misfolded species. This does not exclude that in particular cases the cage-like structures may also act to prevent the aggregation of unfoldase-resistant misfolded polypeptides into potentially more toxic species, but such antiaggregation activity would expectedly inhibit the catalytic unfolding activity.

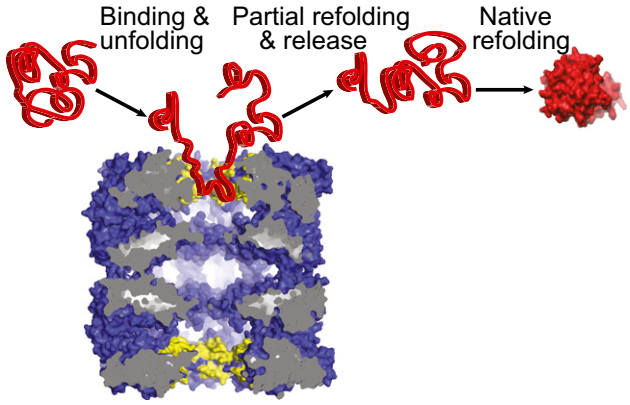

Fig. 5. Scheme of apoGroEL acting as an unfolding catalyst. ApoGroEL (Blue) mediates iterative cycles of binding to the upper cavity (yellow), unfolding, release, and out-of-cage refolding, thereby converting high-affinity misfolded polypeptide substrates (*Left*) into partially unfolded intermediates (*Center*) that fold spontaneously in solution into low-affinity native products (*Right*). Here, native rhodanese is more voluminous than the collapsed upper cavity of apoGroEL.

Relevance of Chaperonins Acting as Unfoldases in the Cell. A particular class of substrates has been identified by immune pull-down on the basis of their selective ability to remain tightly associated either to GroES-less GroEL particles or exclusively to GroES–GroEL–ADP complexes (29, 30), suggesting that similar to our in vitro data, some polypeptide substrates in cells also may require assistance from GroEL without GroES. Noticeably, we showed here that once unfolded, yet another class of FTrho-like substrates might readily dissociate from GroEL and consequently fail to be identified by immune pull-downs as GroEL substrates.

Given that chaperonins hydrolyze ATP very slowly (0.1–0.5 min^{-1}), this raises the possibility that despite the presence in human cells of millimolars of ATP and equimolar protomers of GroES (Table S2), the misfolded polypeptides sporadically forming during synthesis and under stress may become readily unfolded and released in solution before ATP is significantly hydrolyzed by the chaperonins (Fig. 5). ATP hydrolysis would thus strictly be necessary to fuel structural changes in the chaperonins to increase, against a gradient of free energy, the time they stay in the low-affinity releasing state and thus to recover over-sticky intermediates as native proteins. Together with FTluc and MDH, FTrho might serve as an attractive paradigm for very early-misfolded species on the proteotoxic aggregation pathway, to study the role of chaperones in preventing and curing protein conformational diseases.

Our observation that stable misfolded FTrho-like polypeptides, similar to the 82-kDa aconitase (14), need not fully enter the chamber and stay under a sealed GroES lid suggests that large polypeptides with several misfolded domains might be catalytically unfolded domain by domain, as shown to be the case with chimerical rhodanese fused to GFP or dihydrofolate reductase (31). CCT also was suggested to assist multidomain protein refolding in a domain-by-domain manner, thus mimicking optimal cotranslational folding (32).

Chaperonins are 2% (wt/vol) of the total mass of intracellular proteins in human (HeLa) cells (Table S2) (33). Further experiments beyond the scope of this work are needed to assess the relative importance of iterative catalytic unfolding/refolding and prevention of aggregation by sequestration as complementary mechanisms to delay the onset of protein misfolding diseases and aging (34).

Methods

Proteins. GroEL and GroES were purified according to standard laboratory procedure (35). His-tagged luciferase was purified as described previously (18) and stored in 15% (vol/vol) glycerol at −80 °C. Bovine rhodanese and pig heart mitochondrial MDH (mtMDH) were purchased from Sigma–Aldrich.

Mobile loop peptides were from GenScript. All protein concentrations were estimated by the Bradford Assay and mentioned as protomer concentrations unless otherwise mentioned.

Protein Activity Measurements. Rhodanese activity was measured by a colorimetric method (monitored at 460 nm) based on the formation of the complex between ferric ions and one of the reaction products, thiocyanate (17). Luciferase activity was measured using a Victor Light 1420 Luminescence Counter (Perkin–Elmer) as described previously (18). The activity of MDH was measured by following the time-dependent oxidation of NADH by mtMDH at 340 nm (25).

Chaperone Refolding Assays. Refolding assays were performed in refolding buffer [50 mM Tris acetate (pH 7.8), 150 mM KCl, 20 mM $MgCl_2$] in the presence or in the absence of ATP (5 mM) with different chaperone concentrations, as mentioned in the figure legends. For rhodanese, the refolding buffer also included 50 mM $Na_2S_2O_4$, 10% (vol/vol) glycerol, 2 μM BSA, and 20 mM DTT. Rates of rhodanese, luciferase, and MDH refolding were derived from the linear phase of the time curves of recovered enzymatic activity.

Trypsin Sensitivity of Rhodanese. For trypsin digestion, 1 μM FTrho was incubated with trypsin (0.02 mg/mL) for 3 min and the digestion was stopped by adding 100 μM of the trypsin inhibitor TLCK (Sigma–Aldrich). The trypsin digestion during GroEL-assisted unfolding/refolding of FTrho at different time points was followed by measuring yields 60 min after GroEL addition, regardless of when the transient trypsin treatment was applied. Time 0: the 3′ trypsin treatment was applied to FTrho and stopped by TLCK addition before GroEL addition at T = 0 min.

Th-T fluorescence and light-scattering measurements were as described earlier (19).

Denaturation of Rhodanese. The misfolded monomeric luciferase was prepared by freeze–thawing as described in ref. 18. The misfolded monomeric rhodanese was prepared in general according to Natalello et al. (19). In short, 2 μM Nrho in 20 mM Na phosphate (pH 7.5), 12.5 mM Na thiosulfate, and 20 mM DTT was denatured by five to eight consecutive cycles of rapid freezing at −160 °C and slow thawing at 18 °C. When inactivated more than 90%, aggregates were removed by 5′ centrifugation at 20,000 × *g* and the supernatant was concentrated to a final concentration of 2–3 μM of mostly inactive FTrho species. For heat denaturation, rhodanese (5 μM) was incubated for 10 min at 62 °C in 50 mM Tris·HCl, 150 mM KCl, and 20 mM $MgCl_2$, pH 7.5. The residual activity after heat exposure was <2% of the initial. For urea-unfolded rhodanese, rhodanese was incubated in different concentrations of urea up to a maximum of 8 M for 1 h at 25 °C.

Size-Exclusion Chromatography. To isolate GroEL stalled with misfolded inhibitory rhodanese, mixtures of GroEL and rhodanese at time 0 and 60 min were passed through size-exclusion chromatography in buffer (50 mM Tris·HCl, 150 mM potassium chloride, and 20 mM magnesium chloride, pH 7.5) using a Superose 6 HR10/30 gel filtration column (Amersham Pharmacia Biotech, GE Healthcare) at a flow rate of 0.5 mL/min. The absorbance was monitored at 280 nm. Apparent molecular weights were estimated by gel filtration of standard proteins (Bio-Rad).

ACKNOWLEDGMENTS. We thank Elena Bochkareva for the gift of GroEL and GroES, José Maria Valpuesta for the gift of CCT, Matthias Mayer for HtpG, Avital Parnas for unshown preliminary experiments with acid-denatured MDH, Dan S. Tawfik for discussions, and Alberto Merli and Anika Braune for discussions and technical assistance. We also thank the Herbette Foundation of the University of Lausanne for partial financing of P.G.'s research in the A.A. laboratory. This project was financed by Swiss National Science Foundation Grants 125502/1 and 140512/1 (to P.G.) and Israel Science Foundation Grant 452/09 (to A.A.).

1. Sharma SK, De Los Rios P, Goloubinoff P (2011) Probing the different chaperone activities of the bacterial HSP70-HSP40 system using a thermolabile luciferase substrate. *Proteins* 79(6):1991–1998.
2. Dobson CM (2003) Protein folding and misfolding. *Nature* 426(6968):884–890.
3. Jaenicke R (1991) Protein stability and protein folding. *Ciba Found Symp* 161:206–216, discussion 217–221.
4. Sharma SK, Christen P, Goloubinoff P (2009) Disaggregating chaperones: An unfolding story. *Curr Protein Pept Sci* 10(5):432–446.
5. Hartl FU, Hayer-Hartl M (2002) Molecular chaperones in the cytosol: From nascent chain to folded protein. *Science* 295(5561):1852–1858.
6. Hinault MP, Ben-Zvi A, Goloubinoff P (2006) Chaperones and proteases: Cellular fold-controlling factors of proteins in neurodegenerative diseases and aging. *J Mol Neurosci* 30(3):249–265.
7. Goloubinoff P, Christeller JT, Gatenby AA, Lorimer GH (1989) Reconstitution of active dimeric ribulose bisphosphate carboxylase from an unfoleded state depends on two chaperonin proteins and Mg-ATP. *Nature* 342(6252):884–889.
8. Buchner J, et al. (1991) GroE facilitates refolding of citrate synthase by suppressing aggregation. *Biochemistry* 30(6):1586–1591.
9. Fenton WA, Kashi Y, Furtak K, Horwich AL (1994) Residues in chaperonin GroEL required for polypeptide binding and release. *Nature* 371(6498):614–619.
10. Motojima F, Yoshida M (2010) Polypeptide in the chaperonin cage partly protrudes out and then folds inside or escapes outside. *EMBO J* 29(23):4008–4019.
11. Clare DK, et al. (2012) ATP-triggered conformational changes delineate substrate-binding and -folding mechanics of the GroEL chaperonin. *Cell* 149(1):113–123.
12. Horovitz A, Willison KR (2005) Allosteric regulation of chaperonins. *Curr Opin Struct Biol* 15(6):646–651.
13. Horovitz A, Fridmann Y, Kafri G, Yifrach O (2001) Review: Allostery in chaperonins. *J Struct Biol* 135(2):104–114.
14. Farr GW, et al. (2003) Folding with and without encapsulation by cis- and trans-only GroEL-GroES complexes. *EMBO J* 22(13):3220–3230.
15. Inbar E, Horovitz A (1997) GroES promotes the T to R transition of the GroEL ring distal to GroES in the GroEL-GroES complex. *Biochemistry* 36(40):12276–12281.
16. Landry SJ, Zeilstra-Ryalls J, Fayet O, Georgopoulos C, Gierasch LM (1993) Characterization of a functionally important mobile domain of GroES. *Nature* 364(6434):255–258.
17. Mendoza JA, Rogers E, Lorimer GH, Horowitz PM (1991) Chaperonins facilitate the in vitro folding of monomeric mitochondrial rhodanese. *J Biol Chem* 266(20):13044–13049.
18. Sharma SK, De los Rios P, Christen P, Lustig A, Goloubinoff P (2010) The kinetic parameters and energy cost of the Hsp70 chaperone as a polypeptide unfoldase. *Nat Chem Biol* 6(12):914–920.
19. Natalello A, et al. (2013) Biophysical characterization of two different stable misfolded monomeric polypeptides that are chaperone-amenable substrates. *J Mol Biol* 425(7):1158–1171.
20. Weissman JS, Rye HS, Fenton WA, Beechem JM, Horwich AL (1996) Characterization of the active intermediate of a GroEL-GroES-mediated protein folding reaction. *Cell* 84(3):481–490.
21. Laminet AA, Ziegelhoffer T, Georgopoulos C, Plückthun A (1990) The Escherichia coli heat shock proteins GroEL and GroES modulate the folding of the beta-lactamase precursor. *EMBO J* 9(7):2315–2319.
22. Zahn R, Spitzfaden C, Ottiger M, Wüthrich K, Plückthun A (1994) Destabilization of the complete protein secondary structure on binding to the chaperone GroEL. *Nature* 368(6468):261–265.
23. Zahn R, Perrett S, Fersht AR (1996) Conformational states bound by the molecular chaperones GroEL and secB: A hidden unfolding (annealing) activity. *J Mol Biol* 261(1):43–61.
24. Lin Z, Madan D, Rye HS (2008) GroEL stimulates protein folding through forced unfolding. *Nat Struct Mol Biol* 15(3):303–311.
25. Ben-Zvi AP, Chatellier J, Fersht AR, Goloubinoff P (1998) Minimal and optimal mechanisms for GroE-mediated protein folding. *Proc Natl Acad Sci USA* 95(26):15275–15280.
26. Chen LL, Sigler PB (1999) The crystal structure of a GroEL/peptide complex: Plasticity as a basis for substrate diversity. *Cell* 99(7):757–768.
27. Yébenes H, Mesa P, Muñoz IG, Montoya G, Valpuesta JM (2011) Chaperonins: Two rings for folding. *Trends Biochem Sci* 36(8):424–432.
28. Smith KE, Fisher MT (1995) Interactions between the GroE chaperonins and rhodanese. Multiple intermediates and release and rebinding. *J Biol Chem* 270(37):21517–21523.
29. Houry WA, Frishman D, Eckerskorn C, Lottspeich F, Hartl FU (1999) Identification of in vivo substrates of the chaperonin GroEL. *Nature* 402(6758):147–154.
30. Kerner MJ, et al. (2005) Proteome-wide analysis of chaperonin-dependent protein folding in Escherichia coli. *Cell* 122(2):209–220.
31. Kipnis Y, Papo N, Haran G, Horovitz A (2007) Concerted ATP-induced allosteric transitions in GroEL facilitate release of protein substrate domains in an all-or-none manner. *Proc Natl Acad Sci USA* 104(9):3119–3124.
32. Rivenzon-Segal D, Wolf SG, Shimon L, Willison KR, Horovitz A (2005) Sequential ATP-induced allosteric transitions of the cytoplasmic chaperonin containing TCP-1 revealed by EM analysis. *Nat Struct Mol Biol* 12(3):233–237.
33. Finka A, Goloubinoff P (2013) Proteomic data from human cell cultures refine mechanisms of chaperone-mediated protein homeostasis. *Cell Stress Chaperones*, 10.1007/s12192-013-0413-3.
34. Hinault MP, et al. (2010) Stable alpha-synuclein oligomers strongly inhibit chaperone activity of the Hsp70 system by weak interactions with J-domain co-chaperones. *J Biol Chem* 285(49):38173–38182.
35. Todd MJ, Viitanen PV, Lorimer GH (1993) Hydrolysis of adenosine 5′-triphosphate by Escherichia coli GroEL: Effects of GroES and potassium ion. *Biochemistry* 32(33):8560–8567.
36. Azem A, Diamant S, Kessel M, Weiss C, Goloubinoff P (1995) The protein-folding activity of chaperonins correlates with the symmetric GroEL14(GroES7)2 hetero-oligomer. *Proc Natl Acad Sci USA* 92(26):12021–12025.
37. Schmidt M, et al. (1994) Symmetric complexes of GroE chaperonins as part of the functional cycle. *Science* 265(5172):656–659.

Supporting Information

Priya et al. 10.1073/pnas.1219867110

SI Text

S1. Mathematical Modeling and Discussion for Figs. S3–S5. ***Mathematical model.*** We propose a scheme for the catalytic unfolding process mediated by GroEL in which the free energy levels of the various molecular states of GroEL and the protein are represented qualitatively (Fig. S3*A*). First, the misfolded substrate can bind to GroEL, resulting in a decrease of the free energy. To catalyze substrate unfolding so that the thermally driven conversion of freeze–thaw denatured rhodanese (FTrho) to native rhodanese (Nrho) may be accelerated, chaperonin binding must lower the free energy of the transition state (**T**) more than that of the misfolded state (**M**) of the substrate (1), whereas the free energy of bound **T** may be higher by a few k_BT than bound **M**. In other words, the unfolded transitory intermediate **T** must have the highest affinity for the chaperonin. Passing through the transition state, the substrate **T** must then spontaneously convert into a lower free-energy intermediate that can either reacquire some native-like structures in regions that are between the direct contact points with the chaperonin and thus fold on-pathway (**I**) or fail to partially refold and thus misfold off-pathway (**J**). Once released from the chaperonin in solution, the on-pathway intermediate **I** can either rebind or complete refolding to the lowest-affinity native state. The off-pathway intermediate J fails to reduce its high affinity (because of its unsuccessful partial local refolding) and remains stalled onto the chaperonin. The kinetics of the cycle are represented pictorially in Fig. S3 *A* and *B*.

Because we did not observe aggregation during the time scale of the reaction (Fig. S1A), no aggregated state is included in the model. Moreover, simple geometrical considerations argue against the occupation of a single apoGroEL$_7$ ring by more than one 33-kDa rhodanese molecule (compare the size of native Rho with that of the cavity in apoGroEL; see Fig. 5) and thus the model considered only 1:1 substrate–GroEL$_7$ ring complexes. Each GroEL$_7$ ring liberated by a substrate molecule is readily available to bind another substrate, allowing multiple unfolding turnovers per GroEL$_7$ ring. Given that in Fig. 1*A*, two SR1 single-ring mutants are as active as a single GroEL$_{14}$, in our modeling of the GroES- and ATP-independent cycle, the two rings bind and process the substrate independently of each other, allowing us to represent one GroEL$_{14}$ molecule by two effective GroEL$_7$ rings in the mathematical equations below. The model depends on several parameters that are kept to a minimum on the basis of several considerations:

i) Binding/unbinding of FTrho to and from the chaperonin is fast compared with the time scale of the unfolding and refolding reactions, determined by looking at Fig. 2*B* for unfolding (T_{50} = 2.5 min) and at Fig. 2*A* for refolding (T_{50} = 5 min); as a consequence, we described the binding/unbinding of FTrho as an equilibrium with a dissociation constant K_m. Any misfolded molecule is either bound to a GroEL$_7$ ring or not, and at equilibrium we can express the amount of bound misfolded ([*GM*]) as a fraction of the total amount of misfolded protein.

ii) As the transition state T is not detected in our experiments, we did not include it explicitly in the mathematical formulae of the model. Rather, we accounted directly for the transitions from bound M to the bound on-pathway intermediate I and the bound off-pathway intermediate J, which proceed at rates k_I and k_J, respectively.

iii) The bound intermediate I can be released (with rate k_{rel}) or be recaptured (with rate λ_i).

iv) In solution, the intermediate can irreversibly natively refold (with rate k_F).

v) In addition, we included an initial contribution of a minority of native rhodanese species in the FTrho preparation at T = 0 (N_{bg}), which is independent of GroEL and remains fixed in min, and a fittable total amount of refoldable substrate (M_0). The model thus is described by eight parameters, and the governing equations are

$$[M]_{total} = [M] + [GM],$$

$$[GM] = \frac{[G]}{[G] + K_m} M_{total},$$

$$\frac{d[M]_{total}}{dt} = -(k_I + k_J)[GM],$$

$$\frac{d[GI]}{dt} = k_I[GM] + \lambda_i[G][I] - k_{rel}[GI],$$

$$\frac{d[GJ]}{dt} = k_J[GM],$$

$$\frac{d[I]}{dt} = k_{rel}[GI] - \lambda_i[G][I] - k_F[I].$$

We determined the best values of the parameters by fitting the model results to the folding curves for three different values of [GroEL] (Fig. S4). The parameter values are reported in Table S1.

The fitted dissociation constant (K_m) for the misfolded **M** is very low, suggesting that **M** has a high affinity for the chaperonin. The formation of on-pathway **I** and off-pathway **J** intermediates proceeds at fairly high rates (time scale of seconds). This is reasonable, considering the thioflavin T (Th-T) and trypsin data from Fig. 1 *A* and *B*, showing that the bound M becomes unfolded within 2 min. The two rates for intermediate release (k_{rel}) and binding (λ_i) are the fastest of all the processes we have modeled, whereas native folding proceeds at the slowest rate and hence determines the overall T_{50} = 10 min. Thus, in our model, the release of I from the chaperonin is fast, whereas the final folding to the native state in solution is a slower process.

The Th-T and time-lapse trypsin treatments are an independent check that the rates of the upstream processes of **M** binding and unfolding are at least five times faster than the subsequent process of native refolding and, therefore, that the latter is rate limiting. The best fits we obtained produced a very fast rate of release and much slower refolding. In fact, replacing the intermediate release and binding by an equilibrium process by an effective dissociation constant of $k_{rel}/\lambda_i = 792$ nM had a negligible effect on our fits. However, the value of using a kinetic description for this binding/release process is to explore other ways in which the overall refolding time is shared by intermediate release and refolding. Despite its good fit, we ruled out the model with slow intermediate release and fast refolding on the grounds that the amount of free intermediate remained very low (Fig. S3). This was incompatible with the trypsin digestion data, which showed the released intermediate to be most susceptible to trypsin digestion compared with the GroEL-bound intermediate assumed to be more protected

from digestion, because of the plausible decreased accessibility of the 23-kDa trypsin molecules to the bound species in the upper cavity of GroEL.

In-cage folding. The model we have discussed so far involved only out-of-cage refolding. However, we also considered the in-cage folding hypothesis, wherein the native polypeptide is released with a rate k_N from the cage directly into the solution in addition to the folding intermediate I. In contrast to the out-of-cage folding hypothesis, the intermediate does not fold to native in solution.

In Fig. S4 (dashed lines), the fits for in-cage folding clearly were worse than the fits for out-of-cage folding: the χ^2 value was much larger (184 vs. 46) and, more importantly, in-cage folding predicted that a GroEL excess would accelerate the reaction, whereas experimentally it slowed the refolding reaction while reaching the same yields.

We thus reintroduced out-of-cage, in which the released intermediate I could refold slowly free in the solution. In the resulting model with both in-cage and out-of-cage folding, the extra parameter can only improve the fit. However, the χ^2 improved by less than 1 with respect to the only out-of-cage model. The fitted value of the rate of in-cage folding k_N was 0.02 per minute, whereas out-of-cage folding k_F was fivefold higher at 0.11 per minute, implying that the partitioning between in-cage and out-of-cage was shifted greatly in favor of out-of-cage folding.

1. Fersht AR (1998) *Structure and Mechanism in Protein Science: A Guide to Enzyme Catalysis and Protein Folding* (Freeman, New York).

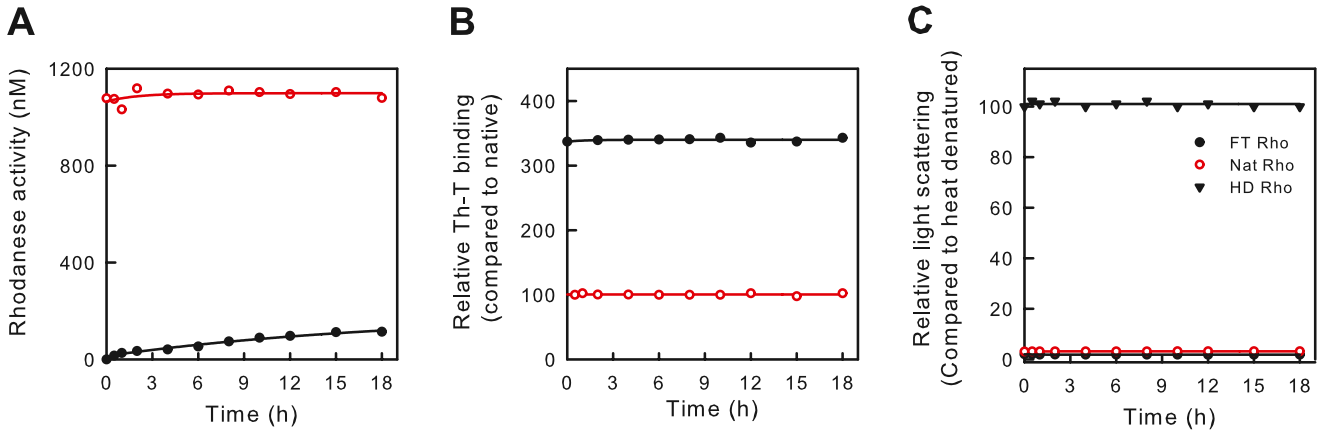

Fig. S1. FTrho is a stable misfolded species. Activity (*A*), relative Th-T fluorescence (*B*), and relative light scattering (*C*) of Nrho (red ○), FTrho (●), and heat-denatured rhodanese (HDrho) (▼) during 18-h incubation in folding buffer at 22 °C.

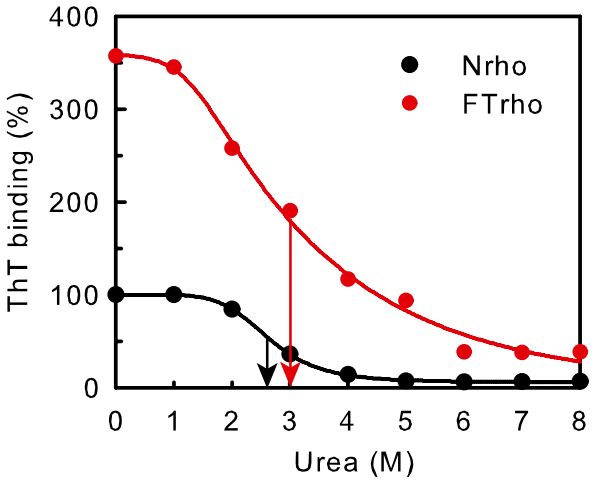

Fig. S2. FTrho is more resistant than Nrho to urea unfolding. One micromolar of FTrho (black line) or Nrho (red line) was incubated for 60 min at 25 °C in the presence of 60 μM Th-T and different increasing urea concentrations, as indicated. Steady-state Th-T fluorescence was measured as in Natalello et al. (1) and normalized to the signal of Nrho without urea (100%). The EC_{50} value for Nrho was at 2.6 M urea (black ↓) and for FTrho at 3.0 M urea (red ↓).

1. Natalello A, et al. (2013) Biophysical characterization of two different stable misfolded monomeric polypeptides that are chaperone-amenable substrates. *J Mol Biol* 425(7):1158–1171.

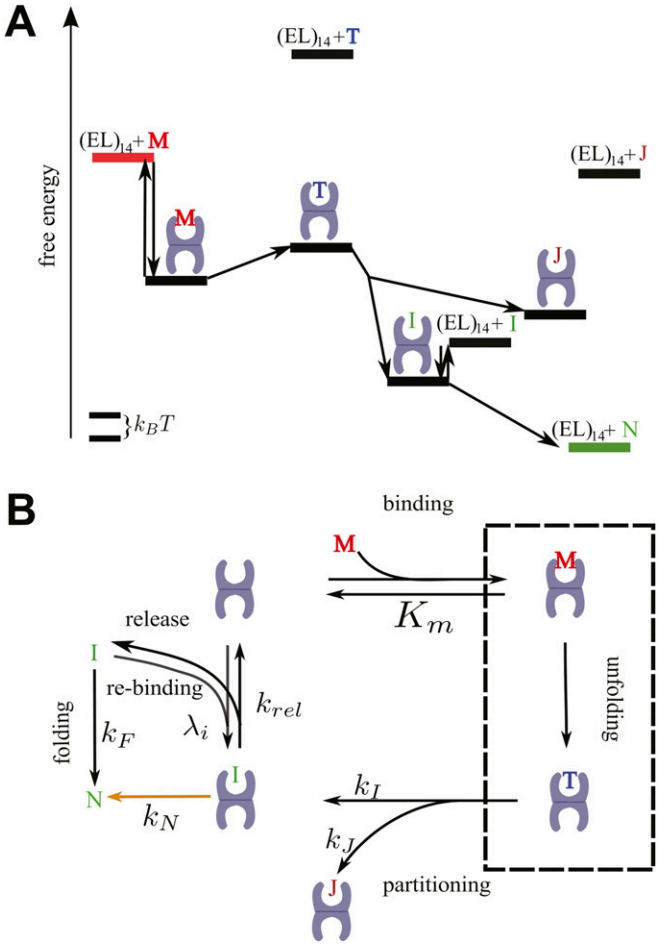

Fig. S3. Model for the catalytic action of GroEL and CCT chaperonins. (*A*) The qualitative free energies (horizontal bars) of the various complexes and the major reaction steps involved in the binding, unfolding, release, and refolding of the polypeptide substrate are shown. The misfolded substrate (FTrho) *M*, has a high affinity for the chaperonin, to which it binds readily; the bound *M* rapidly unfolds on the surface of the apical domains, passing through a very highaffinity transient state *T*. A consequent spontaneous local refolding leads to a medium-affinity intermediate I that may dissociate spontaneously in the external solution, where it refolds slowly to the lowest-affinity native state. Alternatively, *T* may fail to refold locally and stay stalled as a high-affinity intermediate *J*. The thermal energy available for the spontaneous dissociation is shown in the lower left corner. (*B*) Chemical kinetic scheme with its parameters used to produce the formula we used to simulate the reactivation curves shown in Fig. S4. The orange arrow represents in-cage folding, which results in the direct release of a native product. This branch of the reaction has been turned on and off to explore the differences between in-cage and out-of-cage folding.

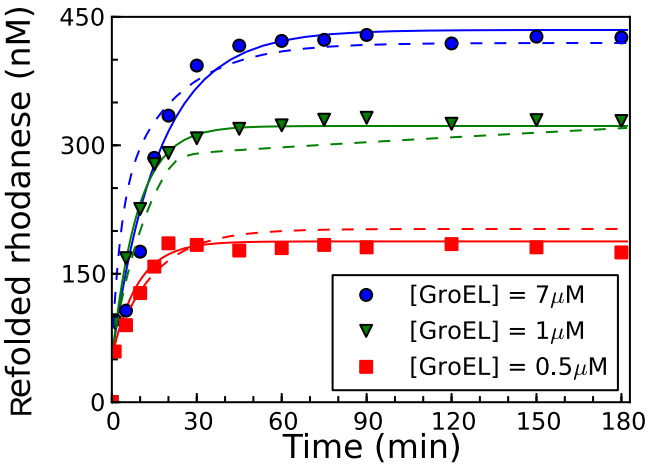

Fig. S4. Simulations of the out-of-cage and in-cage folding model that fit experimental refolding rates and yields at three GroEL concentrations. Symbols are the experimental data from the time-dependent refolding of FTrho (1 μM) supplemented at T = 0 min (without ATP) with 0.5 μM (red ■), 1 μM (green ▼), or 7 μM (blue ●) GroEL (protomers). The simulated activity of 0.5 μM GroEL (red line), 1 μM GroEL (green line), or 7 μM GroEL (blue line) is according to the equation described in SI Text, section S1. The best fits are obtained with parameter values shown in Table S1. Solid lines indicate out-of-cage folding, whereas dotted lines show in-cage folding.

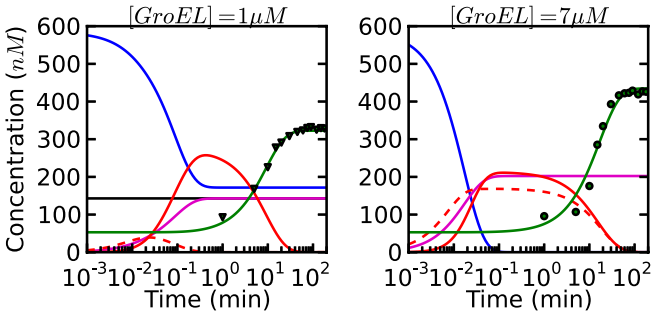

Fig. S5. Time evolution of the various species according to the model. For two different concentrations of chaperonin (Left, equimolar GroEL; Right, excessGroEL), the solid blue line indicates the amount of free refolding amenable FTrho, the solid green line free Nrho, the solid red line free on-pathway intermediate,the dashed red line intermediate bound to GroEL rings, and the solid violet line stalled intermediate on GroEL rings; ▼ (Left) and ● (Right) areexperimental Nrho data. (*Left*) Binding of FTrho and release of the unfolded on-pathway intermediate are fast, so only a minor fraction of the substrate maybe found transiently bound to GroEL rings. Instead, the gradual accumulation of stalled species progressively inhibits the full GroEL population (with a 1:1ratio, at about 170 nM; solid black line). Once all rings are inactivated, no free amenable FTrho can be processed. (*Right*) Free FTrho is consumed readily, andthere is a substantial increase in the amount of transiently bound substrate. This is a consequence of GroEL rebinding of the released substrate. Only later, when native refolding is slowly occurring, does the concentration of both bound and released intermediate decrease. Inhibition of GroEL rings, in this case, isnot complete and is determined mostly by the partitioning between stalling and productive intermediate accumulation. A major difference between the twocases is the number of turnovers per GroEL ring: whereas with equimolar GroEL protomers (substoichiometric GroEL rings), each ring processes, on average, about two substrate molecules before being stalled, when GroEL protomers are in excess (equimolar GroEL rings), at most one substrate molecule per ring canbe produced on average, but actually fewer because of inhibition.

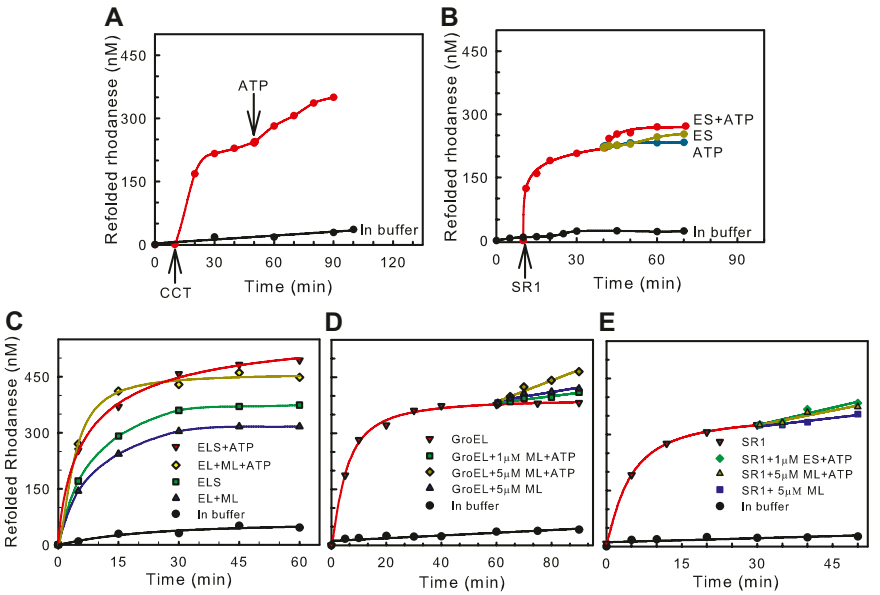

Fig. S6. Sequential chaperonin-assisted refolding by CCT, GroEL or SR1. (*A*) FTrho (1 μM) was first incubated for 10 min in buffer at 22 °C, then supplemented with equimolar CCT as in (Fig. 1*A*), then supplemented at T = 40 min with ATP and allowed to refold for 50 additional minutes. (*B*) FTrho (1 μM) was first incubated for 10 min then supplemented with equimolar SR1 (protomers) as in Fig. 2*B*, then at T = 40 min supplemented with only ATP (5 mM), or with only equimolar GroES or with both, as indicated. Mobile loop peptides (N-ETKSAGGIVLTGS-C) can replace whole GroES7 complexes at decreasing the affinity of sticky FTrho inhibitory species for GroEL or SR1. FTrho (1 μM) was supplemented with GroEL (1 μM) without or with GroES (1 μM) or mobile loops (ML, 5μM), without or with ATP (5 mM), as indicated. (*C*) GroES, and/or ML and/or ATP was added at T = 0 min. ATP and increasing concentrations of ML as indicated were added at 60 min to GroEL (*D*), or to SR1 (*E*).

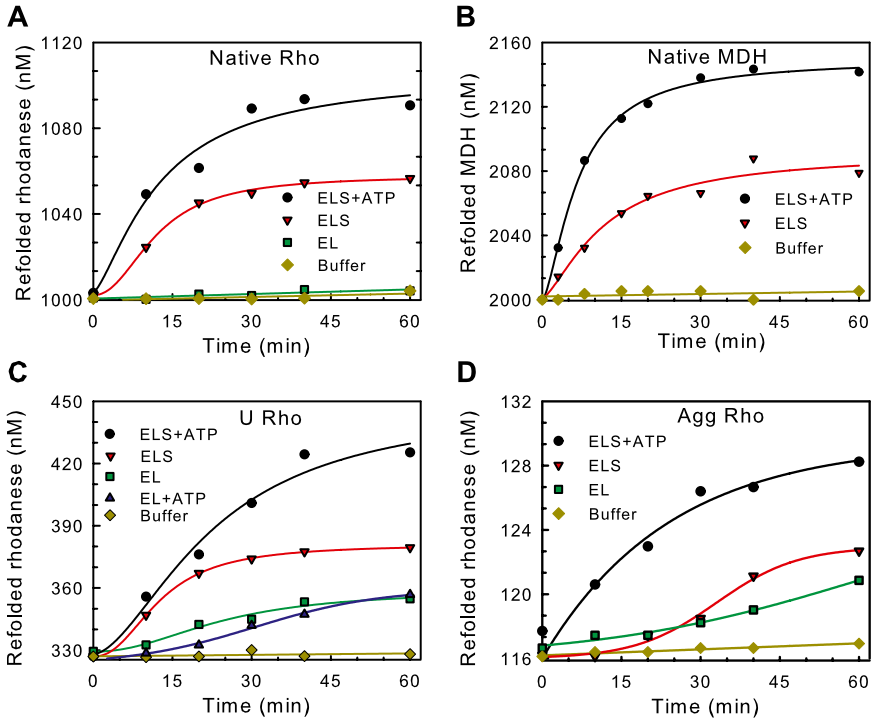

Fig. S7. Protocols other than FT can generate GroEL-amenable species. Time-dependent reactivation of "native" Nrho (1 μM) (*A*) or native mitochondrial malate dehydrogenase (mtMDH; 2 μM) (*B*) from the native stocks provided by the suppliers, or Nrho that first was urea denatured (*C*) or heat denatured (*D*) then incubated at 22 °C either in buffer (♦) or supplemented with equimolar GroEL and GroES without (red ▼) or with 5 mM ATP (●). For *C*, 40 μM Nrho first was denatured in 8 M urea for 60 min then diluted 40-fold in folding buffer and allowed to refold spontaneously for 3 h at 22 °C, and then was supplemented with 1 μM chaperonins. For *D*, 1 μM Nrho was denatured at 62 °C for 10 min until it lost 89% activity, then was supplemented with chaperonins.

Table S1. Parameter values obtained by numerically fitting the model to the data for three different concentrations in Fig. S4

Parameter	Fitted value
K_m	1 nM
k_I	38.34/min
k_J	20.32/min
k_{rel}	59.46/min
λ_i	75/(μM min)
k_F	0.11/min
N_{bg}	53 nM
M_0	584 nM

Quality of the fit was defined by the error, $X^2 = \Sigma_{t,g}[(N_{g,t} - n_{g,t})^2/n_{g,t}$, where $n_{g,t}$ are obtained from the model and $n_{g,t}$ are the experimentally observed values for data points corresponding to time and GroEL values indexed by t (time) and g (GroEL protomer concentration), respectively. We found a value of $X^2 \sim 46$ for a total of 8 parameters and 36 data points.

Table S2. Copy number of cytosolic and mitochondrial chaperonins in HeLa cells

	Gene			Protein amount	
Protein name	Name	% (wt/wt)	*P* value	Copy number (10^6)	*P* value
Chaperonin-containing TCP1, subunit 1 (alpha)	CCT1	0.16	0.020	2.38	0.022
Chaperonin-containing TCP1, subunit 2 (beta)	CCT2	0.16	0.002	2.51	0.003
Chaperonin-containing TCP1, subunit 3 (gamma)	CCT3	0.17	0.004	2.48	0.003
Chaperonin-containing TCP1, subunit 4 (delta)	CCT4	0.16	0.013	2.56	0.016
Chaperonin-containing TCP1, subunit 5 (epsilon)	CCT5	0.19	0.006	2.87	0.006
Chaperonin-containing TCP1, subunit 6 (zeta 1)	CCT6A	0.17	0.037	2.68	0.039
Chaperonin-containing TCP1, subunit 7 (eta)	CCT7	0.12	0.000	1.84	0.001
Chaperonin-containing TCP1, subunit 8 (theta)	CCT8	0.21	0.006	3.22	0.005
TCP/CCT complex*	$(CCT1\text{-}8)_{16}$	1.34	0.002	1.28	0.000
Actin, alpha, cardiac muscle 1	ACTC	0.11	0.144	2.38	0.149
Tubulin, beta 4B class IVb	TUBB2C	0.63	0.035	11.38	0.031
mtHsp60 (GROEL)	HSPD1	0.53	0.015	7.91	0.016
mtHsp10 (GROES)	HSPE1	0.07	0.001	5.51	0.001
mtHsp60 complex	$(HSPD1)_{14}$	0.53	0.015	0.57	0.016
mtHsp10 complex	$(HSPE1)_7$	0.07	0.001	0.78	0.001

Concentrations of cytosolic CCTs and their main actin and tubulin substrates and of mitochondrial Hsp60 and Hsp10 in HeLa cells were obtained from ref. 1. Mean copy numbers per cell from all three independent measurement and *P* values are shown. Mean copy numbers and *P* values for the entire 16-mer CCT complex (*) were estimated from the 24 measurements, assuming that the eight different CCT1–8 subunits are equimolar in the complex (2). We deduced the cellular concentrations of individual proteins, assuming a total protein mass of 150 pg per HeLa cell (3) with an estimated volume of 2,600 μm^3 (4), containing a total of 2×10^9 polypeptides (5). Each protein first was expressed as a percentage of the total protein mass and then was converted into polypeptide copy number per cell. mtHsp60, mitochondrial GroEL; mtHsp10, mitochondrial GroES.

1. Geiger T, Wehner A, Schaab C, Cox J, Mann M (2012) Comparative proteomic analysis of eleven common cell lines reveals ubiquitous but varying expression of most proteins. *Mol Cell Proteomics* 11(3):M111.014050.
2. Dekker C, Willison KR, Taylor WR (2011) On the evolutionary origin of the chaperonins. *Proteins* 79(4):1172–1192.
3. Volpe P, Eremenko-Volpe T (1970) Quantitative studies on cell proteins in suspension cultures. *Eur J Biochem* 12(1):195–200.
4. Zhao L, et al. (2008) Intracellular water-specific MR of microbead-adherent cells: The HeLa cell intracellular water exchange lifetime. *NMR Biomed* 21(2):159–164.
5. Nagaraj N, et al. (2011) Deep proteome and transcriptome mapping of a human cancer cell line. *Mol Syst Biol* 7:548.

CHAPTER 5

Stable α-Synuclein oligomers strongly inhibit chaperone activity of the Hsp70 system by weak interactions with J-domain co-chaperones

Stable α-Synuclein oligomers strongly inhibit chaperone activity of the Hsp70 system by weak interactions with J-domain co-chaperones.

Hinault, M.P., Cuendet, A.F.H., Mattoo, R.U., Mensi, M., Dietler, G., Lashuel, H.A. and Goloubinoff, P.

I contributed to the writing of the manuscript.

I provided the data for Fig. S3 (A and B), Fig. S4 and Fig. S5.

THE JOURNAL OF BIOLOGICAL CHEMISTRY VOL. 285, NO. 49, pp. 38173–38182, December 3, 2010

Stable α-Synuclein Oligomers Strongly Inhibit Chaperone Activity of the Hsp70 System by Weak Interactions with J-domain Co-chaperones*[S]

Received for publication, March 26, 2010, and in revised form, September 14, 2010 Published, JBC Papers in Press, September 16, 2010, DOI 10.1074/jbc.M110.127753

Marie-Pierre Hinault[‡], America Farina Henriquez Cuendet[‡], Rayees U. H. Mattoo[‡], Mounir Mensi[§], Giovanni Dietler[§], Hilal A. Lashuel[¶], and Pierre Goloubinoff[‡1]

From the [‡]Plant Molecular Biology Department, University of Lausanne, Biophore, 1015 Lausanne, Switzerland and the [§]Laboratoire de Physique de la Matière Vivante, IPMC-SB and [¶]Laboratory of Molecular Neurobiology and Neuroproteomics, Brain Mind Institute, Ecole Polytechnique Fédérale de Lausanne, Lausanne 1015, Switzerland

α-Synuclein aggregation and accumulation in Lewy bodies are implicated in progressive loss of dopaminergic neurons in Parkinson disease and related disorders. In neurons, the Hsp70s and their Hsp40-like J-domain co-chaperones are the only known components of chaperone network that can use ATP to convert cytotoxic protein aggregates into harmless natively refolded polypeptides. Here we developed a protocol for preparing a homogeneous population of highly stable β-sheet enriched toroid-shaped α-Syn oligomers with a diameter typical of toxic pore-forming oligomers. These oligomers were partially resistant to *in vitro* unfolding by the bacterial Hsp70 chaperone system (DnaK, DnaJ, GrpE). Moreover, both bacterial and human Hsp70/Hsp40 unfolding/refolding activities of model chaperone substrates were strongly inhibited by the oligomers but, remarkably, not by unstructured α-Syn monomers even in large excess. The oligomers acted as a specific competitive inhibitor of the J-domain co-chaperones, indicating that J-domain co-chaperones may preferably bind to exposed bulky misfolded structures in misfolded proteins and, thus, complement Hsp70s that bind to extended segments. Together, our findings suggest that inhibition of the Hsp70/Hsp40 chaperone system by α-Syn oligomers may contribute to the disruption of protein homeostasis in dopaminergic neurons, leading to apoptosis and tissue loss in Parkinson disease and related neurodegenerative diseases.

A number of neurodegenerative disorders, such as Alzheimer, amyotrophic lateral sclerosis, Huntington, prion encephalopathy, and Parkinson diseases (PDs)[2] are characterized by a loss of neurons associated with protein misfolding and the accumulation in and outside cells of stable protein aggregates composed of specific proteins, such as tau tangles, amyloid-β plaques, α-Syn fibrils, and Lewy bodies (1). Under ideal *in vitro* conditions, such as low protein concentrations and low temperatures, the primary amino acid sequence may suffice to dictate the spontaneous folding of polypeptides into discrete three-dimensional, active structures called the native state (2). Yet in the crowded environment of the cell (for review, see Ref. 3) and especially under stress conditions, such as heat shock, *de novo* synthesized or imported polypeptides and mutant or damaged proteins may undergo transient unfolding, thereby exposing hydrophobic segments that readily self-associate to form stable non-functional high molecular weight, β-sheet-enriched, oligomers and fibrillar assemblies, generally named "aggregates" and amyloids (4, 5).

PD is characterized by the selective degeneration of dopaminergic neurons in the substantia nigra of human brain alongside with the presence of cytoplasmic neuronal inclusions called Lewy bodies (LBs). LBs are proteinaceous inclusions mainly composed of aggregates and insoluble fibrillar α-Syn (6) associated with different members of the protein homeostasis machinery. LBs and other types of α-Syn inclusions are also found in cases of dementia in some types of Alzheimer disease, Down syndrome, and several other neurological diseases, collectively denominated synucleinopathies (for review, see Ref. 7).

α-Syn is a 14.5-kDa protein mainly expressed in the central and peripheral nervous system of vertebrates, from torpedo fish to humans (8). In humans, it is expressed mostly in presynaptic terminals (9), astrocytic and oligodendroglial cells (10). Under physiological conditions, native soluble α-Syn is involved in the differentiation of dopaminergic cells, where it functions as an activity-dependent negative regulator of dopamine neurotransmission (for review, see Ref. 11). Because in the purified state, human α-Syn is a monomer apparently devoid of stable secondary structures, it has been described as "natively" unfolded or intrinsically unstructured (12, 13). Yet, in the membrane-rich crowded environment of the cell, α-Syn may become structured and upon binding to membranes is thought to adopt partially an α-helical conformation (14). During PD pathogenesis or aging, loose α-helical or natively unfolded α-Syn monomers may spontaneously convert, by a mechanism still unclear, into highly stable β-sheet-enriched oligomers, some of which protofibrils (15) that can ultimately form more compact, protease-resistant and apparently less toxic fibrils in LBs (for review, see Ref. 16). Three specific point mutations in α-Syn have been

* This work was supported by Swiss National Science Foundation Grant 3100A0-109290 and by a Zwahlen grant from the Faculty of Biology and Medicine of Lausanne University.

[S] The on-line version of this article (available at http://www.jbc.org) contains supplemental Figs. S1–S6.

[1] To whom correspondence should be addressed: Plant Molecular Biology Dept., University of Lausanne, Biophore, 1015 Lausanne, Switzerland. Tel.: 41216924232; Fax: 41216924195; E-mail: pierre.goloubinoff@unil.ch.

[2] The abbreviations used are: PD, Parkinson disease; LB, Lewy bodies; G6PDH, glucose-6-phosphate dehydrogenase; Th-T, thioflavin T; AS, α-synuclein; NEF, Nucleotide Exchange Factor; PEP, phosphoenolpyruvate; PK, pyruvate kinase.

linked to autosomal dominant inherited forms of PD and correlate with early onset of the disease (17–19). Interestingly, all three also accelerate the *in vitro* oligomerization and fibril formation of α-Syn and promote the spontaneous formation of toxic oligomers, including amyloid pores (20).

There is strong evidence that the soluble, low molecular weight forms of β-sheet-enriched oligomers are the primary toxic species in the disease (21), whereas fibril formation is already part of a detoxification mechanism whereby toxic oligomers become sequestered and, thus, incapacitated at participating in aberrant interactions with membranes and other proteins of the cell (for review, see Ref. 1). In solution and at high concentrations (>200 μM), α-Syn spontaneously forms annular pore-like structures (20, 21) that, when added externally to the culture medium, can cause toxic ion leakage in neuroblastoma cells (22).

Here, we developed a reproducible protocol for preparing and purifying a homogeneous population of highly stable β-sheet enriched, toroid-shaped α-Syn oligomers with a diameter typical of toxic protofibrils. We then compared the effect of purified native monomeric α-Syn to that of the purified oligomers on the *in vitro* ATP-dependent chaperone unfolding/refolding activity of bacterial (DnaK, DnaJ or CbpA, GrpE) or human (HSPA1A, DNAJA1) Hsp70/Hsp40 chaperones. We found that α-Syn oligomers can specifically inhibit the function of the Hsp70/Hsp40 chaperone systems, suggesting that α-Syn oligomer-induced toxicity may also result from the specific stalling of the cellular chaperone machinery, leading to the collapse of protein homeostasis and pathogenesis.

EXPERIMENTAL PROCEDURES

Purification and Characterization of Recombinant α-Syn—pT7 plasmid carrying the human wild-type (WT) *α-Syn* gene was expressed in BL21 (DE3) *Escherichia coli* cells. Cells were grown in 1.2 liters of Lysogeny (Luria) Broth medium containing 100 mg/liter ampicillin at 37 °C with shaking. At $A_{0.6}$, 0.2 mM isopropyl-β-D-thiogalactopyranoside was added, and cells were further grown for 3 h. Centrifuged cells were sonicated in buffer A (50 mM Tris, pH 8.0, 50 mM KCl, 5 mM $Mg(Ac)_2$, 0.1% Na azide), 0.2 mg/ml lysozyme, and the protease inhibitor mixture from Sigma (catalog no. P8465). After 15 min of centrifugation at 6000 rpm, the supernatant was heated at 73 °C for 4.5 min. After a second 15-min centrifugation at 10,000 rpm, the supernatant was precipitated in 40% $(NH4)_2SO_4$ and incubated overnight at 4 °C. After a 15-min centrifugation at 6000 rpm, the pellet was then resuspended in Buffer A, filtered through a 0.2-μm membrane, and loaded on a Superose 6 gel filtration column (Amersham Biosciences). Proteins were eluted in buffer A at a flow rate of 0.5 ml/min. For each eluted peak, fractions were pooled and concentrated by ultrafiltration in a 100-kDa cut-off membrane (Sartorius 13269E) and analyzed on a 15% SDS-PAGE or on a 5.5% native PAGE and stained with Coomassie Blue. The total protein concentration was determined at 560 nm with the bicinchoninic acid assay (BCA) (Sigma) using bovine serum albumin as a standard and then stored in buffer A supplemented with 20% glycerol at −80 °C.

Immunoblotting—Samples were separated on a 7.5% native PAGE or on a 12% SDS-PAGE (Fig. 1) and transferred by electroblotting to a nitrocellulose membrane (Bio-Rad) using standard protocols. Membranes were blocked in 1% skimmed milk and incubated overnight at 4 °C with a rabbit anti-α-Syn polyclonal antibody (Stressgen, Ann Arbor, MI, catalog no. 905-565) (1/1000, v/v) and then incubated with a HRP-labeled goat anti-rabbit antibody (Bio-Rad, catalog no. 170-5046) (1/15000, v/v). Immune complexes were visualized using the chemiluminescent Immunstar™Kit (Bio-Rad) according to the manufacturer's instructions.

Proteins—DnaK, DnaJ, and CbpA were purified according to Gur *et al.* (24); ClpB was purified according to Woo *et al.* (25). His-tagged Luciferase was expressed from the pT7lucC-His plasmid from A. S. Spirin (The Protein Research Institute, Moscow Region, Russia) and purified according to Svetlov *et al.* (26). GrpE was a gift from H.-J. Schönfeld, F. Hoffmann-La Roche, Basel, Switzerland. Glucose-6-phosphate Dehydrogenase (G6PDH) from *Leuconostoc mesenteroides* and BSA were from Sigma. Heat denaturation of the G6PDH was as described in Ben-Zvi *et al.* (27). Cold inactivation of His-tagged Luciferase was achieved by four consecutive cycles of freezing in liquid nitrogen and slow thawing at 4 °C (62).

Atomic Force Microscopy—10 μl of α-Syn monomers or oligomers (1 μM each, expressed in protomers) in buffer (50 mM Tris, 50 mM KCl, 10 mM $MgCl_2$, pH 7.5) were deposited onto freshly cleaved mica at room temperature. After 1 min, the sample was gently rinsed with 1 ml of nanopure H_2O and dried. Samples were imaged using a Nanoscope III (Digital Instrument, Santa Barbara, CA) in the tapping mode. The probes were NSC35 (NT-MDT, Troisk, Russia).

Reactivation of Heat-preaggregated G6PDH by Chaperones—Heat-preaggregated G6PDH was refolded by the DnaK chaperone system as described in Ben-Zvi *et al.* (27) with the following modifications; 0.75 μM heat-aggregated G6PDH (final concentration) was reactivated in the presence of 5 μM DnaK, 5 μM DnaJ, 0.5 μM GrpE (the full DnaK chaperone system) or 5 μM HSPA1A and 5 μM DNAJA1 (the minimal human Hsp70/40 system), and 4 mM ATP. G6PDH activity was measured at different times of chaperone-mediated refolding reaction at 30 °C.

Luciferase Assays—Luciferase activity was measured as described previously (26) using a Victor Light 1420 Luminescence Counter from PerkinElmer Life Sciences.

Inhibition of G6PDH Reactivation by α-Syn Species—Aliquots from each eluted fraction resulting from the gel filtration chromatography were diluted to a final concentration of 2.2 μM α-Syn and added to 0.75 μM heat-inactivated G6PDH and incubated in the presence of the full DnaK/DnaJ/GrpE bacterial system or the minimal Hsp70/Hsp40 human system at 30 °C for 1 h. G6PDH activity was measured at different times of chaperone-mediated refolding reaction.

Thioflavin T Fluorescence Assays—The β-sheet content of G6PDH and α-Syn were evaluated by measuring the fluorescence in a luminescence spectrometer, PerkinElmer Life Sciences LS 55 (excitation, 446 nm; emission, 480 nm), in a 500-μl cuvette containing 10 μM thioflavin T (Th-T) (final concentration) in the refolding buffer: 100 mM Tris-HCl, pH 7.5, 100 mM KCl, 10 mM MgAc, 10 mM DTT, 4 mM ATP, 4 mM PEP, and 0.02 mg/ml PK.

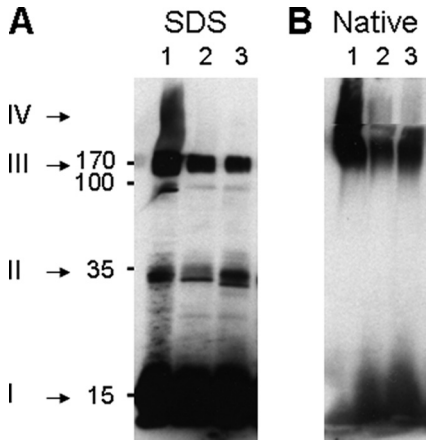

FIGURE 1. **The initial stages in the purification of recombinant α-synuclein protofibrils.** Shown is an immunoblot with an anti-α-synuclein antibody from a SDS gel (*A*) or a native gel (*B*) of cell extracts from BL21 *E. coli* cells expressing WT human α-synuclein. *Lane 1*, soluble initial crude extract. *Lane 2*, soluble extract after heat treatment. *Lane 3*, resolubilized ammonium sulfate pellet from the heat-treated soluble extract in *lane 2*. *Numbers*, estimated molecular masses from the SDS gel in kDa. *Roman numbers with arrows*: *I*, monomers; *II*, dimers; *III*, soluble oligomers; *IV*, large oligomers that do not enter the resolution gel.

RESULTS

To address the possible effects of unstructured α-Syn monomers and structured oligomers on the *in vitro* activity of a typical Hsp70/Hsp40/NEF chaperone system (here, the *E. coli* DnaK/DnaJ/GrpE chaperone machinery), we first designed a protocol to purify a distinct population of stable α-Syn oligomers with reproducible characteristics. Immunoblots from SDS gels of soluble extracts from *E. coli* cells overexpressing plasmid-encoded human α-Syn revealed a predominant fraction of SDS-soluble 14.5-kDa α-Syn monomers (Fig. 1*A*, *lane 1*, I) and a minor fraction of SDS-resistant oligomers: some dimers (Fig. 1*A*, *lane 1*, *II*), high molecular weight species that migrated as 10–14-mers (Fig. 1*A*, *lane 1*, *III*), and very large insoluble oligomers that did not enter the resolution gel (Fig. 1*A*, *lane 1*, *IV*). To deplete this last insoluble fraction of very large SDS-resistant oligomers (fraction IV), the extract was heat-treated at 73 °C for 4.5 min and centrifuged (14,000 rpm, 15 min) (Fig. 1*A*, *lane 2*). After ammonium sulfate precipitation, we obtained a much reduced fraction, albeit of ~95% pure α-Syn, that was devoid of large insoluble species, composed of fully soluble, discrete oligomers that resolved on native gel mainly as 10–14 mers (140–200 kDa) as well as some dimers and monomers (Fig. 1*B*, *lane 3*).

To better understand the relative size distribution of monomeric and oligomeric α-Syn complexes, this soluble fraction was further separated by gel filtration (Fig. 2*A*, *blue line*). As expected from the native gel (Fig. 1*B*), we observed two broad peaks; one corresponding to soluble high molecular weight (M_r) α-Syn oligomers ranging from 10^2 to 10^3 kDa (7.5–11 ml) with a very high specific affinity for the amyloid specific dye, Th-T, and a second that was resolved at the expected position of the 14.5-kDa α-Syn monomer (15–18 ml) with a very low specific affinity for Th-T (Fig. 2*A*, *dark line*). SDS and native gel electrophoresis confirmed that this low M_r fraction contained a uniform population of SDS-soluble 14.5-kDa monomers whose low affinity for Th-T is indicative of a lack of β-sheet structures, in agreement with the intrinsically unfolded state that is predominantly observed in the case of α-Syn monomers *in vitro* (13). In contrast, SDS and native gel electrophoresis confirmed that the high M_r, β-sheet-enriched fraction from the 7.5–11 ml peak was partially SDS-resistant (Fig. 2*B*) and formed on the native gel a remarkably discrete soluble α-Syn oligomer whose high stability was reflected by its ability to withstand extensive dilutions during gel filtration and native gel electrophoresis (Fig. 2*C*).

The discrete nature of this stable high M_r, yet soluble α-Syn oligomer was confirmed by atomic force microscopy (Fig. 2, *D–G*); whereas the low M_r fraction contained mostly α-Syn monomers, undetectable at this low resolution (Fig. 2*D*), the high M_r fraction showed a dense, remarkably homogeneous population of globular, mildly flattened oligomers (Fig. 2*E*), with a narrow size distribution (average diameter of 21 nm ± 3 nm) (Fig. 2*G*). The tapping procedure revealed a weaker region at the center of the particles, suggesting a less dense interior or a pore-like toroid (Fig. 2*F*) indistinguishable in size and shape from previously described toxic pore-forming α-Syn oligomers (20).

This protocol of production of stable α-Syn oligomers was highly reproducible. Yet, depending on the batches, α-Syn oligomers bound about 20 times more Th-T than monomeric α-Syn and about 8 times more than heat-aggregated G6PDH (Fig. 3*A*). G6PDH is a heat-generated misfolded protein substrate that is commonly used to test the unfolding/refolding activity of molecular chaperones (5, 27). The high stability of the β-sheet structures in the α-Syn oligomers was confirmed by their relative high resistance to prolonged (48 h) incubations after extensive dilutions; whereas prolonged incubations of heat-aggregated G6PDH caused a 33% loss of Th-T binding (Fig. 3*B*), only ~8% loss of Th-T binding was observed in the case of α-Syn oligomers under identical conditions (Fig. 3*C*).

We next addressed the biochemical properties of α-Syn oligomers as a possible substrate of the full *E. coli* Hsp70 chaperone machinery. Confirming earlier observations (27), in the presence of DnaK, DnaJ, GrpE, and ATP, heat-preaggregated G6PDH lost 25% of its Th-T binding structures within 50 min (Fig. 4*A*, *open squares*) and correspondingly formed 25% of natively refolded G6PDH enzyme (Fig. 4*A*, *filled circles*). In contrast, the α-Syn oligomers lost less than 10% of their Th-T binding structures (Fig. 4*A*, *filled squares*), indicating that although interacting with the aggregates, the chaperones are less effective at unfolding the misfolded β-sheets structures in α-Syn oligomers than in heat-aggregated G6PDH substrate. Remarkably, immunoblots of native gels confirmed that the Hsp70 chaperone machinery can convert a significant fraction of the stable α-Syn oligomers into monomers in an ATP-dependent manner (Fig. 4*B*). This indicates that the chaperone machinery, although capable of interacting and causing the partial disassociation of the oligomers, are poorly effective at fully unfolding stably misfolded β-sheets structures into unstructured polypeptide segments.

Thus, we next addressed the possibility that the oligomers may stall the Hsp70/40 chaperone machinery. The *in vitro* chaperone-mediated ATP-dependent reactivation of G6PDH was tested in the presence of increasing amounts of monomeric

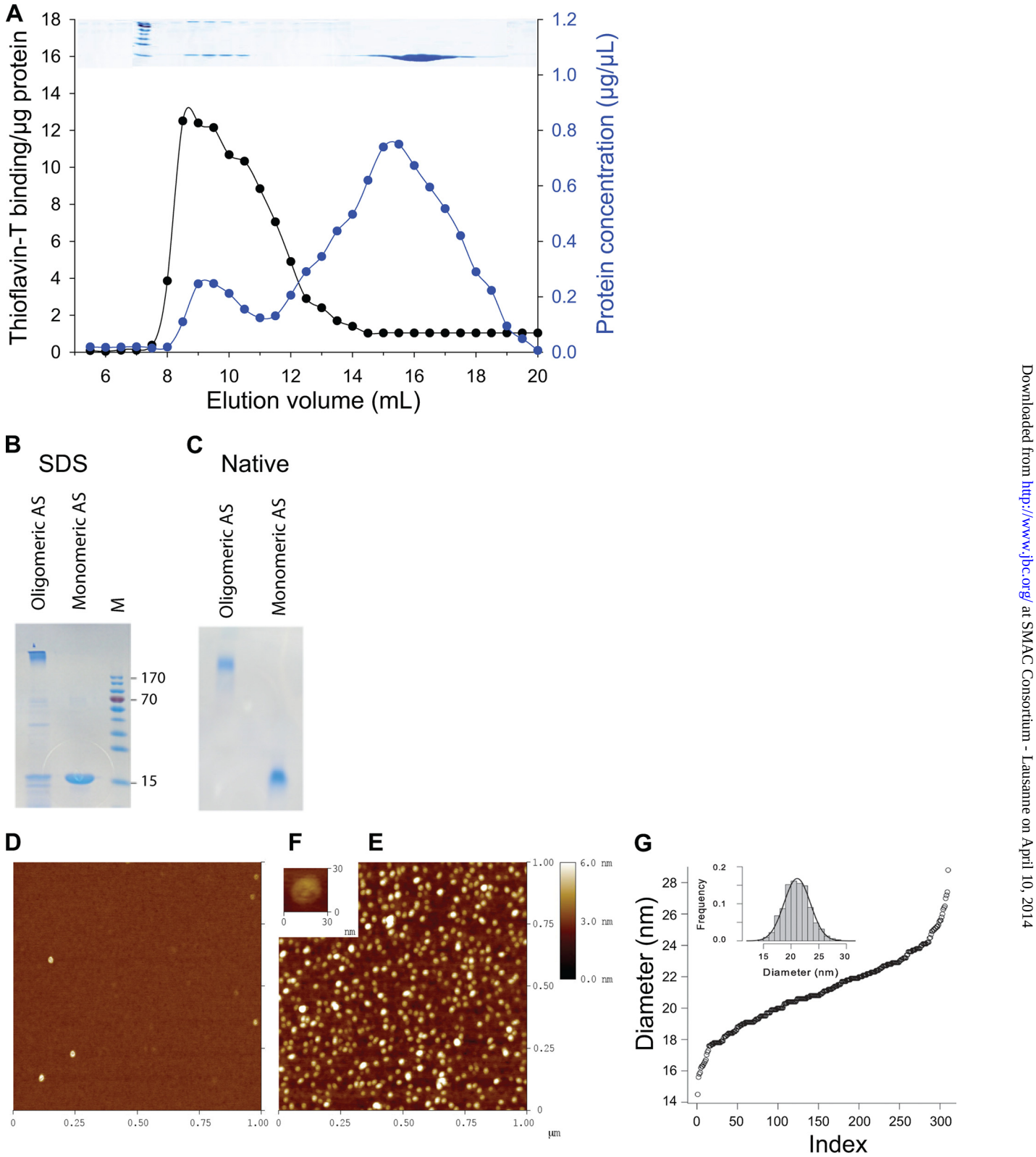

FIGURE 2. **Characterization of recombinant human α-synuclein (*AS*).** *A,* shown is size exclusion chromatography of recombinant α-synuclein from the resolubilized amonium sulfate pellet of the heat-treated crude extract shown in *lane 3* of Fig. 1, *A* and *B*. Elution profile from the Superose 6 column shows the protein concentration profile according to the absorbance at 280 nm (*blue circles*) and the Th-T fluorescence profile (*black circles*). Above the *inset,* Coomassie stain of the corresponding eluted fractions after separation on 12% SDS-PAGE is shown. *B* and *C*, two fractions were pooled from 15–18 ml as *monomeric AS* and from 7.5–11 ml as *oligomeric AS*, concentrated, and further separated by SDS-PAGE (*B*) or native-PAGE (*C*) and Coomassie-stained. Standard molecular masses (*M*) in kDa are indicated for the SDS-gel. *D–F,* shown are atomic force microscopy morphological studies of AS monomers and AS oligomers, as in *B* and *C*. Atomic force microscopy images (1 μm × 1 μm) of AS monomers (*D*) and AS oligomers (*E*) are shown. At higher magnitude, AS oligomers present a globular flattened-shape structure (*F*). *G*, shown is cumulative function of the diameter distribution of the AS oligomers with a mean size of 21.1 nm and a S.D. $s = 2.4$ nm. *Inset*, shown is s histogram of the distribution superimposed with a Gaussian (mean = 21.1 nm, $s = 2.4$ nm).

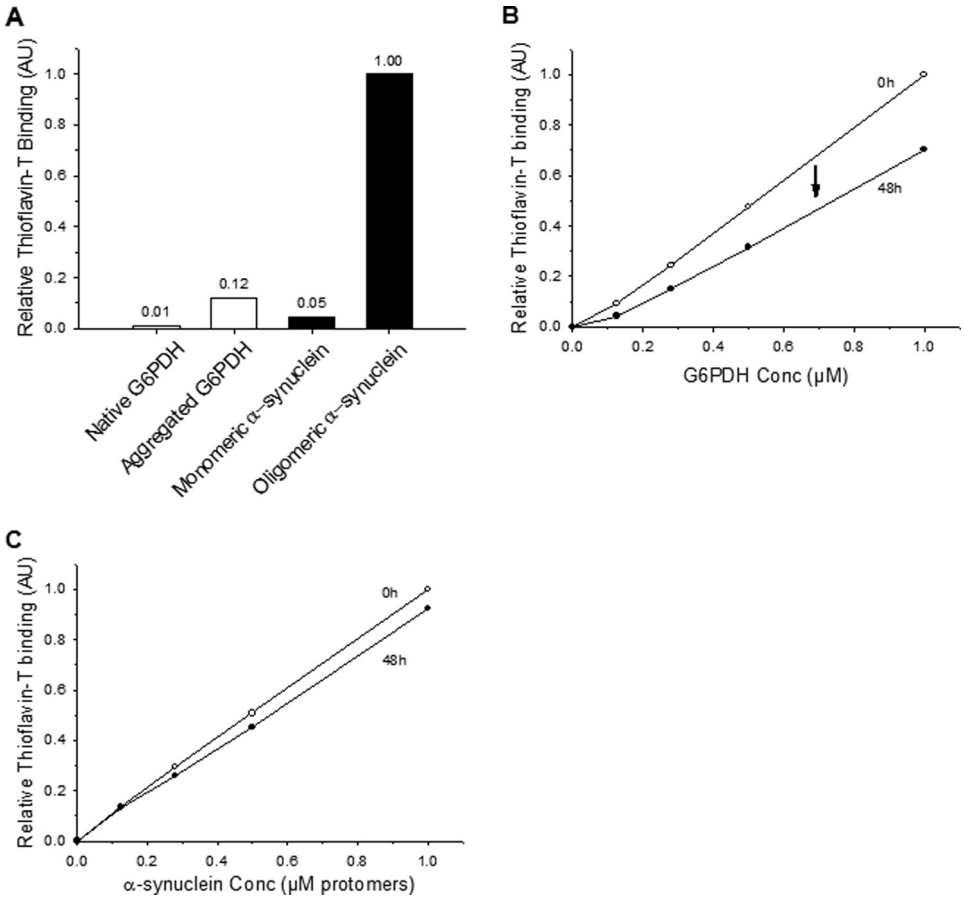

FIGURE 3. **AS oligomers are stable and β-sheet-enriched.** *A*, the specific β-sheet content of various protein forms is shown. The relative Th-T fluorescence by a constant amount (1 μM, expressed in protomers) of AS oligomers was compared with AS monomers (*black bars*) to heat pre-aggregated and to native G6PDH (*white bars*). *B* and *C*, shown is an estimation of the relative stability of various oligomers. The relative Th-T fluorescence (normalized to 1 μM, expressed in protomers) of heat-pre-aggregated G6PDH (*B*) and AS oligomers (*C*) was measured either immediately after dilutions from 1 to 0.1 μM (*open circles*) or 48 h after dilutions (*filled symbols*). *AU*, absorbance units.

or oligomeric α-Syn (Fig. 5*A*). We found that the refolding rate of heat-pre-aggregated G6PDH by an excess of chaperones (5.0 μM DnaK, 1 μM DnaJ, and 0.5 μM GrpE) was strongly inhibited by α-Syn oligomers but not by the monomers. Half-inhibition of the chaperone reaction was observed in the presence of 2 μM α-Syn oligomers (expressed in protomers) (Fig. 5*B*). Remarkably, up to a 10-fold molar excess of monomeric α-Syn did not inhibit and was even slightly beneficial to the chaperone reaction (Fig. 5*A*, *open circles*). Chaperone inhibition was specific to α-Syn oligomers and not to other types of protein aggregates, as equimolar amounts of heat-aggregated MDH or of cold-inactivated luciferase did not compete with the chaperone-mediated reactivation of heat-denatured G6PDH (supplemental Fig. S1). Moreover, the oligomers inhibited the chaperone-mediated refolding of cold-inactivated Luciferase to the same extent as they did in the case of heat-denatured G6PDH (supplemental Fig. S2), indicating that inhibition is not caused by the competition between the different substrates for a limited amount of chaperones but rather by a non-competitive action mediated by a specific interaction of the oligomers with a component of the chaperone system. This specific chaperone inhibitory effect was further tested on different α-Syn oligomers with increasing apparent molecular masses (and/or shapes, as elongated proteins may elute with larger than real apparent molecular masses) obtained by gel filtration fractionation. Remarkably, the size/shape-dependent profile of the specific chaperone inhibitory activity (Fig. 5*C*) matched that of the specific Th-T binding (Figs. 2*A* and 5*C*), suggesting a strong correlation between the β-sheet or amyloid-like content of the α-Syn oligomers and their ability to inhibit the chaperone activity.

The specific *in vitro* inhibitory effect of the α-Syn oligomers was confirmed with HSPA1A and DNAJA1, which represent a central hub of the stress-induced chaperone network and are among the most strongly expressed Hsp70 chaperone and Hsp40 co-chaperones of the cytoplasm of human cells, including PD neurons prone to α-Syn aggregation (61). We found that, similar to *E. coli* Dnak/DnaJ/GrpE chaperones, α-Syn oligomers, but not monomers, strongly inhibited the human HSPA1A/DNAJA1 chaperone machinery (supplemental Fig. S3*A*). Moreover, in the presence of 1.5 μM DNAJA1, inhibition was half, and in the presence of 3 μM DNAJA1, inhibition was fully alleviated. This confirms that, as with bacterial chaperones, the inhibition of the human chaperone system by the α-Syn oligomers, but not by the monomers, is also predominantly caused by the incapacitation of the Hsp40 co-chaperone (supplemental Fig. S3*B*).

Both chaperone and co-chaperone can bind to unfolded or misfolded proteins, albeit in different manners (28). Whereas in its ADP-liganded and substrate-bound state, DnaK may tightly bind only to protruding unfolded hydrophobic polypeptide segments by tightly enclosing them, DnaJ may directly bind with much less steric limitations to bulky hydrophobic surfaces on misfolded structures on the substrate (28–30). Therefore, we next considered the possibility that β-sheet-enriched oligomers expose binding sites with a particular affinity for DnaJ, thereby potentially stalling the chaperone reaction. This was addressed by measuring the rates of ATP- and chaperone-mediated refolding without or with a fixed amount of oligomeric α-Syn in the presence of increasing concentrations of DnaK (Fig. 6*A*) or of DnaJ (or the DnaJ-like co-chaperone CbpA) (Fig. 6, *B* and *C*) or of chaperone substrate (Fig. 6*D*). The half inhibitory effect (IC_{50}), which was observed at 5 μM DnaK, was not alleviated by higher DnaK concentrations of up to 13 μM (Fig. 6*A*), suggesting that inhibition is not because DnaK becomes sequestered by the oligomers. As expected, excess GrpE did not alleviate inhibition (data not shown), consistent with the fact

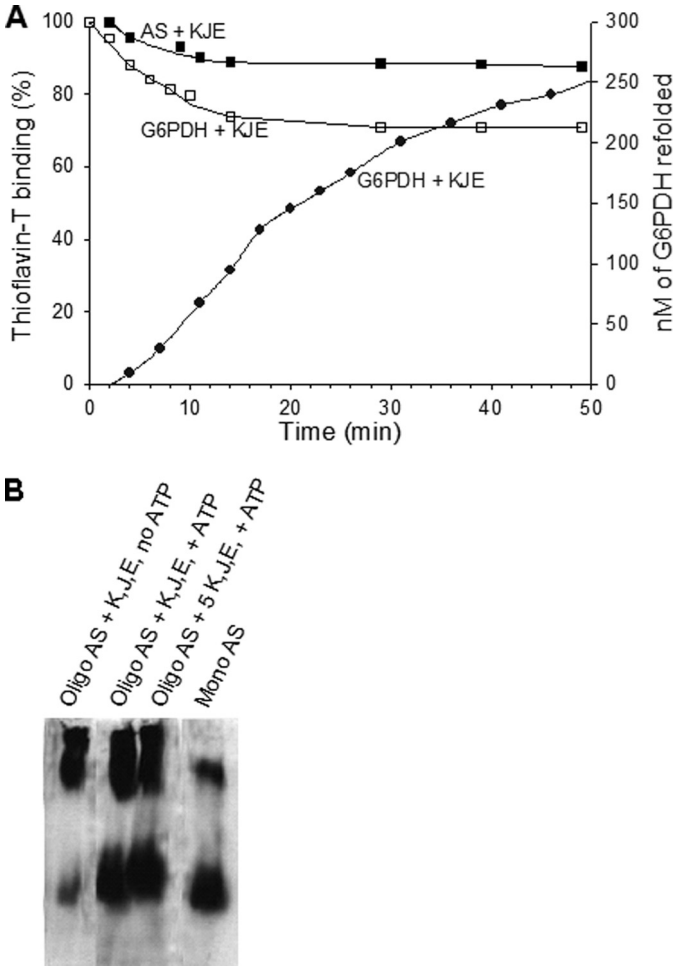

FIGURE 4. **AS oligomers are partially resistant to the Hsp70 chaperone machinery.** *A,* AS oligomers are more resistant to the unfolding chaperones than G6PDH aggregates. Time-dependent loss of Th-T fluorescence (*squares*) of 1 μM heat pre-aggregated G6PDH (*open squares*) or 1 μM (protomers) AS oligomers (*filled squares*) in the presence of 5 μM DnaK, 0.75 μM DnaJ, and 1 μM GrpE (*KJE*) and ATP and the corresponding time-dependent reactivation of native G6PDH (*filled circles*) is shown. *B,* AS oligomers are partially dissociated by the ATP-fueled DnaK/DnaJ/GrpE chaperone system. AS oligomers were incubated as in *A* but for 3 h at 30 °C with or without ATP and chaperones, as specified. Samples were separated on native gel, and α-synuclein was detected by Western blot analysis as in Fig. 1.

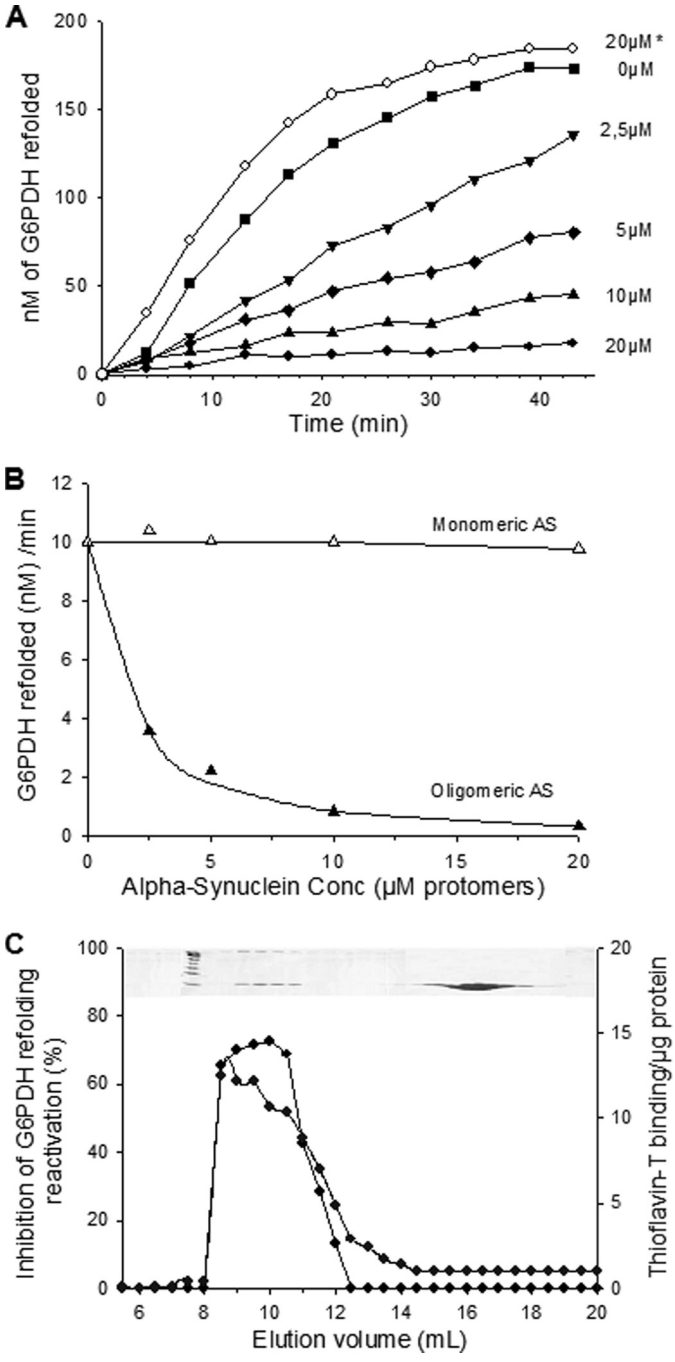

FIGURE 5. **AS oligomers inhibit the unfolding/refolding activity of the Hsp70 chaperone system.** *A,* time-dependent reactivation of heat-pre-aggregated G6PDH by the full DnaK chaperone system is shown. The heat pre-aggregated G6PDH (0,75 μM) was first incubated with increasing concentrations of AS oligomers (0- 20 μM protomers) (*filled symbols*) or 20 μM AS monomers (*open symbols*, *asterisk*) and then incubated with 5 μM DnaK, 1 μM DnaJ, 0.5 μM GrpE, and ATP. *B,* optimal G6PDH refolding rates from *A* as a function of increasing concentrations of AS monomers (*open triangles*) or oligomers (*filled triangles*) are shown. *C,* the specific chaperone inhibitory activity profile (*open circles*) compared with the Th-T binding profile (*filled circles*) of AS species in the different fractions from the size exclusion chromatography in Fig. 2*B* is shown.

that GrpE is a mere nucleotide exchange factor that exclusively interacts with DnaK. In contrast, increasing concentrations of the J-domain co-chaperones were found to gradually alleviate chaperone inhibition by oligomers (Fig. 6, *B* and *C*); inhibition was strongly diminished above 2.5 μM DnaJ and was negligible at 5 μM DnaJ (Fig. 6*B*). This was confirmed using CbpA, which can substitute for DnaJ in our type of *in vitro* DnaK-mediated protein disaggregation assays (24); the inhibition, which was initially set to 50%, remained so below 1 μM CbpA. The inhibition gradually decreased above 1 μM CbpA and in the presence of 5 μM CbpA was reduced to 10% (Fig. 6*C*). This suggests that α-Syn oligomers may inhibit the chaperone reaction by way of specifically sequestering the J-domain co-chaperones.

Because the same quality of G6PDH aggregates cannot be obtained when they have been heat-denatured at different concentrations (31), we chose to use freeze-inactivated luciferase, which shows no differences of chaperone reactivity once inactivated at different concentrations (62) to test the effect of increasing concentrations of a chaperone substrate. Here again, the same amount of oligomers, which inhibited by half the chaperone-mediated refolding of 125 nM luciferase, kept inhibiting by more than half the refolding of five times more lucifer-

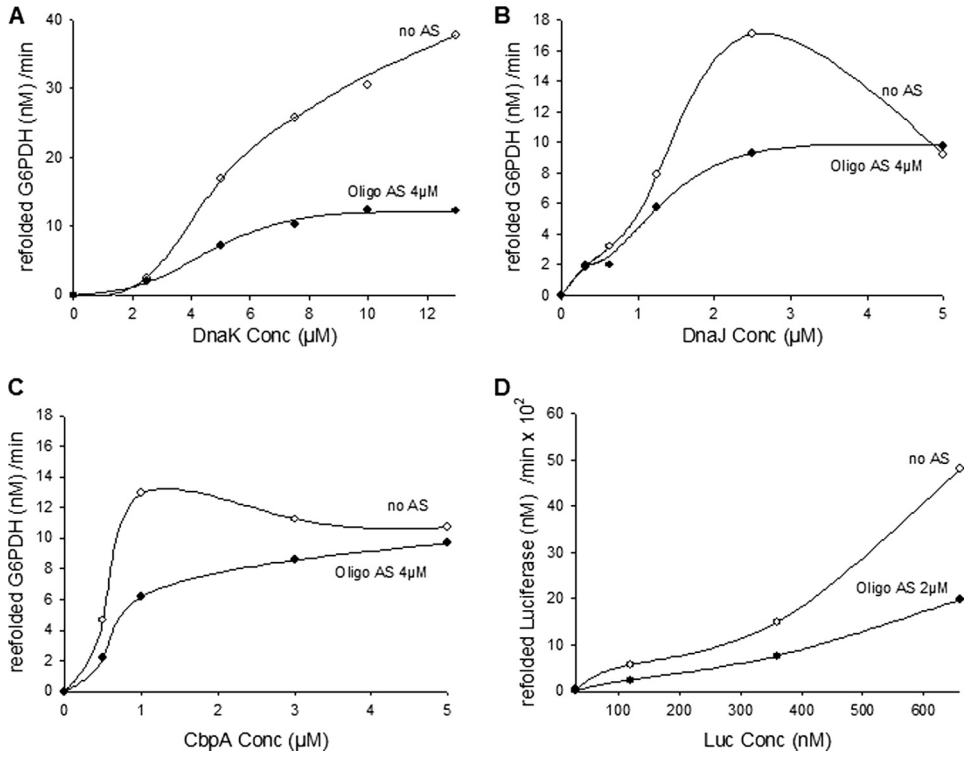

FIGURE 6. **AS protofibrils interact with J-domain chaperones.** The reactivation of heat-pre-aggregated G6PDH was performed under the same conditions as in Fig. 4*A* with constant GrpE (0.5 μM) and increasing DnaK, DnaJ, or CbpA or luciferase substrate concentrations without (*open circles*) or with AS oligomers (4 μM protomers) (*filled circles*). *A,* shown are optimal rates of G6PDH reactivation by constant (1 μM) DnaJ and increasing DnaK concentrations. *B,* shown are optimal rates of G6PDH reactivation by constant (5 μM) DnaK and increasing DnaJ concentrations. *C,* procedures are as in *B* but with increasing CbpA concentrations instead of DnaJ. *D,* shown is optimal rates of luciferase reactivation by constant (0.8 μM) DnaK, (0.4 μM) DnaJ, and (0.8 μM) GrpE and increasing concentrations of inactive luciferase substrate without (*open circles*) or with AS oligomers (2 μM protomers) (*filled circles*).

ase (650 nM) substrate (Fig. 6*D*). Thus, inhibition cannot be attributed to the sequestering of the chaperone substrate by α-Syn oligomers.

DnaJ and α-Syn being devoid of Trp residues, we could follow the changes in the steady-state intrinsic fluorescence of the unique Trp residue, which is in the nucleotide binding domain of DnaK, in the presence of ATP and increasing amounts of monomeric or oligomeric α-Syn with or without DnaJ. Fluorescence changes (supplemental Fig. S4) showed that in the absence of DnaJ, DnaK had the same low apparent affinity for monomeric α-Syn as for oligomeric α-Syn. In contrast, in the presence of DnaJ, increasing amounts of oligomeric α-Syn caused a dramatic change in the DnaK fluorescence, whereas increasing amounts of monomeric α-Syn caused similar minor fluorescence changes, as without DnaJ. This confirms that it is the DnaJ co-chaperone rather than the DnaK chaperone that is able to specifically distinguish between oligomeric and monomeric α-Syn. Moreover, DnaJ acts as if it instructed DnaK to interact with the oligomers and specifically act upon them as a disaggregating/unfolding chaperone.

DISCUSSION

Recombinant α-Syn Oligomers Recapitulate Biochemical Properties of Oligomers from PD Tissues—The physiological non-toxic species of α-Syn is presumably a soluble monomer that in healthy neurons may loosely bind to membranes as amphiphilic α-helices (14). In the purified state the full-length α-Syn polypeptide is found in a so-called natively unfolded or unstructured state, apparently devoid of secondary structures. At high concentrations, β-sheet-enriched oligomers may spontaneously form by a yet unclear mechanism and undergo subsequent growth and/or self-assembly to form the mature fibrils found in the Lewy bodies of PD brains (32). Soluble oligomers, typically composed of about 12–24 subunits, were isolated from the cerebral cortex of PD and dementia with LBs patients and from α-Syn-transgenic mesencephalic neuronal (MES) cells and mouse brains (33). Because oligomers have a higher surface/volume ratio as compared with large fibrils and amyloids, they can be very toxic, and their apparition in cells correlates with a general failure of the protein homeostasis (proteostasis) machinery, the onset of apoptosis, tissue loss, and neurodegeneration (34, 35).

Both artificially formed and *in vivo* formed α-Syn oligomers are partially resistant to detergents such as Triton and SDS (36) and have a typical high affinity for the amyloid-specific dyes like Congo red or Th-T (37). Upon reconstitution in synthetic membranes, they can spontaneously form discrete spheroid pore-like structures that cause ion leakage (38). α-Syn oligomers have been previously isolated from cold-induced dissociation of amyloid fibrils (39). Here, we described a protocol to isolate recombinant human α-Syn oligomers that recapitulate a number of important properties of the toxic α-Syn oligomers found in PD neuronal tissues; they were very stable soluble oligomeric species that were partially resistant to SDS. They could withstand extensive dilutions and native gel electrophoresis and bound much more Th-T (here about 20 times) than the monomeric form. Moreover, the α-Syn oligomers were a remarkably uniform population of discrete spheroid-like flattened structures of the same diameter as previously described for the toxic species shown to spontaneously form pores in artificial membranes and cause ion leakage in cell cultures.

Yet, in contrast to classic protofibrils, we found that these oligomers remained ineffective as seeds of spontaneous α-Syn fibril formation *in vitro* (supplemental Fig. S5). This suggests that our specific α-Syn oligomers are off-fibrillation pathway species whose negative effects on the chaperone network and possibly on the cell cannot be neutralized by the spontaneous or aggresome-mediated formation of less toxic larger fibrils and amyloids.

The α-Syn Oligomers Feebly but Effectively Interact with the Hsp70 Chaperone Machinery—Although Th-T fluorescence showed that, as compared with denatured G6PDH or luciferase, the α-Syn oligomers were relatively resistant, Western blot analysis of native gels revealed that oligomers were relatively efficiently disaggregated by the bacterial ATP-dependent Hsp70 chaperone machinery. This is consistent with earlier finding (40) showing that human Hsp70 can efficiently inhibit α-Syn fibril formation *in vitro* and further suggests that partial ATP-fuelled, chaperone-mediated unfolding can lead to the partial disaggregation of α-Syn oligomers. It should be noted, however, that incomplete chaperone-mediated unfolding of more compact and, therefore, less toxic aggregates could lead to a transient increase of protein toxicity when more active species are formed but are not further converted into nontoxic monomers. The concomitant binding of more than one Hsp70 molecule to the same misfolded polypeptide has been shown to be essential for the effective cooperative unfolding action of the chaperone on relatively resistant protein aggregates such as heat-denatured G6PDH species (27, 41). According to the algorithm of Rüdiger *et al.* (29), the α-Syn sequence has only one good potential Hsp70 binding site (instead of the three-four sites expected on an average polypeptide of the same size). The lack of another chaperone binding site would strongly limit the ability of the single chaperone molecule to efficiently pull and unfold the stable β-sheets and could explain the apparent resistance of misfolded α-Syn conformers to the protein quality control machineries in neurons affected by PD (for review, see Ref. 4).

α-Syn Oligomers Inhibit the Unfolding Activity of the Hsp70/40 System—Consistent with the observed co-localization of human Hsp40 proteins (and Hsp70) with α-Syn in Lewy Bodies (34), our α-Syn oligomers behaved *in vitro* as a competitive inhibitor of the human and bacterial (*E. coli*) Hsp70/40 chaperone machineries by interacting with J-domain co-chaperones. Noticeably, we found that DnaJ preincubated either with α-Syn monomers or with oligomers did not show differences of elution profiles on gel filtration and, moreover, that DnaJ did not co-immunoprecipitate with α-Syn oligomers better than with monomers (data not shown). We conclude that the specific strong inhibitory effect that is exerted by the α-Syn oligomers on the J-domain co-chaperones must be mediated by rather weak interactions. This is not entirely surprising given that a very ubiquitous "generalist" chaperone, such as Hsp70/Hsp40 could hardly afford having very strong affinities for hundreds of different substrate proteins in various misfolded and aggregated states in the same cell.

We found that tryptophan fluorescence independently supported the evidence from the chaperone assays and confirmed that the J-domain co-chaperone is the primary component of the Hsp70 chaperone system that can specifically distinguish between the oligomeric and the monomeric form of α-Syn and, moreover, direct Hsp70 to interact with α-Syn oligomers in a limited attempt to disaggregate them.

The binding of *de novo*-forming oligomers to Hsp40 co-chaperones would partially sequester and, therefore, neutralize the whole Hsp70/Hsp40 chaperone system, adding to the direct deleterious effects of oligomers on membrane integrity (38) and the indirect effects on the stability of other labile and mutant proteins in the cell, as observed in the case of polyQ aggregates in thermo-sensitive mutants of *Caenorhabditis elegans* (42). In addition, because Hsp70/Hsp40 activity can repress IkB and, therefore, repress NF-κB-mediated apoptosis (43), the blockage of Hsp70/Hsp40 by α-Syn oligomers could promote neuroinflammation, cell death, and tissue loss in PD.

Moreover, the toxicity of α-Syn oligomers may not only result from the inhibition of the Hsp70/40 chaperone machinery. α-Syn oligomers have also been shown to strongly inhibit *in vitro* protein degradation mediated by the 26 S proteasome (44). Likewise, PC12 cells expressing the pathogenic A53T and/or A30P α-Syn diseases-associated mutants showed an altered lysosomal activity as compared with WT α-Syn (45). This fits *in vivo* observations of altered proteasomal and/or lysosomal pathways in dopamine neurons of the *substantia nigra* from PD patients (35). Together, this suggests that α-Syn oligomers may impair their own degradation along with that of other damaged proteins in the cell, leading to a vicious cycle of proteostasis imbalance, causing cell death (for review, see Ref. 46).

The Hsp70/Hsp40 Is the Main Chaperone That Can Unfold Toxic Protein Conformers in Neurons—Previous studies have demonstrated the positive effect of molecular chaperones, more particularly of the Hsp70/40 chaperone system, on the cytotoxicity of α-Syn oligomers. Hsp70 overexpression in flies expressing α-Syn prevents dopaminergic neuronal loss caused by α-Syn oligomers. It also reduces α-Syn oligomerization both in mice and in H4 cells expressing α-Syn. In the mouse model Hsp70 overexpression leads to a significant reduction both in high molecular weight and detergent-insoluble α-Syn species (47). Moreover, purified Hsp70 effectively inhibits α-Syn fibril formation *in vitro* and suppresses the permeabilization of synthetic vesicles induced by prefibrillar α-Syn (40). Chaperones other than Hsp70/Hsp40 may also contribute to the reduction of toxic oligomers in the cytoplasm of mammalian cells; the expression of Hsp27 or of the yeast Hsp104 can reduce toxicity associated with α-Syn oligomers in human H4 neuroglioma cells or rat models of PD, respectively (48, 49). However, the contribution of sHSPs is expected to be limited to the passive prevention of protein aggregation as, unlike Hsp70/Hsp40, they cannot use the energy of ATP hydrolysis to unfold misfolded proteins. It can, however, stabilize and deliver misfolded proteins to the Hsp70/Hsp40 chaperone system (50).

True functional homologues of ClpB acting together with Hsp70/Hsp40/NEF in the disaggregation of large compact aggregates (51) have been identified only in bacteria in the organelles and the cytoplasm of plants, yeast, and fungi (for review, see Ref. 5). In animal cells, among the many cytoplasmic AAA+ proteins with conserved Walker motives, none has been convincingly shown thus far to function as true ClpB/Hsp104 homologues. Our immunoblot analysis showed that, unlike with a classic heat-aggregated chaperone substrate, α-Syn oligomers remained resistant to the unfolding action of ClpB, which remained unable to improve the limited disaggregating activity of DnaK/DnaJ/GrpE alone (data not shown). Hence, the Hsp70/40/NEF remains thus the only known chaperone machinery in the cytoplasm of mammalian cells that can use the

energy of ATP hydrolysis to unfold toxic misfolded protein conformers, such as α-Syn oligomers, into non-toxic natively refoldable or protease-degradable species (5, 27).

Recruiting Hsp70/Hsp40/NEF to Reduce PD Is a Promising Therapeutic Approach—An age-dependent progressive failure of the protein clearance machinery, including the Hsp70/Hsp40 chaperone system, has been shown in aging organisms (for review, see Ref. 52). Interestingly, in agreement with our finding that J-domain co-chaperones play a central role in aggregate recognition and processing, a systematic screen in human cell cultures expressing disease-associated polyglutamine proteins (polyQ) revealed that two human DnaJ homologues, DNAJB6b and DNAJB8, are effective suppressors of polyQ aggregation and toxicity (53). This suggests new avenues of therapeutic approaches using chaperone-inducing drugs, such as Hsp90 inhibitors (54) or non-steroidal anti-inflammatory drugs (55). Alternatively, vectors could mediate the specific expression of particular effective J-domain co-chaperones in aging or diseased neurons, thus, targeting more effectively the unfoldase activity of the cytoplasmic Hsp70/Hsp40s to the cytotoxic α-Syn oligomers in PD.

Mechanistic Implications; J-domain Co-chaperones May Preferably Bind Misfolded Structures—Although the native unstructured monomeric form of human α-Syn apparently optimally exposes a typical high affinity binding motive, ^{32}KTKEGVLYVGSKTR^{45}, for the potential binding and locking of Hsp70 (29) (see supplemental Fig. S6), we found that even in large molar excess, it did not inhibit the ATP- and DnaK/DnaJ/GrpE-mediated unfolding/refolding reaction of classic amenable chaperone substrates. This is consistent with NMR and gel filtration studies that show no interaction of Hsp70 with monomeric α-Syn (56, 57). Our work further shows that DnaJ too has no apparent affinity for the unstructured monomeric form of α-Syn. In contrast, we found that the three J-domain co-chaperones, DnaJ, CbpA, and DNAJA1, have an apparent specific affinity for the structured oligomeric form of the same protein. This is consistent with earlier findings showing that the yeast Sis1 and Ydj1 Hsp40s co-chaperones have a stronger affinity for Sup35 prionogenic oligomers than for the soluble monomers (58). Thus, unlike Hsp70, which in the ADP-liganded state may only "lock" around extended loops extruding from the aggregate, J-domain co-chaperones may directly bind surfaces of bulky misfolded structures made of hydrophobic residues joined in *trans*, which are otherwise individually scattered in the primary sequence. This could explain why in the unfolded α-Syn monomer, for lack of a DnaJ binding site, DnaK lacks the ability to lock onto the DnaK binding site and moreover could justify why J-domain co-chaperones do not necessarily compete with Hsp70 for substrate binding and why chaperone and co-chaperone best collaborate when they are bound alongside rather than instead of each other on the same native (59) or unfolded polypeptide substrate (23, 28). Moreover, this would explain for the first time how, subsequent to their initial binding to the substrate, J-domain co-chaperones tend to dissociate from the product of the Hsp70-mediated ATP-fueled unfolding reaction (60); with the co-chaperones preferentially binding the composite trans-assembled structures, the unfolding action of substrate-bound Hsp70 (41) would result in the progressive destruction of the co-chaperone-binding sites on substrate.

Acknowledgments—We thank Paolo De Los Rios for discussions, Eliora Ron and Eyal Gur for CbpA and DjlA plasmids, and Sandeep Sharma and Valerie Grimminger for technical assistance.

REFERENCES

1. Muchowski, P. J. (2002) *Neuron* **35,** 9–12
2. Anfinsen, C. B. (1973) *Science* **181,** 223–230
3. Hartl, F. U., and Hayer-Hartl, M. (2009) *Nat. Struct. Mol. Biol.* **16,** 574–581
4. Hinault, M. P., Ben-Zvi, A., and Goloubinoff, P. (2006) *J. Mol. Neurosci.* **30,** 249–265
5. Sharma, S. K., Christen, P., and Goloubinoff, P. (2009) *Curr. Protein Pept. Sci.* **10,** 432–446
6. Mezey, E., Dehejia, A. M., Harta, G., Tresser, N., Suchy, S. F., Nussbaum, R. L., Brownstein, M. J., and Polymeropoulos, M. H. (1998) *Mol. Psychiatry* **3,** 493–499
7. Spillantini, M. G., and Goedert, M. (2000) *Ann. N.Y. Acad. Sci.* **920,** 16–27
8. Lavedan, C. (1998) *Genome Res.* **8,** 871–880
9. Murphy, D. D., Rueter, S. M., Trojanowski, J. Q., and Lee, V. M. (2000) *J. Neurosci.* **20,** 3214–3220
10. Wakabayashi, K., Hayashi, S., Yoshimoto, M., Kudo, H., and Takahashi, H. (2000) *Acta Neuropathol.* **99,** 14–20
11. Tofaris, G. K., and Spillantini, M. G. (2007) *Cell. Mol. Life Sci.* **64,** 2194–2201
12. Weinreb, P. H., Zhen, W., Poon, A. W., Conway, K. A., and Lansbury, P. T., Jr. (1996) *Biochemistry* **35,** 13709–13715
13. Uversky, V. N. (2003) *J. Biomol. Struct. Dyn.* **21,** 211–234
14. Davidson, W. S., Jonas, A., Clayton, D. F., and George, J. M. (1998) *J. Biol. Chem.* **273,** 9443–9449
15. Goldberg, M. S., and Lansbury, P. T., Jr. (2000) *Nat. Cell Biol.* **2,** E115–E119
16. Volles, M. J., and Lansbury, P. T., Jr. (2003) *Biochemistry* **42,** 7871–7878
17. Polymeropoulos, M. H., Lavedan, C., Leroy, E., Ide, S. E., Dehejia, A., Dutra, A., Pike, B., Root, H., Rubenstein, J., Boyer, R., Stenroos, E. S., Chandrasekharappa, S., Athanassiadou, A., Papapetropoulos, T., Johnson, W. G., Lazzarini, A. M., Duvoisin, R. C., Di Iorio, G., Golbe, L. I., and Nussbaum, R. L. (1997) *Science* **276,** 2045–2047
18. Krüger, R., Kuhn, W., Müller, T., Woitalla, D., Graeber, M., Kösel, S., Przuntek, H., Epplen, J. T., Schöls, L., and Riess, O. (1998) *Nat. Genet.* **18,** 106–108
19. Zarranz, J. J., Alegre, J., Gómez-Esteban, J. C., Lezcano, E., Ros, R., Ampuero, I., Vidal, L., Hoenicka, J., Rodriguez, O., Atarés, B., Llorens, V., Gomez Tortosa, E., del Ser, T., Muñoz, D. G., and de Yebenes, J. G. (2004) *Ann. Neurol.* **55,** 164–173
20. Lashuel, H. A., Petre, B. M., Wall, J., Simon, M., Nowak, R. J., Walz, T., and Lansbury, P. T., Jr. (2002) *J. Mol. Biol.* **322,** 1089–1102
21. Volles, M. J., and Lansbury, P. T., Jr. (2002) *Biochemistry* **41,** 4595–4602
22. Furukawa, K., Matsuzaki-Kobayashi, M., Hasegawa, T., Kikuchi, A., Sugeno, N., Itoyama, Y., Wang, Y., Yao, P. J., Bushlin, I., and Takeda, A. (2006) *J. Neurochem.* **97,** 1071–1077
23. Laufen, T., Mayer, M. P., Beisel, C., Klostermeier, D., Mogk, A., Reinstein, J., and Bukau, B. (1999) *Proc. Natl. Acad. Sci. U.S.A.* **96,** 5452–5457
24. Gur, E., Biran, D., Shechter, N., Genevaux, P., Georgopoulos, C., and Ron, E. Z. (2004) *J. Bacteriol.* **186,** 7236–7242
25. Woo, K. M., Kim, K. I., Goldberg, A. L., Ha, D. B., and Chung, C. H. (1992) *J. Biol. Chem.* **267,** 20429–20434
26. Svetlov, M. S., Kolb, V. A., and Spirin, A. S. (2007) *Mol. Biol.* **41,** 86–92
27. Ben-Zvi, A., De Los Rios, P., Dietler, G., and Goloubinoff, P. (2004) *J. Biol. Chem.* **279,** 37298–37303
28. Han, W., and Christen, P. (2004) *FEBS Lett.* **563,** 146–150
29. Rüdiger, S., Germeroth, L., Schneider-Mergener, J., and Bukau, B. (1997) *EMBO J.* **16,** 1501–1507
30. Rüdiger, S., Schneider-Mergener, J., and Bukau, B. (2001) *EMBO J.* **20,**

1042–1050
31. Diamant, S., Ben-Zvi, A. P., Bukau, B., and Goloubinoff, P. (2000) *J. Biol. Chem.* **275,** 21107–21113
32. Conway, K. A., Harper, J. D., and Lansbury, P. T. (1998) *Nat. Med.* **4,** 1318–1320
33. Sharon, R., Bar-Joseph, I., Frosch, M. P., Walsh, D. M., Hamilton, J. A., and Selkoe, D. J. (2003) *Neuron* **37,** 583–595
34. Auluck, P. K., Chan, H. Y., Trojanowski, J. Q., Lee, V. M., and Bonini, N. M. (2002) *Science* **295,** 865–868
35. Chu, Y., Dodiya, H., Aebischer, P., Olanow, C. W., and Kordower, J. H. (2009) *Neurobiol. Dis.* **35,** 385–398
36. Campbell, B. C., McLean, C. A., Culvenor, J. G., Gai, W. P., Blumbergs, P. C., Jäkälä, P., Beyreuther, K., Masters, C. L., and Li, Q. X. (2001) *J. Neurochem.* **76,** 87–96
37. Conway, K. A., Harper, J. D., and Lansbury, P. T., Jr. (2000) *Biochemistry* **39,** 2552–2563
38. Volles, M. J., Lee, S. J., Rochet, J. C., Shtilerman, M. D., Ding, T. T., Kessler, J. C., and Lansbury, P. T., Jr. (2001) *Biochemistry* **40,** 7812–7819
39. Kim, H. Y., Cho, M. K., Kumar, A., Maier, E., Siebenhaar, C., Becker, S., Fernandez, C. O., Lashuel, H. A., Benz, R., Lange, A., and Zweckstetter, M. (2009) *J. Am. Chem. Soc.* **131,** 17482–17489
40. Huang, C., Cheng, H., Hao, S., Zhou, H., Zhang, X., Gao, J., Sun, Q. H., Hu, H., and Wang, C. C. (2006) *J. Mol. Biol.* **364,** 323–336
41. De Los Rios, P., Ben-Zvi, A., Slutsky, O., Azem, A., and Goloubinoff, P. (2006) *Proc. Natl. Acad. Sci. U.S.A.* **103,** 6166–6171
42. Gidalevitz, T., Ben-Zvi, A., Ho, K. H., Brignull, H. R., and Morimoto, R. I. (2006) *Science* **311,** 1471–1474
43. Weiss, Y. G., Bromberg, Z., Raj, N., Raphael, J., Goloubinoff, P., Ben-Neriah, Y., and Deutschman, C. S. (2007) *Crit. Care Med.* **35,** 2128–2138
44. Zhang, N. Y., Tang, Z., and Liu, C. W. (2008) *J. Biol. Chem.* **283,** 20288–20298
45. Cuervo, A. M., Stefanis, L., Fredenburg, R., Lansbury, P. T., and Sulzer, D. (2004) *Science* **305,** 1292–1295
46. Balch, W. E., Morimoto, R. I., Dillin, A., and Kelly, J. W. (2008) *Science* **319,** 916–919
47. Klucken, J., Shin, Y., Masliah, E., Hyman, B. T., and McLean, P. J. (2004) *J. Biol. Chem.* **279,** 25497–25502
48. Outeiro, T. F., Klucken, J., Strathearn, K. E., Liu, F., Nguyen, P., Rochet, J. C., Hyman, B. T., and McLean, P. J. (2006) *Biochem. Biophys. Res. Commun.* **351,** 631–638
49. Lo Bianco, C., Shorter, J., Régulier, E., Lashuel, H., Iwatsubo, T., Lindquist, S., and Aebischer, P. (2008) *J. Clin. Invest.* **118,** 3087–3097
50. Veinger, L., Diamant, S., Buchner, J., and Goloubinoff, P. (1998) *J. Biol. Chem.* **273,** 11032–11037
51. Goloubinoff, P., Mogk, A., Zvi, A. P., Tomoyasu, T., and Bukau, B. (1999) *Proc. Natl. Acad. Sci. U.S.A.* **96,** 13732–13737
52. Koga, H., Kaushik, S., and Cuervo, A. M. (2010) *Ageing Res. Rev.*, doi: 10.1016/j.arr.2010.02.001
53. Hageman, J., Rujano, M. A., van Waarde, M. A., Kakkar, V., Dirks, R. P., Govorukhina, N., Oosterveld-Hut, H. M., Lubsen, N. H., and Kampinga, H. H. (2010) *Mol. Cell* **37,** 355–369
54. Putcha, P., Danzer, K. M., Kranich, L. R., Scott, A., Silinski, M., Mabbett, S., Hicks, C. D., Veal, J. M., Steed, P. M., Hyman, B. T., and McLean, P. J. (2010) *J. Pharmacol. Exp. Ther.* **332,** 849–857
55. Hirohata, M., Ono, K., Morinaga, A., and Yamada, M. (2008) *Neuropharmacology* **54,** 620–627
56. Dedmon, M. M., Christodoulou, J., Wilson, M. R., and Dobson, C. M. (2005) *J. Biol. Chem.* **280,** 14733–14740
57. Ahmad, A. (2010) *Int. J. Biol. Macromol.* **46,** 275–279
58. Shorter, J., and Lindquist, S. (2008) *EMBO J.* **27,** 2712–2724
59. Rodriguez, F., Arsène-Ploetze, F., Rist, W., Rüdiger, S., Schneider-Mergener, J., Mayer, M. P., and Bukau, B. (2008) *Mol. Cell* **32,** 347–358
60. Summers, D. W., Douglas, P. M., Ramos, C. H., and Cyr, D. M. (2009) *Trends Biochem. Sci.* **34,** 230–233
61. Finka, A., Mattoo, R. U., and Goloubinoff, P. (2010) *Cell Stress Chaperon.*, doi:10.1007/s12192-010-0216-8
62. Sharma, S. K., De Los Rios, P., Christen, P., Lustig, A., and Goloubinoff, P. (2010) *Nat. Chem. Biol.*, doi:10.1038/nchembio.455

SUPPLEMENTARY FIGURES

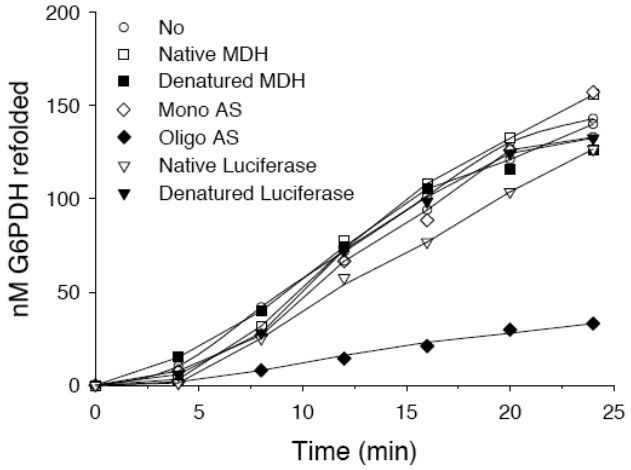

SUPPLEMENTAL FIG. S1. The inhibition of the G6PDH refolding is specific to oligomeric species. Time-dependent reactivation of heat pre-aggregated G6PDH by the DnaK chaperone machinery was performed as in Figure 4. Heat pre-aggregated G6PDH (0,75 µM, ie 38 µg/mL) was incubated in absence (opened circles) or in presence of 58 µg/mL Malate dehydrogenase (MDH) (native or heat-denatured, (squares)), or with 58 µg/mL Luciferase (native or cold-denatured, (triangles)), or with 58µg/mL α-synuclein (monomeric or oligomeric, (diamonds)).

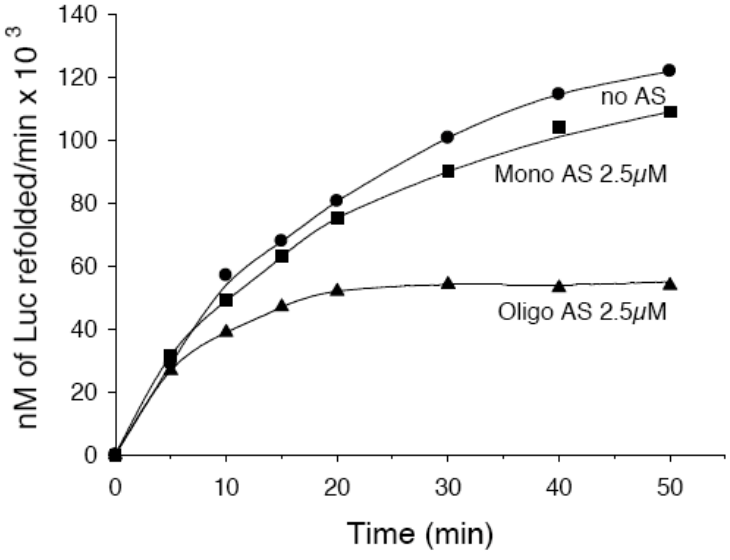

SUPPLEMENTAL FIG. S2. The oligomeric species of α-synuclein inhibit the refolding of freeze-inactivated luciferase mediated by the DnaK chaperone system. Time-dependent reactivation of freeze-inactivated luciferase (0,5µM) by the DnaK chaperone system (2.5µM DnaK, 0.5 µM DnaJ, 0.5 µM GrpE), in absence (circles) or in presence of either 2.5µM oligomeric α-synuclein (triangles) or 2.5µM monomeric α-synuclein (squares). 5 mM ATP were supplemented at time 0min, and aliquots were assayed for Luciferase activity at the indicated time points, as described in Sharma *et al,* 2008.

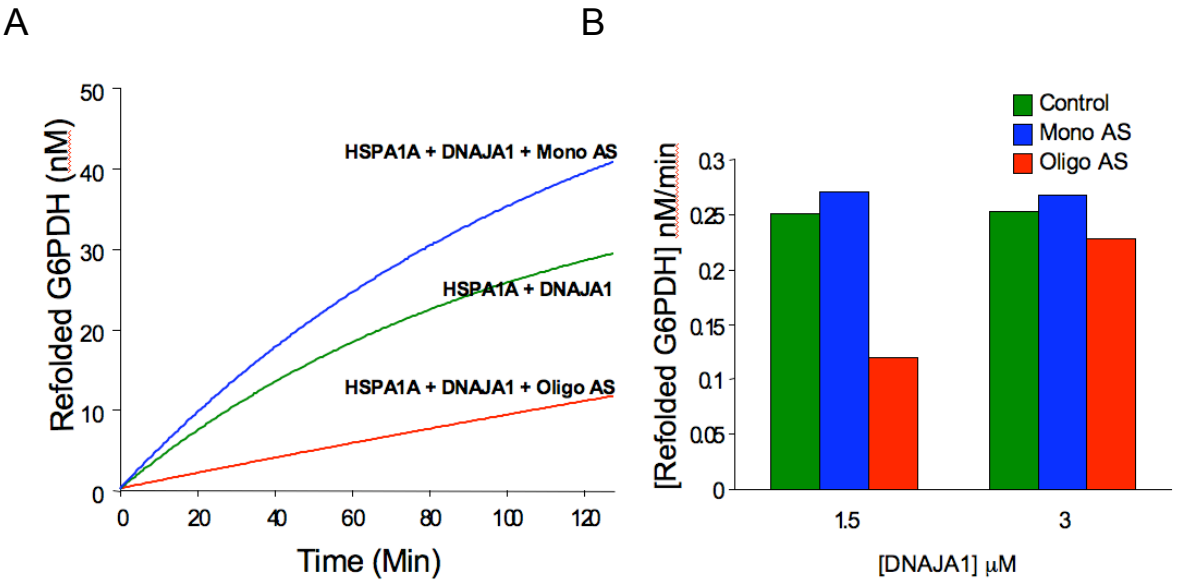

SUPPLEMENTAL FIG. S3. α-Syn oligomers inhibit human Hsp70/40 chaperone mediated refolding of heat denatured G6PDH. G6PDH (750 nM) was heat-denatured 7 minutes at 52°C without chaperones, as in Diamant et al., 2000, then supplemented with purified recombinant human HSP70 (HSPA1A, 5 µM) and Hsp40 (DNAJA1, 1 µM), without (green line), or with 4µM monomeric α-syn (blue line) or 4 µM oligomeric α-syn (red line). The reaction was initiated by addition of 5 mM ATP. *A,* time-dependent refolding of G6PDH at 30°C. *B,* refolding rates in the presence of 5 µM HSPA1A and 1.5 or 3.0 µM DNAJA1.

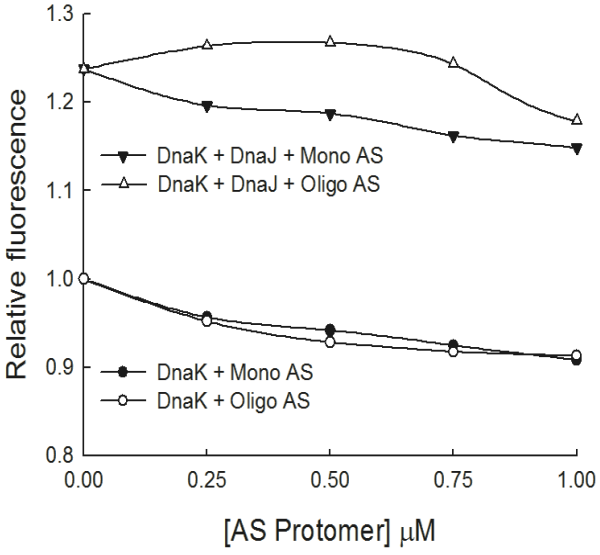

SUPPLEMENTAL FIG. S4: Steady-state tryptophan fluorescence using a LS50 spectrofluorimeter from Perkin Elmer. 1 µM DnaK in refolding buffer was incubated at 25°C in the presence of 1 mM ATP, 5 µg/ml pyruvate kinase and 4 mM PEP, without or with of 0.5 µM DnaJ and increasing concentrations of monomeric or oligomeric α-syn, as indicated (concentrations expressed in protomers). Excitation was at 300 nm and emission at 348 nm.

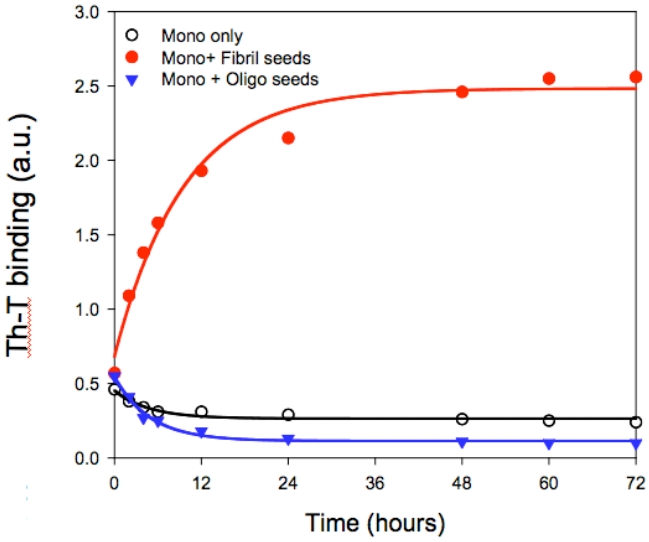

SUPPLEMENTAL FIG. S5. α-Syn oligomers do not seed the fibrilization of α-Syn monomers. α-Syn monomers (50 µM; black line) were incubated at **37°C** for the indicated time without or with freshly sonicated α-syn fibrils (10 µM protomers; red line) or α-Syn oligomers (1 µM protomers; blue line)**.** At indicated times, fibril formation was measured by fluorescence in the presence of 60 µM ThT (excitation: 450 nm; emission: 485 nm) and expressed in arbitrary units (a.u.).

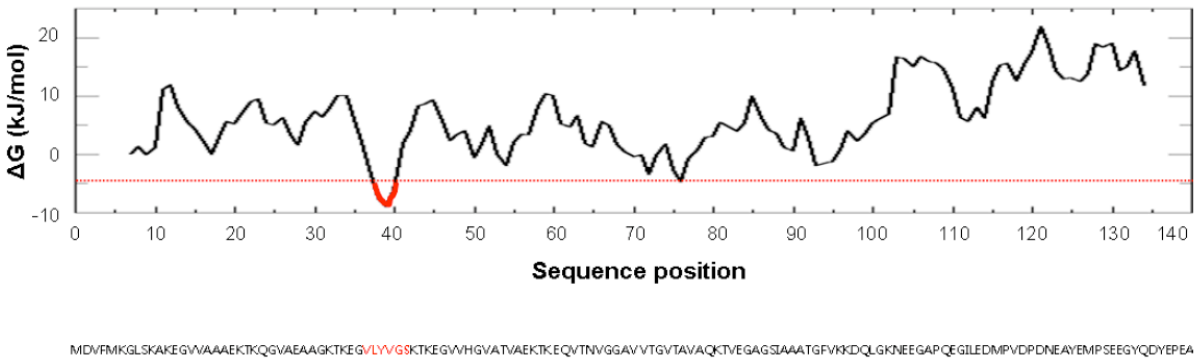

SUPPLEMENTAL FIG. S6. α-synuclein possess a single Hsp70 binding site. Free energies of binding shown as a function of the residue number within the α-synuclein primary sequence, as deduced from the algorithm of Rudiger and co-workers (Rudiger *et al*, 1997), using a sliding window approach. The red dotted line indicates a -5 kJ/mol threshold of confidence, and the red segment of the solid line indicates the region within the α-syn primary sequence predicted to be the Hsp70 binding site (residues 36-41, highlighted in red).

CHAPTER 6

Meta-analysis of heat- and chemically upregulated chaperone genes in plant and human cells

Meta-analysis of heat- and chemically upregulated chaperone genes in plant and human cells.

Finka, A., Mattoo, R.U. and Goloubinoff, P.

I contributed to this work conceptually and in the writing of the manuscript.
I contributed with Dr. Finka in the data acquisition for the Fig. 1(A and B), Fig. 2(A and B), Fig. 3(A-C), Fig. 4, Fig. 5(A and B), Fig. 6 and supplementary material (available online): Fig S1, Fig. S2, Fig S3, Table 1(A and B) and Table 2.

Cell Stress and Chaperones (2011) 16:15–31
DOI 10.1007/s12192-010-0216-8

ORIGINAL PAPER

Meta-analysis of heat- and chemically upregulated chaperone genes in plant and human cells

Andrija Finka · Rayees U. H. Mattoo · Pierre Goloubinoff

Received: 18 June 2010 / Revised: 16 July 2010 / Accepted: 19 July 2010 / Published online: 9 August 2010

Abstract Molecular chaperones are central to cellular protein homeostasis. In mammals, protein misfolding diseases and aging cause inflammation and progressive tissue loss, in correlation with the accumulation of toxic protein aggregates and the defective expression of chaperone genes. Bacteria and non-diseased, non-aged eukaryotic cells effectively respond to heat shock by inducing the accumulation of heat-shock proteins (HSPs), many of which molecular chaperones involved in protein homeostasis, in reducing stress damages and promoting cellular recovery and thermotolerance. We performed a meta-analysis of published microarray data and compared expression profiles of HSP genes from mammalian and plant cells in response to heat or isothermal treatments with drugs. The differences and overlaps between HSP and chaperone genes were analyzed, and expression patterns were clustered and organized in a network. HSPs and chaperones only partly overlapped. Heat-shock induced a subset of chaperones primarily targeted to the cytoplasm and organelles but not to the endoplasmic reticulum, which organized into a network with a central core of Hsp90s, Hsp70s, and sHSPs. Heat was best mimicked by isothermal treatments with Hsp90 inhibitors, whereas less toxic drugs, some of which non-steroidal anti-inflammatory drugs, weakly expressed different subsets of Hsp chaperones. This type of analysis may uncover new HSP-inducing drugs to improve protein homeostasis in misfolding and aging diseases.

Keywords Chaperone network · Heat shock proteins · Foldase · NSAID · Cellular stress response · Unfolded protein response

Introduction

The term "heat-shock proteins" (HSPs) was first used to describe *Drosophila melanogaster* proteins that massively accumulate during heat stress (Tissieres et al. 1974). When subject to a sharp increase in temperature, prokaryotes and eukaryotes alike transiently reallocate their general house-keeping protein synthesis machinery to the specific accumulation of a small subset of highly conserved Hsps, initially named according to their molecular weight on sodium dodecyl sulfate polyacrylamide gels: Hsp100 (ClpB/A/C), Hsp90 (HtpG), Hsp70 (DnaK), Hsp60 (GroEL), Hsp40 (DnaJ), the small Hsps (IbpA/B), and Hsp10 (GroES) (*E. coli* proteins in brackets; Daniels et al. 1984; Tissieres et al. 1974; Kimpel and Key 1985). A general mechanism was then proposed for Hsp70 by Pelham (1986) and for GroEL by Ellis, whereby these two major classes of Hsps may prevent the aggregation of stress-denatured or nascent proteins in the cell and thus "chaperone" the correct native folding and/or assembly of other proteins, without being part of the final native protein structures (Ellis et al. 1989).

Under physiological and stress conditions, the various chaperone families act in a tightly interconnected network (Csermely et al. 2008). Genetic and biochemical studies show that in bacteria, the chaperone network has a key role in housekeeping (Deuerling et al. 1999) and in the cellular response to various stresses (Liberek and Georgopoulos 1993). Eukaryotes may use different subsets of redundant, partially overlapping chaperones to fold and translocate

Electronic supplementary material The online version of this article (doi:10.1007/s12192-010-0216-8) contains supplementary material, which is available to authorized users.

A. Finka · R. U. H. Mattoo · P. Goloubinoff (✉)
Department of Plant Molecular Biology, University of Lausanne, 1015 Lausanne, Switzerland
e-mail: Pierre.Goloubinoff@unil.ch

proteins under physiological conditions, to prevent protein misfolding and aggregation during stress (Albanese et al. 2006), and to recover misfolded proteins after stress (Mogk et al. 1999; Tomoyasu et al. 2001). During a noxious heat shock, an overload of the cellular chaperones may occur (Csermely 2001; Nardai et al. 2002), overwhelming chaperone- and protease-based cellular proteostasis (Morimoto 2008). When the stress is over, the cellular protein network is restructured, and the so-called hubs, which, under stress were transiently replaced by molecular chaperones, regain control of cellular functions (Soti et al. 2005; Szabadkai et al. 2006; Szalay et al. 2007). The general purpose of this study was to gain knowledge on HSP- and chaperone-inducing treatments and drugs that best recapitulate natural patterns of HSP chaperone gene expression in tissues challenged by heat or cellular stresses, to improve proteostasis, particularly in deficient tissues, in aging or degenerative diseases associated to protein misfolding (for a review, see Hinault et al. 2006).

Hsp70s and co-chaperones With the exception of some *archaea* (Large et al. 2009), members of the evolutionary conserved Hsp70 chaperone family are present in all the ATP-containing compartments of living organisms (Macario and de Macario 1999). Thus, in human, the major isoform Hsp72 (HSPA1A) and the heat shock cognate 70 (Hsc70/HSPA8) are located in the cytosol and nucleus, whereas BiP (Grp78/HSPA5) is in the endoplasmic reticulum, mtHsp70 (Grp75/mortalin/HSPA9) is in mitochondria (Hageman and Kampinga 2009), and there are possibly also Hsp70s in peroxisomes (Hageman et al. 2007). In addition, plant chloroplasts and protozoan apicoplasts contain Hsp70s most similar to cyanobacteria (Soll 2002; Tarun et al. 2008). The functional Hsp70 chaperone network entails ATP-driven interactions between many diverse substrate-specific and less specific J-domain co-chaperones (49 in human) that target the fewer Hsp70 isoforms (Kampinga et al. 2009) onto hundreds of protein substrates in the cell and are regulated by various nucleotide exchange factors (NEF) such as GrpE (Harrison 2003), BAG (Kabbage and Dickman 2008), HspBP1 (Kabani et al. 2002), and Hsp110 proteins (Shaner and Morano 2007). These networks are crucial to the co-translational folding of nascent polypeptides, the remodeling of native protein complexes, the transduction of cellular signals, the regulation of the cell cycle, proliferation and apoptosis (Jolly and Morimoto 2000), the regulation of the heat shock response, the unfolding and refolding of stress-denatured proteins, and the import of proteins into the mitochondria (De los Rios et al. 2006), chloroplasts (Shi and Theg 2010), and the endoplasmic reticulum (reviewed in Zimmermann et al. 2010). Moreover, the Hsp70/Hsp40 networks control the stability and activity of native proteins such as σ^{32} and the oligomeric state of native protein complexes, such as repE (Rodriguez et al. 2008), clathrin cages (Schuermann et al. 2008), and IkB (Weiss et al. 2007) and yeast prions (Wickner 1994; Shorter and Lindquist 2008).

The Hsp100 The Hsp100 chaperones are ATPase members of the AAA+ superfamily, including bacterial ClpB, mitochondrial Hsp78, chloroplast ClpC/D, and eukaryotic orthologues in the cytoplasm of fungi, yeast (Hsp104), and plants (Hsp101), (Mogk et al. 2008). The Hsp100 chaperones share sequence, structural, and functional similarities with the AAA+-gated proteases, such as the lid of the eukaryotic proteasome, the ATPase moiety of the bacterial proteases HslU/V, ClpA/P, ClpX/P, and Lon (for a review, see Sharma et al. 2009). Whereas the sole bacterial Hsp70/Hsp40/NEF chaperone network can effectively disaggregate and unfold small soluble protein aggregates (Diamant et al 2000; Ben-Zvi et al. 2004), it best acts in concert with Hsp100 (ClpB) in bacteria and in the cytoplasm of plants and fungi (but not in animals), to disaggregate large insoluble aggregates into natively refoldable polypeptides (Glover and Lindquist 1998; Goloubinoff et al. 1999; Motohashi et al. 1999). As with the other major classes of molecular chaperone, Hsp100 plays a vital role in the survival of bacteria, yeast, and plant cells during and following exposures to high temperatures or chemical stresses (Sanchez and Lindquist 1990).

Hsp60/10 Whereas the proper folding of nascent proteins in bacteria mostly depends on the activity of the Hsp70/40/NEF network, 10–15% of newly synthesized polypeptides are better substrates for bacterial Hsp60/Hsp10 network (for a review, see Liberek et al. 2008). Class I chaperonins represented by Hsp60 homologues are found in bacteria (GroEL), mitochondria, and chloroplasts. A functional Hsp60/Hsp10 complex comprises 14 identical subunits arranged in two stacked heptameric rings, requiring two heptameric co-chaperones, Hsp10/GroES (Azem et al. 1995). Seminal observations showed that artificially denatured proteins become prevented from aggregating upon binding to purified GroEL and, moreover, become subsequently refolded to the native state in a strict GroES- and ATP-dependent manner (Goloubinoff et al. 1989).The class II of chaperonins, which are present in *archaea* and in the cytoplasm of eukaryotes (Large et al. 2009), forms TCP-1 ring complex (TRiC, also named CCT for chaperonin-containing TCP1) consisting of two stacked rings with eight different paralogous subunits per ring (Booth et al. 2008). The TRiCs act as ATP-dependent central mediators of cytosolic protein folding and assembly (Hartl and Hayer-Hartl 2009), which are also important to prevent protein aggregation and toxicity (Kitamura et al. 2006).

Hsp90 family and co-chaperones Whereas the physiological and stress-related functions of HtpG, the bacterial Hsp90, and of the mitochondrial and chloroplast Hsp90s remain unclear (Sato et al. 2010; Hasan and Shimizu 2008), in vitro, Hsp90 can prevent protein aggregation in an ATP-independent manner (Wiech et al. 1992). Owing to the early discovery of specific Hsp90 inhibitors (Whitesell et al. 1994), the cellular functions of endoplasmic reticulum (ER) (Grp94), cytosol, and nuclear located Hsp90s in eukaryotes are better known than a role of prokaryotic HtpG. The EEVD motif at the carboxy-terminus of cytoplasmic Hsp90 and some cytoplasmic Hsp70s is a docking site for connecting proteins with tetratricopeptide repeats (TPR) (Blatch and Lassle 1999; van der Spuy et al. 2000). Bridged by TPR-containing co-chaperones, both chaperones can form functional super-complexes that modify in a yet ill-defined ATP-dependent mechanism, the structure, and consequently the function, of hundreds of the so-called native "client" proteins in the cell (Whitesell and Lindquist 2005; Zhao et al. 2005). Thus, the Hop co-chaperone containing three TPR repeats bridges Hsp70 and Hsp90, which, together with Hsp40 and p23 co-chaperone, drive structural and functional changes in native protein complexes in the cell, such as the progesterone receptor (Cintron and Toft 2006; Onuoha et al. 2008). CHIP is another TPR co-chaperone of Hsp90 with a U-box domain, whose activity promotes "protein triage" of Hsp70- or Hsp90-bound proteins fated to proteasomal degradation (Connell et al. 2001). Taken together, in eukaryotic cells, heterocomplexes of Hsp90 with about a dozen co-chaperones (Picard 2006; for an updated list of Hsp90 co-chaperones, see http://www.picard.ch/downloads/Hsp90interactors.pdf) with Hsp70 and protein clients are key to various physiological processes, in particular signal transduction.

Small Hsps Unlike the ATPase chaperones Hsp100, Hsp90, Hsp70, and Hsp60, the small Hsps (sHSPs) have a conserved α-crystalline domain that passively binds misfolded intermediates, independently from ATP hydrolysis (Jakob et al. 1993). Without stress, sHsps are mostly assembled into large oligomeric complexes (Garrido et al. 2006), which, under stress conditions, may dissociate into amphiphilic dimers that prevent misfolding polypeptides from aggregating (Jakob et al. 1993) and protect membranes from heat disruption (Horvath et al. 2008; Haslbeck et al. 2005). sHsps cooperate with Hsp70/Hsp40 and Hsp100 or the GroEL/GroES chaperone networks in refolding of misfolded proteins (for a review, see Nakamoto and Vigh 2007). Human Hsp27 and Hsp70 are often, although not obligatorily, co-expressed in response to a variety of physiological and environmental stimuli (Garrido et al. 2006) (Vigh et al. 2007). As sHsps have strong cytoprotective properties (Garrido et al. 2006), their inhibition is an important target in pharmacological therapies to cancer (Didelot et al. 2007), whereas the upregulation sHsp may prevents liver damage (Kanemura et al. 2009) or pathologies caused by protein misfolding, such as Alzheimer's (Fonte et al. 2008; Wu et al. 2010), Parkinson's (Zourlidou et al. 2004), and Huntington's disease (Perrin et al. 2007).

Here, we used published microarray data from *Homo sapiens* and the land plant *Arabidopsis thaliana* to perform a meta-analysis of the expression profiles of bioinformatically predicted chaperones, co-chaperones, and foldase genes (together called the chaperome), following various abiotic and chemical stresses. Clustering of induction profiles revealed that heat shock primarily induces cytoplasmic and mitochondrial but not ER chaperone networks, a profile that was best mimicked by isothermal treatments with Hsp90 inhibitors or less faithfully by other compounds, many of which are known as anti-inflammatory drugs. Sequence analysis of HSP promoters showed that canonical heat hock elements (HSEs) were unexpectedly rare in HSP genes. This type of analysis may uncover new HSP-inducing drugs that best recapitulate natural patterns of HSP chaperone gene expression in undamaged tissues, to improve protein homeostasis in defective aging tissues and in protein misfolding pathologies.

Methods

List of human and plant chaperones, co-chaperones, and foldases

Two lists of bio-informatically identified "chaperomes" were compiled for the human and the *A. thaliana* genomes (Supplemental Tables 1a and 2, respectively), which included all the predicted protein sequences sharing at least 40% homology with one of the conserved canonical chaperone families in eukaryotes and their corresponding, identifiable prokaryotic homologues (prokaryote genes named in brackets): Hsp70 (DnaK), Hsp90 (HtpG), Hsp100/Hsp78 (ClpB/C), Hsp40 (DnaJ), Hsp60 (GroEL), and the α-crystalline domain containing small HSPs (IbpA/B), trigger factors, co-chaperones and nucleotides exchange factors (such as Hsp110, Grp170, Bag2, GrpE, GroES, Cpn10, and Cpn20), all J-domain containing proteins with a conserved HPD motive, over a dozen of Hsp90 co-chaperones (interactors) as listed by Picard (http://www.picard.ch/downloads/Hsp90interactors.pdf). Because peptidyl prolyl isomerases (PPIs) and protein disulfide isomerases (PDIs) are clearly involved in cellular protein homeostasis in general and although they do not belong to the canonical chaperone families, we

chose to add them to this analysis (for a review, see Sharma et al. 2009).

Bioinformatic analysis

All data are MIAME compliant. The raw data were extracted from the National Center for Biotechnology Information (NCBI) Gene Expression Omnibus (GEO). For the *A. thaliana* chaperome metadata analysis, the microarray data for dithiothreitol (DTT), tunicamycin, and the five heat treatments were extracted from the GEO (ATH1-121501 Affymetrix *Arabidopsis* ATH1 Genome Array), under the following series accession numbers: GSE4021 (leaf disks), GSE11758 (mature leaves), GSE4760 (seedlings), GSE16222 (seedlings), GSE12619 (seedlings), GSE4062 (shoots), and GSE11758 (mature leaves), respectively. Microarray datasets for salicylic acid (seedlings), ibuprofen (seedlings), 2,3,5-triiodobenzoicacid (TIBA, seedlings), and 2,4,6-trihydroxybenzamide (2,4,6-T, seedlings) were obtained from Genevestigator (Zimmermann et al. 2004). Array metadata for DTT, tunicamycin, and one heat treatment denoted in GEO as GSE16222 were joined to the rest of metadata obtained from Genevestigator as a tab delimited file.

For the human and *Arabidopsis* chaperome metadata analysis, respectively, 167 and 281 probes (Supplemental Tables 1a and b and 2) corresponding to unique genes were chosen as described (Hageman and Kampinga 2009). The microarray data for the predicted human chaperome was searched in NCBI GEO (HG_U133 Plus 2.0 Affymetrix Human Genome Array): sapphyrin PCI-5002 GSE6962 (A549 tumor), echinomycin GSE7835 (U251 cells), etoposide GSE11954 (hepatic stellate cells), simvastatin GSE4883 (human peripheral blood monocytes macrophages), 2-deoxyglucose GSE13548 (HeLa cells), tunicamycin GSE13548 (HeLa cells), phorbol 12-myristate 13-acetate GSE12736 (K562 cells), cadmium (early) GSE9951 (immortalized human normal prostate epithelial cell line), paclitaxel GSE11552 (294T cells), heat shock study GSE9916 (THP-1 cells), elesclomol study GSE11552 (294T cells), smoking study six brands of cigarettes (early) GSE10718 (normal human bronchial epithelial cells), propiconazole GSE10410 (human primary hepatocytes), *N*-acetylcystein GSE11552 (294T cells), rifampicin GSE10410 (human primary hepatocytes), myclobutanil GSE10410 (human primary hepatocytes), estrogen (late) GSE11324 (MCF7 cells), dihydrotestosterone GSE7708 (LNCaP cells), doxycycline GSE7678 (SW480 cells), VAF347 GSE10463 (immature monocyte-derived dendritic cells), and apple procyanidin GSE9647 (human vascular endothelial cells). The array metadata for 2-deoxyglucose and tunicamycin were from GEO and joined to the rest of the metadata obtained from Genevestigator as a tab delimited file. Solar ultraviolet, Hsp90 inhibitors and non-steroidal anti-inflammatory drug (NSAID) microarray data for available human Hsp70 and Hsp40 genes were searched directly in Genevestigator (HG_U133A Affymetrix Human Genome Array) and joined with data from the heat shock study (GSE9916) as a tab delimited file.

Transcripts were considered responsive only when showing at least a 2-fold change in response to an investigated treatment. The distance matrix was evaluated using the Pearson correlation coefficient, and clusters were created using the complete linkage method by Cluster 3.0 (http://bonsai.ims.u-tokyo.ac.jp/~mdehoon/soft ware/cluster/manual/index.html) and visualized by the JavaTreeView (Saldanha 2004) algorithm, exported as a postscript file, processed by Adobe Illustrator (Adobe Systems, Mountain View, CA, USA). Annotation and presumed subcellular localization of chaperones were performed according to the Uniprot database.

In an attempt to generate a significant network best describing the degree of connectivity between the various chaperones, co-chaperones, and foldases in the human chaperome, we used the STRING database and web resource. STRING weights both physical and functional protein–protein interactions and integrates various informations from different metadatabase sources, to produce a network map showing all possible protein–protein interactions in the chaperome (http://string-db.org) (Jensen et al. 2009). Because under non-stressed conditions, the members of the chaperone network are expected to have more but weaker interactions among themselves than under stressful conditions (Csermely et al. 2008), we chose the low confidence factor of 0.15 for this analysis. The interactions between chaperones was visualized using Medusa (Hooper and Bork 2005)

Using the search PromForm program from the Promoter Database (http://rulai.cshl.edu/cgi-bin/TRED/tred.cgi?process=searchPromForm), a search for HSEs containing direct or inverted repeats of 5′-nGAAn-3′ was performed from 3 kbp upstream to 300 bp downstream from the predicted transcription start site of each bioinformatically identified chaperone gene from mammals (as listed in Supplemental Table 1b).

Results

Most HSPs are not chaperones, and most chaperones are not HSPs

As exemplified by the two seminal reviews, “Molecular chaperone functions of heat-shock proteins” (Hendrick and Hartl 1993) and “Heat-shock proteins as molecular chaperones” (Becker and Craig 1994), the terms “chaper-

ones" and "HSPs" are often indiscriminately used in the literature. In 2009, a survey of 300 articles in PubMed citing both "chaperones" and "Hsp70" in their title, abstract, or introduction, a third stated that molecular chaperones are Hsps and Hsps are molecular chaperones without distinction (data not shown). To estimate the validity of the generally assumed strong linkage between HSPs and molecular chaperones, we examined the microarray responses to mild heat treatments in two very different eukaryotes, a higher plant and a mammal, and compared the messenger RNA (mRNA) expression patterns of bio-informatically identified chaperome genes (listed in Supplemental Tables 1a and 2), to the rest of the corresponding genomes. Because of the high degree of evolutionary conservation, members of the α-crystalline-containing small HSPs and of the four canonical families of ATP-hydrolyzing chaperones Hsp100, Hsp90, Hsp70 and Hsp60 and their respective co-chaperones, as well as the PPIs and the PDIs, were identified by simple bioinformatic analysis (see "Methods"). Hence, of the 23,438 predicted protein-encoding genes in *H. sapiens* (The Genome Reference Consortium, version GRCh37), 168 genes were identified as belonging to "the human chaperome" (Supplemental Table 1b). Similarly, of the 27,379 predicted protein-encoding genes in the terrestrial plant *A. thaliana* (The *Arabidopsis* Information Resource, version TAIR9), 305 genes were identified as "the *Arabidopsis* chaperome" (Supplemental Table 2).

A meta-analysis of microarray data from different organisms and laboratories is always limited by the smallest number of available probes for HSP and chaperome genes, printed on the chips. Thus, we could effectively follow the changes in the expression profiles of up to 167 human chaperome genes and up to 281 *Arabidopsis* chaperome genes. Microarray data showed that a short sub-lethal heat treatment (37°C–>43°C, 60 min for human, 23°C–>38°C, 90 min for the plant) upregulated more than 3.16-fold ($\log_{10}$ value=0.5) about 2% of the human genes and 4% of the plant genes, respectively (Fig. 1). Noticeably, in human and plant, chaperome genes were, respectively, 17 and seven times, more likely to be induced by heat than non-chaperone genes. Moreover, while being only 0.7% of the human genome, 20% of the chaperome was massively (>20-fold) induced by heat (Fig. 1a), a remarkable 28-fold enrichment of expressed mRNA levels. Similarly, while being only 1.1% of the plant genome, 16% of the chaperome was most massively (>20-fold) induced by heat, a 14-fold enrichment of mRNA levels (Fig. 1b). Despite this general high propensity of the chaperomes to be induced by heat, a majority of chaperome genes (66% for human and 72% for plant) yet remained uninduced by heat, confirming the importance not to confuse HSPs for chaperones and vice versa. Hence, molecular chaperones and foldases should be specifically referred as such and not as HSPs, especially in a context of their physiological functions in protein homeostasis, cellular trafficking, signaling, or of their induction by other means than heat.

The heat-inducible chaperones can be upregulated by isothermal chemical treatments

Although heat has a demonstrated strong effect on the induction of a specific subset of chaperome genes, other isothermal chemical or physical stresses may also induce similar or different subsets of chaperome genes (Saidi et al. 2005, 2007).

In *Arabidopsis*, five independent heat treatments (HS) by different laboratories and different temperature conditions showed comparable induction patterns of chaperome genes associated to the cellular stress response (CSR), demonstrating the robustness of our approach (see Supplemental Fig. 1). Isothermal treatments with inhibitors of polar auxin transport, such as TIBA and 2,4,6-T and also with the plant hormone salicylic acid and with ibuprofen, which are both NSAIDs in mammals, showed mildly increased levels of particular chaperones, which, however, only loosely clustered with the heat treatments (Fig. 2, Supplemental Fig. 2). Two main treatment clusters were, however, clearly observed, one following heat or specific chemical treatments, corresponding to a general response associated to the CSR (for a review, see Calabrese et al. 2008; Fig. 2a), in which chaperones mostly targeted to the cytosol, the plasma membrane and the mitochondria were upregulated (Aparicio et al. 2005), and the other following chemical treatments with stressors specific to the ER, corresponding to a response known as the "unfolded protein response" (UPR), in which chaperones mostly targeted to the ER lumen and membranes were upregulated (Schroder and Kaufman 2005, Fig. 2b). Unexpectedly, several plant heat shock cognates, in particular Hsc70s, were also upregulated by heat in plants (Supplemental Fig. 1, arrows) as well as in animal cells. Thus, Hsc70 (HspA8) was induced by heat (Fig. 3, treatment I) or isothermal treatments with *N*-acetylcycteine or estrogen (Fig. 3, treatment E, T). Hsc70s are thus either wrongly named, or their definition as being non-heat inducible chaperone cognates must be corrected.

In cultured animal cells, several seminal studies using isothermal treatments with amino acid analogs (Hightower 1980) or low concentrations of zinc (Whelan and Hightower 1985) caused expression of molecular chaperones. In a similar manner, isothermal treatments of human cells with Hsp90 inhibitors, UV light, elesclomol, or cigarette smoke best recapitulated the expression pattern of heat shock by inducing a similar subset of

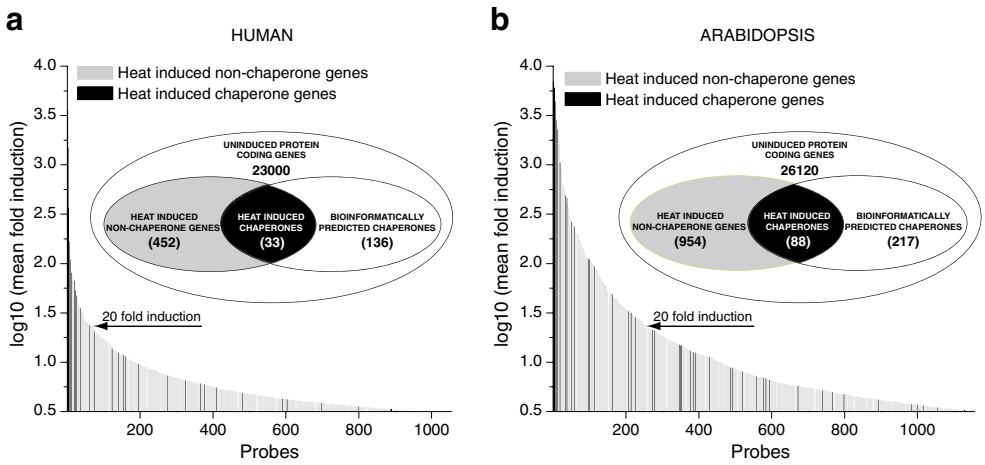

Fig. 1 Distribution and expression levels of heat-induced chaperome genes in human and plant. Distribution and fold-expression levels of heat-induced genes in (**a**) human monocyte leukemia THP-1 cells (37°C–>43°C 1 h and (**b**) plant *Arabidopsis thaliana* (23°C–>38°C, 90 min). Microarray probes corresponding to bio-informatically predicted chaperome genes are in *black* and non-chaperome genes are *grey*. The microarray data for human and plant sets were extracted from the National Center for Biotechnology Information (NCBI) Gene Expression Omnibus under the series accession nos. GSE9916 and GSE16222, respectively

about 45 out of 167 chaperome genes (Supplemental Fig. 3), most of which targeted to the cytoplasm, membranes, and mitochondria, but not to the ER (Fig. 3a). In contrast, treatments with tunicamycin, 2-deoxyglucose, or dithiothreitol induced a very different set of human chaperome genes, whose products were targeted to the ER lumen and membranes (Fig. 3b). Interestingly, the antibiotic rifampicin and two antifungal agents, myclobutanil and propiconazole, induced an additional chaperone cluster (Fig. 3c), which was not apparently related to a given subcellular localization. In conclusion, members of UPR gene cluster should be specifically called "UPR chaperones" and of the CSR gene cluster "CSR chaperones", not HSPs, even when addressed in a context of heat shock.

As with plants, treatments of human cells with several NSAIDs induced various chaperones, in particular members of the Hsp70/40 family. However, expression patterns were generally heterogeneous and at lower intensities than with CSR-inducing treatments (Fig. 4). Together with the fact that NSAIDs also induce CSR chaperones in plants (Saidi et al. 2005), this suggests that different drugs commonly classified as NSAIDs may have unconventional activation mechanisms that may not necessarily involve the inhibition of cyclooxygenases of which plants are devoid.

CSR but not UPR activates the core elements of the chaperone network

Our clustering analysis of the mammalian chaperome was thus far based only on mRNA expression metadata under various physical and chemical treatments (Figs. 3 and 4). We next estimated the robustness of this result using the STRING database that includes additional criteria, such as physical and known functional interactions (co-expression and experimental view) or computational predictions of homology and text mining co-occurrence (Jensen et al. 2009). The STRING analysis revealed a network with a strong core that cumulated most connections with other members of the chaperome that was mainly composed of Hsp90s (HSP90AA1, HSP90AB1, and HSP90B1) and Hsp70s (HSPA1A HSPA1L, HSPA2, and HSPA8), tightly interconnected to each other through common co-chaperones, such as Hip (ST13) and Hop (STIP1) (Fig. 5a). This chaperone network could be simply subdivided into five chaperone subnetworks comprising most of: (1) the Hsp70s and their co-chaperones (green, Fig. 5a, upper right), (2) the Hsp90s and their co-chaperones (magenta, Fig. 5a, upper left), (3) the PPIase and PDIs (yellow, Fig. 5a, lower left), the chaperonins (grey, Fig. 5a, lower right), and the small HSPs (black, Fig. 5a, lower right). Justifying our choice to include PPIases and PDIs in the chaperome, these foldases were nearly all found to be well-connected to the Hsp90s and the chaperonins subnetworks but, unexpectedly, much less connected to the Hsp70s and the small Hsps subnetworks (Fig. 5a).

We next examined the positioning of proteins that were at least 2-fold upregulated by heat, as a paradigm of CSR (Fig. 5b, red), or by tunicamycin, as a paradigm of UPR (Fig. 5b, yellow). Most sHSPs, together with the Hsp70s and Hsp90s core of the whole chaperone network, were strongly enriched with CSR-induced but not with UPR-induced proteins. This confirms that CSR chaperones are not evenly scattered over the whole

Fig. 2 Clustering of upregulated RNA expression levels in *Arabidopsis* chaperome under seven abiotic and chemical treatments: dithiothreitol (DTT), tunicamycin, salicylic acid, ibuprofen, 2,3,5-triiodobenzoicacid (TIBA), 2,4,6-trihydroxybenzamide (2,4,6-T), and heat treatment as indicated. Gene clusters typical of (**a**) the cellular stress response (CSR) or of the (**b**) unfolded protein response (UPR). The presumed subcellular localizations are indicated with *different background colors*

network but rather form a compact, specific core subnetwork (Fig. 5b, red circles). Confirming our transcriptomic analysis (Fig. 3), UPR-induced chaperones were fewer (Fig. 5b, yellow circles) with only three proteins (HSPA5, DNAJC3, and DNAJB9) induced by both treatments. Remarkably, many J-domain, co-chaperones, and Hsp90 co-chaperones and most of the PPIases and PDIs remained uninduced by either heat or ER stressors.

HSEs are frequent but not obligatorily present in promoters of heat-induced chaperone genes

The presence of HSEs is essential to the specific binding of activated heat-shock factors, in particular HSF-1, and to the recruitment of RNA polymerase II at the transcription start sites of HSP genes (Xing et al. 2005; Yao et al. 2006). In animals, yeast, and plants, HSEs are thought to be optimal when composed of three direct repeats of 5′-nGAAn-3′ (Amin et al. 1988; Kroeger and Morimoto 1994; Yamamoto et al. 2009), or less optimal, with inverted repeats of 5′-nTTCn-3′. We next searched for complete or partial, direct or inverted HSE patterns, between positions −3000 and 300 bp from the translation start site of each predicted human chaperome gene (Supplemental Table 1b). Expectedly, HSEs were found to be more frequent in the regulatory sequences of 45 chaperone genes that are induced at least 2-fold by heat (Fig. 6), compared to less- or non-heat induced chaperone genes. Whereas in the CSR chaperone cluster (Fig. 3, cluster a), 17 out of 24 genes (71%) contained an average of two HSEs, in the UPR chaperone cluster (Fig. 3a, cluster b), only two out of 12 genes (17%) contained a single HSE motive. However, a majority of mammalian heat-induced chaperone genes remained devoid of identifiable HSEs, suggesting that HSEs are contributing only partially to the specificity of the heat-shock response and that other specific HSF-binding sites remain to be experimentally identified.

Our combined microarray, networking and sequence promoter analysis, may contribute to the identification of potential chaperone and co-chaperone matches. Thus, the HSPD1 and HSPE1 genes, respectively encoding for mitochondrial Hsp60 and Hsp10, have similar patterns of mRNA expression (Figs. 3, 5) and were also similar in terms of HSEs patterns in their promoters (Fig. 6). Likewise, the Hsp70 chaperone genes, HSPA1A and HSPA6, had expression profiles similar to the Hsp40 co-chaperones DNAJA4, DNAJB6, DNAJB1, DNAJB4, and DNAJA1 and to the nucleotide exchange factors BAG3 or HSPH1. All but two (DNAJA4 and DNAJB1) had one or two HSEs in their promoters, suggesting that they may preferably collaborate with each other under particular stressful or physiological conditions.

Fig. 3 Clustering of upregulated RNA expression levels in the human chaperome under 21 treatments: *A* 2-deoxyglucose, *B* tunicamycin, *C* phorbol 12-myristate 13-acetate, *D* cadmium, *E* *N*-acetylcysteine, *F* paclitaxel, *G* doxycycline, *H* echinomycin, *I* heat shock study, *J* elesclomol, *K* smoking, *L* simvastatin, *M* etoposide, *N* VAF347, *O* sapphyrin PCI-5002, *P* propiconazole, *Q* myclobutanil, *R* rifampicin, *S* dihydrotestosterone, *T* estrogen, and *U* apple procyanidin. Gene clusters typical of the (**a**) cellular stress response (CSR), of the (**b**) unfolded protein response (UPR), and of the (**c**) less specific cell responses are shown. The presumed subcellular localizations are indicated with *different background colors* of the gene names

Discussion

The term molecular chaperone is adequate but incomplete

The term "molecular chaperone" was first used by Laskey to describe the properties of nucleoplasmin (Laskey et al. 1978). In 1989, Ellis adorned protein biochemistry with this social term to describe the new molecular function of a class of proteins that mediate the native folding and/or assembly of other polypeptides (Ellis et al. 1989). Whereas a social chaperone has a rather passive function—it merely prevents improper associations between youngsters—molecular chaperones, in particular the ATP-fuelled GroEL (Shtilerman et al. 1999), ClpB (Goloubinoff et al. 1999), and Hsp70 (Ben-Zvi et al. 2004), have since been found to carry an active function of repairing structural damages by unfolding and promoting native protein refolding or degradation (reviewed in Sharma et al. 2009). Hence, the social term "molecular police" might have better reflected the energy-consuming mechanism by which ATPase chaperones first apprehend, then "rehabilitate" strayed-off misfolded proteins, converting them into non-toxic functional proteins of the cell (Hinault and Goloubinoff 2007). Noticeably, alongside maintaining a "state of law" among cellular proteins, called protein homeostasis (or proteostasis, Morimoto 2008) in the crowded protein population of the cell, the network of chaperones, like a highly coordinated police force, is also involved in non-stress housekeeping functions, such as regulating protein trafficking, signaling, and import into organelles. Thus, although incomplete, the term "molecular chaperone" is not entirely wrong and should be maintained, primarily because it is now well-anchored into the scientific community.

The cellular stress response is likely under the control of the plasma membrane

Sensing temperature changes in eukaryotes has been initially attributed to unspecified thermolabile proteins in the cytoplasm, whose unfolding supposedly recruits inhibitory Hsp90 and Hsc70 chaperones, thereby activating formerly chaperone-repressed Hsfs (Voellmy and Boellmann 2007). However, it has been recently

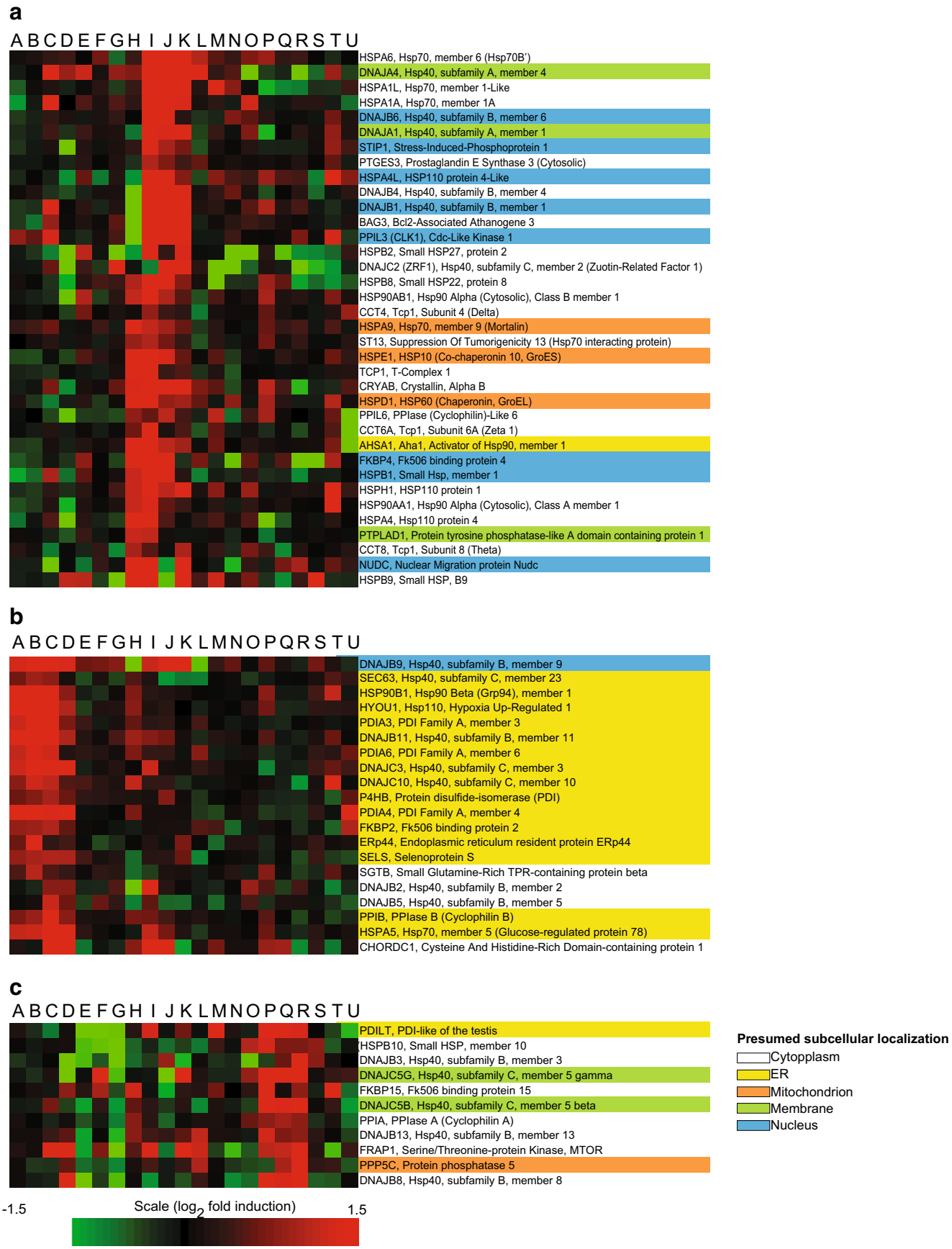
a
A B C D E F G H I J K L M N O P Q R S T U
HSPA6, Hsp70, member 6 (Hsp70B')
DNAJA4, Hsp40, subfamily A, member 4
HSPA1L, Hsp70, member 1-Like
HSPA1A, Hsp70, member 1A
DNAJB6, Hsp40, subfamily B, member 6
DNAJA1, Hsp40, subfamily A, member 1
STIP1, Stress-Induced-Phosphoprotein 1
PTGES3, Prostaglandin E Synthase 3 (Cytosolic)
HSPA4L, HSP110 protein 4-Like
DNAJB4, Hsp40, subfamily B, member 4
DNAJB1, Hsp40, subfamily B, member 1
BAG3, Bcl2-Associated Athanogene 3
PPIL3 (CLK1), Cdc-Like Kinase 1
HSPB2, Small HSP27, protein 2
DNAJC2 (ZRF1), Hsp40, subfamily C, member 2 (Zuotin-Related Factor 1)
HSPB8, Small HSP22, protein 8
HSP90AB1, Hsp90 Alpha (Cytosolic), Class B member 1
CCT4, Tcp1, Subunit 4 (Delta)
HSPA9, Hsp70, member 9 (Mortalin)
ST13, Suppression Of Tumorigenicity 13 (Hsp70 interacting protein)
HSPE1, HSP10 (Co-chaperonin 10, GroES)
TCP1, T-Complex 1
CRYAB, Crystallin, Alpha B
HSPD1, HSP60 (Chaperonin, GroEL)
PPIL6, PPIase (Cyclophilin)-Like 6
CCT6A, Tcp1, Subunit 6A (Zeta 1)
AHSA1, Aha1, Activator of Hsp90, member 1
FKBP4, Fk506 binding protein 4
HSPB1, Small Hsp, member 1
HSPH1, HSP110 protein 1
HSP90AA1, Hsp90 Alpha (Cytosolic), Class A member 1
HSPA4, Hsp110 protein 4
PTPLAD1, Protein tyrosine phosphatase-like A domain containing protein 1
CCT8, Tcp1, Subunit 8 (Theta)
NUDC, Nuclear Migration protein Nudc
HSPB9, Small HSP, B9
b
A B C D E F G H I J K L M N O P Q R S T U
DNAJB9, Hsp40, subfamily B, member 9
SEC63, Hsp40, subfamily C, member 23
HSP90B1, Hsp90 Beta (Grp94), member 1
HYOU1, Hsp110, Hypoxia Up-Regulated 1
PDIA3, PDI Family A, member 3
DNAJB11, Hsp40, subfamily B, member 11
PDIA6, PDI Family A, member 6
DNAJC3, Hsp40, subfamily C, member 3
DNAJC10, Hsp40, subfamily C, member 10
P4HB, Protein disulfide-isomerase (PDI)
PDIA4, PDI Family A, member 4
FKBP2, Fk506 binding protein 2
ERp44, Endoplasmic reticulum resident protein ERp44
SELS, Selenoprotein S
SGTB, Small Glutamine-Rich TPR-containing protein beta
DNAJB2, Hsp40, subfamily B, member 2
DNAJB5, Hsp40, subfamily B, member 5
PPIB, PPIase B (Cyclophilin B)
HSPA5, Hsp70, member 5 (Glucose-regulated protein 78)
CHORDC1, Cysteine And Histidine-Rich Domain-containing protein 1
c
A B C D E F G H I J K L M N O P Q R S T U
PDILT, PDI-like of the testis
HSPB10, Small HSP, member 10
DNAJB3, Hsp40, subfamily B, member 3
DNAJC5G, Hsp40, subfamily C, member 5 gamma
FKBP15, Fk506 binding protein 15
DNAJC5B, Hsp40, subfamily C, member 5 beta
PPIA, PPIase A (Cyclophilin A)
DNAJB13, Hsp40, subfamily B, member 13
FRAP1, Serine/Threonine-protein Kinase, MTOR
PPP5C, Protein phosphatase 5
DNAJB8, Hsp40, subfamily B, member 8
-1.5
Scale (log2 fold induction)
1.5
Presumed subcellular localization
Cytopplasm
ER
Mitochondrion
Membrane
Nucleus

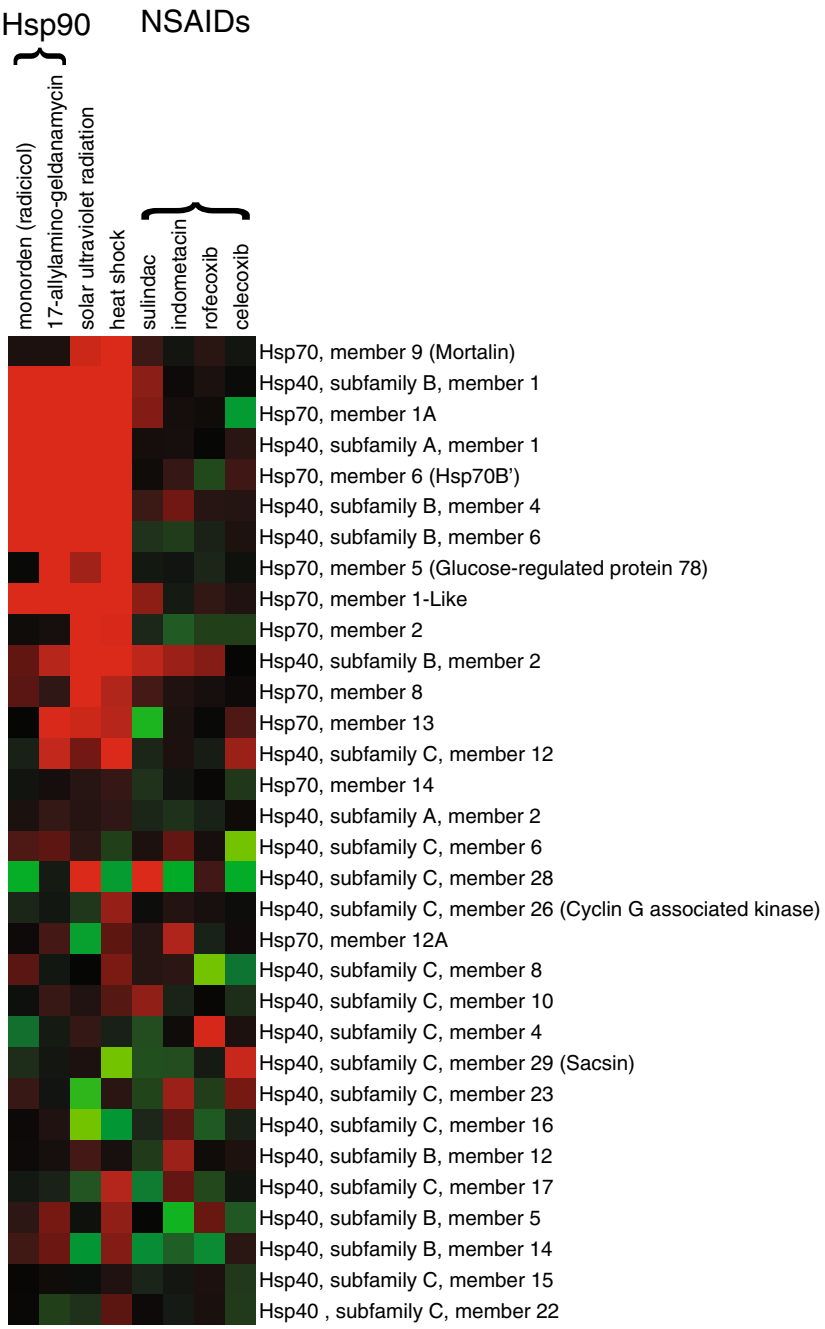

Fig. 4 Expression profile of human Hsp70 and Hsp40 orthologs under different treatments. Heat and UV induced up- and downregulated human Hsp70 and Hsp40 genes, as compared to isothermal treatments with two Hsp90 inhibitors and four different NSAIDs, as indicated

shown in plants that ambient temperature upshifts, for example, from 12 to 27°C, can trigger the upregulation of 2,764 HSP genes, many of which are chaperone genes (Kumar and Wigge 2010). Likewise, isothermal treatments with non-toxic chemicals, such as hormones and NSAIDs unlikely to denature proteins in bacteria, yeast, plants, and animals can upregulate specific HSP and chaperone genes (Saidi et al. 2005, 2007; Vigh et al. 2007). Similarly, the generally observed induction of the CSR in various organisms by treatments with membrane fluidizers strongly suggests that subtle changes in the plasma membrane state (fluidity, the raft/non-raft organization) are the most upstream events of the temperature-sensing and signaling pathway, both in prokaryotes and eukaryotes (de Marco et al. 2005; Vigh et al. 1998, 2007). Because abnormally exposed hydrophobic parts of misfolded proteins often wrongly interact with membranes and because, without a Ca^{2+} entry-

Fig. 5 Chaperone network rearrangements in CSR and UPR. **a** Interaction network of proteins in different cellular functions from STRING analysis of the chaperome (Supplemental Table 1) showing Hsp70 (*green*), Hsp90 (*magenta*), foldases (*orange*), small Hsp (*black*) and chaperonin subnetwork (*gray*). **b** Stress-induced centralization of chaperone hubs in CSR (*red*), UPR (*orange*), or both (*pink*)

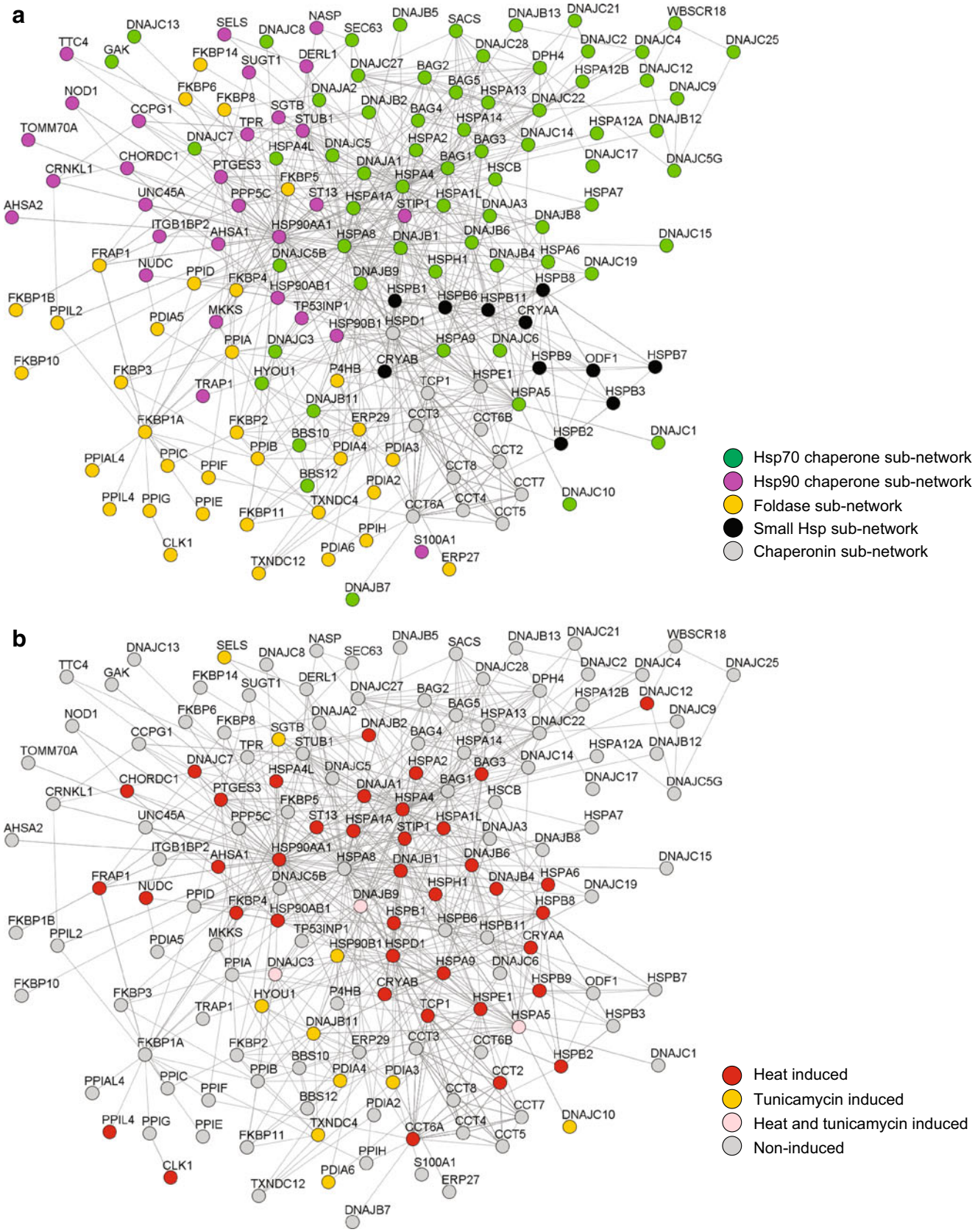
a
DNAJC13
SELS
NASP
DNAJB5
SACS
DNAJB13
DNAJC21
WBSCR18
TTC4
GAK
DNAJC8
SEC63
DNAJC28
DNAJC2
DNAJC4
DNAJC25
FKBP14
SUGT1
DERL1
DNAJC27
BAG2
DPH4
HSPA12B
DNAJC12
NOD1
FKBP6
FKBP8
DNAJA2
BAG5
HSPA13
DNAJC9
CCPG1
SGTB
DNAJB2
DNAJC22
TOMM70A
TPR
STUB1
BAG4
HSPA14
HSPA12A
DNAJB12
DNAJC7
HSPA4L
DNAJC5
HSPA2
BAG3
DNAJC14
CHORDC1
DNAJA1
BAG1
DNAJC17
DNAJC5G
CRNKL1
PTGES3
FKBP5
HSPA4
HSCB
AHSA2
UNC45A
PPP5C
ST13
HSPA1A
STIP1
HSPA1L
DNAJA3
HSPA7
ITGB1BP2
AHSA1
HSP90AA1
HSPA8
DNAJB1
DNAJB6
DNAJB8
DNAJC15
FRAP1
DNAJC5B
HSPH1
DNAJB4
HSPA6
NUDC
PPID
DNAJB9
DNAJC19
FKBP4
HSP90AB1
HSPB1
HSPB8
FKBP1B
PPIL2
HSPB6
HSPB11
TP53INP1
CRYAA
PDIA5
MKKS
HSPD1
HSP90B1
PPIA
DNAJC3
HSPA9
DNAJC6
FKBP10
CRYAB
HSPB9
ODF1
HSPB7
FKBP3
HYOU1
P4HB
HSPE1
TRAP1
TCP1
HSPA5
HSPB3
DNAJB11
FKBP1A
FKBP2
ERP29
CCT3
CCT6B
HSPB2
DNAJC1
BBS10
PPIB
PDIA4
PDIA3
CCT2
PPIAL4
PPIC
PPIF
CCT8
BBS12
PDIA2
CCT7
PPIL4
PPIG
PPIE
TXNDC4
CCT4
DNAJC10
FKBP11
CCT6A
CCT5
PPIH
CLK1
S100A1
PDIA6
ERP27
TXNDC12
DNAJB7
Hsp70 chaperone sub-network
Hsp90 chaperone sub-network
Foldase sub-network
Small Hsp sub-network
Chaperonin sub-network
b
Heat induced
Tunicamycin induced
Heat and tunicamycin induced
Non-induced

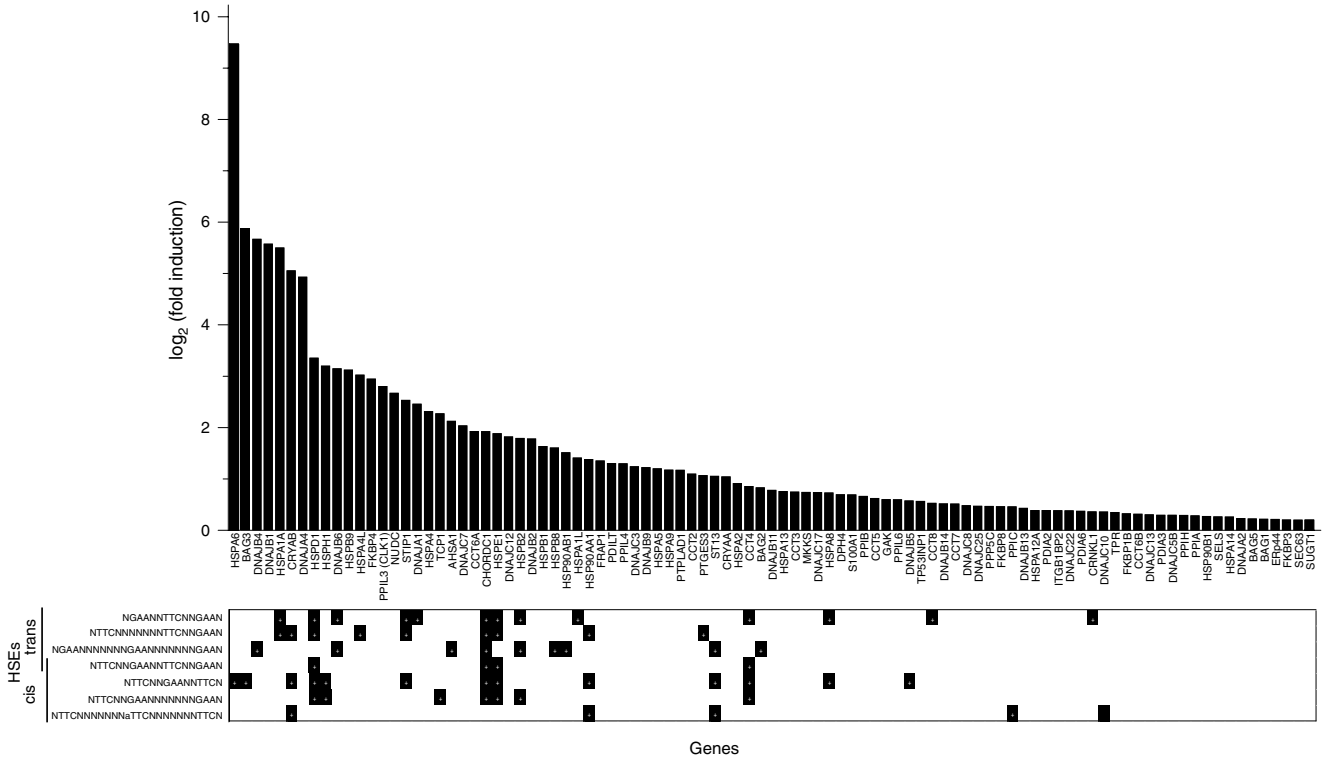

Fig. 6 Heat shock elements found in heat-induced human chaperome genes. Distribution of fold expression levels of heat-induced chaperone genes in human monocyte leukemia THP-1cells (*graph*) and the presence of specific HSEs between −3000 and 300 bp of the translation start site of each genes (*lower panel*). The microarray data for the human chaperome subset (Supplemental Table 1a) is as in Fig. 1a

dependent clearance signal from the plasma membrane, Hsp90 inhibitors cannot directly induce an isothermal HSR in plants, the plasma membrane also stands as a sensor of intra- and extracellular protein aggregates, activating the CSR chaperones to reduce aggregate toxicity (Saidi et al. 2009).

Analysis of the chaperone network under stress

Molecular chaperones with their co-chaperones form a dynamic network with hundreds of so-called client proteins (Picard 2006). During and after stress, a massive reallocation of the cellular resources occurs, which in turn causes dramatic rearrangements in the chaperone network (Szalay et al. 2007). Pallotai et al. (2008) showed that in the stressed interactome in yeast, novel *centralities* or important interactions in the network appeared, which in parallel increased the number of unlinked or isolated network elements or modules. As resources diminish during stress, the function of most protein networks becomes transiently arrested, whereas the few that remains active, such as the CSR chaperone network, become more active and abundant and take control on many of the cellular functions in a centralized and highly hierarchical manner (Szalay et al. 2007). Thus, in *Escherichia coli*, heat shock places the transcription factor σ^{32} as a central hub regulating other protein networks (El-Samad et al. 2005), while in yeast, refolding of damaged proteins by stress-induced chaperones is prioritized, compared to the folding of newly synthesized proteins indicating a massive rearrangement in the cellular protein networks (Albanese et al. 2006). Our comparative analysis of mRNA co-expression under various physical and chemical treatments revealed a modular organization of the chaperone networks, whereby the UPR, involving only a small set of ER chaperones, can be clearly distinguished from CSR chaperones, mainly located to the cytoplasm and organelles. This was confirmed using additional comparative criteria in the STRING-generated network map that showed that CSR chaperones contribute mostly to a core of Hsp70s, Hsp90s, and sHSPs, and to a much lesser extent to chaperone regulators such as the co-chaperones and to the foldases. Mechanistically, a massive increase in the cellular concentrations of Hsp90s and Hsp70s without an equivalent accumulation of co-chaperones is expected to create an imbalance resulting, at least in the case of Hsp70, in a higher binding/holdase capacity than processive unfolding/folding activity (Sharma et al. 2009). Such a pro-holdase tendency under heat shock is corroborated by our data (Fig. 5b), showing strong over-representation of heat-induced sHSPs, which are holdases par excellence of the whole chaperone network (Veinger et al. 1998). This suggests that the primary concern of heat-stressed cells is to prevent protein misfolding

and aggregation during stress, while ATP-consuming unfoldase/refoldase activities depending on co-chaperones are postponed to the recovery phase after the stress, a condition under which the proteins refolded by the chaperones can become and stably remain native.

Treatments that increase the cellular chaperone load

Aging and protein misfolding diseases apparently result from a general failure of the cellular protein homeostasis machinery, which is most relevantly composed of molecular chaperones, foldases, and proteases. Whereas environmental stresses, pollutants, and mutations may increase the rate at which toxic misfolded protein conformers accumulate in cells, aging cells show decreasing abilities to respond to proteotoxic species by upregulating their cellular chaperone load (Ben-Zvi et al. 2009; Hinault et al. 2006). To combat aging and protein misfolding diseases, it is therefore central to identify the reasons for the failure of the CSR in aging and diseased cells. One possible reason could be an increased rigidity of membranes commonly observed in aging cells, as lipid saturation and loss of fluidity may strongly decrease the cell's ability to sense a heat stress and induce an appropriate HSR (Horváth et al. 1998), implying that in old cells, the CSR too could become deficient when challenged by intra- or extracellular proteotoxic species (Vigh et al. 2007). An additional possibility is that particular toxic protein conformers, such as oligomers or protofibrils of α-synuclein, tau or polyglutamine proteins, respectively found in diseased neurons in Parkinson, Alzheimer, and Huntington diseases, act as non-competitive inhibitors of the various layers of cellular defenses, such as the chaperones themselves, the proteasome, the aggresome, and lysosomal autophagy (reviewed in Kopito 2000; Ross and Poirier 2004). Moreover, toxic protein conformers can directly damage membranes by spontaneously forming pores that cause ion leakage and cell death (Lashuel et al. 2002).

One therapeutic approach would be to identify treatments that can restore the expression levels and the activity of the CSR chaperones in particular. Mild repetitive heat-shocks, as with daily saunas, would probably be the most natural way to induce the accumulation of protective and repairing CSR chaperones in tissues suffering from stress damages or chronic protein misfolding diseases. However, arguing against long-term beneficial effects of thermotherapy (Pouppirt 1929), increased temperatures also increase the propensity of proteins to unfold and form toxic misfolded species. Rather, isothermal exposures to non-toxic HSP-inducing drugs might better treat protein misfolding diseases and aging, especially drugs that cross the blood–brain barrier (Hinault et al. 2006).

Alongside Hsp90 inhibitors that are very toxic and cause apoptosis through oxidative stress (Kirshner et al. 2008) and are therefore used in cancer therapy (Solit and Chiosis 2008), we found that the thiobenzoylhydrazide, elesclomol, best recapitulated in human cells the heat-induced chaperome pattern (Fig. 3). Thus, despite their ability to best mimic the induction of anti-inflammatory, anti-aggregation CSR chaperones load, Hsp90 inhibitors and elesclomol may counter-productively accelerate, rather than delay, neuronal death in protein misfold ing diseases.

In contrast, other hydroxylamines, such as arimoclomol and bimoclomol, are apparently much less toxic than elesclomol and are also inducers of CSR chaperones, although not nearly as effective (Vigh et al. 1997; Kieran et al. 2004; Lanka et al. 2009). Likewise, but less pronounced, several NSAIDs, such as aspirin, diclofenac, ibuprofen, and indomethacin, also upregulated the expression of some chaperone genes, albeit not in clearly recognizable clusters, as with elesclomol or tunicamycin. NSAIDs are known to decrease inflammation and fever via inhibitory mechanisms of prostaglandin synthesis, and, in parallel, they induce the accumulation of some CSR chaperones (Hinault et al. 2006; Smalley et al. 1995). It is thus possible that in mammals, specific NSAIDs may decrease the pro-apoptotic consequences of inflammation and oxidative stress while at the same time maintain an artificially elevated load of protective anti-apoptotic chaperones.

Possibly, the use of various NSAID combinations, together with other of CSR-chaperone-inducing drugs, such as hydroxylamine derivatives (Vigh et al. 1997), vanilloids, such as curcumin (Kanitkar and Bhonde 2008), flavonoids, such as quercetin (Aalinkeel et al. 2008), or omega-3-fatty acids (Narayanan et al. 2006), with anti-aging and anti-apoptotic effects on developing brain (Sinha et al. 2009), may improve protein misfolding diseases and aging in general (Gidalevitz et al. 2010). Combinations of non-toxic HSP drugs could directly decrease the cellular concentration of cytotoxic protein conformers and indirectly block neuroinflammation and apoptosis signals, leading to an arrest of tissue loss. This type of mRNA expression meta-analysis, combined with network analysis, thus provides important tools to test known and new drugs for their potential specific chaperone-inducing ability, to combat protein-misfolding diseases and aging.

Acknowledgments This research was financed in part by grant no. 3100A0-109290 from the Swiss National Science Foundation, the Alzheimer's Drug Discovery Foundation New York, and the Zwahlen Grant from the Faculty of Biology and Medicine from Lausanne University.

References

Aalinkeel R, Bindukumar B, Reynolds JL, Sykes DE, Mahajan SD, Chadha KC, Schwartz SA (2008) The dietary bioflavonoid, quercetin, selectively induces apoptosis of prostate cancer cells by down-regulating the expression of heat shock protein 90. Prostate 68(16):1773–1789. doi:10.1002/Pros.20845

Albanese V, Yam AYW, Baughman J, Parnot C, Frydman J (2006) Systems analyses reveal two chaperone networks with distinct functions in eukaryotic cells. Cell 124(1):75–88

Amin J, Ananthan J, Voellmy R (1988) Key features of heat-shock regulatory elements. Mol Cell Biol 8(9):3761–3769

Aparicio F, Thomas CL, Lederer C, Niu Y, Wang DW, Maule AJ (2005) Virus induction of heat shock protein 70 reflects a general response to protein accumulation in the plant cytosol. Plant Physiol 138(1):529–536. doi:10.1104/pp.104.058958

Azem A, Diamant S, Kessel M, Weiss C, Goloubinoff P (1995) The protein-folding activity of chaperonins correlates with the symmetric GroEL(14)(GroES(7))(2) heterooligomer. Proc Natl Acad Sci USA 92(26):12021–12025

Becker J, Craig EA (1994) Heat-shock proteins as molecular chaperones. Eur J Biochem 219(1–2):11–23

Ben-Zvi A, De los Rios P, Dietler G, Goloubinoff P (2004) Active solubilization and refolding of stable protein aggregates by cooperative unfolding action of individual Hsp70 chaperones. J Biol Chem 279(36):37298–37303. doi:10.1074/jbc.M405627200

Ben-Zvi A, Miller EA, Morimoto RI (2009) Collapse of proteostasis represents an early molecular event in *Caenorhabditis elegans* aging. Proc Natl Acad Sci USA 106(35):14914–14919. doi:10.1073/pnas.0902882106

Blatch GL, Lassle M (1999) The tetratricopeptide repeat: a structural motif mediating protein–protein interactions. Bioessays 21 (11):932–939

Booth CR, Meyer AS, Cong Y, Topf M, Sali A, Ludtke SJ, Chiu W, Frydman J (2008) Mechanism of lid closure in the eukaryotic chaperonin TRiC/CCT. Nat Struct Mol biol 15(7):746–753. doi:10.1038/Nsmb.1436

Calabrese V, Cornelius C, Mancuso C, Pennisi G, Calafato S, Bellia F, Bates TE, Stella AMG, Schapira T, Kostova ATD, Rizzarelli E (2008) Cellular stress response: a novel target for chemoprevention and nutritional neuroprotection in aging, neurodegenerative disorders and longevity. Neurochem Res 33(12):2444–2471. doi:10.1007/s11064-008-9775-9

Cintron NS, Toft D (2006) Defining the requirements for Hsp40 and Hsp70 in the Hsp90 chaperone pathway. J Biol Chem 281 (36):26235–26244. doi:10.1074/jbc.M605417200

Connell P, Ballinger CA, Jiang JH, Wu YX, Thompson LJ, Hohfeld J, Patterson C (2001) The co-chaperone CHIP regulates protein triage decisions mediated by heat-shock proteins. Nat Cell Biol 3 (1):93–96

Csermely P (2001) Chaperone overload is a possible contributor to 'civilization diseases'. Trends Genet 17(12):701–704

Csermely P, Korcsmáros T, Kovács IA, Szalay MS, Soti C (2008) Systems biology of molecular chaperone networks. In: Derek J, Chadwick JG (eds) The biology of extracellular molecular chaperones., pp 45–58

Daniels CJ, Mckee AHZ, Doolittle WF (1984) Archaebacterial heat-shock proteins. EMBO J 3(4):745–749

De los Rios P, Ben-Zvi A, Slutsky O, Azem A, Goloubinoff P (2006) Hsp70 chaperones accelerate protein translocation and the unfolding of stable protein aggregates by entropic pulling. Proc Natl Acad Sci USA 103(16):6166–6171. doi:10.1073/pnas.0510496103

de Marco A, Vigh L, Diamant S, Goloubinoff P (2005) Native folding of aggregation-prone recombinant proteins in Escherichia coli by osmolytes, plasmid- or benzyl alcohol-overexpressed molecular chaperones. Cell Stress Chaperones 10(4):329–339

Deuerling E, Schulze-Specking A, Tomoyasu T, Mogk A, Bukau B (1999) Trigger factor and DnaK cooperate in folding of newly synthesized proteins. Nature 400(6745):693–696

Diamant S, Ben-Zvi AP, Bukau B, Goloubinoff P (2000) Size-dependent disaggregation of stable protein aggregates by the DnaK chaperone machinery. J Biol Chem 275(28):21107–21113

Didelot C, Lanneau D, Brunet M, Joly AL, De Thonel A, Chiosis G, Garrido C (2007) Anti-cancer therapeutic approaches based on intracellular and extracellular heat shock proteins. Curr Med Chem 14(27):2839–2847

El-Samad H, Kurata H, Doyle JC, Gross CA, Khammash M (2005) Surviving heat shock: control strategies for robustness and performance. Proc Natl Acad Sci USA 102(8):2736–2741. doi:10.1073/pnas.0403510102

Ellis RJ, Vandervies SM, Hemmingsen SM (1989) The molecular chaperone concept. Biochem Soc Symp 55:145–153

Fonte V, Kipp DR, Yerg J, Merin D, Forrestal M, Wagner E, Roberts CM, Link CD (2008) Suppression of in vivo beta-amyloid peptide toxicity by overexpression of the HSP-16.2 small chaperone protein. J Biol Chem 283(2):784–791. doi:10.1074/jbc.M703339200

Garrido C, Brunet M, Didelot C, Zermati Y, Schmitt E, Kroemer G (2006) Heat shock proteins 27 and 70. Cell Cycle 5(22):2592–2601

Gidalevitz T, Kikis EA, Morimoto RI (2010) A cellular perspective on conformational disease: the role of genetic background and proteostasis networks. Curr Opin Struck Biol 20(1):23–32. doi:10.1016/j.sbi.2009.11.001

Glover JR, Lindquist S (1998) Hsp104, Hsp70, and Hsp40: a novel chaperone system that rescues previously aggregated proteins. Cell 94(1):73–82

Goloubinoff P, Christeller JT, Gatenby AA, Lorimer GH (1989) Reconstitution of active dimeric ribulose bisphosphate carboxylase from an unfolded state depends on 2 chaperonin proteins and Mg-ATP. Nature 342(6252):884–889

Goloubinoff P, Mogk A, Ben Zvi AP, Tomoyasu T, Bukau B (1999) Sequential mechanism of solubilization and refolding of stable protein aggregates by a bichaperone network. Proc Natl Acad Sci USA 96(24):13732–13737

Hageman J, Kampinga HH (2009) Computational analysis of the human HSPH/HSPA/DNAJ family and cloning of a human HSPH/HSPA/DNAJ expression library. Cell Stress Chaperones 14(1):1–21. doi:10.1007/s12192-008-0060-2

Hageman J, Vos MJ, van Waarde MAWH, Kampinga HH (2007) Comparison of intra-organellar chaperone capacity for dealing with stress-induced protein unfolding. J Biol Chem 282 (47):34334–34345. doi:10.1074/jbc.M703876200

Harrison C (2003) GrpE, a nucleotide exchange factor for DnaK. Cell Stress Chaperones 8(3):218–224

Hartl FU, Hayer-Hartl M (2009) Converging concepts of protein folding in vitro and in vivo. Nat Struct Mol biol 16(6):574–581. doi:10.1038/Nsmb.1591

Hasan CMM, Shimizu K (2008) Effect of temperature up-shift on fermentation and metabolic characteristics in view of gene expressions in *Escherichia coli*. Microb Cell Fact 7:35. doi:10.1186/1475-2859-7-35

Haslbeck M, Franzmann T, Weinfurtner D, Buchner J (2005) Some like it hot: the structure and function of small heat-shock proteins. Nat Struct Mol biol 12(10):842–846. doi:10.1038/Nsmb993

Hendrick JP, Hartl FU (1993) Molecular chaperone functions of heat-shock proteins. Annu Rev Biochem 62:349–384

Hightower LE (1980) Cultured animal-cells exposed to amino-acid-analogs or puromycin rapidly synthesize several polypeptides. J Cell Physiol 102(3):407–427

Hinault MP, Goloubinoff P (2007) Molecular crime and cellular punishment: active detoxification of misfolded and aggregated

proteins in the cell by the chaperone and protease networks. Adv Exp Mol Biol 594:47–54
Hinault MP, Ben-Zvi A, Goloubinoff P (2006) Chaperones and proteases—cellular fold-controlling factors of proteins in neurodegenerative diseases and aging. J Mol Neurosci 30(3):249–265. doi:10.1385/Jmn/30:03:249
Hooper SD, Bork P (2005) Medusa: a simple tool for interaction graph analysis. Bioinformatics 21(24):4432–4433. doi:10.1093/bioinformatics/bti696
Horváth I, Glatz A, Varvasovszki V, Török Z, Pali T, Balogh G, Kovacs E, Nadasdi L, Benko S, Joo F, Vígh L (1998) Membrane physical state controls the signaling mechanism of the heat shock response in Synechocystis PCC 6803: identification of hsp17 as a "fluidity gene". Proc Natl Acad Sci USA 95(7):3513–3518
Horvath I, Multhoff G, Sonnleitner A, Vigh L (2008) Membrane-associated stress proteins: more than simply chaperones. Biochim Biophys Act 1778(7–8):1653–1664. doi:10.1016/j.bbamem.2008.02.012
Jakob U, Gaestel M, Engel K, Buchner J (1993) Small heat-shock proteins are molecular chaperones. J Biol Chem 268(3):1517–1520
Jensen LJ, Kuhn M, Stark M, Chaffron S, Creevey C, Muller J, Doerks T, Julien P, Roth A, Simonovic M, Bork P, von Mering C (2009) STRING 8—a global view on proteins and their functional interactions in 630 organisms. Nucleic Acids Res 37: D412–D416. doi:10.1093/Nar/Gkn760
Jolly C, Morimoto RI (2000) Role of the heat shock response and molecular chaperones in oncogenesis and cell death. J Natl Cancer Inst 92(19):1564–1572
Kabani M, McLellan C, Raynes DA, Guerriero V, Brodsky JL (2002) HspBP1, a homologue of the yeast Fes1 and S1s1 proteins, is an Hsc70 nucleotide exchange factor. FEBS Lett 531(2):339–342. doi:S0014-5793(02)03570-6
Kabbage M, Dickman MB (2008) The BAG proteins: a ubiquitous family of chaperone regulators. Cell Mol Life Sci 65(9):1390–1402. doi:10.1007/s00018-008-7535-2
Kampinga HH, Hageman J, Vos MJ, Kubota H, Tanguay RM, Bruford EA, Cheetham ME, Chen B, Hightower LE (2009) Guidelines for the nomenclature of the human heat shock proteins. Cell Stress Chaperones 14(1):105–111. doi:10.1007/s12192-008-0068-7
Kanemura H, Kusumoto K, Miyake H, Tashiro S, Rokutan K, Shimada M (2009) Geranylgeranylacetone prevents acute liver damage after massive hepatectomy in rats through suppression of a CXC chemokine GRO1 and induction of heat shock proteins. J Gastrointest Surg 13(1):66–73. doi:10.1007/s11605-008-0604-x
Kanitkar M, Bhonde RR (2008) Curcumin treatment enhances islet recovery by induction of heat shock response proteins, Hsp70 and heme oxygenase-1, during cryopreservation. Life Sci 82(3–4):182–189. doi:10.1016/j.lfs.2007.10.026
Kieran D, Kalmar B, Dick JRT, Riddoch-Contreras J, Burnstock G, Greensmith L (2004) Treatment with arimoclomol, a coinducer of heat shock proteins, delays disease progression in ALS mice. Nat Med 10(4):402–405. doi:10.1038/Nm1021
Kimpel JA, Key JL (1985) Presence of heat-shock mRNAs in field grown soybeans. Plant Physiol 79(3):672–678
Kirshner JR, He SQ, Balasubramanyam V, Kepros J, Yang CY, Zhang M, Du ZJ, Barsoum J, Bertin J (2008) Elesclomol induces cancer cell apoptosis through oxidative stress. Mol Cancer Ther 7 (8):2319–2327. doi:10.1158/1535-7163.Mct-08-0298
Kitamura A, Kubota H, Pack CG, Matsumoto G, Hirayama S, Takahashi Y, Kimura H, Kinjo M, Morimoto RI, Nagata K (2006) Cytosolic chaperonin prevents polyglutamine toxicity with altering the aggregation state. Nat Cell Biol 8(10):1163–1224. doi:10.1038/Ncb1478
Kopito RR (2000) Aggresomes, inclusion bodies and protein aggregation. Trends Cell Biol 10(12):524–530
Kroeger PE, Morimoto RI (1994) Selection of new Hsf1 and Hsf2 DNA-binding sites reveals differences in trimer cooperativity. Mol Cell Biol 14(11):7592–7603
Kumar SV, Wigge PA (2010) H2A.Z-Containing nucleosomes mediate the thermosensory response in *Arabidopsis*. Cell 140 (1):136–147. doi:10.1016/j.cell.2009.11.006
Lanka V, Wieland S, Barber J, Cudkowicz M (2009) Arimoclomol: a potential therapy under development for ALS. Expert Opin Investig Drugs 18(12):1907–1918. doi:10.1517/13543780903357486
Large AT, Goldberg MD, Lund PA (2009) Chaperones and protein folding in the archaea. Biochem Soc Trans 37:46–51. doi:10.1042/Bst0370046
Lashuel HA, Hartley D, Petre BM, Walz T, Lansbury PT (2002) Neurodegenerative disease—amyloid pores from pathogenic mutations. Nature 418(6895):291
Laskey RA, Honda BM, Mills AD, Finch JT (1978) Nucleosomes are assembled by an acidic protein which binds histones and transfers them to DNA. Nature 275(5679):416–420
Liberek K, Georgopoulos C (1993) Autoregulation of the *Escherichia coli* heat-shock response by the Dnak and Dnaj heat-shock proteins. Proc Natl Acad Sci USA 90(23):11019–11023
Liberek K, Lewandowska A, Zietkiewicz S (2008) Chaperones in control of protein disaggregation. EMBO J 27(2):328–335. doi:10.1038/sj.emboj.7601970
Macario AJL, de Macario EC (1999) The archaeal molecular chaperone machine: peculiarities and paradoxes. Genetics 152(4):1277–1283
Mogk A, Tomoyasu T, Goloubinoff P, Rudiger S, Roder D, Langen H, Bukau B (1999) Identification of thermolabile *Escherichia coli* proteins: prevention and reversion of aggregation by DnaK and ClpB. EMBO J 18(24):6934–6949
Mogk A, Hasiberger T, Tessarz P, Bukau B (2008) Common and specific mechanisms of AAA plus proteins involved in protein quality control. Biochem Soc Trans 36:120–125. doi:10.1042/Bst0360120
Morimoto RI (2008) Proteotoxic stress and inducible chaperone networks in neurodegenerative disease and aging. Gen Dev 22 (11):1427–1438. doi:10.1101/Gad.1657108
Motohashi K, Watanabe Y, Yohda M, Yoshida M (1999) Heat-inactivated proteins are rescued by the DnaK.J-GrpE set and ClpB chaperones. Proc Natl Acad Sci USA 96(13):7184–7189
Nakamoto H, Vigh L (2007) The small heat shock proteins and their clients. Cell Mol Life Sci 64(3):294–306. doi:10.1007/s00018-006-6321-2
Narayanan NK, Narayanan BA, Bosland M, Condon MS, Nargi D (2006) Docosahexaenoic acid in combination with celecoxib modulates HSP70 and p53 proteins in prostate cancer cells. Int J Cancer 119(7):1586–1598. doi:10.1002/Ijc.22031
Nardai G, Csermely P, Soti C (2002) Chaperone function and chaperone overload in the aged. A preliminary analysis. Exp Gerontol 37(10–11):1257–1262. doi:S0531-5565(02)00134-1
Onuoha SC, Couistock ET, Grossmann JG, Jackson SE (2008) Structural studies on the co-chaperone hop and its complexes with Hsp90. J Mol Biol 379(4):732–744. doi:10.1016/j.jmb.2008.02.013
Palotai R, Szalay MS, Csermely P (2008) Chaperones as integrators of cellular networks: changes of cellular integrity in stress and diseases. IUBMB Life 60(1):10–18. doi:10.1002/Iub.8
Pelham HRB (1986) Speculations on the functions of the major heat-shock and glucose-regulated proteins. Cell 46(7):959–961
Perrin V, Regulier E, Abbas-Terki T, Hassig R, Brouillet E, Aebischer P, Luthi-Carter R, Deglon N (2007) Neuroprotection by Hsp104 and Hsp27 in lentiviral-based rat models of Huntington's disease. Mol Ther 15(5):903–911. doi:10.1038/mt.sj.6300141
Picard D (2006) Chaperoning steroid hormone action. Trends Endocrinol Metab 17(6):229–235. doi:10.1016/j.tem.2006.06.003
Pouppirt PS (1929) Treatment of Parkinson's syndrome with fever produced by baths: report of case. Cal West Med 31(3):192–195

Rodriguez F, Arsene-Ploetze F, Rist W, Rudiger S, Schneider-Mergener J, Mayer MP, Bukau B (2008) Molecular basis for regulation of the heat shock transcription factor sigma(32) by the DnaK and DnaJ chaperones. Mol Cell 32(3):347–358. doi:10.1016/j.molcel.2008.09.016

Ross CA, Poirier MA (2004) Protein aggregation and neurodegenerative disease. Nat Rev Neurosci 10(Suppl):S10–S17. doi:10.1038/Nm1066

Saidi Y, Finka A, Chakhporanian M, Zryd JP, Schaefer DG, Goloubinoff P (2005) Controlled expression of recombinant proteins in *Physcomitrella patens* by a conditional heat-shock promoter: a tool for plant research and biotechnology. Plant Mol Biol 59(5):697–711. doi:10.1007/s11103-005-0889-z

Saidi Y, Domini M, Choy F, Zryd JP, Schwitzguebel JP, Goloubinoff P (2007) Activation of the heat shock response in plants by chlorophenols: transgenic *Physcomitrella patens* as a sensitive biosensor for organic pollutants. Plant Cell Environ 30(6):753–763. doi:10.1111/j.1365-3040.2007.01664.x

Saidi Y, Finka A, Muriset M, Bromberg Z, Weiss YG, Maathuis FJM, Goloubinoff P (2009) The heat shock response in moss plants is regulated by specific calcium-permeable channels in the plasma membrane. Plant Cell 21(9):2829–2843. doi:10.1105/tpc.108.065318

Saldanha AJ (2004) Java Treeview—extensible visualization of microarray data. Bioinformatics 20(17):3246–3248. doi:10.1093/bioinformatics/bth349

Sanchez Y, Lindquist SL (1990) Hsp104 required for induced thermotolerance. Science 248(4959):1112–1115

Sato T, Minagawa S, Kojima E, Okamoto N, Nakamoto H (2010) HtpG, the prokaryotic homologue of Hsp90, stabilizes a phycobilisome protein in the cyanobacterium *Synechococcus elongatus* PCC 7942. Mol Microbiol 76(3):576–589. doi:10.1111/j.1365-2958.2010.07139.x

Schroder M, Kaufman RJ (2005) The mammalian unfolded protein response. Annu Rev Biochem 74:739–789. doi:10.1146/annurev.biochem.73.011303.074134

Schuermann JP, Jiang JW, Cuellar J, Llorca O, Wang LP, Gimenez LE, Jin SP, Taylor AB, Demeler B, Morano KA, Hart PJ, Valpuesta JM, Lafer EM, Sousa R (2008) Structure of the Hsp110: Hsc70 nucleotide exchange machine. Mol Cell 31(2):232–243. doi:10.1016/j.molcel.2008.05.006

Shaner L, Morano KA (2007) All in the family: atypical Hsp70 chaperones are conserved modulators of Hsp70 activity. Cell Stress Chaperones 12(1):1–8

Sharma SK, Christen P, Goloubinoff P (2009) Disaggregating chaperones: an unfolding story. Curr Prot Pept Sci 10:432–446

Shi LX, Theg SM (2010) A stromal heat shock protein 70 system functions in protein import into chloroplasts in the moss *Physcomitrella patens*. Plant Cell 22(1):205–220. doi:10.1105/tpc.109.071464

Shorter J, Lindquist S (2008) Hsp104, Hsp70 and Hsp40 interplay regulates formation, growth and elimination of Sup35 prions. EMBO J 27(20):2712–2724. doi:10.1038/emboj.2008.194

Shtilerman M, Lorimer GH, Englander SW (1999) Chaperonin function: folding by forced unfolding. Science 284(5415):822–825

Sinha RA, Khare P, Rai A, Maurya SK, Pathak A, Mohan V, Nagar GK, Mudiam MKR, Godbole MM, Bandyopadhyay S (2009) Anti-apoptotic role of omega-3-fatty acids in developing brain: perinatal hypothyroid rat cerebellum as apoptotic model. Int J Dev Neurosci 27(4):377–383. doi:10.1016/j.ijdevneu.2009.02.003

Smalley WE, Ray WA, Daugherty JR, Griffin MR (1995) Nonsteroidal antiinflammatory drugs and the incidence of hospitalizations for peptic-ulcer disease in elderly persons. Am J Epidemiol 141(6):539–545

Solit DB, Chiosis G (2008) Development and application of Hsp90 inhibitors. Drug Discov Today 13(1–2):38–43

Soll J (2002) Protein import into chloroplasts. Curr Opin Plant Biol 5 (6):529–535

Soti C, Pal C, Papp B, Csermely P (2005) Molecular chaperones as regulatory elements of cellular networks. Curr Opin Cell Biol 17 (2):210–215. doi:10.1016/j.ceb.2005.02.012

Szabadkai G, Bianchi K, Varnai P, De Stefani D, Wieckowski MR, Cavagna D, Nagy AI, Balla T, Rizzulo R (2006) Chaperone-mediated coupling of endoplasmic reticulum and mitochondrial Ca^{2+} channels. J Cell Biol 175(6):901–911

Szalay MS, Kovacs IA, Korcsmaros T, Bode C, Csermely P (2007) Stress-induced rearrangements of cellular networks: consequences for protection and drug design. FEBS Lett 581(19):3675–3680. doi:10.1016/j.1ebsiet.2007.03.083

Tarun AS, Peng X, Dumpit RF, Ogata Y, Silva-Rivera H, Camargo N, Daly TM, Bergman LW, Kappe SHI (2008) A combined transcriptome and proteome survey of malaria parasite liver stages. Proc Natl Acad Sci USA 105(1):305–310. doi:10.1073/pnas.0710780104

Tissieres A, Mitchell HK, Tracy UM (1974) Protein synthesis in salivary glands of *Drosophila melanogaster*—relation to chromosome puffs. J Mol Biol 84(3):389–398

Tomoyasu T, Mogk A, Langen H, Goloubinoff P, Bukau B (2001) Genetic dissection of the roles of chaperones and proteases in protein folding and degradation in the *Escherichia coli* cytosol. Mol Microbiol 40(2):397–413

van der Spuy J, Kana BD, Dirr HW, Blatch GL (2000) Heat shock cognate protein 70 chaperone-binding site in the co-chaperone murine stress-inducible protein 1 maps to within three consecutive tetratricopeptide repeat motifs. Biochem J 345:645–651

Veinger L, Diamant S, Buchner J, Goloubinoff P (1998) The small heat-shock protein IbpB from Escherichia coli stabilizes stress-denatured proteins for subsequent refolding by a multichaperone network. J Biol Chem 273(18):11032–11037

Vigh L, Literati PN, Horvath I, Torok Z, Balogh G, Glatz A, Kovacs E, Boros I, Ferdinandy P, Farkas B, Jaszlits L, Jednakovits A, Koranyi L, Maresca B (1997) Bimoclomol: a nontoxic, hydroxylamine derivative with stress protein-inducing activity and cytoprotective effects. Nat Med 3(10):1150–1154

Vigh L, Maresca B, Harwood JL (1998) Does the membrane's physical state control the expression of heat shock and other genes? Trends Biochem Sci 23(10):369–374

Vigh L, Horvath I, Maresca B, Harwood JL (2007) Can the stress protein response be controlled by 'membrane-lipid therapy'? Trends Biochem Sci 32(8):357–363. doi:10.1016/j.tibs.2007.06.009

Voellmy R, Boellmann F (2007) Chaperone regulation of the heat shock protein response. Adv Exp Mol Biol 594:89–99

Weiss YG, Bromberg Z, Raj N, Raphael J, Goloubinoff P, Ben-Neriah Y, Deutschman CS (2007) Enhanced heat shock protein 70 expression alters proteasomal degradation of I kappa B kinase in experimental acute respiratory distress syndrome. Crit Care Med 35(9):2128–2138. doi:10.1097/01.Ccm.0000278915.78030.74

Whelan SA, Hightower LE (1985) Induction of stress proteins in chicken-embryo cells by low-level zinc contamination in amino acid-free media. J Cell Physiol 122(2):205–209

Whitesell L, Lindquist SL (2005) HSP90 and the chaperoning of cancer. Nat Rev Cancer 5(10):761–772

Whitesell L, Mimnaugh EG, Decosta B, Myers CE, Neckers LM (1994) Inhibition of heat-shock protein Hsp90-Pp60(V-Src) heteroprotein complex-formation by benzoquinone ansamycins—essential role for stress proteins in oncogenic transformation. Proc Natl Acad Sci USA 91(18):8324–8328

Wickner RB (1994) [Ure3] as an altered Ure2 protein—evidence for a prion analog in *Saccharomyces cerevisiae*. Science 264 (5158):566–569

Wiech H, Buchner J, Zimmermann R, Jakob U (1992) Hsp90 chaperones protein folding in vitro. Nature 358(6382):169–170

Wu YJ, Cao ZM, Klein WL, Luo Y (2010) Heat shock treatment reduces beta amyloid toxicity in vivo by diminishing oligomers. Neurobiol Aging 31(6):1055–1058. doi:10.1016/j.neurobiolaging.2008.07.013

Xing HY, Wilkerson DC, Mayhew CN, Lubert EJ, Skaggs HS, Goodson ML, Hong YL, Park-Sarge OK, Sarge KD (2005) Mechanism of Hsp70i gene bookmarking. Science 307 (5708):421–423. doi:10.1126/science.1106478

Yamamoto N, Takemori Y, Sakurai M, Sugiyama K, Sakurai H (2009) Differential recognition of heat shock elements by members of the heat shock transcription factor family. FEBS J 276(7):1962–1974. doi:10.1111/j.1742-4658.2009.06923.x

Yao J, Munson KM, Webb WW, Lis JT (2006) Dynamics of heat shock factor association with native gene loci in living cells. Nature 442(7106):1050–1053. doi:10.1038/Nature05025

Zhao RM, Davey M, Hsu YC, Kaplanek P, Tong A, Parsons AB, Krogan N, Cagney G, Mai D, Greenblatt J, Boone C, Emili A, Houry WA (2005) Navigating the chaperone network: an integrative map of physical and genetic interactions mediated by the Hsp90 chaperone. Cell 120(5):715–727. doi:10.1016/j.cell.2004.12.024

Zimmermann P, Hirsch-Hoffmann M, Hennig L, Gruissem W (2004) GENEVESTIGATOR. *Arabidopsis* microarray database and analysis toolbox. Plant Physiol 136(1):2621–2632. doi:10.1104/pp.104.046367

Zimmermann R, Eyrisch S, Ahmad M, Helms V (2010) Protein translocation across the ER membrane. Biochim Biophys Acta. doi:10.1016/j.bbamem.2010.06.015

Zourlidou A, Smith MDP, Latchman DS (2004) HSP27 but not HSP70 has a potent protective effect against alpha-synuclein-induced cell death in mammalian neuronal cells. J Neurochem 88 (6):1439–1448. doi:10.1046/j.1471-4159.2003.02273.x

CHAPTER 7

Conclusion of the thesis: A review

Molecular chaperones are nano-machines that catalytically unfold misfolded and alter-natively folded proteins

Molecular chaperones are nano-machines that catalytically unfold misfolded and alter-natively folded proteins.

Mattoo, R.U. and Goloubinoff, P.

I contributed to this work conceptually and in the writing of the manuscript. I provided the data for Fig 1, Fig 2 and Table 1.

Cell. Mol. Life Sci.
DOI 10.1007/s00018-014-1627-y

Cellular and Molecular Life Sciences

REVIEW

Molecular chaperones are nanomachines that catalytically unfold misfolded and alternatively folded proteins

Rayees U. H. Mattoo · Pierre Goloubinoff

Received: 19 December 2013 / Revised: 4 April 2014 / Accepted: 7 April 2014

Abstract By virtue of their general ability to bind (hold) translocating or unfolding polypeptides otherwise doomed to aggregate, molecular chaperones are commonly dubbed "holdases". Yet, chaperones also carry physiological functions that do not necessitate prevention of aggregation, such as altering the native states of proteins, as in the disassembly of SNARE complexes and clathrin coats. To carry such physiological functions, major members of the Hsp70, Hsp110, Hsp100, and Hsp60/CCT chaperone families act as catalytic unfolding enzymes or unfoldases that drive iterative cycles of protein binding, unfolding/pulling, and release. One unfoldase chaperone may thus successively convert many misfolded or alternatively folded polypeptide substrates into transiently unfolded intermediates, which, once released, can spontaneously refold into low-affinity native products. Whereas during stress, a large excess of non-catalytic chaperones in holding mode may optimally prevent protein aggregation, after the stress, catalytic disaggregases and unfoldases may act as nanomachines that use the energy of ATP hydrolysis to repair proteins with compromised conformations. Thus, holding and catalytic unfolding chaperones can act as primary cellular defenses against the formation of early misfolded and aggregated proteotoxic conformers in order to avert or retard the onset of degenerative protein conformational diseases.

Keywords Hsp70 · Hsp110 · Hsp40 · GroEL · Disaggregase · Polypeptide unfoldase · Holdase · Translocase

R. U. H. Mattoo · P. Goloubinoff (✉)
Department of Plant Molecular Biology, Faculty of Biology and Medicine, University of Lausanne, Biophore Building, 1015 Lausanne, Switzerland
e-mail: pierre.goloubinoff@unil.ch

Introduction

Anfinsen demonstrated that under optimal non-physiological conditions of low protein concentrations and low temperatures, the primary amino acid sequence of a polypeptide contains the necessary instructions for its spontaneous acquisition of a narrow range of relatively stable but dynamic functional structures, generally referred to as the "native state" [1]. Yet, the refolding process is often inefficient because hydrophobic residues that in stress-unfolded or de novo-synthesized polypeptides become abnormally exposed to the aqueous phase, may spontaneously seek intra-molecular stability by forming wrong beta sheets and improper inter-molecular ensembles generally called aggregates. Because of cooperativity, a simple increase in the number of surface-exposed hydrophobic residues may result in a synergic increase of the affinity between several misfolded polypeptides. Thus, aggregate-entrapped polypeptides may become precluded from dissociating and reaching their native state within a biologically relevant time-scale [2, 3]. Moreover, aggregates may be cytotoxic, especially to animal cells, and cause aging-induced degenerative disorders, such as Parkinson's, Huntington's and Alzheimer's diseases [4]. In youth, however, a cellular network composed of molecular chaperones and of chaperone-controlled proteases can efficiently counteract toxic protein aggregation by a mechanism generally termed as "holdase", corresponding to the non-catalytic tight binding of aggregation-prone misfolding intermediates to the chaperone surface. For a general review on the main chaperone families, their structures, and their anti-aggregation activities, see [5]. Here, we focus on chaperones that seem to function as catalytic unfolding enzymes and are of importance in combating early proteotoxic intermediates in protein conformational diseases.

Published online: 24 April 2014

Several independent studies have reported unfolding of misfolded polypeptides by chaperonins and Hsp70 chaperones [6–11]. Recently, members of conserved chaperone families Hsp70, Hsp110, and Hsp60/CCT have been shown to drive catalytic polypeptide unfolding activity, where sub-stoichiometric quantities of chaperones could process a molar excess of high-affinity misfolded substrates into low-affinity native products [12, 13]. A clear understanding of the passive "holding" and the catalytic unfolding mechanisms by which some chaperones can oppose the formation of toxic protein conformers, and others actively revert already-formed toxic aggregated conformers into harmless native or degraded polypeptides, is central to the design of new therapeutic solutions to protein conformational diseases. Here, we review the different molecular functions of chaperones and critically discuss the adequacy of the terms that are used in the literature to describe them.

The role of chaperones in protein misfolding diseases

Under physiological conditions, molecular chaperones and proteases control house-keeping processes of cellular proteostasis, such as assisting the proper de novo folding of polypeptides exiting the ribosome, or of cytoplasmic proteins exiting the import pores in the *endoplasmic reticulum* lumen or the mitochondrial matrix. Molecular chaperones also activate or inhibit various signaling pathways [14–16]. For example, Hsc70 regulates SNARE complexes [17, 18]. After exocytosis, when the *cis*-SNARE complex is stuck on the target membrane, the AAA+ ATPase *N*-ethylmaleimide sensitive factor disassembles it and after disassembly, Hsc70 together with cysteine-string protein-alpha and small guanine-rich tetratricopeptide protein, are then required for the refolding of the SNARE SNAP-25, converting it into an active form [19]. Chaperones can also disassemble native complexes such as clathrin cages [20] and they may target short-lived or stress-damaged proteins to proteasomal or lysosomal degradation and reorient mutant proteins prone to aggregation back on track of the native pathway, to undergo functional folding and assembly [4].

The expression of molecular chaperones is markedly increased under different environmental stress conditions, for example following hyperthermia or heat shock, hypoxia, oxidative stress, or exposure to toxins [5, 21–23]. The stress response is thought to be activated by the accumulation of unfolded or misfolded proteins, eliciting chaperone expression by turning on a signaling pathway that engages the transcription factor heat shock factor 1 (HSF-1) [22–25]. Under stress, such as heat shock, all organisms massively synthesize heat-shock proteins (HSPs), many, but not all, belonging to the molecular chaperone category. Compared to average human genes, members of the human "chaperome" network [26] are 20 times more likely to be stress-inducible [21]. Yet, noticeably, two-thirds of the human chaperome is constitutively expressed without stress and constitutes up to 10 % of the total protein mass of HeLa cells [27]. In young animals, molecular chaperones can effectively retard the formation of cytotoxic protein aggregates such as fibrils, tangles, and amyloids, which are hallmarks of degenerative diseases, such as Alzheimer's, Parkinson's, Huntington's, diabetes type 2, and Prion diseases.

The involvement of molecular chaperones in neurodegenerative diseases can be exemplified with the particular case of Parkinson's disease (PD). Indeed, Hsp90, Hsp70, Hsp60, Hsp40, and Hsp27 were found in Lewy bodies and Hsp70 in particular was inferred to be an important chaperone to mitigate α-synuclein toxicity [28–31]. Further, exposure of cells and whole mice to toxins like rotenone or 1-methyl-4-phenyl-1,2,3,6-tetrahydropyridine, or to the proteasome inhibitor lactacystin, showed a marked increase in chaperone levels, particularly of Hsp70 [32, 33]. Likewise, targeted overexpression of α-synuclein using viral-vector in the *substantia nigra* of mice resulted in increased mRNA levels of Hsp70, Hsp40 and Hsp27 [34]. Moreover, the sequestration of molecular chaperones into protein aggregates results in their cellular depletion and thus a subsequent loss of chaperone function that may promote neurodegeneration [35]. Consistently, in vitro, α-synuclein oligomers caused the depletion of Hsp40 (DnaJ) rendering the Hsp70 machinery (DnaK–DnaJ–GrpE) inefficient at unfolding/refolding misfolded proteins [36]. A systematic study of the interaction of several small Hsps (αB-crystallin, Hsp27, Hsp20, HspB8, and HspB2B3) showed that transient binding to the various forms of α-synuclein resulted in the inhibition of mature α-synuclein fibril formation [37]. Further, in vitro experiments showed that the small HSP, αB-crystallin (HspB5) can mediate the depolymerization of α-synuclein fibers with the help of other chaperones, including Hsp70 and its co-chaperones [38]. Moreover, in an in vitro system, mammalian Hsp110 can synergize Hsp70 to drive the catalytic disaggregation of α-synuclein amyloid fibrils [39]. All these studies show a close linkage between cellular stress, toxic protein misfolding, and chaperone induction, suggesting that protein misfolding diseases could result from chaperone failure and that the artificial increase of the cellular chaperone load by ectopic expression or drugs mimicking various stresses could combat protein misfolding diseases [4].

Noticeably, under mildly stressful conditions, protein aggregates in the cell and in vitro can serve as nucleating seeds to the aggregation of other metastable proteins that would otherwise spontaneously revert to the native state [40, 41]. Chaperones are thus key factors to neutralize the aggregation seeds, thereby disallowing a prion-like

propagation-of-aggregation effect even among regular labile proteins [4, 40]. Hence, small amounts of arsenite-, lead-, or cadmium-induced protein aggregates can serve as seeds that commit other labile proteins in excess to misfold and aggregate even after all traces of heavy metals have been removed from the seeds. Fortunately, this seeding process can be effectively counteracted by "holding" and unfolding chaperones such as Hsp70 and CCTs [42, 43].

The various chaperone activities

Whereas many but not all chaperones can passively bind misfolding proteins and thus arrest further aggregation into insoluble, potentially cytotoxic species, chaperone activity goes much beyond mere passive stoichiometric binding of metastable polypeptide species. Because binding or tight holding are not catalytic processes, the term "holdase" that is often used in the chaperone literature should be avoided. Moreover, many molecular chaperones function under physiological conditions as regulators of native protein folding, translocation, and assembly that do not call for their ability to prevent aggregation. Significantly, at least three out of five main chaperone families can act as bona fide polypeptide unfoldase enzymes.

In unstressed cells, molecular chaperones play a central role in protein homeostasis and regulate structural transitions between native and "alternative" states of proteins, such as between the oligomeric active versus the monomeric inactive states of native IκB, caspases or HSF-1 [44–47], or between inactive and active steroid hormone receptors [48–50]. In stressed cells, molecular chaperones become a primary line of cellular defenses against stress-induced protein misfolding and aggregation events [51] that otherwise become increasingly toxic by compromising the stability of other proteins and the integrity of membranes [52]. In aging mammalian neurons, toxic protein aggregates generally cause neuro-inflammation, oxidative stress, apoptosis, and tissue loss, leading to neurodegeneration and diseases.

Most molecular chaperones fall into five main families of highly conserved proteins: the Hsp100s (ClpB), the Hsp90s (HtpG), the Hsp70/Hsp110 (DnaK), Hsp60/CCTs (GroEL), and the α-crystalline-containing domain generally called the "small Hsps" (IbpA/B) (*Escherichia coli* orthologues shown in parentheses). Apparently, all families share the ability to screen for proteins with hydrophobic residues that are abnormally exposed to the solvent, and are thus prone to associate and form stable inactive aggregates [3, 4, 53]. With the exception of the small Hsps, the major classes of molecular chaperones are also ATPases, suggesting that their function can implicate an ATP-driven increase of the free energy in their bound misfolded or alternatively folded polypeptide substrates [54].

Chaperones with holdase activity

The first in vitro chaperone assay showed that the *E. coli* Hsp60, GroEL, could passively prevent the aggregation of a urea-, acid- or Guanidium HCl-denatured RuBisCO substrate. Importantly, in addition to the GroEL ability to "hold" the inactive RuBisCO in a soluble inactive state, the addition of GroES and ATP subsequently released the substrate from the holding GroEL, which then refolded into native active RuBisCO [55]. Yet, rather than referring to this remarkable ability of chaperones to drive the stringent native refolding of unfolded proteins, which would have otherwise remained inactive and aggregated, most subsequent papers chose to adopt the definition of chaperone activity as being the ability to prevent aggregation of heat- or Guanidium HCl-denatured proteins. In addition to chaperonin, many but not all chaperone families, including Hsp40, Hsp90, CCTs, and sHsps but not Hsp104 (ClpB), were shown to effectively prevent the aggregation of proteins in the absence of ATP [5, 56]. The term "holdase" thus was dubbed to describe the physical tight interaction of a chaperone with a non-native unfolded or misfolded polypeptide, which thus became prevented from forming larger aggregates that scatter light [4]. The "holdase" activity could be qualitatively observed with a previously unfolded polypeptide set to aggregate in a fluorometer cuvette: the presence of a given amount of chaperone caused the lowering and slowing down of the time-dependent increase in the light scattering signal [57]. However, the "holdase" activity of chaperones remained mostly a mere qualitative observation, since light-scattering assays suffer from low sensitivity and signals lack a direct connection with the size distribution of the aggregates.

A further depreciation of the concept that chaperones are "holdases", is the fact that the Hsp100/ClpB chaperones are unable to passively prevent the aggregation of unfolding or unfolded polypeptides, but rather act as very effective disaggregase chaperones, which together with HSP70, use ATP to forcefully solubilize already preformed, stable protein aggregates [58]. Although not all chaperones have a "holdase" activity, there is a general agreement to describe the activity, at least of the small-HSPs, as such, possibly because the α-crystallin domain-containing small heat shock protein (sHSPs) are devoid of ATPase activity of their own. Thus, under stress conditions, small-Hsps like Hsp25 or IbpB can bind very tightly to non-native unfolding or unfolded proteins and maintain them in an inactive non-aggregated state, which may be subsequently fed to an ATP-dependent unfoldase chaperone machinery such as

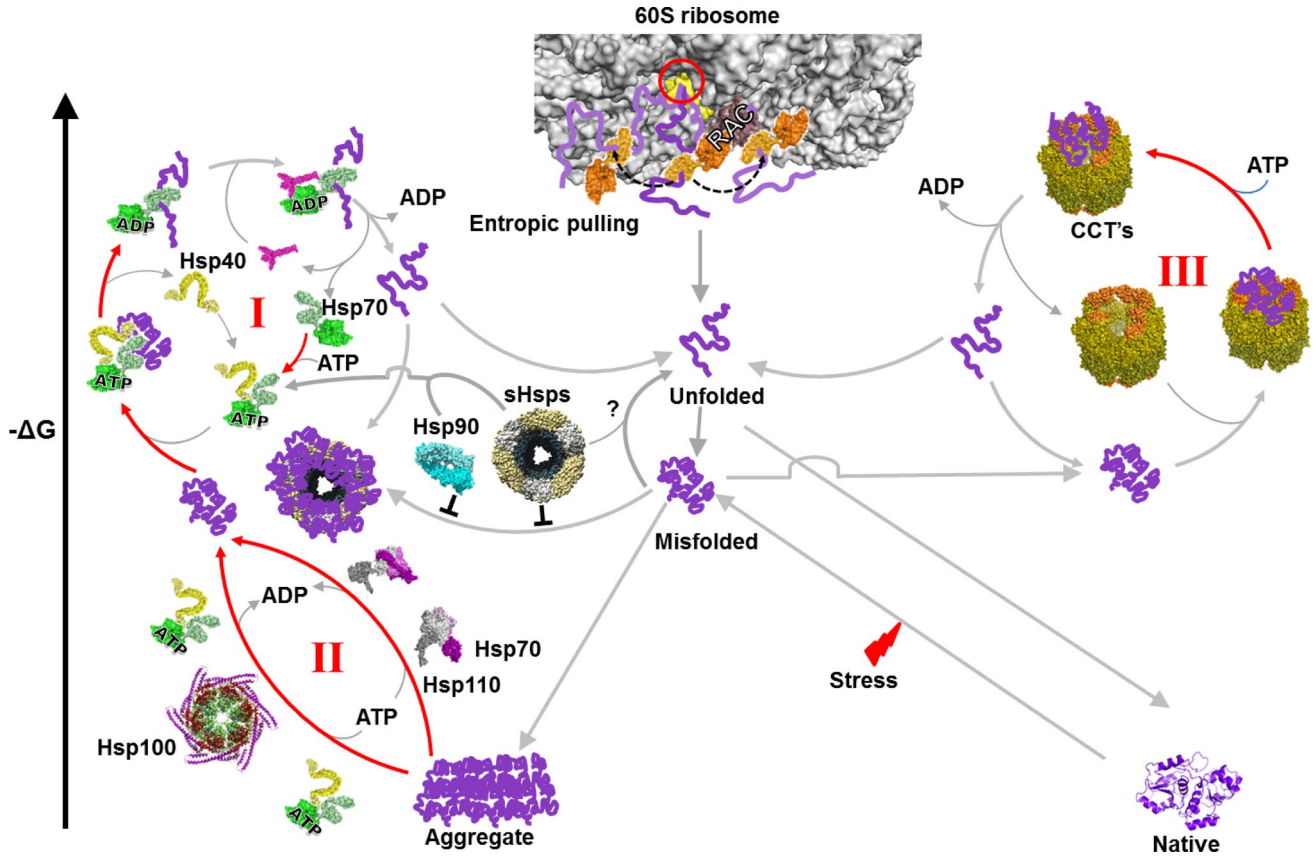

Fig. 1 Folding of nascent and misfolded polypeptides by the cytosolic chaperone network. A newly synthesized polypeptide emerging from the eukaryotic ribosome (PDB:3O2Z) tunnel (*red circle*) encounters in a typical eukaryotic cell such as yeast, ribosome-associated chaperones that can apply an entropic pulling force to unfold misfolded secondary structures in the growing nascent polypeptide chain. Upon exposure of the nascent polypeptide to the crowded environment of cytosol it may expose hydrophobic residues leading to misfolding. The misfolded conformers may then become a substrate of Hsp70 (PDB:1KHO) system (Hsp70–Hsp40 and nucleotide exchange factor, PDB:1DKG), which by reiterative cycles of binding, ATP-fueled unfolding and spontaneous refolding, converts the misfolded polypeptide into a native protein (cycle I). In case of failure, the misfolded substrate can bind instead to holding chaperones such as Hsp90 or sHsps that may keep the substrate in a non-aggregated, folding competent state, which may be subsequently passed on to the unfolding machinery of Hsp70 system for refolding to the native state. Possible unfolding of misfolded substrate by sHsps, structure adapted from [157], is unclear and is shown as a *question mark*. The aggregated protein in the cytosol of metazoans can be reverted to the native state by the Hsp110–Hsp70 system (PDB:3C7N) and also by the Hsp100s (structure adapted from [158]) and Hsp70 system in yeasts and plants (cycle II). In case of failure, the misfolded polypeptide can bind instead the CCT chaperonin (PDB:4A13), where it will undergo cycles of binding, unfolding, and ATP-fueled release, leading to the native state (cycle III). The structures are from highly homologous chaperone orthologs from various organisms, because they are not all available from yeast

Hsp70–Hsp40, to become reactivated after the stress (Fig. 1) [59–61]. Several in vitro studies using purified sHsps from various organisms have demonstrated that sHsps can effectively prevent the thermal aggregation of other proteins in an ATP-independent manner. They describe "holding" by sHsps as a single step, which is nearly irreversible in biological timescales, rather than a dynamic binding/release process [62–65]. Whereas small Hsps (sHsps) do not generally drive dissociation at a useful rate and are energy independent, other chaperones can bind (and unfold) already-formed stable misfolded proteins, as in the case GroEL and CCT, which need energy to drive dissociation at a useful rate. Yet, other chaperones bind and disaggregate already-formed large insoluble stable protein aggregates, as in the case of Hsp110–Hsp70 and Hsp100–Hsp70 bichaperone machineries [58, 66]. It should be noticed that because all enzymes need to bind their substrate, it is futile to mention protein binding as a particular property of the chaperones. Even when non-enzymatic polypeptides bind other macromolecules, as with histones binding DNA, this does not qualify them to be named DNA *bindases* or *holdases*. In another example, glucose-6-phosphate dehydrogenase (G6PDH) binds glucose-6-phosphate (G6P) and NADP with high affinity and converts them into 6-phosphoglucono-lactone and NADPH + H [67]. It would be misleading and poorly informative to name G6PDH "G6P holdase". Thus, it would

seem inappropriate to assign a holdase activity to chaperones that drive the forceful unfolding and translocation of polypeptides across membranes [20]. Polypeptide *translocases*, *unfoldases*, and/or even *pullases* would better fit the definition of their function.

In order to label a given protein as an enzyme, it should carry basic properties common to all enzymes. Like all catalysts, it should act by way of lowering the energy of activation of a spontaneous reaction and thus increase the rate at which equilibrium is reached and it should not remain stably associated to its products. It should not be consumed by the reactions, nor should it alter the equilibrium of the catalyzed reaction. The International Union of Biochemistry and Molecular Biology (IUBMB) has formulated several principles to name new enzymes. First, the name should end with suffix "-ase", implying that it has a catalytic mode of action, driving iterative cycles of substrate binding, substrate conversion into product, and product release. The use of the suffix "-ase" is strongly discouraged for non-enzyme molecules. Second, efforts should be made to classify new enzymes among the six existing classes of the *Oxidoreductases*, *Transferases*, *Hydrolases*, *Lyases*, *Isomerases*, and *Ligases*. Third, enzymes should be named according to the main reaction they catalyze (Enzyme Nomenclature 1992, Academic Press, San Diego, California, ISBN 0-12-227164-5).

The term "*holdase*" is thus an oxymoron: Either a chaperone is an enzyme deserving the suffix "-ase", in which case it should act as a catalyst, i.e., it should also be able to carry many cycles and in particular to *release* its products within a biologically relevant time-scale at the end of every cycle, or it should not harbor the suffix "-ase" and rather be called "holding" chaperones. Noticeably, even the small HSPs for the activity of which, the term "*holdases*" is most often used, can also accelerate the native refolding of artificially unfolded proteins, raising the possibility that small HSPs might also act as polypeptide foldases [68].

Chaperones with catalytic polypeptide unfoldase activity

Molecular chaperones such as Hsp70, Hsp110, Hsp100, or Hsp60s can use ATP to unfold stable misfolded or aggregated proteins and convert them into natively refoldable species [6, 13, 66]. Hsp70, in collaboration with co-chaperones Hsp40 and nucleotide exchange factor (NEF), function as an efficient unfolding or disaggregation machinery [69–71]. The bacterial Hsp70 system that includes DnaK (Hsp70), DnaJ (Hsp40), and GrpE (NEF), can work at V_{max} in multiple turnovers, converting a molar excess of stable inactive misfolded protein species into the active native state, in a strict ATP-dependent manner [13]. This conversion by

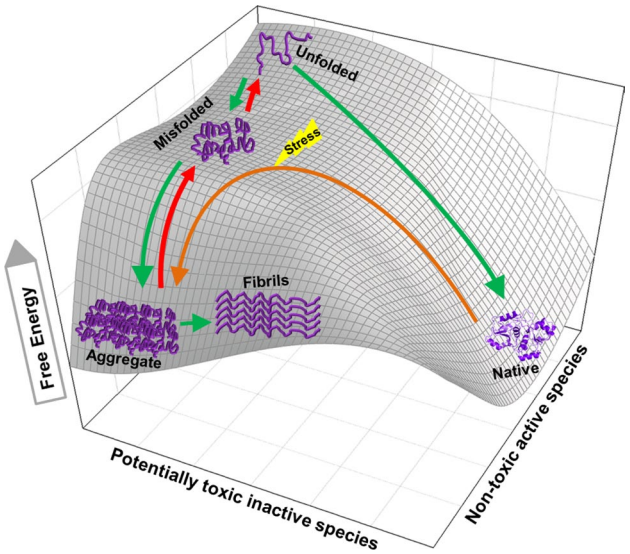

Fig. 2 Disaggregating and unfolding chaperones transiently increase the free energy of misfolded or alternatively folded substrates but not of natively folded products. The 3D mesh-plot shows a typical unfolded polypeptide with the highest free energy, which can spontaneously reach to lower free energy states, either by folding to the native conformation (*right*) or by misfolding to the aggregated state (*left*). When conditions are not favorable for native folding, the unfolded polypeptide may prefer undertaking the misfolding pathway to aggregation (*green arrows*). Native proteins under stress gaining free energy may partially unfold to a state from which it can readily seek a more stable misfolded state [3] and further aggregate (*brown arrow*) [2]. ATP-fueled unfoldase chaperones drive the substrate uphill the free energy barrier (*red arrows*) by converting stable aggregates and misfolded species into unfolded products with a higher free energy. From there, if conditions are favorable to the end product, the unfolded species can collapse to the stable native state

Hsp70s of stable misfolded polypeptides into the native species is accomplished by working against a free energy barrier, converting a stable misfolded protein with a low free energy into a transiently unfolded species with a higher free energy, which, after release may spontaneously fold to a native species with a lower free energy (Fig. 2). Demonstrating that unfolding of stable misfolded species is highly conserved in evolution, a similar unfolding mechanism leading to spontaneous native refolding was shown in the case of human Hsp70 (and Hsp40) and its ortholog Hsp110 (with Hsp40), which was indistinguishable from that of bacterial DnaK, except that is was energetically much more expensive [66] and also that NEF activity was not involved, as this was the case in the bacterial system [13]. Likewise, a similar unfolding mechanism leading to spontaneous native refolding was shown in the case of bovine CCT, which was indistinguishable from that of bacterial GroEL [12]. Indeed, the mere binding of a stable misfolded fluorescently labeled rhodanese was shown by fluorescent spectroscopy to cause significant unfolding in the substrate, which was exacerbated further upon ATP addition [6].

The catalytic unfolding of stable misfolded polypeptides by Hsp70s and Hsp60s, like other enzymatic reactions, starts with the misfolded polypeptide acting as a high-affinity substrate, the unfolded species as an unstable intermediate of the reaction with a yet higher affinity for the catalytic site of the enzyme, and the natively refolding/refolded protein as the low-affinity product of the reaction. Owing to their demonstrated abilities to convert a stoichiometric excess of misfolded polypeptide substrates through successive cycles of binding, unfolding, release, and native refolding, Hsp70/Hsp110s and Hsp60/CCTs have thus earned the qualification of bona fide polypeptide unfoldases [13, 66].

The mechanism by which Hsp70 can use ATP hydrolysis to pull and unfold polypeptide segments in stably misfolded and aggregated proteins, or pull and unfold alternative proteins across the membranes, involves a possible direct unfolding effect on the bulky substrate, possibly by the clamping of the lid of the chaperone protein binding domain towards its base [72, 73], as well as by a subsequent more global cooperative entropic pulling action [74] between the Hsp70 molecule and the import pore or between several Hsp70s concomitantly bound at different places on the same misfolded polypeptide [20]. In vitro, the ATPase chaperonins GroEL (organized in two homo-heptameric rings) and CCT (organized in two hetero-octameric rings) that consequently show multiple substrate binding sites, can mediate several consecutive cycles of binding-unfolding-release-refolding [12, 75, 76]. ATP is mostly used to fuel the forceful eviction of high-affinity over-sticky intermediates that following several cycles may start to accumulate on catalytic unfoldase sites and act as competitive inhibitors of the catalytic unfoldase reaction [12]. Other chaperones, such as the small HSPs, which are not ATPases, could also act as polypeptide unfoldases, provided an eviction mechanism of the over-sticky intermediates exists. In the case of the small HSPs, the Hsp70 chaperone system has been shown to carry such a regenerative function for over-sticky misfolded protein substrates associated to sHSPs [61]. Recently, bacterial and mammalian Hsp90 has been shown to carry an ATP-dependent activity leading, in collaboration with the Hsp70 chaperone system, to the refolding of some misfolded polypeptides such as luciferase and of native proteins, such as p53 (Fig. 1) [77–79].

Noticeably, depending on the conditions, catalytic unfoldases can reversibly switch into "holding" chaperones. Under heat stress, heat-labile proteins such as firefly luciferase or malate dehydrogenase tend to spontaneously convert into stable inactive aggregates [80, 81]. Under such unfavorable unstable conditions for the native product of the reaction, an active polypeptide unfoldase in the cell could result in the deleterious acceleration of protein misfolding and aggregation [80]. Thus, whereas at 25 °C, equimolar GroEL and GroES can optimally catalyze the in vitro release and the native refolding of a pre-bound inactive malate dehydrogenase, at 43 °C, the affinity of GroES for GroEL is reversely decreased with the consequence that as long as the denaturing elevated temperature is maintained, GroEL binds (but does not release) the misfolded MDH substrate, despite the presence of equimolar GroES and ATP in the solution. Thus, the GroEL-bound MDH is prevented from aggregating until the temperature is decreased and GroES rebinding can resume, inducing substrate release and native refolding [82]. Similarly, the chaperone activity of bacterial DnaK–DnaJ–GrpE can be reversibly arrested at elevated temperatures due to the reversible decrease of the substrate-release factor GrpE at high temperature [82, 83].

Given that various molecular chaperones are expected to arrest their catalytic polypeptide unfoldase activity under stress and thus become transiently passive "holding" chaperone that merely prevent aggregation, they may need to be present at much higher cellular concentrations than if they were only catalytic unfoldases. This could account for the observed very high cellular concentrations of core members of the chaperome network, which can reach up to 10 % of the total to protein mass [27]. Noticeably, an abundant chaperone is not evidence of its inefficiency as an unfolding catalyst. Suffice it to be slow, as in the case of RuBisCO, which owing to its relative slowness at catalytically incorporating inorganic carbon into the planet's food chain [84], it also needs to be the most abundant protein in the biosphere [85].

Chaperones with disaggregase activity

Bacterial Hsp70 (DnaK), in the presence of its DnaJ and GrpE co-chaperones and ATP, has been shown in vitro to be able to convert stable preformed small soluble aggregates [70]. Yet, for the disaggregation-unfolding-refolding reaction to be optimal, a large molar excess of the Hsp70 chaperone over the substrate was necessary, a constraint that could be explained by a mechanism of entropic pulling [69, 70, 74]. To alleviate the necessity for a non-physiological excess of Hsp70 over its aggregated substrates, nature may have designed specific Hsp70 co-chaperones in the form of the AAA+ rings of ClpB/Hsp104 or the Hsp70-like Sse/Hsp110s.

Hsp100s (also named ClpB in bacteria, Hsp104 in yeast, and Hsp101 in plants) are AAA+ hexameric ring-like chaperones termed "*disaggregases*" because they act as nanomachines harnessing the energy of ATP hydrolysis to the forceful unfolding and solubilization of large stable protein aggregates to be converted in collaboration with Hsp70s (DnaK) into natively refolded proteins (cycle

II, Fig. 1) [58, 86]. The disaggregase activity of the bacterial Hsp100–Hsp70 (ClpB-DnaK) system is attributed to both their individual and reciprocally regulated concerted unfolding actions on the stable misfolded and aggregated substrates (Fig. 1) [58, 70, 87, 88]. Demonstrating that disaggregation of stable misfolded species is highly conserved in evolution, a similar disaggregation mechanism, leading to spontaneous native refolding, was initially shown in the case of yeast Hsp70 (and Hsp40) and the ClpB ortholog Hsp104 [89, 90]. Unlike yeast and plants, metazoans lack bona fide ClpB/Hsp104-like disaggregases. Yet, they possess another disaggregating chaperone couple composed of a bona fide Hsp70, loosely associated to an evolutionarily related chaperone called Hsp110. Noticeably, Hsp110 in animals, also called Sse in yeast, structurally and functionally belongs to the Hsp70 family [66, 91]. It is not to be confused with the Hsp100 chaperones, which are unrelated to Hsp70s and are rather AAA+ proteins. Hsp110 and Sse were initially described as mere NEF of the Hsp70 (Ssa in yeast) chaperones [92–94] and indeed, even without ATP, human Hsp110 was shown to induce the release of an unfolded substrate from human Hsp70, exactly as bacterial GrpE induced the release of unfolded protein bound to bacterial DnaK [13, 66]. Moreover, suggesting a tight link between ATP-fueled unfolding and disaggregation, Hsp110 with Hsp40 (but without Hsp70) was found to be able to unfold misfolded luciferase monomers, but not large aggregates [66]. In contrast, human Hsp110 and Hsp70 chaperones (with Hsp40) were shown to concertedly act as equal partners that use ATP hydrolysis to disaggregate and unfold large stable luciferase aggregates [39, 66, 91, 95, 96] (Fig. 1). The NEF, Bag1, could not substitute for Hsp110 as a co-chaperone of the disaggregation mechanism [95]. Interestingly, the cytoplasm of plants, yeast, and fungi harbors both Hsp100–Hsp70 and Hsp110–Hsp70 disaggregating machineries, suggesting that the two do not quite overlap in terms of their respective aggregate specificity. Thus, although the human cytoplasm propitiously carries at least one effective disaggregation system (Hsp110–Hsp70), compared to yeast it may still suffer from lacking the Hsp104–Hsp70-based disaggregating machinery, a loss of function that possibly contributes to the excessive sensitivity of aging metazoan neurons to toxic protein aggregates.

Chaperones with polypeptide translocase activity

Trigger factor (TF), initially described as a putative peptidyl-prolyl *cis–trans* isomerase, is a bacterial chaperone that transiently associates to the ribosomal protein L23, where the growing polypeptide chain exits the ribosome and enters into the crowded cytosol. TF lacks ATPase activity. It passively interacts with most polypeptides early during synthesis where it possibly acts as a peptidyl prolyl isomerase, i.e., as a *foldase*, accelerating native folding. It is the first chaperone to associate with nascent chains, thereby acting upstream to the cytosolic DnaK and GroEL *unfoldase* chaperone machineries [97–103]. Already during passage through the ribosomal tunnel, nascent chains may acquire some wrong secondary structures [104]. TF is reported to "hold" the nascent chain and thus apply some pulling and unfolding on the exiting polypeptides [105, 106]. Moreover, TF's particular shape allows it to mould the de novo folding of small polypeptide domains [107] in a direct assisted-folding mechanism of the nascent chains that is clearly distinct from the pulling and unfolding mechanism by DnaK. In addition to its role at the ribosomal exit in de novo protein folding, in vitro assays with artificially unfolded polypeptides have shown that TF can also promote proper native refolding without ribosomes, by transient holding/pulling and/or by acting as a peptidyl prolyl *cis-trans* isomerase [108–110].

Eukaryotes have evolved a different co-translational folding machinery that involves specific variants of Hsp70 and Hsp40. In yeast, this system consists of an Hsp70-like chaperone, *Ssz1* (Hsp70L1 in humans), a J-protein, *Zuo1* (MPP11 in humans), and a stable, ribosome-associated heterodimer named RAC, with two functionally interchangeable Hsp70s, *Ssb1* and *Ssb2*, thus forming a chaperone triad at the ribosome tunnel exit (Fig. 1). When expressed in *S. cerevisiae*, *E. coli* TF can bind to the yeast ribosomes and partially complement a knockout of the yeast ribosomal chaperone triad [111]. In mammals, *Ssb* is absent, but is functionally replaced by the abundant cytosolic Hsc70 [112, 113]. RAC acts as a co-chaperone that stimulates the ATPase activity of *Ssb* (Hsp70) through the J-domain of Zuo1 [114]. Like other J-proteins, Zuo1 associates with ribosomes and target Hsp70 (Ssb) onto the growing polypeptide at the exit of the ribosomal tunnel [113] (Fig. 1).

Moreover, Hsp70 chaperones can assist in general in the post-translational translocation of polypeptides across the membranes of organelles, such as the *endoplasmic reticulum* (ER), mitochondria, and chloroplast [115–117]. The energy necessary to unfold a cytoplasmic precursor protein and translocate it unidirectionally into an organelle through a narrow pore allowing only unfolded polypeptides to cross, may come from the membrane potential driving the polypeptide initial insertion into the pore [118] and ATP hydrolysis by the Hsp70 (mtHsp70, also known as Mortalin, in mitochondria, and BiP in the ER) acting as an import motor on the acceptor side of the membrane [119–122]. The reversible docking of mtHsp70 to the pore and binding (locking) onto the entering polypeptide is simultaneously regulated by the pore-anchoring proteins Tim44 and the J-domain proteins Pam18/Pam16, and by the nucleotide exchange factor, Mge1. Similarly, the

post-translational translocation of specific proteins across the membrane of the ER to the lumen involves a pore-like protein, Sec63, which exposes a J-domain on the lumen side and by doing so, acts as a reversible anchor to BiP, the ER Hsp70 [116].

Two divergent models were initially proposed to explain the mechanism of chaperone-mediated unfolding and unidirectional translocation of precursor protein to the mitochondria. The first was the *Brownian ratchet* model, where polypeptide-bound mtHsp70 was suggested to act as a ratchet that passively prevents backsliding to the cytoplasm and thus driving the polypeptide's inward translocation [121, 123–126]. The second model, called *power stroke*, suggested that a polypeptide and pore-bound mtHsp70 could use the energy of ATP hydrolysis to undergo a conformational transition that, exploiting the pore as a *fulcrum*, would act as a lever arm applying an inward force on the polypeptide and causing its unfolding on the cytoplasmic side and subsequent import [127–133]. Taking advantage of new mechanistic information in the absence of an import pore, on the involvement of Hsp70 (DnaK) and Hsp40 (DnaJ), in the ATP-fueled solubilization and unfolding of stable protein aggregates, a unifying model called *entropic pulling* was proposed. It reproduced the combined effects of the two models above by drawing attention to the fact that upon release from the pore (or from the aggregates), an Hsp70 molecule locked onto a substrate polypeptide applies a pulling force of entropic origin on the polypeptide that needs neither coordinated structural transformations in Hsp70 nor a mechanical fulcrum. Instead, the pore and the surrounding membrane, or a large aggregate, constrain the freedom of movement (thus, the entropy) of the polypeptide–chaperone complex, with an effect that decreases as the distance of the complex from the constraint increases. As a consequence, because of thermodynamics, the complex is entropically pulled away from the pore or from the aggregate. In entropic pulling, the energy of ATP is not directly converted into a mechanical force, as postulated by the power-stroke model, but rather into an indirect thermodynamic force. In the case of translocation, such force remains operative only until 30–40 amino acids have been imported, reducing thereafter to a pure ratchet, unless a new Hsp70 molecule binds [74, 134].

Chaperones with targetase activity

J-domain proteins are also described as holdases [135] but they are principally obligate co-chaperones of the Hsp70/Hsp110s ATPases. J-proteins bind first to misfolded [69, 70], alternatively folded chaperone substrates [136], or to unfolded polypeptides at the ribosomal exit pore [137], or at the import pores of mitochondria or ER [138–140], and may thus attract Hsp70 molecules onto their putative protein substrates. The docking of the highly conserved J-domain to the nucleotide binding domain of Hsp70 (or Hsp110) molecule poises the latter to hydrolyze ATP and, by allostery, causes the locking of the protein binding domain upon a misfolded, unfolded, or alternatively folded polypeptide substrate. The locking of a single Hsp70 molecule may cause the global unfolding of a single domain protein, as in the case of firefly luciferase that acts virtually as a single domain protein [13]. However, in the case of a multidomain polypeptide, such as G6PDH, the locking of a single Hsp70 is expected to cause only a local partial unfolding of the bound polypeptide segment [69, 141, 142]. In this case, the collaborative action of several concomitantly bound Hsp70s at different places on the same polypeptide can cause an additional pulling effect of entropic origin, leading to the global unfolding of the protein (cycle I and II, Fig. 1) [69, 74]. Subsequent to Hsp70-mediated unfolding of the substrate, a nucleotide exchange factor, such as bacterial GrpE, or eukaryotic Bag3, may cause the dissociation of ADP and of the unfolded product from Hsp70 [143]. The product may then spontaneously refold to the native state [13]. If at this stage, misfolding happens rather than native refolding, further unfolding cycles may be needed until all molecules have reached the most stable native state (cycle I, Fig. 1).

Recently, it was reported that mere binding of Hsp40s (DnaJ) could cause some unfolding within a polypeptide [144]. This is, however, not a general effect as a large molar excess of bacterial DnaJ was shown not to disturb wrong beta sheets in a stable misfolded luciferase species, whereas substoichiometric amounts of DnaJ supplemented with DnaK and ATP readily unfolded it [13]. In the cytoplasm and the ER of human cells, the total copy number of J-proteins is respectively 6.4- and 9.6-fold less than the sum of the copy number of Hsp70 and Hsp110 present in the same compartments, confirming that J-proteins unlikely act as equal stoichiometric partners of the Hsp70/Hsp110 unfoldase machinery, but rather as catalysts [27]. Indeed, in vitro refolding assays show that J-proteins (Hsp40s) are optimally acting when present in sub-stoichiometric ratios compared to their Hsp70 partners as in the cell [36, 91]. Thus, 20 times less DnaJ than DnaK can drive at half optimal rates the active refolding of stably heat-preaggregated G6PDH enzyme [36]. This apparent catalytic mode of action by J-proteins implies that J-proteins should not act as holding chaperones but would rather need to be able to readily dissociate from their substrates as soon as Hsp70 has hydrolyzed ATP and thus evicted the bound J-domain from the nucleotide binding domain, while concomitantly locking and unfolding the polypeptide substrate in the protein binding domain. Remarkably, once the DnaJ has bound to an aggregated substrate and recruited the DnaK

Table 1 The major conserved families of molecular chaperones with their established functions, as well as their yet-to-be-demonstrated possible additional functions

Function(s)	Hsp100 (ClpB)	Hsp70/110 (DnaK)	Hsp60 (GroEL)	Hsp90 (HtpG)	Small-Hsps	J-Proteins
Generally accepted function	Disaggregase [58, 86]	Unfoldase [13] Translocase [159]	Holding [160] Folding [161]	Holding [162]	Holding [61]	Holding [135]
Possible additional function	Unfoldase [163]	Disaggregase [39, 66, 70] Holding [164]	Unfoldase [6, 12]	Unfolding [77]	Folding [68]	Hsp70/110 Targetase [74]

and once ATP-fueled DnaK locking onto the misfolded polypeptide has caused the substrate to unfold, this disentanglement is observed to effectively drive DnaJ dissociation, likely because the ATP-fueled DnaK-mediated unfolding destroyed the high affinity DnaJ-binding sites (cycle I, Fig. 1) [36, 145]. In the cell, this may be illustrated in the case of the J-protein auxilin, which in collaboration with Hsc70 mediates the de-oligomerization of clathrin baskets in an ATP-dependent manner. Auxilin, which is ~2,700 times less abundant than Hsc70 in the cytoplasm, initially binds to the clathrin heavy chain, then it entraps Hsc70 by way of inserting its high affinity J-domain in the nucleotide-binding domain. This triggers ATP hydrolysis and causes the locking of the protein binding domain of Hsc70 onto the heavy chain [27, 146, 147]. In vitro, the binding of auxilin to clathrin saturates at three auxilin molecules per clathrin triskelion [148]. However, when auxilin acts as co-chaperone for the targeting Hsc70 onto clathrin baskets in the uncoating reaction, only catalytic amounts of auxilin are required, compared to the Hsc70 and the triskelions [149]. Thus, rather than being referred to as *holdases*, J-proteins in general would better answer to the definition of the "Hsp70/110-*targetases*" (Table 1).

In conclusion, various well-known conserved families of molecular chaperones share the ability to bind more or less tightly and less or more reversibly, to misfolded, aggregated, unfolded, or alternatively folded proteins, but not to native proteins. They may, however, strongly differ in the outcome of polypeptide binding. Upon binding, some chaperones may cause spontaneous unfolding of the polypeptide substrate, others merely prevent aggregation, and yet others may need to use the energy of ATP hydrolysis to forcefully unfold, pull apart, de-oligomerize, and/or disaggregate various polypeptide substrates. Because passive, tight polypeptide binding by a chaperone is not a catalytic process, the suffix "-ase" should be avoided, and the term "holding" chaperones used instead. Because there is a growing number of molecular chaperones that upon substrate binding and unfolding, end up releasing their bound polypeptides in a folding competent state within a biologically reasonable time scale, these chaperones deserve the label of polypeptide *unfoldases* acting as bona fide enzymes. They are functionally related to the class 5 isomerases. Like peptidyl prolyl *cis–trans* isomerases, Hsp70s, or GroEL/CCTs, they do not obligatorily require the breakage of a covalent bond in their polypeptide substrates to catalytically unfold them. Like topoisomerase, they may need to hydrolyze ATP to drive the conformational changes in the misfolded substrates, although catalysis does not change the overall chemical composition [54].

Type I and type II J-proteins can apparently bind to unfolded or misfolded polypeptides and thus incidentally also prevent their aggregation to some degree. Other J-domain proteins can bind to alternatively folded substrates, such as sigma 32 [150], and SNARES that are substrates that do not tend to aggregate under physiological conditions. Likewise, auxilin is a J-protein that can bind only to the alternatively folded clathrin cages and Pam16/18 of the mitochondrial import pore do not directly bind to any substrate protein per se but only indirectly by way of the nearby pore [18, 20, 151, 152]. Rather, J-domain proteins principally act as chaperone targeting devices. In sub-stoichiometric amounts, they drive the binding and "locking" of Hsp70s and/or Hsp110s onto their various alternative, misfolded, or translocating unfolded polypeptides substrates, leading to effective pulling, unfolding, and, upon product release, to native refolding. J-domain co-chaperones should thus best be termed *Hsp70/110 targetases*.

Table 1 summarizes the main classes of conserved molecular chaperones, the various well-established and yet ill-characterized molecular activities, from passive holding and targeting to spontaneous and ATP-fueled catalytic unfolding, disaggregating, pulling, and translocating.

Proteins that need to alternate between various states in order to carry their physiological functions may also bear an intrinsic sensitivity to environmental changes. Thus, labile proteins in cells under mild stresses may tend to unfold and transiently expose hydrophobic residues to the crowded hydrophilic environment, which, depending on the stress intensity and duration, may lead to intra-molecular misfolding and the gradual formation of increasingly stable inter-molecular ensembles called aggregates or amyloids. Likely owing to wrong hydrophobic interactions, the earliest forms of misfolded and aggregated species can compromise the integrity of cellular membranes and the stability of other labile native proteins [153–155]. Moreover, in animal cells, misfolded

conformers induce apoptotic signals, which can lead to a gradual loss of neural tissue, as in Alzheimer's and Parkinson's diseases [4]. These ensuing degenerative conditions are late-onset diseases, likely because they correlate with an age-dependant decreased ability of neurons to sense various abiotic stresses and thus to appropriately produce protective HSPs [156]. In youth, however, when the cellular stress response is optimal, the HSP chaperone network can effectively prevent and avert the formation of early misfolded and aggregated proteotoxic conformers. It is therefore essential to understand which of the specific holding, unfolding, targeting, pulling, and/or disaggregating mechanisms the various members of the cellular chaperone network are using, individually and in collaboration, to reduce proteotoxic species and convert them into harmless, degraded or "rehabilitated" functional native proteins [100]. Detailed knowledge of the various chaperone mechanisms is central to the design of future chaperone-based therapies against protein conformational diseases and aging.

Acknowledgments This work was supported in part by the Faculty of Biology and Medicine of Lausanne University of Lausanne and by Grant 31003A-140512/1 from the Swiss National Fund.

References

1. Anfinsen CB (1973) Principles that govern the folding of protein chains. Science 181(4096):223–230
2. Dobson CM (2003) Protein folding and misfolding. Nature 426(6968):884–890. doi:10.1038/nature02261
3. Natalello A, Mattoo RU, Priya S, Sharma SK, Goloubinoff P, Doglia SM (2013) Biophysical characterization of two different stable misfolded monomeric polypeptides that are chaperone-amenable substrates. J Mol Biol 425(7):1158–1171. doi:10.1016/j.jmb.2012.12.025
4. Hinault MP, Ben-Zvi A, Goloubinoff P (2006) Chaperones and proteases: cellular fold-controlling factors of proteins in neurodegenerative diseases and aging. J Mol Neurosci 30(3):249–265. doi:10.1385/JMN:30:3:249
5. Hartl FU, Bracher A, Hayer-Hartl M (2011) Molecular chaperones in protein folding and proteostasis. Nature 475(7356):324–332. doi:10.1038/nature10317
6. Lin Z, Madan D, Rye HS (2008) GroEL stimulates protein folding through forced unfolding. Nat Struct Mol Biol 15(3):303–311. doi:10.1038/nsmb.1394
7. Lin Z, Rye HS (2004) Expansion and compression of a protein folding intermediate by GroEL. Mol Cell 16(1):23–34. doi:10.1016/j.molcel.2004.09.003
8. Rassow J, Hartl FU, Guiard B, Pfanner N, Neupert W (1990) Polypeptides traverse the mitochondrial envelope in an extended state. FEBS Lett 275(1–2):190–194 (pii:0014-5793(90)81469-5)
9. Schwartz MP, Huang S, Matouschek A (1999) The structure of precursor proteins during import into mitochondria. J Biol Chem 274(18):12759–12764
10. Sharma S, Chakraborty K, Muller BK, Astola N, Tang YC, Lamb DC, Hayer-Hartl M, Hartl FU (2008) Monitoring protein conformation along the pathway of chaperonin-assisted folding. Cell 133(1):142–153. doi:10.1016/j.cell.2008.01.048
11. Shtilerman M, Lorimer GH, Englander SW (1999) Chaperonin function: folding by forced unfolding. Science 284(5415):822–825
12. Priya S, Sharma SK, Sood V, Mattoo RU, Finka A, Azem A, De Los Rios P, Goloubinoff P (2013) GroEL and CCT are catalytic unfoldases mediating out-of-cage polypeptide refolding without ATP. Proc Natl Acad Sci USA 110(18):7199–7204. doi:10.1073/pnas.1219867110
13. Sharma SK, De Los Rios P, Christen P, Lustig A, Goloubinoff P (2010) The kinetic parameters and energy cost of the Hsp70 chaperone as a polypeptide unfoldase. Nat Chem Biol 6(12):914–920. doi:10.1038/Nchembio.455
14. Picard D (2006) Chaperoning steroid hormone action. Trends Endocrinol Metab 17(6):229–235. doi:10.1016/j.tem.2006.06.003
15. Voellmy R, Boellmann F (2007) Chaperone regulation of the heat shock protein response. Adv Exp Med Biol 594:89–99. doi:10.1007/978-0-387-39975-1_9
16. Weiss YG, Bromberg Z, Raj N, Raphael J, Goloubinoff P, Ben-Neriah Y, Deutschman CS (2007) Enhanced heat shock protein 70 expression alters proteasomal degradation of IkappaB kinase in experimental acute respiratory distress syndrome. Crit Care Med 35(9):2128–2138
17. Zinsmaier KE, Bronk P (2001) Molecular chaperones and the regulation of neurotransmitter exocytosis. Biochem Pharmacol 62(1):1–11 (pii:S0006-2952(01)00648-7)
18. Joglekar AP, Hay JC (2005) Evidence for regulation of ER/Golgi SNARE complex formation by hsc70 chaperones. Eur J Cell Biol 84(5):529–542. doi:10.1016/j.ejcb.2004.12.028
19. Sharma M, Burre J, Sudhof TC (2011) CSPalpha promotes SNARE-complex assembly by chaperoning SNAP-25 during synaptic activity. Nat Cell Biol 13(1):30–39. doi:10.1038/ncb2131
20. Sousa R, Lafer EM (2006) Keep the traffic moving: mechanism of the Hsp70 motor. Traffic 7(12):1596–1603. doi:10.1111/j.1600-0854.2006.00497.x
21. Finka A, Mattoo RU, Goloubinoff P (2011) Meta-analysis of heat- and chemically upregulated chaperone genes in plant and human cells. Cell Stress Chaperones 16(1):15–31. doi:10.1007/s12192-010-0216-8
22. Gidalevitz T, Prahlad V, Morimoto RI (2011) The stress of protein misfolding: from single cells to multicellular organisms. Cold Spring Harb Perspect Biol 3(6). doi:10.1101/cshperspect.a009704
23. Tyedmers J, Mogk A, Bukau B (2010) Cellular strategies for controlling protein aggregation. Nat Rev Mol Cell Biol 11(11):777–788. doi:10.1038/nrm2993
24. Richter K, Haslbeck M, Buchner J (2010) The heat shock response: life on the verge of death. Mol Cell 40(2):253–266. doi:10.1016/j.molcel.2010.10.006
25. Vabulas RM, Raychaudhuri S, Hayer-Hartl M, Hartl FU (2010) Protein folding in the cytoplasm and the heat shock response. Cold Spring Harb Perspect Biol 2(12):a004390. doi:10.1101/cshperspect.a004390
26. Kampinga HH, Hageman J, Vos MJ, Kubota H, Tanguay RM, Bruford EA, Cheetham ME, Chen B, Hightower LE (2009) Guidelines for the nomenclature of the human heat shock proteins. Cell Stress Chaperones 14(1):105–111. doi:10.1007/s12192-008-0068-7

27. Finka A, Goloubinoff P (2013) Proteomic data from human cell cultures refine mechanisms of chaperone-mediated protein homeostasis. Cell Stress Chaperones 18(5):591–605. doi:10.1007/s12192-013-0413-3
28. Uryu K, Richter-Landsberg C, Welch W, Sun E, Goldbaum O, Norris EH, Pham CT, Yazawa I, Hilburger K, Micsenyi M, Giasson BI, Bonini NM, Lee VM, Trojanowski JQ (2006) Convergence of heat shock protein 90 with ubiquitin in filamentous alpha-synuclein inclusions of alpha-synucleinopathies. Am J Pathol 168(3):947–961 (pii:S0002-9440(10)62155-4)
29. McLean PJ, Kawamata H, Shariff S, Hewett J, Sharma N, Ueda K, Breakefield XO, Hyman BT (2002) TorsinA and heat shock proteins act as molecular chaperones: suppression of alpha-synuclein aggregation. J Neurochem 83(4):846–854 (pii:1190)
30. Leverenz JB, Umar I, Wang Q, Montine TJ, McMillan PJ, Tsuang DW, Jin J, Pan C, Shin J, Zhu D, Zhang J (2007) Proteomic identification of novel proteins in cortical Lewy bodies. Brain Pathol 17(2):139–145. doi:10.1111/j.1750-3639.2007.00048.x
31. Auluck PK, Chan HY, Trojanowski JQ, Lee VM, Bonini NM (2002) Chaperone suppression of alpha-synuclein toxicity in a *Drosophila* model for Parkinson's disease. Science 295(5556):865–868. doi:10.1126/science.1067389389
32. Zhou Y, Gu G, Goodlett DR, Zhang T, Pan C, Montine TJ, Montine KS, Aebersold RH, Zhang J (2004) Analysis of alpha-synuclein-associated proteins by quantitative proteomics. J Biol Chem 279(37):39155–39164. doi:10.1074/jbc.M405456200
33. Kuhn K, Wellen J, Link N, Maskri L, Lubbert H, Stichel CC (2003) The mouse MPTP model: gene expression changes in dopaminergic neurons. Eur J Neurosci 17(1):1–12 (pii:2408)
34. St Martin JL, Klucken J, Outeiro TF, Nguyen P, Keller-McGandy C, Cantuti-Castelvetri I, Grammatopoulos TN, Standaert DG, Hyman BT, McLean PJ (2007) Dopaminergic neuron loss and up-regulation of chaperone protein mRNA induced by targeted over-expression of alpha-synuclein in mouse substantia nigra. J Neurochem 100(6):1449–1457. doi:10.1111/j.1471-4159.2006.04310.x
35. Ebrahimi-Fakhari D, Saidi LJ, Wahlster L (2013) Molecular chaperones and protein folding as therapeutic targets in Parkinson's disease and other synucleinopathies. Acta Neuropathol Commun 1(1):79. doi:10.1186/2051-5960-1-79
36. Hinault MP, Cuendet AF, Mattoo RU, Mensi M, Dietler G, Lashuel HA, Goloubinoff P (2010) Stable alpha-synuclein oligomers strongly inhibit chaperone activity of the Hsp70 system by weak interactions with J-domain co-chaperones. J Biol Chem 285(49):38173–38182. doi:10.1074/jbc.M110.127753
37. Bruinsma IB, Bruggink KA, Kinast K, Versleijen AA, Segers-Nolten IM, Subramaniam V, Kuiperij HB, Boelens W, de Waal RM, Verbeek MM (2011) Inhibition of alpha-synuclein aggregation by small heat shock proteins. Proteins 79(10):2956–2967. doi:10.1002/prot.23152
38. Duennwald ML, Echeverria A, Shorter J (2012) Small heat shock proteins potentiate amyloid dissolution by protein disaggregases from yeast and humans. PLoS Biol 10(6):e1001346. doi:10.1371/journal.pbio.1001346
39. Shorter J (2011) The mammalian disaggregase machinery: Hsp110 synergizes with Hsp70 and Hsp40 to catalyze protein disaggregation and reactivation in a cell-free system. PLoS One 6(10):e26319. doi:10.1371/journal.pone.0026319
40. Ben-Zvi AP, Goloubinoff P (2002) Proteinaceous infectious behavior in non-pathogenic proteins is controlled by molecular chaperones. J Biol Chem 277(51):49422–49427. doi:10.1074/jbc.M209163200
41. Sharma SK, Christen P, Goloubinoff P (2009) Disaggregating chaperones: an unfolding story. Curr Protein Pept Sci 10(5):432–446 (pii:CPPS-4)
42. Jacobson T, Navarrete C, Sharma SK, Sideri TC, Ibstedt S, Priya S, Grant CM, Christen P, Goloubinoff P, Tamas MJ (2012) Arsenite interferes with protein folding and triggers formation of protein aggregates in yeast. J Cell Sci 125(Pt 21):5073–5083. doi:10.1242/jcs.107029
43. Sharma SK, Goloubinoff P, Christen P (2008) Heavy metal ions are potent inhibitors of protein folding. Biochem Biophys Res Commun 372(2):341–345. doi:10.1016/j.bbrc.2008.05.052
44. Baler R, Zou J, Voellmy R (1996) Evidence for a role of Hsp70 in the regulation of the heat shock response in mammalian cells. Cell Stress Chaperones 1(1):33–39
45. Beere HM, Wolf BB, Cain K, Mosser DD, Mahboubi A, Kuwana T, Tailor P, Morimoto RI, Cohen GM, Green DR (2000) Heat-shock protein 70 inhibits apoptosis by preventing recruitment of procaspase-9 to the Apaf-1 apoptosome. Nat Cell Biol 2(8):469–475. doi:10.1038/35019501
46. Ghosh S, Baltimore D (1990) Activation in vitro of NF-kappa B by phosphorylation of its inhibitor I kappa B. Nature 344(6267):678–682. doi:10.1038/344678a0
47. Rabindran SK, Wisniewski J, Li L, Li GC, Wu C (1994) Interaction between heat shock factor and hsp70 is insufficient to suppress induction of DNA-binding activity in vivo. Mol Cell Biol 14(10):6552–6560
48. Dittmar KD, Banach M, Galigniana MD, Pratt WB (1998) The role of DnaJ-like proteins in glucocorticoid receptor.hsp90 heterocomplex assembly by the reconstituted hsp90.p60.hsp70 foldosome complex. J Biol Chem 273(13):7358–7366
49. Dittmar KD, Hutchison KA, Owens-Grillo JK, Pratt WB (1996) Reconstitution of the steroid receptor.hsp90 heterocomplex assembly system of rabbit reticulocyte lysate. J Biol Chem 271(22):12833–12839
50. Pratt WB, Toft DO (2003) Regulation of signaling protein function and trafficking by the hsp90/hsp70-based chaperone machinery. Exp Biol Med (Maywood) 228(2):111–133
51. De Los Rios P, Goloubinoff P (2012) Protein folding: chaperoning protein evolution. Nat Chem Biol 8(3):226–228. doi:10.1038/nchembio.791
52. Lashuel HA, Hartley D, Petre BM, Walz T, Lansbury PT Jr (2002) Neurodegenerative disease: amyloid pores from pathogenic mutations. Nature 418(6895):291. doi:10.1038/418291a
53. Hartl FU, Hayer-Hartl M (2002) Molecular chaperones in the cytosol: from nascent chain to folded protein. Science 295(5561):1852–1858. doi:10.1126/science.1068408
54. Priya S, Sharma SK, Goloubinoff P (2013) Molecular chaperones as enzymes that catalytically unfold misfolded polypeptides. FEBS Lett 587(13):1981–1987. doi:10.1016/j.febslet.2013.05.014
55. Goloubinoff P, Gatenby AA, Lorimer GH (1989) GroE heat-shock proteins promote assembly of foreign prokaryotic ribulose bisphosphate carboxylase oligomers in *Escherichia coli*. Nature 337(6202):44–47. doi:10.1038/337044a0
56. Wiech H, Buchner J, Zimmermann R, Jakob U (1992) Hsp90 chaperones protein folding in vitro. Nature 358(6382):169–170. doi:10.1038/358169a0
57. Buchner J, Kiefhaber T (1990) Folding pathway enigma. Nature 343(6259):601–602. doi:10.1038/343601b0
58. Goloubinoff P, Mogk A, Zvi AP, Tomoyasu T, Bukau B (1999) Sequential mechanism of solubilization and refolding of stable protein aggregates by a bichaperone network. Proc Natl Acad Sci USA 96(24):13732–13737
59. Ehrnsperger M, Graber S, Gaestel M, Buchner J (1997) Binding of non-native protein to Hsp25 during heat shock creates a reservoir of folding intermediates for reactivation. EMBO J 16(2):221–229. doi:10.1093/emboj/16.2.221
60. Lee GJ, Roseman AM, Saibil HR, Vierling E (1997) A small heat shock protein stably binds heat-denatured model substrates

and can maintain a substrate in a folding-competent state. EMBO J 16(3):659–671. doi:10.1093/emboj/16.3.659
61. Veinger L, Diamant S, Buchner J, Goloubinoff P (1998) The small heat-shock protein IbpB from *Escherichia coli* stabilizes stress-denatured proteins for subsequent refolding by a multichaperone network. J Biol Chem 273(18):11032–11037
62. Chang Z, Primm TP, Jakana J, Lee IH, Serysheva I, Chiu W, Gilbert HF, Quiocho FA (1996) Mycobacterium tuberculosis 16-kDa antigen (Hsp16.3) functions as an oligomeric structure in vitro to suppress thermal aggregation. J Biol Chem 271(12):7218–7223
63. Horwitz J (1992) Alpha-crystallin can function as a molecular chaperone. Proc Natl Acad Sci USA 89(21):10449–10453
64. Jakob U, Gaestel M, Engel K, Buchner J (1993) Small heat shock proteins are molecular chaperones. J Biol Chem 268(3):1517–1520
65. Jinn TL, Chen YM, Lin CY (1995) Characterization and physiological function of class I low-molecular-mass, heat-shock protein complex in soybean. Plant Physiol 108(2):693–701 (pii:108/2/693)
66. Mattoo RU, Sharma SK, Priya S, Finka A, Goloubinoff P (2013) Hsp110 is a bona fide chaperone using ATP to unfold stable misfolded polypeptides and reciprocally collaborate with Hsp70 to solubilize protein aggregates. J Biol Chem. doi:10.1074/jbc.M113.479253
67. Cosgrove MS, Naylor C, Paludan S, Adams MJ, Levy HR (1998) On the mechanism of the reaction catalyzed by glucose 6-phosphate dehydrogenase. Biochemistry 37(9):2759–2767. doi:10.1021/bi972069y
68. Lee GJ, Pokala N, Vierling E (1995) Structure and in vitro molecular chaperone activity of cytosolic small heat shock proteins from pea. J Biol Chem 270(18):10432–10438
69. Ben-Zvi A, De Los Rios P, Dietler G, Goloubinoff P (2004) Active solubilization and refolding of stable protein aggregates by cooperative unfolding action of individual hsp70 chaperones. J Biol Chem 279(36):37298–37303. doi:10.1074/jbc.M405627200
70. Diamant S, Ben-Zvi AP, Bukau B, Goloubinoff P (2000) Size-dependent disaggregation of stable protein aggregates by the DnaK chaperone machinery. J Biol Chem 275(28):21107–21113. doi:10.1074/jbc.M001293200
71. Skowyra D, Georgopoulos C, Zylicz M (1990) The *E. coli* dnaK gene product, the hsp70 homolog, can reactivate heat-inactivated RNA polymerase in an ATP hydrolysis-dependent manner. Cell 62(5):939–944 (pii:0092-8674(90)90268-J)
72. Baneyx F, Nannenga BL (2010) Chaperones: a story of thrift unfolds. Nat Chem Biol 6(12):880–881. doi:10.1038/nchembio.468
73. Schlecht R, Erbse AH, Bukau B, Mayer MP (2011) Mechanics of Hsp70 chaperones enables differential interaction with client proteins. Nat Struct Mol Biol 18(3):345–351. doi:10.1038/nsmb.2006
74. De Los Rios P, Ben-Zvi A, Slutsky O, Azem A, Goloubinoff P (2006) Hsp70 chaperones accelerate protein translocation and the unfolding of stable protein aggregates by entropic pulling. Proc Natl Acad Sci USA 103(16):6166–6171. doi:10.1073/pnas.0510496103
75. Braig K, Otwinowski Z, Hegde R, Boisvert DC, Joachimiak A, Horwich AL, Sigler PB (1994) The crystal structure of the bacterial chaperonin GroEL at 2.8 A. Nature 371(6498):578–586. doi:10.1038/371578a0
76. Rivenzon-Segal D, Wolf SG, Shimon L, Willison KR, Horovitz A (2005) Sequential ATP-induced allosteric transitions of the cytoplasmic chaperonin containing TCP-1 revealed by EM analysis. Nat Struct Mol Biol 12(3):233–237. doi:10.1038/nsmb901
77. Walerych D, Gutkowska M, Klejman MP, Wawrzynow B, Tracz Z, Wiech M, Zylicz M, Zylicz A (2010) ATP binding to Hsp90 is sufficient for effective chaperoning of p53 protein. J Biol Chem 285(42):32020–32028. doi:10.1074/jbc.M110.112110
78. Nakamoto H, Fujita K, Ohtaki A, Watanabe S, Narumi S, Maruyama T, Suenaga E, Misono TS, Kumar PK, Goloubinoff P, Yoshikawa H (2014) Physical interaction between bacterial heat shock protein 90 (Hsp90) and Hsp70 chaperones mediates their cooperative action to refold denatured proteins. J Biol Chem. doi:10.1074/jbc.M113.524801
79. Genest O, Hoskins JR, Camberg JL, Doyle SM, Wickner S (2011) Heat shock protein 90 from *Escherichia coli* collaborates with the DnaK chaperone system in client protein remodeling. Proc Natl Acad Sci USA 108(20):8206–8211. doi:10.1073/pnas.1104703108
80. Sharma SK, De Los Rios P, Goloubinoff P (2011) Probing the different chaperone activities of the bacterial HSP70–HSP40 system using a thermolabile luciferase substrate. Proteins 79(6):1991–1998. doi:10.1002/prot.23024
81. Saidi Y, Domini M, Choy F, Zryd JP, Schwitzguebel JP, Goloubinoff P (2007) Activation of the heat shock response in plants by chlorophenols: transgenic *Physcomitrella patens* as a sensitive biosensor for organic pollutants. Plant Cell Environ 30(6):753–763. doi:10.1111/j.1365-3040.2007.01664.x
82. Goloubinoff P, Diamant S, Weiss C, Azem A (1997) GroES binding regulates GroEL chaperonin activity under heat shock. FEBS Lett 407(2):215–219 (pii:S0014-5793(97)00348-7)
83. Diamant S, Goloubinoff P (1998) Temperature-controlled activity of DnaK–DnaJ–GrpE chaperones: protein-folding arrest and recovery during and after heat shock depends on the substrate protein and the GrpE concentration. Biochemistry 37(27):9688–9694. doi:10.1021/bi980338u
84. Ellis RJ (2010) Biochemistry: tackling unintelligent design. Nature 463(7278):164–165. doi:10.1038/463164a
85. Spreitzer RJ, Salvucci ME (2002) RuBisCO: structure, regulatory interactions, and possibilities for a better enzyme. Annu Rev Plant Biol 53:449–475. doi:10.1146/annurev.arplant.53.100301.135233
86. Glover JR, Lindquist S (1998) Hsp104, Hsp70, and Hsp40: a novel chaperone system that rescues previously aggregated proteins. Cell 94(1):73–82 (pii:S0092-8674(00)81223-4)
87. Oguchi Y, Kummer E, Seyffer F, Berynskyy M, Anstett B, Zahn R, Wade RC, Mogk A, Bukau B (2012) A tightly regulated molecular toggle controls AAA plus disaggregase. Nat Struct Mol Biol 19(12):1338–1346. doi:10.1038/Nsmb.2441
88. Seyffer F, Kummer E, Oguchi Y, Winkler J, Kumar M, Zahn R, Sourjik V, Bukau B, Mogk A (2012) Hsp70 proteins bind Hsp100 regulatory M domains to activate AAA+ disaggregase at aggregate surfaces. Nat Struct Mol Biol 19(12):1347–1355. doi:10.1038/nsmb.2442
89. Desantis ME, Sweeny EA, Snead D, Leung EH, Go MS, Gupta K, Wendler P, Shorter J (2014) Conserved distal loop residues in the Hsp104 and ClpB middle domain contact nucleotide-binding domain 2 and enable Hsp70-dependent protein disaggregation. J Biol Chem 289(2):848–867. doi:10.1074/jbc.M113.520759
90. Lee J, Kim JH, Biter AB, Sielaff B, Lee S, Tsai FT (2013) Heat shock protein (Hsp) 70 is an activator of the Hsp104 motor. Proc Natl Acad Sci USA 110(21):8513–8518. doi:10.1073/pnas.1217988110
91. Schuermann JP, Jiang J, Cuellar J, Llorca O, Wang L, Gimenez LE, Jin S, Taylor AB, Demeler B, Morano KA, Hart PJ, Valpuesta JM, Lafer EM, Sousa R (2008) Structure of the Hsp110:Hsc70 nucleotide exchange machine. Mol Cell 31(2):232–243. doi:10.1016/j.molcel.2008.05.006

92. Dragovic Z, Broadley SA, Shomura Y, Bracher A, Hartl FU (2006) Molecular chaperones of the Hsp110 family act as nucleotide exchange factors of Hsp70s. EMBO J 25(11):2519–2528. doi:10.1038/sj.emboj.7601138
93. Polier S, Dragovic Z, Hartl FU, Bracher A (2008) Structural basis for the cooperation of Hsp70 and Hsp110 chaperones in protein folding. Cell 133(6):1068–1079. doi:10.1016/j.cell.2008.05.022
94. Raviol H, Sadlish H, Rodriguez F, Mayer MP, Bukau B (2006) Chaperone network in the yeast cytosol: Hsp110 is revealed as an Hsp70 nucleotide exchange factor. EMBO J 25(11):2510–2518. doi:10.1038/sj.emboj.7601139
95. Rampelt H, Kirstein-Miles J, Nillegoda NB, Chi K, Scholz SR, Morimoto RI, Bukau B (2012) Metazoan Hsp70 machines use Hsp110 to power protein disaggregation. EMBO J 31(21):4221–4235. doi:10.1038/emboj.2012.264
96. Torrente MP, Shorter J (2013) The metazoan protein disaggregase and amyloid depolymerase system: Hsp110, Hsp70, Hsp40, and small heat shock proteins. Prion 7(6):457–463
97. Valent QA, Kendall DA, High S, Kusters R, Oudega B, Luirink J (1995) Early events in preprotein recognition in *E. coli*: interaction of SRP and trigger factor with nascent polypeptides. EMBO J 14(22):5494–5505
98. Valent QA, de Gier JW, von Heijne G, Kendall DA, ten Hagen-Jongman CM, Oudega B, Luirink J (1997) Nascent membrane and presecretory proteins synthesized in *Escherichia coli* associate with signal recognition particle and trigger factor. Mol Microbiol 25(1):53–64
99. Schaffitzel E, Rudiger S, Bukau B, Deuerling E (2001) Functional dissection of trigger factor and DnaK: interactions with nascent polypeptides and thermally denatured proteins. Biol Chem 382(8):1235–1243. doi:10.1515/BC.2001.154
100. Jong WSP, ten Hagen-Jongman CM, Genevaux P, Brunner J, Oudega B, Luirink J (2004) Trigger factor interacts with the signal peptide of nascent Tat substrates but does not play a critical role in Tat-mediated export. Eur J Biochem 271(23–24):4779–4787
101. Ullers RS, Luirink J, Harms N, Schwager F, Georgopoulos C, Genevaux P (2004) SecB is a bona fide generalized chaperone in *Escherichia coli*. Proc Natl Acad Sci USA 101(20):7583–7588. doi:10.1073/pnas.0402398101
102. Ullers RS, Houben EN, Raine A, ten Hagen-Jongman CM, Ehrenberg M, Brunner J, Oudega B, Harms N, Luirink J (2003) Interplay of signal recognition particle and trigger factor at L23 near the nascent chain exit site on the *Escherichia coli* ribosome. J Cell Biol 161(4):679–684. doi:10.1083/jcb.200302130
103. Ullers RS, Houben EN, Brunner J, Oudega B, Harms N, Luirink J (2006) Sequence-specific interactions of nascent *Escherichia coli* polypeptides with trigger factor and signal recognition particle. J Biol Chem 281(20):13999–14005. doi:10.1074/jbc.M600638200
104. Wilson DN, Beckmann R (2011) The ribosomal tunnel as a functional environment for nascent polypeptide folding and translational stalling. Curr Opin Struct Biol 21(2):274–282. doi:10.1016/j.sbi.2011.01.007
105. Hoffmann A, Becker AH, Zachmann-Brand B, Deuerling E, Bukau B, Kramer G (2012) Concerted action of the ribosome and the associated chaperone trigger factor confines nascent polypeptide folding. Mol Cell 48(1):63–74. doi:10.1016/j.molcel.2012.07.018
106. Hebert DN, Chandrasekhar KD, Gierasch LM (2012) You got to know when to hold (or unfold) 'em. Mol Cell 48(1):3–4. doi:10.1016/j.molcel.2012.09.022
107. Ferbitz L, Maier T, Patzelt H, Bukau B, Deuerling E, Ban N (2004) Trigger factor in complex with the ribosome forms a molecular cradle for nascent proteins. Nature 431(7008):590–596. doi:10.1038/nature02899
108. Merz F, Hoffmann A, Rutkowska A, Zachmann-Brand B, Bukau B, Deuerling E (2006) The C-terminal domain of *Escherichia coli* trigger factor represents the central module of its chaperone activity. J Biol Chem 281(42):31963–31971. doi:10.1074/jbc.M605164200
109. Kramer G, Rutkowska A, Wegrzyn RD, Patzelt H, Kurz TA, Merz F, Rauch T, Vorderwulbecke S, Deuerling E, Bukau B (2004) Functional dissection of *Escherichia coli* trigger factor: unraveling the function of individual domains. J Bacteriol 186(12):3777–3784. doi:10.1128/Jb.186.12.3777-3784.2004
110. Huang GC, Li ZY, Zhou JM, Fischer G (2000) Assisted folding of D-glyceraldehyde-3-phosphate dehydrogenase by trigger factor. Protein Sci 9(6):1254–1261. doi:10.1110/ps.9.6.1254
111. Rauch T, Hundley HA, Pfund C, Wegrzyn RD, Walter W, Kramer G, Kim SY, Craig EA, Deuerling E (2005) Dissecting functional similarities of ribosome-associated chaperones from *Saccharomyces cerevisiae* and *Escherichia coli*. Mol Microbiol 57(2):357–365. doi:10.1111/j.1365-2958.2005.04690.x
112. Otto H, Conz C, Maier P, Wolfle T, Suzuki CK, Jeno P, Rucknagel P, Stahl J, Rospert S (2005) The chaperones MPP11 and Hsp70L1 form the mammalian ribosome-associated complex. Proc Natl Acad Sci USA 102(29):10064–10069. doi:10.1073/pnas.0504400102
113. Preissler S, Deuerling E (2012) Ribosome-associated chaperones as key players in proteostasis. Trends Biochem Sci 37(7):274–283. doi:10.1016/j.tibs.2012.03.002
114. Huang P, Gautschi M, Walter W, Rospert S, Craig EA (2005) The Hsp70 Ssz1 modulates the function of the ribosome-associated J-protein Zuo1. Nat Struct Mol Biol 12(6):497–504. doi:10.1038/nsmb942
115. Chacinska A, Koehler CM, Milenkovic D, Lithgow T, Pfanner N (2009) Importing mitochondrial proteins: machineries and mechanisms. Cell 138(4):628–644. doi:10.1016/j.cell.2009.08.005
116. Rapoport TA, Matlack KE, Plath K, Misselwitz B, Staeck O (1999) Posttranslational protein translocation across the membrane of the endoplasmic reticulum. Biol Chem 380(10):1143–1150. doi:10.1515/BC.1999.145
117. Shi LX, Theg SM (2011) The motors of protein import into chloroplasts. Plant Signal Behav 6(9):1397–1401. doi:10.4161/psb.6.9.16916
118. Schleiff E, Becker T (2011) Common ground for protein translocation: access control for mitochondria and chloroplasts. Nat Rev Mol Cell Biol 12(1):48–59. doi:10.1038/nrm3027
119. Bauer MF, Sirrenberg C, Neupert W, Brunner M (1996) Role of Tim23 as voltage sensor and presequence receptor in protein import into mitochondria. Cell 87(1):33–41 (pii:S0092-8674(00)81320-3)
120. Martin J, Mahlke K, Pfanner N (1991) Role of an energized inner membrane in mitochondrial protein import. Delta psi drives the movement of presequences. J Biol Chem 266(27):18051–18057
121. Schneider HC, Berthold J, Bauer MF, Dietmeier K, Guiard B, Brunner M, Neupert W (1994) Mitochondrial Hsp70/MIM44 complex facilitates protein import. Nature 371(6500):768–774. doi:10.1038/371768a0
122. Ungermann C, Neupert W, Cyr DM (1994) The role of Hsp70 in conferring unidirectionality on protein translocation into mitochondria. Science 266(5188):1250–1253
123. Berthold J, Bauer MF, Schneider HC, Klaus C, Dietmeier K, Neupert W, Brunner M (1995) The MIM complex mediates preprotein translocation across the mitochondrial inner membrane and couples it to the mt-Hsp70/ATP driving system. Cell 81(7):1085–1093 (pii:S0092-8674(05)80013-3)

124. Milisav I, Moro F, Neupert W, Brunner M (2001) Modular structure of the TIM23 preprotein translocase of mitochondria. J Biol Chem 276(28):25856–25861. doi:10.1074/jbc.M102132200
125. Moro F, Sirrenberg C, Schneider HC, Neupert W, Brunner M (1999) The TIM17.23 preprotein translocase of mitochondria: composition and function in protein transport into the matrix. EMBO J 18(13):3667–3675. doi:10.1093/emboj/18.13.3667
126. Schneider HC, Westermann B, Neupert W, Brunner M (1996) The nucleotide exchange factor MGE exerts a key function in the ATP-dependent cycle of mt-Hsp70-Tim44 interaction driving mitochondrial protein import. EMBO J 15(21):5796–5803
127. Bomer U, Maarse AC, Martin F, Geissler A, Merlin A, Schonfisch B, Meijer M, Pfanner N, Rassow J (1998) Separation of structural and dynamic functions of the mitochondrial translocase: Tim44 is crucial for the inner membrane import sites in translocation of tightly folded domains, but not of loosely folded preproteins. EMBO J 17(15):4226–4237. doi:10.1093/emboj/17.15.4226
128. Bukau B, Horwich AL (1998) The Hsp70 and Hsp60 chaperone machines. Cell 92(3):351–366 (pii:S0092-8674(00)80928-9)
129. Glick BS (1995) Can Hsp70 proteins act as force-generating motors? Cell 80(1):11–14 (pii:0092-8674(95)90444-1)
130. Jensen RE, Johnson AE (1999) Protein translocation: is Hsp70 pulling my chain? Curr Biol 9(20):R779–R782. doi:10.1016/S0960-9822(00)80012-3
131. Pfanner N, Geissler A (2001) Versatility of the mitochondrial protein import machinery. Nat Rev Mol Cell Biol 2(5):339–349. doi:10.1038/35073006
132. Pfanner N, Meijer M (1995) Protein sorting. Pulling in the proteins. Curr Biol 5(2):132–135 (pii:S0960-9822(95)00033-9)
133. Ryan MT, Pfanner N (2001) Hsp70 proteins in protein translocation. Adv Protein Chem 59:223–242
134. Goloubinoff P, De Los Rios P (2007) The mechanism of Hsp70 chaperones: (entropic) pulling the models together. Trends Biochem Sci 32(8):372–380. doi:10.1016/j.tibs.2007.06.008
135. Rikhvanov EG, Romanova NV, Chernoff YO (2007) Chaperone effects on prion and nonprion aggregates. Prion 1(4):217–222 (pii:5058)
136. Mayer MP, Schroder H, Rudiger S, Paal K, Laufen T, Bukau B (2000) Multistep mechanism of substrate binding determines chaperone activity of Hsp70. Nat Struct Biol 7(7):586–593. doi:10.1038/76819
137. Gautschi M, Lilie H, Funfschilling U, Mun A, Ross S, Lithgow T, Rucknagel P, Rospert S (2001) RAC, a stable ribosome-associated complex in yeast formed by the DnaK–DnaJ homologs Ssz1p and zuotin. Proc Natl Acad Sci USA 98(7):3762–3767. doi:10.1073/pnas.071057198
138. Truscott KN, Voos W, Frazier AE, Lind M, Li Y, Geissler A, Dudek J, Muller H, Sickmann A, Meyer HE, Meisinger C, Guiard B, Rehling P, Pfanner N (2003) A J-protein is an essential subunit of the presequence translocase-associated protein import motor of mitochondria. J Cell Biol 163(4):707–713. doi:10.1083/jcb.200308004
139. D'Silva PR, Schilke B, Walter W, Craig EA (2005) Role of Pam16's degenerate J domain in protein import across the mitochondrial inner membrane. Proc Natl Acad Sci USA 102(35):12419–12424. doi:10.1073/pnas.0505969102
140. Misselwitz B, Staeck O, Matlack KE, Rapoport TA (1999) Interaction of BiP with the J-domain of the Sec63p component of the endoplasmic reticulum protein translocation complex. J Biol Chem 274(29):20110–20115
141. Zhuravleva A, Clerico EM, Gierasch LM (2012) An interdomain energetic tug-of-war creates the allosterically active state in Hsp70 molecular chaperones. Cell 151(6):1296–1307. doi:10.1016/j.cell.2012.11.002
142. Zhuravleva A, Gierasch LM (2011) Allosteric signal transmission in the nucleotide-binding domain of 70-kDa heat shock protein (Hsp70) molecular chaperones. Proc Natl Acad Sci USA 108(17):6987–6992. doi:10.1073/pnas.1014448108
143. Zuiderweg ER, Bertelsen EB, Rousaki A, Mayer MP, Gestwicki JE, Ahmad A (2013) Allostery in the Hsp70 chaperone proteins. Top Curr Chem 328:99–153. doi:10.1007/128_2012_323
144. Tiwari S, Kumar V, Jayaraj GG, Maiti S, Mapa K (2013) Unique structural modulation of a non-native substrate by cochaperone DnaJ. Biochemistry 52(6):1011–1018. doi:10.1021/bi301543g
145. Jiang J, Maes EG, Taylor AB, Wang L, Hinck AP, Lafer EM, Sousa R (2007) Structural basis of J cochaperone binding and regulation of Hsp70. Mol Cell 28(3):422–433. doi:10.1016/j.molcel.2007.08.022
146. Lindner R, Ungewickell E (1991) Light-chain-independent binding of adaptors, AP180, and auxilin to clathrin. Biochemistry 30(37):9097–9101
147. Jiang J, Taylor AB, Prasad K, Ishikawa-Brush Y, Hart PJ, Lafer EM, Sousa R (2003) Structure-function analysis of the auxilin J-domain reveals an extended Hsc70 interaction interface. Biochemistry 42(19):5748–5753. doi:10.1021/bi034270g
148. Ma Y, Greener T, Pacold ME, Kaushal S, Greene LE, Eisenberg E (2002) Identification of domain required for catalytic activity of auxilin in supporting clathrin uncoating by Hsc70. J Biol Chem 277(51):49267–49274. doi:10.1074/jbc.M203695200
149. Ungewickell E, Ungewickell H, Holstein SE, Lindner R, Prasad K, Barouch W, Martin B, Greene LE, Eisenberg E (1995) Role of auxilin in uncoating clathrin-coated vesicles. Nature 378(6557):632–635. doi:10.1038/378632a0
150. Mayer MP, Laufen T, Paal K, McCarty JS, Bukau B (1999) Investigation of the interaction between DnaK and DnaJ by surface plasmon resonance spectroscopy. J Mol Biol 289(4):1131–1144. doi:10.1006/jmbi.1999.2844
151. Swayne LA, Beck KE, Braun JE (2006) The cysteine string protein multimeric complex. Biochem Biophys Res Commun 348(1):83–91. doi:10.1016/j.bbrc.2006.07.033
152. D'Silva PR, Schilke B, Hayashi M, Craig EA (2008) Interaction of the J-protein heterodimer Pam18/Pam16 of the mitochondrial import motor with the translocon of the inner membrane. Mol Biol Cell 19(1):424–432. doi:10.1091/mbc.E07-08-0748
153. Soto C, Estrada L, Castilla J (2006) Amyloids, prions and the inherent infectious nature of misfolded protein aggregates. Trends Biochem Sci 31(3):150–155. doi:10.1016/j.tibs.2006.01.002
154. Terzi E, Holzemann G, Seelig J (1997) Interaction of Alzheimer beta-amyloid peptide(1–40) with lipid membranes. Biochemistry 36(48):14845–14852. doi:10.1021/bi971843e
155. Zhu M, Li J, Fink AL (2003) The association of alpha-synuclein with membranes affects bilayer structure, stability, and fibril formation. J Biol Chem 278(41):40186–40197. doi:10.1074/jbc.M305326200
156. Heydari AR, Takahashi R, Gutsmann A, You S, Richardson A (1994) Hsp70 and aging. Experientia 50(11–12):1092–1098
157. Haslbeck M, Franzmann T, Weinfurtner D, Buchner J (2005) Some like it hot: the structure and function of small heat-shock proteins. Nat Struct Mol Biol 12(10):842–846. doi:10.1038/nsmb993
158. Lee S, Sowa ME, Choi JM, Tsai FT (2004) The ClpB/Hsp104 molecular chaperone-a protein disaggregating machine. J Struct Biol 146(1–2):99–105. doi:10.1016/j.jsb.2003.11.016
159. Kang PJ, Ostermann J, Shilling J, Neupert W, Craig EA, Pfanner N (1990) Requirement for hsp70 in the mitochondrial matrix for translocation and folding of precursor proteins. Nature 348(6297):137–143. doi:10.1038/348137a0
160. Goloubinoff P, Christeller JT, Gatenby AA, Lorimer GH (1989) Reconstitution of active dimeric ribulose bisphosphate carboxylase from an unfoleded state depends on two

chaperonin proteins and Mg-ATP. Nature 342(6252):884–889. doi:10.1038/342884a0

161. Apetri AC, Horwich AL (2008) Chaperonin chamber accelerates protein folding through passive action of preventing aggregation. Proc Natl Acad Sci USA 105(45):17351–17355. doi:10.1073/pnas.0809794105
162. Buchner J (1999) Hsp90 & Co.—a holding for folding. Trends Biochem Sci 24(4):136–141 (pii:S0968-0004(99)01373-0)
163. Haslberger T, Zdanowicz A, Brand I, Kirstein J, Turgay K, Mogk A, Bukau B (2008) Protein disaggregation by the AAA+ chaperone ClpB involves partial threading of looped polypeptide segments. Nat Struct Mol Biol 15(6):641–650. doi:10.1038/nsmb.1425
164. Mogk A, Tomoyasu T, Goloubinoff P, Rudiger S, Roder D, Langen H, Bukau B (1999) Identification of thermolabile *Escherichia coli* proteins: prevention and reversion of aggregation by DnaK and ClpB. EMBO J 18(24):6934–6949. doi:10.1093/emboj/18.24.6934

PERSPECTIVES

The study presented in this thesis showed that misfolded species which are likely to be the earliest species to form in the toxic aggregation pathway (chapter 2) can be efficiently reverted to the native state by chaperones acting as polypeptide unfoldases, such as Hsp70/Hsp110 and GroEL/CCT (Chapter 3 and 4). The early species in the aggregation pathway are said to be more toxic compared to the final aggregates, amyloids or fibrils. Once aggregation occurs, it can render chaperone systems less efficient e.g. α-synuclein oligomers inhibit Hsp70 unfolding system (chapter 5). From this study, it appears that chaperones, particularly polypeptide unfoldases, must be available when the misfolded species are formed in the cell so that they can become unfolded and reactivated as native proteins before they become inhibitory and toxic after misfolding. Future studies should now address whether the misfolded species that have been isolated and characterized here, are indeed toxic to cells as expected. Moreover, other polypeptide-unfolding chaperone systems need to be explored in addition to the Hsp70/Hsp110 and chaperonins (GroEL/CCT). Our meta-analysis of chaperone expressomic (Chapter 6) revealed that under different stress conditions, cytosolic chaperones are organized in three core chaperone network hubs contributed by Hsp70s, Hsp90s and small-Hsp. It is tempting to speculate that like Hsp70s, Hsp90s and sHsps can also act as polypeptide unfoldases of misfolded proteins. So, exploring the role of Hsp90s and sHsps in the active unfolding and refolding of misfolded proteins is the next important question that needs to be addressed. Finally, the mechanism by which Hsp110 collaborates with Hsp70 (chapter 3) at disaggregating various large stable protein aggregates is completely unknown and it needs to be deciphered in order to control the protein disaggregation in animal cells.

Molecular chaperones are optimally expressed under stress, in youth and in cancerous cells resistant to chemotherapy. The expression of molecular chaperones become defective in aging cells that leads to many neurodegenerative diseases. The defective chaperone expression is thus an apparent central cause for aging and protein-conformational diseases. There are several intuitive questions that need to be addressed, like why chaperone load decreases during aging and what measures may be undertaken to slowdown this process and restore the chaperone load in aging cells as in youth? On the other hand we need to understand and control how chaperone overload may lead to resistance of cancer cells to stress and chemotherapy in particular. The exploration of chaperone-inducing or chaperone-inhibiting drugs could be a therapeutic approach that holds great promise in combating aging and cancer. Yet, chaperone-inducing drugs against protein misfolding diseases could be oncogenic, emphasizing the importance of a detailed understanding and the specific differences of action between various chaperone and co-chaperone orthologs within given conserved chaperone families.